U.PORTO
FACULDADE DE CIÊNCIAS
UNIVERSIDADE DO PORTO

NOVA
NOVA SCHOOL OF
SCIENCE & TECHNOLOGY

universidade
de aveiro

PhD

3rd
CYCLE

FCUP
FCT-NOVA
UA
2024

U.PORTO

MISTRAL: Novel 4-amino- and 4,9-diamino-acridines as multi-stage antimalarials

Mélanie Fernandes Fonte

FC

U.PORTO
FACULDADE DE CIÊNCIAS
UNIVERSIDADE DO PORTO

NOVA
NOVA SCHOOL OF
SCIENCE & TECHNOLOGY

universidade
de aveiro

MISTRAL

Novel 4-amino- and 4,9-diamino-acridines as multi-stage antimalarials

Mélanie Fernandes Fonte
Doctoral Program in Sustainable Chemistry
Department of Chemistry and Biochemistry
Faculty of Sciences of the University of Porto
2024

PhD

MISTRAL

Novel 4-amino- and 4,9-diamino-acridines as multi-stage antimalarials

Mélanie Fernandes Fonte
Thesis carried out as part of the Doctoral Program in Sustainable Chemistry
Department of Chemistry and Biochemistry
2024

Supervisor
Cátia Andreia Silva Teixeira,
Researcher, REQUIMTE

Co-supervisors
Paula Alexandra de Carvalho Gomes,
Associate Professor, Faculty of Science of University of Porto

Miguel Prudêncio,
Researcher, Gulbenkian Institute for Molecular Medicine

All the corrections determined by the jury, and only those, were made.

The Supervisor,

Assinado por: Cátia Andreia Silva Teixeira
Identificação: BI12491362
Data: 2025-01-13 às 11:03:50

Assinado por: **Rui Miguel Prudêncio**
Num. de Identificação: 09111494
Data: 2025.01.13 13:11:53+00'00'

CHAVE MÓVEL

Assinado por: **PAULA ALEXANDRA DE CARVALHO GOMES**
Num. de Identificação: 09536203
Data: 2025.01.13 14:19:53+00'00'

CHAVE MÓVEL

Porto, 13/01/2025

“Success is walking from failure to failure

with no loss of enthusiasm”

Winston Churchill

Acknowledgements

A realização desta tese de doutoramento, financiada pela Fundação para a Ciência e Tecnologia (SFRH/BD/147345/2019), é um marco importante na minha vida académica e profissional, e não teria sido possível sem o apoio e a colaboração de várias pessoas. Foram quatro anos repletos de desafios, tanto a nível profissional quanto pessoal, nos quais aprendi imenso. Ao longo desta jornada, tive a sorte de poder contar com pessoas incríveis na minha vida e o prazer de conhecer muitas outras igualmente extraordinárias. Embora as palavras não sejam suficientes, deixo aqui um sincero agradecimento a todos que fizeram parte desta caminhada.

Primeiramente, gostaria de agradecer à minha orientadora, Cátia Teixeira, e coorientadores, Professora Paula Gomes e Miguel Prudêncio, pelo apoio, valiosas contribuições e encorajamento constante, fundamentais para a concretização deste trabalho.

Agradeço também a todas as pessoas com as quais tive o prazer de colaborar - Xavier Fernàndez-Busquets, Yunuen Avalos-Padilla, Diana Fontinha, Diana Moita, Sofia Santana e Ricardo Ferraz – cuja participação foi essencial para os resultados alcançados.

Aos meus colegas de laboratório, Teresa, Rita, Ana, Luísa, Natália e Pedro, agradeço pela amizade, discussões científicas enriquecedoras e apoio mútuo que foi essencial para manter a motivação e a inspiração ao longo deste percurso. Vivemos muitos bons momentos no laboratório que serão sempre lembrados. Um especial agradecimento à Teresa, Rita e Ana que foram “o meu pilar” em todos os momentos, tanto os bons quanto os desafiadores.

Também não poderia deixar de agradecer à Claúdia e à Mafalda que estiverem sempre presentes nesta etapa e me apoiaram constantemente. As nossas conversas de almoço e lanchinhos sabiam sempre muito bem!

À Sílvia, a minha amiga de longa data, deixo aqui também um especial agradecimento. Obrigada pelo apoio constante e pela compreensão.

Aos meus familiares, em especial aos meus pais e ao meu irmão, agradeço pelo amor incondicional, incentivo constante e compreensão durante os momentos mais difíceis. A vossa presença e apoio foram vitais para que eu pudesse alcançar este objetivo.

Por fim, dedico esta tese a todos aqueles que, direta ou indiretamente, contribuíram para a minha formação académica e para a realização deste trabalho. A todos, o meu mais sincero agradecimento.

LAQV requimte
LABORATÓRIO ASSOCIADO PARA A QUÍMICA VERDE
GIMM Gulbenkian Institute for Molecular Medicine
fct Fundação para a Ciência e a Tecnologia
REPÚBLICA PORTUGUESA
EDUCAÇÃO, CIÊNCIA E INOVAÇÃO
PESSOAS 2030 PROGRAMA DEMOGRAFIA, QUALIFICAÇÕES E INCLUSÃO
PORTUGAL 2030
UNIÃO EUROPEIA
Fundo Social Europeu

Resumo

A malária continua a ser uma das doenças infeciosas mais mortais, especialmente nas regiões tropicais e sub-tropicais dos países em desenvolvimento. A multirresistência do agente etiológico da malária, o parasita *Plasmodium*, constitui o principal obstáculo ao controlo e à erradicação da doença, comprometendo a eficácia de todos os antimaláricos desenvolvidos até à data. Consequentemente, há uma necessidade urgente de desenvolver novos medicamentos para substituir ou complementar os atuais, antes que estes falhem totalmente. Dado que as estratégias anteriores não permitiram atingir o objetivo de erradicação da malária, a pesquisa de novos fármacos redirecionou-se para o desenvolvimento de agentes ativos em várias fases do desenvolvimento do parasita. Um fármaco que afete simultaneamente múltiplos processos no ciclo de vida do parasita poderá exibir maior eficácia e menor probabilidade de induzir o desenvolvimento de estirpes de parasitas resistentes. Neste contexto, este projeto de doutoramento centrou-se no desenvolvimento de um potencial protótipo antimalárico multifásico, através da fusão de dois fármacos antimaláricos amplamente conhecidos, a primaquina e a cloroquina, numa única estrutura molecular. Com este objetivo em mente, a primeira parte deste projeto consistiu na síntese química e na avaliação antiplasmódica *in vitro* de duas famílias de derivados de acridina: 4-aminoacridinas e 4,9-diaminoacridinas. Estes compostos exibiram uma combinação da atividade de cada um dos fármacos de origem, apresentando dupla ação contra as formas sanguíneas e hepáticas de parasitas *Plasmodium*. A segunda parte do projeto incluiu a otimização química destas duas famílias, inspirada no conceito de biterapia covalente, de modo a obter híbridos com atividade superior. Assim, foram desenvolvidas duas novas famílias, resultantes da conjugação das aminoacridinas a uma estrutura bioativa adicional: um ácido *trans*-cinâmico. Estes novos conjugados foram posteriormente avaliados contra três fases distintas do ciclo de vida do parasita e, conforme previsto, a introdução do ácido cinâmico resultou em compostos com maior atividade antiplasmódica.

No seu conjunto, esta tese propõe novos derivados da acridina como potenciais protótipos terapêuticos ativos contra múltiplas fases de desenvolvimento do parasita da malária no hospedeiro humano. Dado que os fármacos antimaláricos continuam a ser a base do controlo e da erradicação da malária, os resultados aqui descritos podem representar um ponto de viragem significativo nesta área de investigação.

Palavras-chave: acridina, ácido cinâmico, biterapia covalente, descoberta de medicamentos, malaria, multi-fase, *Plasmodium*, química heterocíclica, resistência

Abstract

Malaria remains a major burden to global public health, especially in tropical and sub-tropical regions of developing countries. Multi-drug resistance of *Plasmodium* parasites, the etiological agents of malaria, is the main obstacle to malaria control and eradication, compromising the effectiveness of all antimalarial drugs developed to date. Hence, there is a pressing need for the development of new drugs to replace or complement the existing ones before their complete failure. Since prior strategies have not reached the eradication goals proposed, the focus of malaria drug development has shifted to the discovery of multi-stage drugs. A medicine that targets multiple processes in the parasite life cycle may not only have improved efficiency but also reduced probability of inducing development of resistant parasite strains. In this context, this doctoral project focused on the development of a potential multi-stage antimalarial lead through the combination of two well-known antimalarial drugs, primaquine and chloroquine, in a single molecular structure. With this objective in mind, the first part of this project consisted on the chemical synthesis and *in vitro* antiplasmodial evaluation of two families of acridine derivatives: 4-aminoacridines and 4,9-diaminoacridines. The results confirmed that these new compounds displayed the combined activity of both parent drugs, exhibiting dual action against blood and liver forms of *Plasmodium* parasites. Based on this, the second part of the project included the structural optimization of the two families, inspired in the covalent bitherapy concept to obtain hybrids with enhanced multi-stage antiplasmodial activity. Thus, two new families of compounds were produced, by conjugation of the aminoacridines with an additional bioactive moiety, namely, a *trans*-cinnamic acid. The new conjugates were screened *in vitro* against three stages of the malaria parasite lifecycle and, as expected, the introduction of the *trans*-cinnamic acid moiety resulted in enhanced *in vitro* antiplasmodial activity.

Altogether, this thesis proposes new acridine derivatives as potential multi-stage antimalarial leads in the human host. Since antimalarial drugs remain the mainstay for malaria control and eradication, the findings herein described may represent a significant turning point in this area of research.

Keywords: acridine, cinnamic acid, covalent bitherapy, drug discovery, heterocyclic chemistry, malaria, multi-stage, *Plasmodium,* resistance

Preface

Malaria is one of the most devastating parasitic diseases, affecting an estimated 250 million people and causing approximately 600,000 deaths annually. Despite the substantial efforts to eradicate this disease, the declining effectiveness of existing therapies driven by the constant evolution of resistance to the current antimalarial chemotherapeutics, has been aggravating the malaria threat. Moreover, the complex life cycle of the malaria parasite hampers the development of an effective vaccine, leaving the world heavily reliant on antimalarial drugs. To counter these statistics, which are likely to increase, new medicines to replace the existing ones before their complete failure are urgently needed. Furthermore, since prior drug development strategies are not a long-term option, it is essential to explore new approaches to identify novel antimalarial leads. To this end, and prompted by results previously obtained by our research group, the fundamental goal of this project was to develop a potential multi-stage antimalarial lead capable of targeting more than one process in the malaria parasite life cycle. This approach likely contributes to enhance efficacy while reducing the likelihood of emerging resistance.

The rational design of the multi-stage compounds targeted in this work was achieved by merging the chemical structures of two established antimalarial drugs that, together, are effective across three distinct stages of the malaria parasite life cycle. Hence, while chloroquine exerts its activity against the blood forms of *Plasmodium,* primaquine can eliminate all liver forms of the parasite and interrupt disease transmission due to its gametocytocidal action. Based on this, the working hypothesis addressed in this doctoral project was that merging these two drugs into a single molecular construct would likely combine the antimalarial properties of the parent drugs, affording multi-stage activity. It was further hypothesized that conjugation of the new “merged” constructs with a second bioactive building block might contribute to an additional improvement of antiplasmodial efficacy, following the concept of covalent bitherapy advanced by Meunier in 2008.

The research work conducted to test the hypotheses above was reported in five original articles, either already published or submitted for publication in internationally indexed scientific journals with peer review. Therefore, the Results and Discussion section of this doctoral thesis is organized in two main chapters. The articles included in each chapter are preceded by a synopsis and a graphical abstract, and are included the as facsimile of their published versions, i.e., as autonomous units formatted as per the specific

journal's style (sections, figure/table/scheme numbering, reference citation styles). Overall, this doctoral thesis is organized as follows.

The introductory **Chapter I** provides an overview of the current global malaria situation, highlighting the existing therapeutic options and the reasons why there is a pressing need for alternatives. Building on this, several approaches used in drug development are reviewed, with particular emphasis on the covalent bitherapy strategy, which has been devised to create potential multi-stage drugs and inspired the work herein reported.

Chapter II (**articles I** and **II**) presents the rational design, synthesis, structural characterization, and *in vitro* evaluation of the two initial families developed as potential multi-stage drugs – 4-aminoacridines and 4,9-diaminoacridines. As the results obtained validated our working hypothesis, i.e. the newly synthesized compounds displayed a combination of the activities of the parent drugs, we subsequently sought to optimize the synthetic routes used to produce these compounds, as also reported in this chapter.

Chapter III (**articles III**, **IV**, and **V**) encompasses the chemical optimization of 4-aminoacridine and 4,9-diaminoacridine derivatives obtained by conjugation with a *trans*-cinnamic acid moiety, known for its intrinsic antiplasmodial activity. The conjugates targeted were selected on the basis of the results reported in the previous chapter, i.e., the best-performing 4-aminoacridines and 4,9-diaminoacridines were selected and linked to the cinnamic acid moieties following the covalent bitherapy strategy aiming to produce more potent multi-stage molecules. The conjugates were screened for their multi-stage activity *in vitro*, with promising results overall. The fact that these novel conjugates incorporated both the acridine and the cinnamoyl moieties, also known for their antitumoral properties, alerted us to their potential antiproliferative activity. As such, we have additionally tested their action against different tumor cell lines and our relevant findings obtained have also been incorporated into this chapter.

Finally, **Chapter IV** summarizes the overall achievements of this doctoral project and provide an outlook for future work.

List of Publications

The work herein reported and discussed resulted in the following scientific production:

Papers

Mélanie Fonte, Natália Fagundes, Ana Gomes, Ricardo Ferraz, Cristina Prudêncio, Maria João Araújo, Paula Gomes, Cátia Teixeira. Development of a synthetic route towards N^4, N^9-disubstituted 4,9-diaminoacridines: On the way to multi-stage antimalarials. *Tetrahedron Letters*, **2019**, 60, 1166–1169.

DOI: 10.1016/j.tetlet.2019.03.052.

Mélanie Fonte, Natália Tassi, Diana Fontinha, Inés Bouzón-Arnáiz, Ricardo Ferraz, Maria J. Araújo, Xavier Fernàndez-Busquets, Miguel Prudêncio, Paula Gomes, Cátia Teixeira. 4,9-Diaminoacridines and 4-Aminoacridines as Dual-Stage Antiplasmodial Hits. *ChemMedChem*, **2021**, 16, 788–792.

DOI: 10.1002/cmdc.202000740

Mélanie Fonte, Natália Tassi, Paula Gomes, Cátia Teixeira. Acridine-Based Antimalarials—From the Very First Synthetic Antimalarial to Recent Developments. *Molecules*, **2021**, 26, 600.

DOI: 10.3390/molecules26030600

Mélanie Fonte, Diana Fontinha, Diana Moita, Omar Caño-Prades, Yunuen Avalos-Padilla, Xavier Fernàndez-Busquets, Miguel Prudêncio, Paula Gomes, Cátia Teixeira. New 4-(*N*-cinnamoylbutyl)aminoacridines as potential multi-stage antiplasmodial leads. *European Journal of Medicinal Chemistry*, **2023**, 258, 115575.

DOI: 10.1016/j.ejmech.2023.115575

Mélanie Fonte, Cátia Teixeira, Paula Gomes. Improved synthesis of antiplasmodial 4-aminoacridines and 4,9-diaminoacridines. *RSC Advance*, **2024**, 14, 6253–6261.

DOI: 10.1039/d4ra00091a

Mélanie Fonte, Catarina Rôla, Sofia Santana, Yunuen Avalos-Padilla, Xavier Fernàndez-Busquets, Miguel Prudêncio, Paula Gomes, Cátia Teixeira. Disclosure of cinnamic acid/4,9-diaminoacridine conjugates as multi-stage antiplasmodial hits. *Bioorganic & Medicinal Chemistry*, **2024**, 104, 117714.

DOI: 10.1016/j.bmc.2024.117714

Mélanie Fonte, Catarina Rôla, Sofia Santana, Miguel Prudêncio, Joana Almeida, Ricardo Ferraz, Cristina Prudêncio, Cátia Teixeira, Paula Gomes. Repurposing antiplasmodial leads for cancer: exploring the antiproliferative effects of *N*-cinnamoyl-aminoacridines. *Bioorganic & Medicinal Chemistry Letters*, **2024**, 111, 129894.

DOI: 10.1016/j.bmcl.2024.129894

Oral communications

Mélanie Fonte *et al.* "New 4-(*N*-cinnamoylbutyl) aminoacridines as potential multi-stage antiplasmodial leads." Oral communication presented at the LAQV-REQUIMTE Webinar –2024.

Mélanie Fonte *et al.* "New 4-(*N*-cinnamoylbutyl) aminoacridines as potential multi-stage antiplasmodial leads." Oral communication presented at the XXVIII Encontro Nacional da Sociedade Portuguesa de Química – Aveiro, Portugal, 24/07/2023 – 26/07/2023.

Mélanie Fonte *et al.* "Novel 4-amino- and 4,9-diaminoacridines as multi-stage antimalarials." Oral communication presented during an internship at the Wroclaw

University of Science and Technology (Prof. Berlicki's Lab), University of Wroclaw - Poland – 08/10/2022 – 22/10/2022.

Poster communications

Mélanie Fonte *et al.* "Cinnamic acid-acridine hybrids as multi-stage antiplasmodial leads". Poster presented at the 15th National Organic Chemistry Meeting & 8th National Medicinal Chemistry Meeting – Faro, Portugal, 21/01/2024 – 24/04/2024.

Mélanie Fonte *et al.* "Synthesis and in vitro efficiency of 4-(*N*-cinnamoylbutyl)aminoacridines against multi-stages of malaria parasites in the mammalian host". Poster presented at the 10th EFMC Young Medicinal Chemists' Symposium – Zagreb, Croatia, 07/09/2023 – 08/09/2023.

Mélanie Fonte *et al.* "Novel 4-aminoacridinecinnamic acid conjugates as multi-stage antiplasmodial hits". Poster presented at the XXVI Encontro Galego Português de Química – Galiza, Spain, 16/11/2022 – 18/11/2022.

Mélanie Fonte *et al.* "Novel 4-aminoacridinecinnamic acid conjugates as multi-stage antiplasmodial hits". Poster presented at the 9th EFMC Young Medicinal Chemists' Symposium – Nice, France, 08/09/2022 – 09/09/2022.

Mélanie Fonte *et al.* "Novel 4-aminoacridinecinnamic acid conjugates as multi-stage antiplasmodial hits". Poster presented at the XXVII EFMC International Symposium on Medicinal Chemistry – Nice, France, 04/09/2022 – 08/09/2022.

Mélanie Fonte *et al.* "4,9-diaminoacridines and 4-aminoacridines as potential antiproliferative hits". Poster presented at the 7th International Electronic Conference on Medicinal Chemistry – virtual event, 01/11/2021 - 30/11/2021.

Mélanie Fonte *et al.* "4,9-diaminoacridines and 4-aminoacridines as dual-stage antiplasmodial hits". Poster presented at the XXVII Encontro Nacional da Sociedade Portuguesa de Química – Braga, Portugal, 14/07/2021 – 16/07/2021.

Mélanie Fonte *et al.* "Novel dual-stage aminoacridine derivatives targeting the malaria parasite". Poster presented at the Interfacing Chemical Biology and Drug Discovery - virtual event, 07/07/2021 – 09/07/2021.

Mélanie Fonte *et al.* "4,9-diaminoacridines and 4-aminoacridines as antiplasmodial dualstage hits". Poster presented at the 6th International Electronic Conference on Medicinal Chemistry – virtual event, 01/11/2020 – 30/11/2020.

Mélanie Fonte *et al.* "Development of a synthetic route towards N^4, N^9-disubstituted 4,9-diaminoacridines: On the way to multistage antimalarials". Poster presented at the XXVI Encontro Nacional da Sociedade Portuguesa de Química – Porto, Portugal, 24/07/2019 – 26/07/2019.

Mélanie Fonte *et al.* "New 4-aminoacridine analogues as promising dual-stage antimalarials". Poster presented at the IJUP 2018 – Encontro de Investigação Jovem da Universidade do Porto – Porto, Portugal, 07/02/2018 – 08/02/2018.

Mélanie Fonte *et al.* "Novel 4,9-diaminoacridine derivatives as potential multi-target antimalarials.". Poster presented at the IJUP 2018 – Encontro de Investigação Jovem da Universidade do Porto – Porto, Portugal, 07/02/2018 – 08/02/2018.

Mélanie Fonte *et al.* "Novel 4,9-diaminoacridine derivatives as potential multi-target antimalarials". Poster presented at the 12th National Organic Chemistry Meeting & 5th National Medicinal Chemistry Meeting – Coimbra, Portugal, 17/01/2018 – 19/01/2018.

Table of contents

Acknowledgements vii

Resumo ix

Abstract xi

Preface xiii

List of Publications xv

Table of contents xix

List of Tables xxi

List of Schemes xxiii

List of Figures xxv

List of Abbreviations xxvii

CHAPTER I 1

1. Malaria 3

1.1. Malaria Epidemiology 3

1.2. *Plasmodium* Infection and Transmission 4

1.3. Malaria Control and Elimination 6

1.4. Antimalarial Chemotherapy 7

1.4.1. Acridines 8

1.4.2. Quinolines 8

1.4.3. Endoperoxides 11

1.4.4. Antifolates, naphthoquinone, and antibiotics 12

2. The need for novel antimalarials 17

3. Approaches for discovering multi-stage antimalarials: from traditional approaches to the covalent bitherapy concept 21

4. Multi-stage antiplasmodial hybrids 24

4.1. Aminoquinoline-based conjugates 24

4.1.1. AQ-AQ conjugates 24

4.1.2. AQ-Endoperoxide conjugates 26

4.1.3. AQ-Cinnamic acid conjugates 28
4.1.4. AQ-Triazole conjugates 29
4.1.5. AQ-Quinoxaline conjugates 30
4.1.6. AQ-Organometallic conjugates 31
4.1.7. Other AQ conjugates 33
4.2. Acridine-based conjugates 34
4.3. Aminoquinoline-based merged hybrids 36
5. Overview of the present work 39
References 43
CHAPTER II 57
Article I 59
Article II 81
CHAPTER III 109
Article III 111
Article IV 163
Article V 201
CHAPTER IV 211
Summary of main conclusions 213
Future Perspectives 219
Annexes 221

List of Tables

Table 1. Summary of WHO recommendations for the prophylaxis and treatment of uncomplicated and severe malaria based on the current WHO Model List of Essential Medicines 2023.[65, 66] 16

List of Schemes

Scheme 1. Synthesis route developed by Fonte *et al.* for the obtention of 4,9-diaminoacridine derivative. Reagents and conditions: **Part A** (at blue) **- (i)** CH_3I, Cs_2CO_3, dimethylformamide (DMF), room temperature (rt), 90 min; **(ii)** Tf_2O, Et_3N, CH_2Cl_2, N_2 atmosphere, -25 °C, 30 min; **(iii)** 4-methoxy-2-nitroaniline, Cs_2CO_3, $Pd(OAc)_2$, *rac*-BINAP, toluene, N_2 atmosphere, 120 °C, 5 h; **(iv)** (1) $Ba(OH)_2 \cdot 8H_2O$, CH_3OH, 90 °C, 2 h; (2) 1 M aq. HCl; **(v)** $POCl_3$, 120 °C, 2.5 h; **Part B** (at yellow) **– (vi)** Phenol, Cs_2CO_3, dimethylsulfoxide (DMSO), 4 Å molecular sieves, 100 °C, 2 h, then *N,N*-diethylpentan-1,4-diamine, 100°C, 4 h; **(vii)** $SnCl_2$, 37% aq. HCl, 0→40 °C, 30 min; **(viii)** *N*-(4-bromobutyl)phthalimide, CH_3COONa, CH_3CH_2OH, microwave (MW) heating (100 W, 120°C) in a pressurized vial (100 psi), 2.5 h; **(ix)** NH_2NH_2, tetrahydrofuran (THF), 60°C, 72 h.[102] 37

List of Figures

Figure 1. Map of the estimated number of malaria cases in 2022 according to the WHO database (data collected from the WHO's Global Health Observatory and analyzed in Excel).[3] 3

Figure 2. Progress in malaria deaths and cases between 2019-2022 (Data from WHO 2019-2022 reports).[1, 7-10] 4

Figure 3. *Plasmodium* life cycle (Figure designed on BioRender. Adaptation from ref 21). 6

Figure 4. Chemical structure of the quinine alkaloid and the methylene blue dye. 7

Figure 5. The main classes of antimalarial drugs developed so far and introduced in the clinic, most of them still recommended by WHO, as described in **Table 1**. 14

Figure 6. History of the introduction of the principal antimalarials and the first emergence of resistance in the field (Figure designed using Canva). Legend: Single bars refer to monotherapies; double- and triple-bar boxes denote combination therapies. Colors refer to the chemical classes to which the antimalarials belong. CQ – Chloroquine, ADQ – Amodiaquine, AS-ADQ – Artesunate-Amodiaquine, SP – Sulfadoxine-Pyrimethamine, MFQ – Mefloquine, AS-MFQ – Artesunate-Mefloquine, ART – Artemisinin, PPQ – Piperaquine, DHA-PPQ – Dihydroartemisinin-Piperaquine, PND – Pyronaridine, AS-PND – Artesunate-Pyronaridine, AT-LMF – Artemether-Lumefantrine, AS-SP – Artesunate+Sulfadoxine-Pyrimethamine.[21] 18

Figure 7. Summary of MMV's Target Product Profiles (TPPs) and Target Candidate Profiles (TCPs) for malaria medicines to control, eliminate, and eradicate malaria.[84] .. 20

Figure 8. Meunier's pioneering contribution in applying the covalent bitherapy concept to antimalarials: trioxaquines as covalent conjugates of antimalarial quinolines and trioxanes; the structure of **PA1103-SAR116242**, a trioxaquine advanced as candidate for preclinical development, is also shown.[93-95] 22

Figure 9. Classification of hybrids according to the nature of the linker: conjugate,[100] cleavage conjugate,[101] fused hybrids[100] and merged[102] hybrids, and examples of chemical structures of compounds representing antimalarial hybrids in each category. 23

Figure 10. PQ-CQ conjugates developed by Lödige *et al.*[100, 105] (**1a-g**) and Pereira *et al.* (**2, 3**).[106, 107] 26

Figure 11. AQ-Endoperoxide conjugates developed by Capela *et al.*[109-111] (**4-7**) and by Benoit-Vical *et al.* (**8**).[112] 28

Figure 12. AQ-CA conjugates developed by Pérez *et al.*[117, 118] and Gomes *et al*. (**9-11**).[119] 29
Figure 13. AQ-Triazole conjugates developed by Wadi *et al.*[123] (**12**) and Huang *et al.* (**13**).[124] 30
Figure 14. AQ-Quinoxaline conjugates developed by Bonilla-Ramirez *et al.* (**14-15**).[127, 128] 31
Figure 15. AQ-Organometallic conjugates developed by Macedo *et al.*[131, 132] (**16**, **17**) and Matos *et al.* (**18**, **19**).[137] 33
Figure 16. AQ-Triazine, AQ- pyrimidine, AQ-Squaramide, and AQ-adamantane conjugates developed by Rodrigues *et al.* (**20**),[142] Kaur *et al.* (**21**),[145] Ribeiro *et al.* (**22, 23**),[148] and Terzić *et al.* (**24**),[150] respectively. 34
Figure 17. ACR-based conjugates developed by Gomes and co-workers (**25**, **26**).[151, 153] 36
Figure 18. 4,9-diaminoacridine merged hybrid (**27**) recently developed by Gomes and co-workers as a potential multi-stage antiplasmodial,[102] which served as driving force for the doctoral research project herein reported. 36
Figure 19. 4,9-diaminoacridines and 4-aminoacridines developed in this doctoral project as potential multi-stage antimalarial hits, resulting from the “merge” of the chemical structures of the antimalarial AQ drugs CQ and PQ. 39
Figure 20. The four experimental goals set to achieve the global aim of this doctoral project (highlighted in green) 40

List of Abbreviations

A

ACR	Acridine
ACT	Artemisinin-based Combination Therapy
ADQ	Amodiaquine
AQ	Aminoquinoline
ART	Artemisinin
AS	Artesunate
AT	Artemether

C

CA	*trans*-cinnamic acid
CQ	Chloroquine

D

DHA	Dihydroartemisinin
DHFR	Dihydrofolate reductase
DHPS	Dihydropteroate synthetase
DMF	Dimethylformamide
DMSO	Dimethyl sulfoxide
DNA	Deoxyribonucleic acid
DV	Digestive vacuole

E

EC_{50}	Half-maximal Effective Concentration
ESI-MS	Electrospray Ionization Mass Spectrometry

G

GMS	Greater Mekong Subregion
G6PD	Glucose-6-phosphate dehydrogenase

H

Hb	Hemoglobin
HF	Halofantrine
HPLC	High-performance Liquid Chromatography

HPPK	Hydroxymethylpterin pyrophosphokinase
Hz	Hemozoin

I

IC_{50}	Half-maximal Inhibitory Concentration
iPr	Isopropyl
IPTi	Intermittent Preventive Treatment in infants
IPTp	Intermittent Preventive Treatment in pregnancy

L

LMF	Lumefantrine

M

MFQ	Mefloquine
MMV	Medicines for Malaria Venture
MoA	Mechanism of Action
MW	Microwave

N

NMR	Nuclear Magnetic Ressonance

P

P.	*Plasmodium*
PND	Pyronaridine
PPIX	Protoporphyrin IX
PPQ	Piperaquine
PQ	Primaquine

Q

QN	Quinacrine

R

ROS	Reactive Oxygen Species
rt	Room temperature

S

SAR	Structure-activity Relationships
SI	Selective index
SMP	Seasonal Malaria Chemoprevention
SP	Sulfadoxine-Pyrimethamine
spp	Several species

T

TCP	Target Candidate Profile
TQ	Tafenoquine
TPP	Target Product Profile

W

WHO	World Health Organization

CHAPTER I

Introduction

Contents:

1. Malaria

1.1. Malaria Epidemiology

1.2. *Plasmodium* Infection and Transmission

1.3. Malaria Control and Elimination

1.4. Antimalarial Chemotherapy

1.4.1. Acridines

1.4.2. Quinolines

1.4.3. Endoperoxides

1.4.4. Antifolates, naphthoquinone, and antibiotics

2. The need for novel antimalarials

3. Approaches for discovering multi-stage antimalarials: from traditional approaches to the covalent bitherapy concept

4. Multi-stage antiplasmodial hybrids

4.1. Aminoquinoline-based conjugates

4.1.1. AQ-AQ conjugates

4.1.2. AQ-Endoperoxide conjugates

4.1.3. AQ-Cinnamic acid conjugates

4.1.4. AQ-Triazole conjugates

4.1.5. AQ-Quinoxaline conjugates

4.1.6. AQ-Organometallic conjugates

4.1.7. Other AQ conjugates

4.2. Acridine-based conjugates

4.3. Aminoquinoline-based merged hybrids

5. Overview of the present work

References

1. Malaria

1.1. Malaria Epidemiology

Malaria is a vector-borne parasitic disease that imposes a substantial impact on both morbidity and mortality in the regions where it is endemic. The most recent report by the World Health Organization (WHO) estimated 249 million malaria cases in 2022, an increase of 5 million cases compared with 2021, which resulted in 608,000 deaths.[1] Malaria has a broad impact throughout tropical and subtropical areas of the globe, affecting indigenous populations, especially pregnant women and children under the age of 5, as well as an increasing number of travelers. The WHO African Region accounted for about 82% of the cases and 94% of deaths globally, followed by the WHO Southeast Asia Region with 10% of the cases and 3% of fatalities (**Figure 1**).[1] In these countries, the ecological conditions for transmission and propagation of malaria parasites are highly favorable since (i) the high temperature and humidity, and frequent rainfall, are ideal for vector proliferation, and (ii) poverty is prevalent, with affected populations having limited access to proper sanitation and healthcare systems. This poverty can greatly enhance the impact of malaria by hampering the availability of treatment and preventive measures and/or obstructing patients' compliance with the latter due to insufficient communication and education.[2]

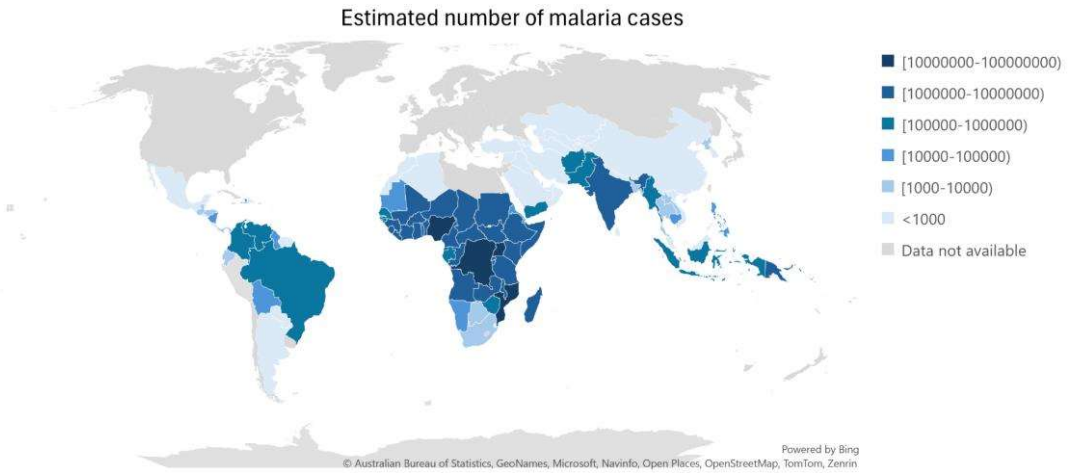


Figure 1. Map of the estimated number of malaria cases in 2022 according to the WHO database (data collected from the WHO's Global Health Observatory and analyzed in Excel).[3]

The global malaria incidence rate was significantly reduced from 2000 to 2019, which was mainly attributed to the introduction of artemisinin-based combination therapies

(ACT) as well as insecticide-treated bed nets. However, despite the WHO's sustained efforts, global malaria progress has stalled in recent years. Previous achievements were threatened by drug resistance spread and the COVID-19 pandemic, leading to higher mortality in 2020 and even greater increases in the subsequent years (**Figure 2**).[4] If the current trend continues, it is likely that the 2025 targets delineated in the Global Technical Strategy for Malaria, which include a 75% reduction of malaria cases by 2025 compared to the 2015 baseline, will not be achieved.[5] Moreover, there is an urgent concern that climate change could drive the spread of malaria vectors to regions where malaria has been previously eradicated or which have never been exposed to the disease.[6]

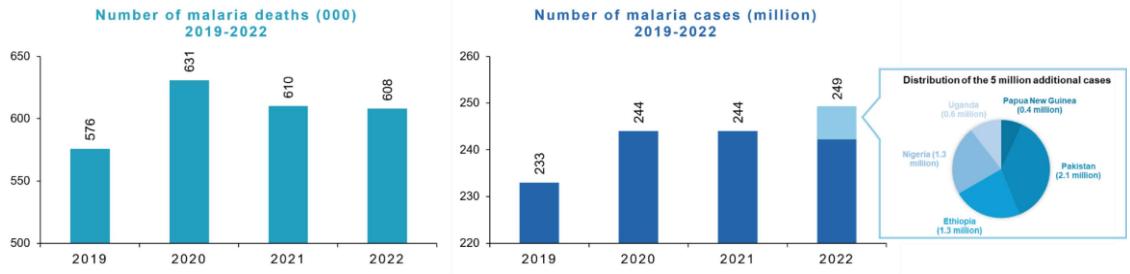


Figure 2. Progress in malaria deaths and cases between 2019-2022 (Data from WHO 2019-2022 reports).[1, 7-10]

1.2. *Plasmodium* Infection and Transmission

Malaria is caused by a protozoan parasite from the genus *Plasmodium*, transmitted to humans through the bites of infected female *Anopheles* mosquitoes. There are five different species of *Plasmodium* capable of infecting humans: *P. falciparum*, *P. vivax*, *P. ovale* spp, *P. malariae,* and *P. knowlesi*.[1, 7, 9, 10] However, recently, *P. ovale curtisi* and *P. ovale wallikeri* have been described as two distinct species due to their differences in clinical, prognostic, and sensitivity to antimalarial drugs.[11, 12] Most infections are caused by *P. falciparum* and *P. vivax*, where *P. falciparum* is the predominant cause of mortality, especially in Africa. Conversely, *P. vivax* is mainly spread in most countries outside sub-Saharan Africa and, despite causing benign malaria, is also increasingly recognized as an important contributor to the malaria toll, due to the high morbidity that it causes. This is mainly because, alongside *P. ovale*, it can generate liver-resident latent forms termed hypnozoites that can be reactivated months or years later to initiate a relapse infection.[13] All the infectious *Plasmodium* species share a common and complex life cycle, which involves alternate developmental asexual and sexual stages within the human host and the *Anopheles* mosquito, respectively (**Figure 3**).[14, 15] In humans, *Plasmodium* infection

begins when an infected female *Anopheles* mosquito takes a blood meal and injects sporozoites present in its salivary glands into the person's skin. Then, the sporozoites enter the bloodstream, where they travel to the liver and invade the hepatocytes. There, they multiply asexually and differentiate into liver schizonts containing thousands of merozoites. The schizonts eventually rupture and release the merozoites into the bloodstream, and erythrocytes become quickly infected.[16] In *P. vivax* and *P. ovale* species, the schizonts can, alternatively, transform into dormant hypnozoites, which can persist for months or even years in the liver until they reactivate and cause relapses. The precise mechanisms triggering hypnozoite reactivation are not fully understood and research is ongoing to better comprehend the factors influencing the timing and frequency of relapses. The incidence and temporal patterns of relapse vary geographically, which suggests that relapses may be related to environmental conditions and/or host biology. Some hypotheses include, for example, the reaction of hypnozoites to specific components, such as proteins, in vector saliva or a host immune response to the mosquito bite.[13, 17]

Once inside the red blood cell, the parasite initiates its second asexual multiplication stage in the mammalian host, undergoing different morphological forms, from a ring-like to trophozoite stages and then to schizonts containing multiple merozoites. Eventually, mature schizonts rupture, and the new merozoites are released back into the bloodstream, to initiate another intraerythrocytic replication cycle. This can persist indefinitely in the absence of treatment or an adequate immune response. During this time, the parasite digests host-cell hemoglobin to satisfy its nutritional requirements, and the heme waste produced is polymerized to form the less toxic pigmented waste called hemozoin. It is only at this point of the parasite life cycle that the first symptoms of malaria appear, such as febrile waves, headache, vomiting, anemia, coma, cerebral malaria, and eventually death.[18]

Under some exceptional circumstances and still unclear mechanisms,[19] a subpopulation of ~1% of the merozoites differentiates into male and female gametocytes that will ensure parasite transmission to the mosquito vector. This stage involves five morphologically unique steps for 2–3 weeks to complete maturation. Once mature, gametocytes circulate the mammalian host circulatory systems awaiting uptake by a new *Anopheles* vector. This completes the part of the parasites' life cycle that occurs inside the human body.[19]

The second part of the life cycle in the insect vector begins after the ingestion of gametocytes by a mosquito during a blood meal. In the lumen of the mosquito midgut, gametocytes differentiate into male and female gametes, which fuse to form a zygote that will subsequently develop into a motile ookinete. The ookinete travels through the

gut to produce an oocyst, which continues developing in the epithelium of the midgut forming thousands of sporozoites. When the oocyst matures, it ruptures, and these sporozoites migrate to the salivary glands, where they can infect a new human host during a blood meal (mosquito bite), concluding the complex life cycle of the parasite.[20]

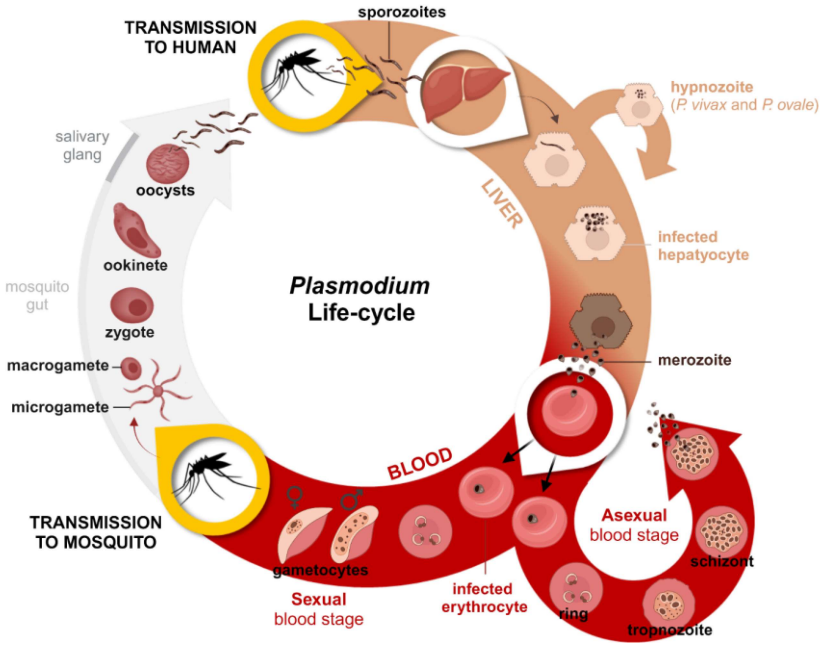


Figure 3. *Plasmodium* life cycle (Figure designed on BioRender. Adaptation from ref 21).

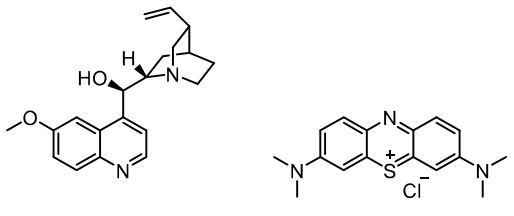
1.3. Malaria Control and Elimination

Each of the developmental stages discussed above provides numerous potential targets for intervention, at which the parasite's life cycle can be interrupted. Therefore, the control and elimination of malaria comprise several measures that act against infection on both the mosquito vector and the human host. The *Anopheles* mosquito is essential to malaria transmission and thus, measures to control and eliminate this vector are important tools in the fight against malaria. Nowadays, vector control is achieved by limiting propagation using long-lasting insecticide-treated bed nets and indoor residual spraying.[1, 22] Another recent, but controversial, strategy consists of genetically modifying mosquitoes to produce sterile or antipathogenic vectors, which will mate with wild mosquitoes and, consequently, transfer this trait to their offspring. However, the release of genetically modified organisms into the environment generates a multitude of ethical concerns in the scientific community and is therefore not consensual.[23, 24]

On the other hand, the measures implemented against infection of the human host by parasites include early diagnosis using rapid diagnostic tests, chemoprophylaxis for risk groups (pregnant women and children) or travelers, and chemotherapy. Recently, the RTS,S/AS01[25] and R21/Matrix-M[26] vaccines were recommended by WHO for malaria prevention caused by *P. falciparum*.[1] However, according to reports from pilot programs and clinical trials, these vaccines provide only partial infection prevention in children from around 5 months of age and do not avoid cases of malaria caused by *Plasmodium* species other than by *P. falciparum*. These limitations in protective efficacy and the need to continuously update vaccine formulations due to antigenic polymorphism highlight the current dependence on antimalarial drugs.[26-28] Therefore, chemoprophylaxis and chemotherapy still play, and will continue to play, a central role in combating malaria infections.

1.4. Antimalarial Chemotherapy

The beginning of malaria chemotherapy can be traced back to the discovery of quinine, a natural alkaloid found in the bark of the *Cinchona tree*. Quinine (**Figure 4**) was isolated for the first time from the bark in 1820 and became the mainstay of antimalarial treatment for over a hundred years. Due to its complex structure, it was only in 1944 that William Perkins accomplished its total synthesis.[29] Meanwhile, in an attempt to obtain quinine, William Perkins accidentally synthesized the first synthetic dye named methylene blue (**Figure 4**). Later, Ehrlich and Guttmann used this dye to cure two malaria patients after noticing that it was selectively toxic to the parasite. Although both patients experienced a reduction in their fever and clearance of the parasites, methylene blue was not used further at that time. However, this work laid the foundation for the development of synthetic antimalarial drugs. The first antimalarial drug classes raised from modifications of this dye were acridines and quinolines. Over the years, these classes of compounds showed some limitations, which led to the development of other classes, such as endoperoxides and antifolates.[29-31]



Quinine **Methylene Blue**

Figure 4. Chemical structure of the quinine alkaloid and the methylene blue dye.

1.4.1. Acridines

Acridines (ACR) were the pioneering synthetic class of compounds resulting from modifications of methylene blue. Their chemical structure is characterized by a planar aromatic surface constituted by three fused six-membered rings and a central nitrogen. Quinacrine (QN, **Figure 5**), an ACR derivative, was the first synthetic antimalarial drug active against blood forms of the malaria parasite. This drug was widely used by soldiers during the Second World War when supplies of quinine were limited. However, QN's use was short-lived due to its substantial undesirable side effects.[29, 31] Since then, several modifications around the QN structure have been conducted to improve its pharmacokinetic and pharmacodynamic properties, as well as to overcome problems of cytotoxicity. However, to date, no compound arising from these studies has yet reached clinical application.[32-34]

1.4.2. Quinolines

As the complexity of quinine's chemical structure challenged its synthesis in the laboratory, researchers started exploring its key structural elements to obtain compounds able to replace QN. At the time, quinoline-based antimalarials were raised as one of the most important and wide classes of compounds in malaria history and were responsible for effectively controlling the disease during the 20th century. The first quinoline-based compound, chloroquine (CQ, **Figure 5**), was discovered in 1934 and its efficiency turned it into the cornerstone of the WHO's efforts to eradicate malaria globally.[29] After the success of CQ, the exploration of antimalarial candidates based around the quinoline's nucleus led to compounds such as primaquine (PQ), tafenoquine (TQ), piperaquine (PPQ), pyronaridine (PND), amodiaquine (ADQ), mefloquine (MFQ), halofantrine (HF) and lumefantrine (LMF).[29, 30] Although each of these compounds shares the quinoline ring system, small variations in their structures allow them to be categorized into three subclasses: the 4-aminoquinolines (CQ, ADQ, PPQ, and PND), the 8-aminoquinolines (PQ and TQ), and the aryl-aminoalcohols (MFQ, HF, and LMF).

4-Aminoquinolines

As previously highlighted, CQ – a 4-aminoquinoline (4-AQ) – was the most successful drug used for the treatment and prophylactic of malaria due to its high efficacy against blood forms of *Plasmodium*, stability, low toxicity, and low cost. However, over years of use, the appearance of parasite strains resistant to this drug led to the search for new 4-AQs.[29-31, 35] CQ comprises a quinoline ring system with a 7-chloro substitution and a flexible pentyl diamine side chain. Structure-activity relationships (SAR) studies indicated

that (i) the quinoline ring itself, (ii) a strong electron-withdrawing and lipophilic group in the 7-position, and (iii) a tertiary amino nitrogen in the alkyl side chain, are required for CQ to exert its antimalarial activity.[36] Based on this, attempts have been made to obtain a superior antimalarial drug. As a lipophilicity enhancement strategy, an aromatic structure (4-aminophenol) was incorporated into the side chain of CQ, thus resulting in ADQ (**Figure 5**), a more potent compound. However, its therapeutic value was significantly reduced by its severe hepatotoxicity and dangerous agranulocytosis, resulting from its metabolization into a quinone-imine. These serious side effects only occur when ADQ is used prophylactically over a prolonged period, while shorter therapeutic regimes are sufficiently safe. Consequently, ADQ is nowadays only used in combination with other drugs (ADQ-artesunate, **Table 1**) for the treatment of uncomplicated *P. falciparum* malaria.[30, 31, 37] Subsequently, PPQ and PND (**Figure 5**), another two 4-AQs, were developed as alternatives to replace CQ. PPQ is a bis-4-AQ linked by a piperazine-alkyl chain, while PND is a benzo-naphthyridine derivative, with an additional ADQ-like side chain. Both drugs are safe and well tolerated with minor side effects and are currently in use as a partner drug of other antimalarials (PPQ-dihydroartemisinin and PND-artesunate, **Table 1**) for curative treatment.[30, 31, 38, 39]

Aryl-aminoalcohols

The aryl-aminoalcohols subclass has the aryl group connected to an amino alcohol moiety. After quinine, MFQ (**Figure 5**) was the first antimalarial drug developed with these structural features, being active against blood forms of *Plasmodium*. It is considered a simpler quinine analog with a piperidine ring in place of the more complex substituted quinuclidine and optimization of the quinine core to a considerably more lipophilic 2,8-disubstituted trifluoromethyl derivative. Despite its efficacy, MFQ is associated with severe adverse neurological effects, which limit its clinical use.[30, 31] Nowadays, MFQ is typically used as a prophylactic agent for travelers, when other antimalarial options are unavailable or ineffective, or in combination with another antimalarial drug for treatment (MFQ-artesunate, **Table 1**).[40] HF and LMF (**Figure 5**) were discovered a few years later. They are two antimalarial drugs structurally similar, highly lipophilic, and also active against all blood forms of *Plasmodium*. The most significant difference between these drugs is that HF is highly cardiotoxic and, therefore, is no longer used in the clinic, while LMF does not have cardiac side effects and is currently used in combination with another antimalarial for the treatment of uncomplicated malaria (LMF-artemether, **Table 1**).[30, 31, 41]

8-Aminoquinolines

The two quinoline subclasses above described possess activity mainly against blood forms of *Plasmodium*, acting as blood schizonticides. In contrast, 8-aminoquinolines (8-AQs) stand as the only class of antimalarials available in clinics that act as tissue schizonticides and hypnozonticides, i.e. acting against liver forms of the malaria parasite, including the latent ones formed by some *Plasmodium* species. Additionally, their gametocytocidal properties against all human malaria species enable them to disrupt the transmission cycle between humans and mosquitoes.[42] PQ (**Figure 5**) was the first 8-AQ approved for medical use and is still a success in treating relapses of *P. vivax* and *P. ovale* malaria (**Table 1**). Despite its efficacy, PQ has low oral bioavailability and is highly hemotoxic in patients with glucose-6-phosphate dehydrogenase (G6PD) deficiency, which limits its clinical application.[30, 31, 43, 44] Thus, continuous efforts to develop 8-AQ analogs with better pharmacological and reduced toxicological profiles have been made, which led to the discovery of TQ (**Figure 5**), an 8-AQ with higher efficacy due to its superior pharmacokinetic properties. TQ was recently approved for use in prophylaxis or radical cure of relapsing *P. vivax* and *P. ovale* infections and is likely to replace PQ in future treatment regimens. However, TQ is also hemotoxic and, like PQ, cannot be used in certain risk groups of the population.[45-48]

With the exception of 8-AQs, the remaining compounds of the quinoline class act as blood schizonticides, and are reported to share a common therapeutic target, the parasite-specific substance hemozoin, although other targets may also be involved in some cases.[35]

During the blood stage of the *Plasmodium* life cycle, the malaria parasite consumes large quantities of hemoglobin (Hb) from its host cell through the endocytosis process. The vesicles containing Hb are transported to the parasite's digestive vacuole (DV), an acidic lysosome, where the Hb is degraded by the parasite as a source of amino acids required for its maturation and growth. Aspartic proteases (plasmepsins I-IV) and cysteine proteases (falcipains) are involved in Hb hydrolysis leading to the release of globin moieties that are further degraded into peptides to provide amino acids for protein synthesis. However, Hb degradation leads to the release of free heme [Fe(II)PPIX], which is toxic for the parasite due to its generation of reactive oxygen species (ROS) that cause oxidative stress and thereby membrane and DNA damage. To reduce this toxicity, the free heme is quickly oxidized by the parasite to form reactive Fe(III)PPIX which is then converted into a non-toxic and insoluble crystal known as hemozoin (Hz), that accumulates in the DV.[30, 35, 49]

The antimalarial activity of the quinoline-containing compounds acting as blood schizonticides seems to correlate with the inhibition of Hz formation. The weak base character of 4-AQs explains their selective accumulation in the DV. Their uncharged forms diffuse freely into acidic compartments, like the *P. falciparum* DV, where they protonate and become trapped. Once inside the DV, the compounds bind to the free heme to form a drug-heme complex, disrupting the detoxification process involved in the formation of inert Hz. Therefore, the level of toxic free heme increases leading to parasite death.[50, 51] However, the mechanism(s) of action (MoA) by which quinoline antimalarial drugs target heme is still a topic under discussion. Also, it is not yet well understood whether the different quinolines inhibit Hz formation via similar or different pathways. Several studies suggest that they may inhibit Hz crystallization by binding to the free heme monomer, the μ-oxo dimer, or the Fe-O41 reciprocal "head-to-tail" dimers, or by acting as capping molecules on Hz crystal faces. Moreover, multiple quinolines can bind simultaneously to heme molecules through π-π stacking interactions between the quinoline ring and the porphyrin ring system of heme, as well as electrostatic interactions between charged groups.[52] Even though the main MoA of these compounds appears to be inhibition of the Hz crystals formation, other possible targets have also been identified, especially in the case of aryl-aminoalcohols. Quinolines may also act through (i) accumulation of Hb in endocytic vesicles,[53] (ii) induction of morphologic changes in DV membrane,[50] (iii) inhibition of cysteine proteases[54] and (iv) inhibition of nucleic acid and protein synthesis.[50, 55]

On the other hand, the antimalarial activity of quinoline-containing compounds acting as tissue schizonticides and hypnozonticides (8-AQs) is not yet fully understood. It is believed that the metabolism within the parasite's mitochondria is disrupted, eventually by interference with the ubiquinone function. A recent study suggested that the more plausible MoA of 8-AQs is related to the generation of ROS through the cycling of hydroxylated metabolites.[45, 56, 57]

1.4.3. Endoperoxides

Endoperoxides are a structural class of compounds developed in an attempt to address some limitations of earlier antimalarials, representing a significant advancement in the treatment of malaria. Artemisinin (ART, **Figure 5**) was the first natural endoperoxide-containing compound extracted from the plant *Artemisia annua*, an herb that was commonly used in Chinese traditional medicine as a remedy for fevers and chills. ART is highly potent against blood forms of *P. falciparum*. Despite its antimalarial efficacy, ART has some limitations such as low oral solubility, poor bioavailability, and short half-

life *in vivo*.[29] To overcome these issues, researchers developed semi-synthetic and fully synthetic derivatives with improved pharmacokinetic properties and efficacy. The most used ones are artemether (AT), artesunate (AS), and arteether (**Figure 5**). These semi-synthetic derivatives of ART act as prodrugs that are transformed into the active ART metabolite, dihydroartemisinin (DHA). Importantly, due to the high clearance rate of ART and of its derivatives, these compounds are currently combined with other antimalarial drugs, such as AQs, that have extended half-lives (**Table 1**).[30, 31]

The MoA(s) of endoperoxide antimalarials remain unclear, even though they are most likely associated with the endoperoxide bridge (1,2,4-trioxane), the key structural feature of all ART derivatives. One of the most accepted theories proposes that ART and its derivatives act via a two-step mechanism: ART is first activated by Fe(II)PPIX, a side-product of Hb digestion present in high amounts inside the parasite that catalyzes the cleavage of this endoperoxide; as a result of this cleavage, ROS are produced that further rearrange into carbon-centered radicals, which cause damage to specific cellular targets through alkylation.[30, 51, 58, 59] Still, several other potential targets of ART and derivatives have been proposed such as P-type ATPases, phosphatidylinositol-3-kinase, and the respiratory chain in mitochondria.[58, 60, 61]

1.4.4. Antifolates, naphthoquinone, and antibiotics

Antifolates are a class of drugs that target specific enzymes responsible for the synthesis or conversion of folate derivatives, which play a crucial role in DNA synthesis. By disrupting folate metabolism, these drugs inhibit the growth and reproduction of the parasite, eventually leading to its death. Proguanil (**Figure 5**) was the first antifolate with reported activity against erythrocytic stages of all *Plasmodium* species pathogenic to humans. Shortly afterwards, and based on the proguanil structure, another antifolate drug, pyrimethamine (**Figure 5**), was advanced as a very effective and safe antimalarial with a good pharmacokinetic profile. Both proguanil and pyrimethamine target the dihydrofolate reductase (DHFR) activity of the parasite's bifunctional DHFR-thymidylate synthetase protein, acting as competitive inhibitors of the enzymes' natural substrates.[30] Currently, pyrimethamine and proguanil are used in a synergistic combination with sulfadoxine (**Figure 5**), another antifolate, and atovaquone (**Figure 5**), a naphthoquinone, respectively, for chemoprevention of malaria in pregnancy, young children and travelers[62] or for treatment of *P. falciparum* infections (Sulfadoxine-Pyrimethamine (SP) and Proguanil-Atovaquone, **Table 1**).[29, 31] Sulfadoxine is a sulfonamide derivative that inhibits the dihydropteroate synthetase (DHPS) activity of the bifunctional hydroxymethylpterin pyrophosphokinase (HPPK)-DHPS protein. Compared

to pyrimethamine, sulfadoxine has a longer half-life and an improved toxicological profile. In turn, atovaquone is the only antimalarial naphthoquinone used in the clinic; it acts as a cytochrome *bc*1 complex inhibitor, blocking mitochondrial electron transport and thus interfering with the exoerythrocytic and erythrocytic stages of malaria parasites.[31]

Noteworthy, besides the aforementioned classes of antimalarial compounds that were specifically designed to target *Plasmodium* parasites, broad-spectrum tetracycline antibiotics such as doxycycline, have also shown effectiveness as a prophylactic agent.[63] Doxycycline (**Figure 5**, **Table 1**) attacks the parasite by interfering with protein synthesis during the blood phase of the parasite's life cycle. This drug acts in the essential apicoplast organelle, specifically blocking the genome expression and protein translation, which results in the distribution of nonfunctional apicoplasts into daughter merozoites and consequently to a slow but potent antimalarial effect. Nowadays, doxycycline is used in combination with quinine for the treatment of both uncomplicated and severe malaria, or as a single drug as a chemoprevention measure.[64]

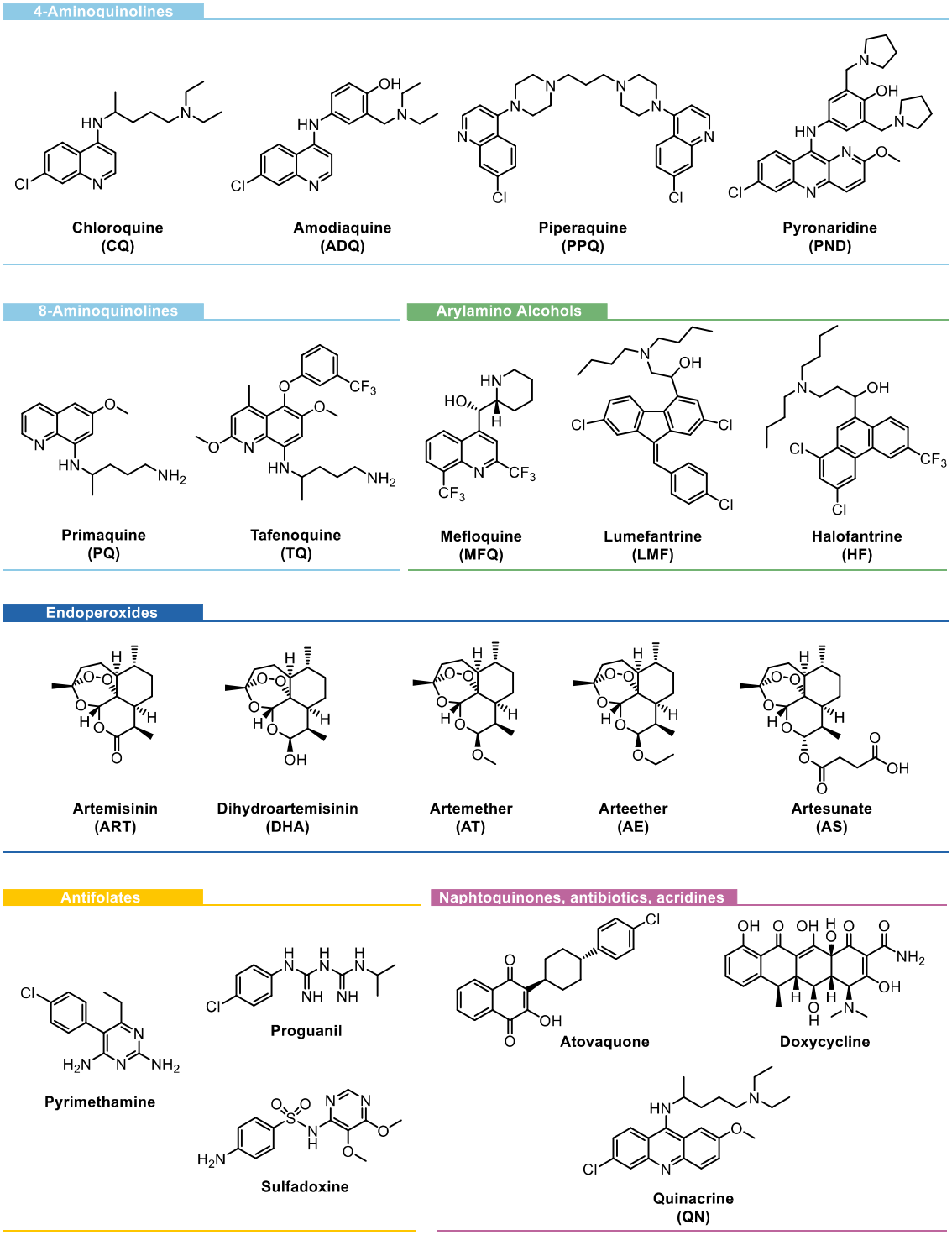


Figure 5. The main classes of antimalarial drugs developed so far and introduced in the clinic, most of them still recommended by WHO, as described in **Table 1.**

Most of the antimalarials previously described are included in the current WHO Model List of Essential Medicines, which comprises 14 medicines for curative and 6 medicines for prophylactic treatments.[65] According to the most recent WHO recommendations, some medicines are formulated as a single compound while others are used in combination, as depicted in **Table 1.** The dosing therapies depend on the geographic location of the infection, the *Plasmodium* species, and the severity of the clinical condition.[65, 66]

Drugs for chemoprevention aim to prevent infection in, for example, high-risk groups such as non-immune travelers, and pregnant women and children living in endemic countries. The first group refers to people not previously exposed to the parasite, who should initiate treatment before entering endemic areas to prevent severe malaria. In the case of pregnant women and children, the WHO recommends three main different strategies: (i) intermittent preventive treatment in pregnancy (IPTp), which is given during antenatal care starting in the 2nd trimester; (ii) intermittent preventive treatment in infants (IPTi), given to children under 5 years old; and (iii) seasonal malaria chemoprevention (SMC) specifically for Sub-Saharan Africa children during the period of greatest risk (rainy season).

Regarding chemotherapy, ACTs are the current first-line treatment for uncomplicated malaria, especially in endemic areas where *P. falciparum* is prevalent. To prevent relapses in *P. vivax* and *P. ovale* infections, PQ is also administered. In severe cases of malaria, adults and children are usually treated with intravenous or intramuscular AS or AT. Once the patient can tolerate oral therapy, the treatment is continued with ACT. [1, 66-68] ACTs combine a short-acting ART derivative (AT, AS, or DHA) with one complementary long-acting drug (ADQ, MFQ, PPQ, LMF, or PND). The two drugs must have different MoA(s) and unrelated structures, as well as display well-matched pharmacokinetic and pharmacodynamic profiles. These combination therapies benefit from the ability of ART and derivatives to rapidly reduce the parasite biomass leading to a rapid clinical response and a rapid relief of symptoms. The few remaining parasites that have not been cleared by ART will be eliminated by the long half-life partner drug.[69]

Table 1. Summary of WHO recommendations for the prophylaxis and treatment of uncomplicated and severe malaria based on the current WHO Model List of Essential Medicines 2023.[65, 66]

Chemoprophylaxis

General Indications	*P. vivax* and *P. ovale*
Amodiaquine + Sulfadoxine-Pyrimethamine (SMP)	Chloroquine
Sulfadoxine-Pyrimethamine (IPTp/IPTi)	Primaquine
Proguanil + Chloroquine*	
Mefloquine	
Doxycycline	

* for use in regions where parasites are still susceptible to CQ

Chemotherapy

Uncomplicated malaria

General Indications	*P. vivax* and *P. ovale*
ACTs - Artesunate + Amodiaquine - Artesuntate + Mefloquine - Arthemether + Lumefantrine - Artesunate + Sulfadoxine-Pyrimethamine - Artesunate + Pyronaridine - Dihydroartemisinin + Piperaquine	Chloroquine Primaquine
Atovaquone - Proguanil	
Quinine + doxycycline*	

* for use in recurrent malaria *P. falciparum* infection

Severe malaria

General Indications		
Artesunate	Artemether	Quinine + Doxycycline

2. The need for novel antimalarials

Despite the existence of effective antimalarials in the clinic, parasites and mosquito vectors have demonstrated a persistent ability to evolve mechanisms to circumvent the available arsenal for malaria control. This ongoing adaptative evolution is the main reason why malaria control and/or eradication remains a significant challenge.[70]

According to the WHO, resistance has been defined as the ability of a parasite strain to survive and/or multiply despite the adequate administration and absorption of medicine given in the dose normally recommended.[71] In general, drug resistance appears to be caused by a change in the structure, function, or quantity of a target protein. These changes occur through spontaneous single or multiple genetic mutations or gene amplifications that confer reduced susceptibility to the antimalarials. The development of drug resistance is influenced by factors such as transmission in specific geographical areas, levels of immunity, parasite load, and the pharmacokinetic-pharmacodynamic properties of the drugs used. Besides, resistance may also arise due to incorrect drug dosage, use of cheap and poor-quality counterfeit drugs, and self-medication.[72]

The first well-documented case of antimalarial drug resistance was reported for CQ in the late 1950s and early 1960s in Southeast Asia, specifically in regions like Cambodia and Thailand, where *P. falciparum* was prevalent.[73] Over the years, CQ-resistant strains of *P. falciparum* spread to other parts of Asia, Africa, and South America. The spread of resistant parasites significantly compromised the effectiveness of CQ as a treatment for malaria, which increased morbidity and mortality worldwide.[74] This event marked a turning point in malaria treatment, leading to the pursuit of alternative antimalarial drugs. Despite the efforts since then, as represented in **Figure 6**, this problem expanded to most of the antimalarial drugs developed, which consequently led to an increase in mortality and morbidity.[70] The discovery of ART, during the 1990s, followed by the introduction of ACTs in 2005 created a new hope in controlling and eradicating malaria. However, resistance to ART has also emerged in several malaria-endemic regions, first in the Greater Mekong Subregion (GMS) of Southeast Asia, and subsequently in South America, Papua New Guinea, and Eastern Africa.[75, 76] In the GMS, the decreased susceptibility to ART exposed its partner drugs, causing the emergence of resistance to them as well, which consequently led to high rates of ACT failure.[77] The major concern revolves around the risk of ACT resistance spread to regions such as Myanmar, Bangladesh, India, and all sub-Saharan Africa, similar to the previous spread of resistance to CQ that contributed to millions of malaria-related deaths, mainly in African children.[75, 78] To date, resistance to ACT partner drugs has not been confirmed in Africa,

and the treatment remains highly efficacious. However, given the heavy reliance on ACTs in Africa, full-blown treatment failure could have very serious consequences. Until new antimalarials become available, triple ACTs, which combine artemisinin and two existing partner drugs, are being employed to delay the emergence and spread of resistant parasites to ACTs.[79-82]

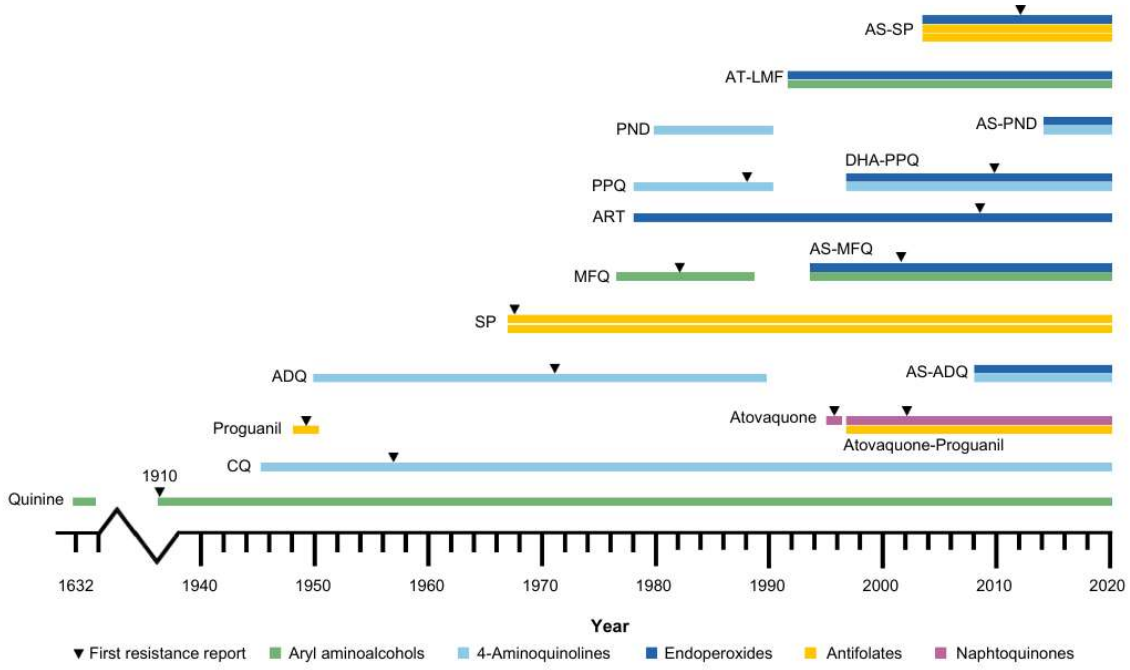


Figure 6. History of the introduction of the principal antimalarials and the first emergence of resistance in the field (Figure designed using Canva). Legend: Single bars refer to monotherapies; double- and triple-bar boxes denote combination therapies. Colors refer to the chemical classes to which the antimalarials belong. CQ – Chloroquine, ADQ – Amodiaquine, AS-ADQ – Artesunate-Amodiaquine, SP – Sulfadoxine-Pyrimethamine, MFQ – Mefloquine, AS-MFQ – Artesunate-Mefloquine, ART – Artemisinin, PPQ – Piperaquine, DHA-PPQ – Dihydroartemisinin-Piperaquine, PND – Pyronaridine, AS-PND – Artesunate-Pyronaridine, AT-LMF – Artemether-Lumefantrine, AS-SP – Artesunate+Sulfadoxine-Pyrimethamine.[21]

This emergence and spread of multidrug-resistant parasites, including to current first-line treatments, highlights the ongoing challenge of combatting malaria. In anticipation of complete failure of ACTs, it becomes extremely important to quickly develop novel and inexpensive antimalarial drugs for their replacement. Notably, most of the malaria chemotherapy arsenal available today targets the blood stage of the malaria parasite life cycle, the symptomatic phase responsible for the morbidity and mortality associated with this disease. However, tissue schizonticides and hypnozonticides, which act against all liver forms of *Plasmodium*, including the dormant ones, and gametocytocidal drugs, which prevent transmission, are also important to achieve radical cure.[83] Indeed,

according to the Medicines for Malaria Venture (MMV), an organization dedicated to the discovery and development of new medicines, future antimalarial treatments need to cure the disease efficiently, by rapid clearance of asexual blood-stage parasitemia in patients (Target Candidate profile (TCP)-1), blocking transmission between human and mosquito (TCP-5 and TCP-6), and eliminating all liver forms of the parasite including dormant hypnozoites (TCP-3 and TCP-4). Ideally, these new medicines should possess new MoA(s) and good pharmacokinetic properties to reduce the risk of resistance emergence and allow for single-dose administration to increase compliance. Moreover, given that malaria cases are prevalent in tropical regions, the medicines need to be chemically stable in high temperatures and humid environments and, ultimately, must exhibit favorable tolerance in the risk groups: children below the age of 5 and pregnant women.[83-85] In order words, the Target Product Profiles (TPP-1 and TPP-2) proposed by MMV emphasize that the most feasible option to control and eliminate malaria goes through the development of a multi-stage antimalarial drug, capable of targeting more than one process in the parasite life cycle and therefore reducing the probability of emergence of resistant parasites (**Figure 7**). This shift in the strategy for malaria drug development from single- to multi-stage compounds may offer several advantages. When compared to single-stage drugs, multi-stage drugs may likely have improved effectiveness in preventing or treating the disease as a result of targeting more than one process in the pathogen's life cycle. They may lead to a faster clearance of the infection and provide a broader spectrum of activity, effectively addressing various strains of a pathogen. Both characteristics are crucial in drugs used to treat infectious diseases such as malaria, for which a rapid response is essential to prevent complications and the spread of the disease, and the pathogen exhibits genetic diversity. However, one of the main reasons behind the relevance of multi-stage drugs, is that they diminish the likelihood of selection of resistant strains, as the resistance to a drug that acts simultaneously on multiple targets would require the unlikely event of concurrent mutations appearing in multiple protein targets or genes. Conversely, a drug that hits a single target is more prone to induce resistance by, e.g., mutations in such target. Additionally, when compared to ACT, the use of one single multi-stage drug may avoid side effects arising from drug-drug interactions and the dosing regimen is also relatively simpler, thereby improving patients' compliance.[86, 87] Overall, the development and use of multi-stage drugs have been regarded as a more sustainable and durable treatment option that, combined with the increased use of bed nets and insecticides and the promise of an efficient vaccine, may lead to a significant reduction in the malaria burden.

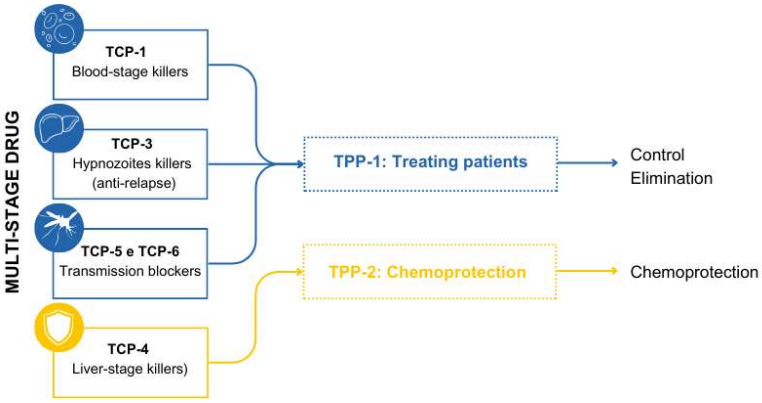


Figure 7. Summary of MMV's Target Product Profiles (TPPs) and Target Candidate Profiles (TCPs) for malaria medicines to control, eliminate, and eradicate malaria.[84]

3. Approaches for discovering multi-stage antimalarials: from traditional approaches to the covalent bitherapy concept

There are several strategies for the development of novel antimalarial drugs, the most traditional ones comprising *in silico* (virtual) and *in vitro* (experimental) screening of known structures, as well as rational chemistry-based approaches.[83, 88]

Virtual screening predicts bioactive compounds through computational structure- or ligand-based methods, which use the knowledge of the 3D structure of the biological target, typically a protein, or the structure of compounds exhibiting the desired activity, respectively. Virtual screening relies on receptor-ligand interactions, and therefore is limited by the substantial gap in our understanding of the biology of malaria parasites. *In vitro* screening, such as that employing high-throughput methods, is another approach that involves systematically testing large libraries of chemical compounds to identify those active against the parasite through "whole-cell" or "target-based" approaches. In the whole-cell assay, a culture of the whole parasite is exposed to the test compounds, whereas in the target-based approach, the compounds are only tested against specific therapeutic targets which are crucial for parasite survival. Although both strategies are powerful tools for the identification of new compounds, they are quite long and expensive processes to advance new candidates, since the hit compounds identified in such screenings invariably require further investigation and optimization to progress in the drug development pipeline.[83, 88] On the other hand, the rational chemistry-based approaches use the pharmacophores of known antimalarial drugs that have been successfully introduced in the clinic as a basis for new improved compounds. In this sense, these scaffolds are modified to optimize their therapeutic properties and to reduce limitations to their use such as resistance and bioavailability using SAR studies and whole-cell or biochemical assays.[83, 88, 89] Although this approach has been successful over the years and given rise to a wide range of chemical compounds, the major limitation is that there is no model compound active against all stages of the parasite life cycle, therefore hindering the current goal of obtaining a multi-stage drug.

To speed up the antimalarial drug development process, while concomitantly pursuing multi-stage action, Meunier proposed the covalent bitherapy concept as a new rational-chemical approach of higher efficacy and lower cost compared to traditional strategies.[90-94] The pioneering contribution of Meunier in this regard was in malaria field and refers to

the trioxaquines (**Figure 8**), molecules comprising a trioxane motif covalently linked to an aminoquinoline entity. Among 120 molecules resulting from this study, the favorable *in vitro* and *in vivo* activity profile of trioxaquine **PA1103-SAR116242** (**Figure 8**) led to its selection as candidate for preclinical development and confirmation of this approach as a valuable tool in malaria drug discovery.[94-96] In the covalent biotherapy approach, two or more different pharmacophores with different MoAs are covalently linked to each other to form a new single entity. The resulting hybrid molecule is expected to display, at least, a dual mode of action by additive or even synergistic combination of the therapeutic properties of its parent scaffolds; in other words, the hybrid should be able to affect multiple targets simultaneously, consequently with greater effectiveness at lower doses and less vulnerability to resistance, compared to the parent individual drugs. Consequently, this strategy encloses the potential to offer significant benefits including a decreased chance of drug-drug interactions, which is frequent in combination therapies, lower cost, and improved patient compliance.[90, 91]

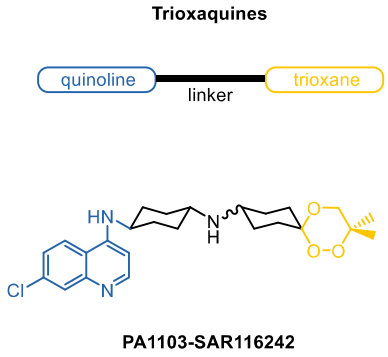


Figure 8. Meunier's pioneering contribution in applying the covalent bitherapy concept to antimalarials: trioxaquines as covalent conjugates of antimalarial quinolines and trioxanes; the structure of **PA1103-SAR116242**, a trioxaquine advanced as candidate for preclinical development, is also shown.[94-96]

Hybrids can be categorized into four main groups according to the nature of the linker: conjugates, cleavage conjugates, fused hybrids, and merged hybrids (**Figure 9**).[97] Typically, pharmacophores can be directly linked to each other by a stable covalent bond (e.g., amide, ether, thioether, among others) or through a linker which may also add a specific function (e.g., solubilizing moiety) to the final compound. The resulting molecules, called ***conjugates***, are markedly larger than the parent drugs, and often more lipophilic, and thus the linker must be as simple as possible. If the size of the linker is so small that the frameworks of the pharmacophores are essentially touching each other, the conjugates become classified as ***fused hybrids***. More recent approaches combine the hybrid and prodrug concepts, known as ***cleavage conjugates***, where the selective

cleavage of the linker triggers the release of the pharmacophores at the site of action. The ***merged hybrids*** have simpler and smaller molecular structures formed by merging the commonalities of parent drugs.[97]

The pharmacophores chosen for the hybrids' conception can be an entire drug or only the structural part of it that is responsible for therapeutic activity (pharmacophore). When the knowledge beyond the antimalarial activity of a compound is not fully understood, the best strategy involves the use of the entire drug with the desired activity. During this process, chemical modifications towards the improvement of the physicochemical and pharmacokinetic profiles of the resulting molecule are also taken into consideration.[87, 92] Thus, several hybrids comprising whole drugs, or parts of them, with multi-stage action, reduced toxicity, and improved activity as compared to the individual parent drugs, have been developed over the years.[90, 98, 99] The following section focuses on multi-stage antiplasmodial hybrids (conjugates and merged hybrids) that incorporate AQ scaffolds, which are amongst the most important in the malaria chemotherapy arsenal.

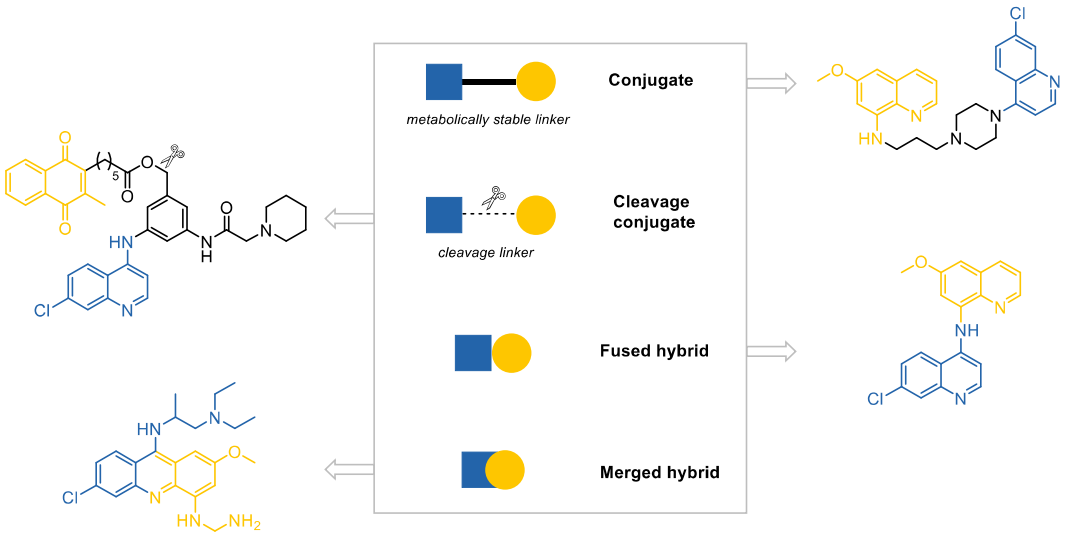


Figure 9. Classification of hybrids according to the nature of the linker: conjugate,[100] cleavage conjugate,[101] fused hybrids[100] and merged[102] hybrids, and examples of chemical structures of compounds representing antimalarial hybrids in each category.

4. Multi-stage antiplasmodial hybrids

4.1. Aminoquinoline-based conjugates

The quinoline core is considered one of the most valuable building blocks in malaria drug development history. Since the isolation of quinine from the bark of *Cinchona*, the quinoline moiety was the inspiration of the main part of antimalarial compounds developed to date, which includes 4-AQs, 8-AQs, and ACR.

4-AQs received much attention owing to the remarkable success of CQ, which exhibited great biological properties and was widely employed. Besides, other derivatives from this class, such as ADQ, is extensively used as a component of an ACT combination so far efficient. The 8-AQs, constituted exclusively by PQ and TQ, on the other hand, are the only class with the ability to kill all the hepatic forms of the parasite, including hypnozoites, and therefore are quite relevant as well. The ACR, while not as prominent in malaria history, possess an aromatic core that resembles the fusion between a 4-AQ and an 8-AQ, therefore offering an intriguing option to explore for multi-stage hybrids. In this sense, due to their unique features, in the last two decades, AQs emerged as a scaffold of choice to develop antiplasmodial hybrid compounds with dual- or multi-stage activity.[91, 98] To date, AQs have been linked to a diverse range of moieties with different activities, as next described, to obtain a multi-stage candidate with improved efficiency and pharmacokinetic-pharmacodynamic properties.[103, 104]

4.1.1. AQ-AQ conjugates

The conjugation of the two well-known AQs targeting different stages of the *Plasmodium* life cycle was one of the simpler and first strategies explored for obtaining multi-stage compounds with enhanced activities and pharmacodynamic-pharmacokinetic profiles. In this sense, Lödige *et al.* hypothesized that the combination of CQ and PQ scaffolds might lead to an increase in PQ's half-life and consequently allow to decrease dosage/frequency of administration, therefore reducing the levels of potentially harmful metabolites; moreover, its conjugation to CQ might as well decrease the risk of CQ-induced development of resistant parasites.[100, 105] The authors tested different types of linkage between the heteroaromatic pharmacophores of both drugs: PQ's side chain linker (**1a**), a piperazine diamine (**1b-c**) or diamide (**1d-e**) linker, an aromatic linker (**1f**), and no linker at all (**1g**) (**Figure 10**). Hybrids retained the activity of the parent drugs since they displayed multi-stage activity against the pathogen. Conjugate **1a** was the most promising, exhibiting low micromolar activity against asexual blood stages of CQ-sensitive 3D7 and CQ-resistant K1 and Dd2 *P. falciparum* strains (3D7: IC_{50}(**1a**) = 0.64

± 0.046 μM; IC_{50}(PQ)= 3.11 ± 1.536 μM, IC_{50}(CQ)= 0.03 ± 0.002 μM; Dd2: IC_{50}(**1a**) = 0.58 ± 0.185 μM, IC_{50}(PQ)= 1.12 ± 0.351 μM, IC_{50}(CQ)= 0.26 ± 0.126 μM; K1: IC_{50}(**1a**) = 0.08 ± 0.0048 μM, IC_{50}(PQ)= 0.46 ± 0.08 μM, IC_{50}(CQ)= 0.146 ± 0.02 μM). Moreover, **1a** showed an inhibitory effect against gametocytes of *P. falciparum* with a % gametocytemia of 0.7 ± 0.04, which was slightly superior to that of CQ but inferior to that of PQ (% gametocytemia (CQ) = 0.9 ± 0.07; % gametocytemia (PQ) = 0.2 ± 0.05). The *in vitro* inhibitory activity against the development of liver-stage *P. berghei* was similar to that of PQ. These findings were validated *in vivo*, where **1a** elicited activity against liver and blood stages of *P. berghei* ANKA in mice, prevented blood-stage patency, and was therapeutic to the symptoms of experimental cerebral malaria.[100, 105]

Years later, Pereira *et al.* reported the linkage of two AQs by coordination to gold(I), which was reported as having inhibitory activity of the thioredoxin reductase of *P. falciparum*, an enzyme essential for the parasite's survival.[106, 107] Conjugates **2** and **3**, which connected PQ and CQ or PQ and ADQ, respectively, exhibited potent dual-stage activity (**Figure 10**). Both hybrids were active against blood forms of *Plasmodium*, especially against the CQ-sensitive 3D7 strain, and liver forms of *P. berghei* (3D7: IC_{50}(**2**) = 27.7 ± 3.9 nM, IC_{50}(**3**)= 35.5 ± 2.1 nM, IC_{50}(CQ) = 18.0 ± 1.7 nM, IC_{50}(ADQ) = 18.0 ± 1.6 nM, IC_{50}(PQ) = 1117 ± 53 nM; W2: IC_{50}(**2**) = 166 ± 25.7 nM; IC_{50}(**3**)= 2.97 ± 0.96 nM, IC_{50}(CQ) = 460 ± 17.4 nM, IC_{50}(ADQ) = 86.2 ± 9.4 nM, IC_{50}(PQ) = 182.3 ± 18.9 nM). Conjugate **3** was additionally tested against young and mature gametocytes and found to be highly potent as well (early gametocytes: IC_{50}(**3**) = 0.035 ± 0.01 μM; IC_{50}(PQ) = 13.7 ± 7.6 μM; IC_{50}(ADQ) = 0.061 ± 0.02 μM; mature gametocytes: IC_{50}(**3**) = 9.5 ± 3.1 μM; IC_{50}(PQ) = 43.2 ± 10.6 μM; IC_{50}(ADQ) = 23.6 ± 5.0 μM). In the experimental malaria infection model, the conjugates exhibited superior efficacy in suppressing the onset of infection compared to references CQ/ADQ and PQ and even to a 1:1 combination of 8-AQ/4-AQ. This confirmed the great potential of covalently binding two bioactive pharmacophores to each other, towards development of novel multi-stage antimalarials.[106, 107]

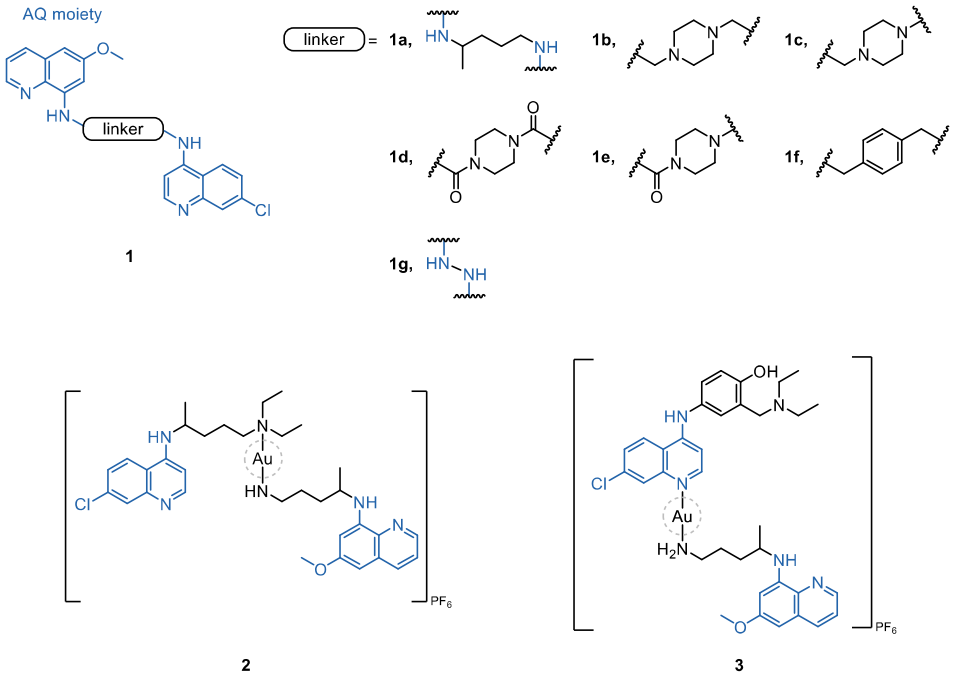


Figure 10. PQ-CQ conjugates developed by Lödige *et al.*[100, 105] (**1a-g**) and Pereira *et al.* (**2, 3**).[106, 107]

4.1.2. AQ-Endoperoxide conjugates

ART and its derivatives are highly effective antimalarials and particularly useful against strains of *P. falciparum* resistant to other agents, which makes them an interesting scaffold for combining with AQs to produce multi-stage hybrids.[108] Based on this, Capela *et al.* evaluated the combination of the 8-AQ PQ to ART against liver and blood stages, both *in vitro* and in animal models of malaria.[109] The two hybrids synthesized in this work differ in the linker used to connect both moieties (**4** and **5**, **Figure 11**). Compared to parent compounds, both hybrids displayed significantly enhanced *in vitro* activities against liver stages of *P. berghei* (IC_{50}(**4**) = 155 nM, IC_{50}(**5**) = 523 nM, IC_{50}(ART+PQ) = 9714 nM). In the blood stage, they displayed activities similar to ART against blood forms of *P. falciparum* (IC_{50}(**4**) = 12.5 ± 1.1 nM; IC_{50}(**5**) = 9.1 ± 0.6 nM; IC_{50} (ART) = 8.2 ± 0.9 nM). Additional *in vivo* experiments demonstrated that hybrid **4** is quite efficient in controlling parasitaemia.[109]

As an alternative to AQ-ART conjugates, the same authors extended their studies towards hybrid compounds containing the 8-AQ and full synthetic endoperoxides (1,2,4-trioxane or 1,2,4,5-tetraoxane).[110] The endoperoxide motif present in ART is reported as responsible for its antiplasmodial activity due to being reductively activated by iron(II) in heme to form carbon-centered radicals capable of reacting with heme and proteins. All conjugates, which only differ in the nature (amide or amine) and length of the linker, showed high potency against both exoerythrocytic and erythrocytic forms of malaria

parasites. From the set, conjugate **6** (**Figure 11**), an AQ-tetraoxane hybrid with an amide linker between the two pharmacophores, stood out for (i) its promising dual-stage activity *in vitro* (blood-stage, CQ-resistant W2 strain: IC_{50}(**6**) = 21.1 nM, IC_{50}(ART) = 8.2 nM, IC_{50}(PQ) = 3300 nM; liver-stage: IC_{50}(**6**) = 538 nM, IC_{50}(PQ) = 7500 nM), (ii) its ability to irreversibly clear parasitemia from *P. berghei*-infected mice and (iii) its transmission-blocking activity on *P. berghei*-infected ANKA *Anopheles gambiae* mosquitoes.[110]

Despite all the above, conjugate **6** displayed high metabolic susceptibility in rat liver microsomes ($t_{1/2}$ = 10 min). Based on this, the authors explored another series of AQ-tetraoxane conjugates, with an aryl or heteroaryl group installed at the metabolically labile C-5 position of the 8-AQ moiety.[111] 5-Hydroxy-8-AQ are thought to be the metabolites responsible for the hemolytic toxicity associated with 8-AQ, and thus blocking C-5 may offer the opportunity to increase the compound's half-live and overcome toxicity issues. As expected, the compound's metabolic stability was quite improved in the conjugates containing an aryl substituent at C-5 of the 8-AQ moiety, and the dual-stage activity against blood forms of the CQ-resistant *P. falciparum* W2 strain and liver forms of *P. berghei* were retained. Conjugate **7** (**Figure 11**) showed the most promising profile (IC_{50}(W2) = 0.045 ± 0.002 μM; IC_{50}(*P. berghei*) = 2.11 ± 0.13 μM; $t_{1/2}$ = 37 min).[111]

Benoit-Vical *et al.* also explored the combination of synthetic endoperoxides and AQs, named trioxaquines.[112] In this case, the authors developed conjugates containing the 4-AQ and the trioxane motifs, which were shown to be highly potent against (i) erythrocytic stages of CQ-sensitive and CQ-resistant strains of *P. falciparum in vitro*, (ii) *P. vinckei petteri* and *P. yoelii nigeriensis* strains in suppressive and curative murine *in vivo* tests, and (iii) early and late gametocytes *in vitro*. Moreover, no toxicity was observed either on cell lines or in mice. Conjugate **8** (**Figure 11**) was the most promising one, with IC_{50} values in the nanomolar range against blood forms of *P. falciparum* and gametocytes, in some cases much better than the references (blood-stage: IC_{50}(**8**) = 4 - 23 nM, IC_{50}(CQ) = 25 – 180 nM, IC_{50}(ART) = 6 – 8 nM; gametocytocidal-stage: IC_{50}(**8**) = 67 - 69 nM, IC_{50}(PQ) = 1320 – 4580 nM).[112]

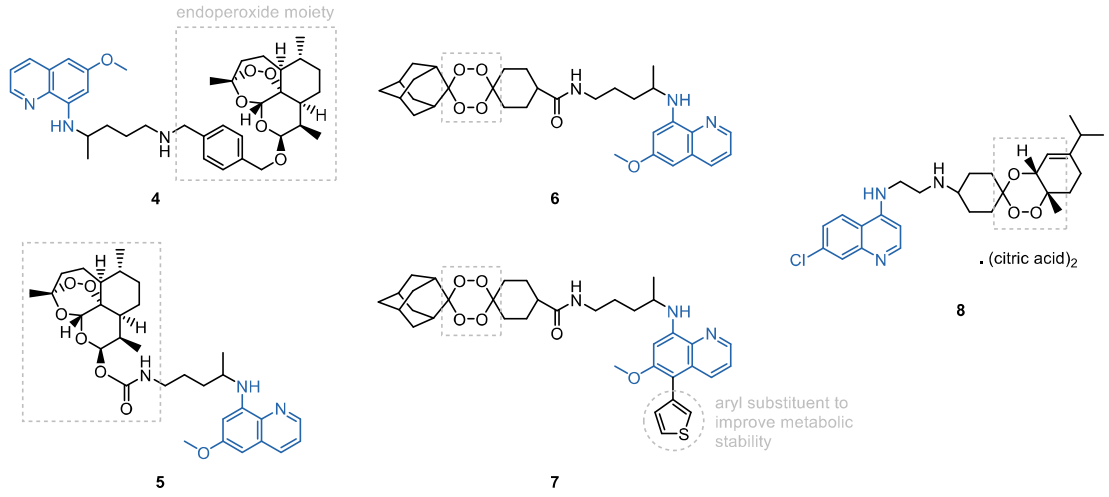


Figure 11. AQ-Endoperoxide conjugates developed by Capela *et al.*[109-111] (**4-7**) and by Benoit-Vical *et al.* (**8**).[112]

4.1.3. AQ-Cinnamic acid conjugates

Besides their combination with other well-known antimalarial drugs, AQs have been linked to other types of pharmacophores that are not in use as individual drugs but have reported effects on essential pathways for parasite survival. One of the first studies in this context was conducted by Pérez *et al.*, which demonstrated the value of *trans*-cinnamic acids (CA) as valuable building blocks for boosting the effectiveness of established antimalarials like CQ and PQ.[113, 114] The antimalarial potential of CAs was first advanced by Kanaani and Ginsburg in 1992, based on their ability to, in *Plasmodium* parasites, (i) reduce energy production by inhibition of lactate transporters, (ii) decrease the translocation of amino acids and carbohydrates, and (iii) change mitochondrial respiration. Besides, the cinnamoyl group has a vinyl carbonyl moiety that can act as a Michael acceptor, enclosing the potential to inhibit parasitic cysteine proteases involved in hemoglobin degradation (falcipains).[115, 116] Based on these observations, the authors reported the synthesis and SAR analysis of an expanded series of CQ- and PQ-CA conjugates.[117, 118] The CQ-CA series showed remarkable dual-stage activity against both blood- and liver-stage malaria parasites *in vitro*, better than those of the reference drugs for each stage. The SAR study suggested that a single substituent (R) on the cinnamoyl group, a butyl spacer, and an amide linkage between the heterocyclic core of CQ and the cinnamoyl group were essential for higher activities. In this sense, conjugates **9a** and **9b** (**Figure 12**) were the most potent and less toxic against the CQ-sensitive 3D7 and CQ-resistant W2 *P. falciparum* strains and liver-forms of *P. berghei* (3D7: IC_{50}(**9a**) = 15.63 ± 5.4 nM, IC_{50}(**9b**) = 26.21 ± 2.0 nM, IC_{50}(CQ) = 52.45 nM; W2: IC_{50}(**9a**) = 11.0 ± 6.2 nM, IC_{50}(**9b**) = 11.6 ± 0.4 nM, IC_{50}(CQ) = 138 nM; liver-stage: IC_{50}(**9a**) = 2.50 ± 0.2 µM, IC_{50}(**9b**) = 1.44 ± 0.3 µM, IC_{50}(PQ) = 7.5 µM). Further studies of these two

compounds with the rodent malaria model confirmed that **9b** had *in vivo* antimalarial activity against blood-stage parasites, however, lower than might be expected based on *in vitro* data, possibly because of bioavailability issues.[117]

Regarding the PQ-CA series, conjugate **10** (**Figure 12**), containing a *para*-isopropyl (iPr) substituent in the cinnamoyl group, was five-fold more potent *in vitro* than PQ against hepatic stage *P. berghei* infection and was non-toxic to Huh7 human hepatoma cells. However, in the erythrocytic stage, its activity against the CQ-resistant *P. falciparum* strain W2 was not better than that of the reference ART (liver-stage: IC_{50}(**10**) = 1.54 ± 0.35 μM, IC_{50}(PQ) = 7.50 μM; blood-stage: IC_{50}(**10**) = 4.84 μM, IC_{50}(ART) = 5.64 nM).[118]

Considering previous results, the same authors decided to investigate more deeply the importance of the cinnamoyl group for antimalarial dual-stage activity. In this context, they developed a series of *N*-acylated CQ conjugates, in which the cinnamoyl group was replaced by alkanoyl groups of various lengths, including linear, branched, and fluorinated groups, or by nonaromatic α,β-vinylcarbonyls.[119] Overall, the new *N*-acylated analogs were found to be somewhat less active and more cytotoxic than their *N*-cinnamoylated counterparts. However, they equally displayed nanomolar activities *in vitro* against CQ-sensitive and CQ-resistant *P. falciparum* strains, and significant *in vitro* liver-stage activity against *P. berghei*. From the set, conjugate **11** (**Figure 12**) stood out for being 4- to 18-fold better than CQ against blood forms and slightly better than PQ against liver forms (Blood-stage: IC_{50}(**11**): 5.30, 27.0, and 12.3 nM against 3D7, Dd2, and W2, respectively; IC_{50}(CQ): 21.0, 108, and 226 nM against 3D7, Dd2, and W2, respectively; Liver-stage: IC_{50}(**3**) = 5.6 μM, IC_{50}(PQ) = 7.5 μM).[119]

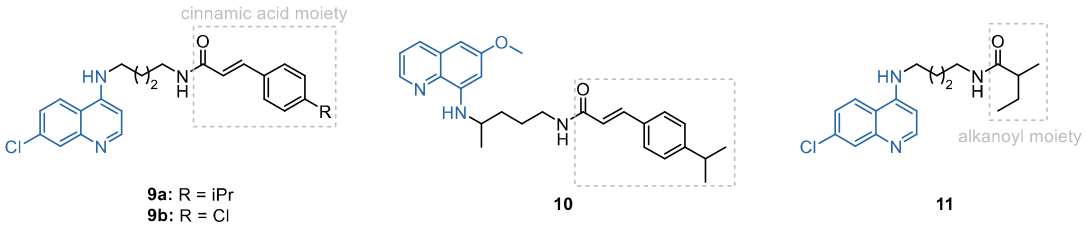


Figure 12. AQ-CA conjugates developed by Pérez *et al.*[117, 118] and Gomes *et al.* (**9-11**).[119]

4.1.4. AQ-Triazole conjugates

The 1,2,3-triazoles are equally interesting scaffolds in antimalarial drug development, not only due to their numerous biological activities, but also because they are nitrogen-containing heterocycles that, due to their lipophilic properties and overall basicity, tend to accumulate in the DV of the parasite and inhibit Hz formation therein.[120-122] In this context, Wadi *et al.* designed hybrid compounds wherein the 1,2,3-triazole moiety was

connected to the CQ core by an aliphatic diamine linker adjacent to a carbonyl group.[123] Overall, these hybrids exhibited dual-stage activity against asexual and sexual blood forms of the malaria parasite with little or no cytotoxicity. Moreover, *in vitro* screening revealed that this antimalarial activity is favored by a shorter aliphatic diamino-linker and a halogen at the *para*-position of the phenoxy group. The best conjugate containing these features (**12**, **Figure 13**) was active in the nanomolar range against the CQ-sensitive and the CQ-resistant 3D7 and RKL-9 *P. falciparum* strains, respectively, being 39-fold more potent than the reference CQ against the latter (3D7: IC_{50}(**12**) = 40.0 nM, IC_{50}(CQ) = 5.8 nM; RKL-9: IC_{50}(**12**) = 2.94 nM, IC_{50}(CQ) = 114.4 nM). Additionally, **12** was shown to target mature gametocytes and induce morphological deformations in them with an IC_{50} value of 19.80 μM.[123]

As a follow-up to this work, years later, Huang *et al.* developed another series of hybrids binding the 1,2,3-triazole moiety to a 4-pyridylvinylquinoline through an alkyl linker.[124] The best conjugate (**13**, **Figure 13**) also possessed dual activity, being highly potent against asexual and sexual blood forms of *P. falciparum* (Dd2: EC_{50}(**13**) = 0.04 ± 0.01 μM; 3D7: EC_{50}(**13**) = 0.07 ± 0.01 μM; gametocytes: EC_{50}(**13**) = 0.89 - 0.95 μM).[124]

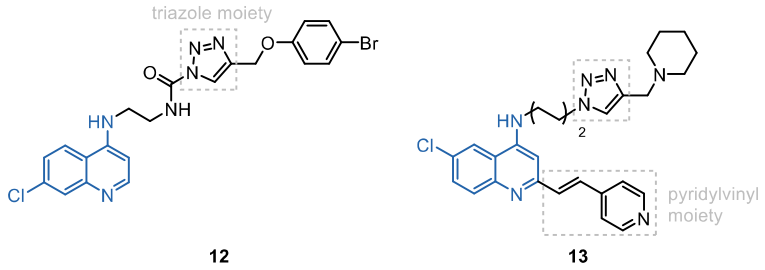
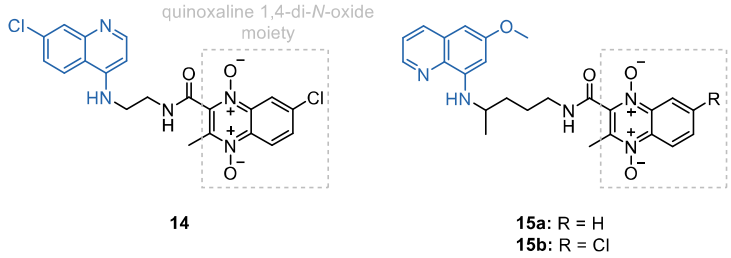


Figure 13. AQ-Triazole conjugates developed by Wadi *et al.*[123] (**12**) and Huang *et al.* (**13**).[124]

4.1.5. AQ-Quinoxaline conjugates

Quinoxalines have displayed therapeutic activity against different parasites, including erythrocytic forms of *P. falciparum*, and consequently have been also explored to produce hybrid compounds with multi-stage activity.[125, 126] In this sense, Bonilla-Ramirez *et al.* developed two series of conjugates with dual-stage action by combining quinoxaline 1,4-di-*N*-oxide hybrids and the pharmacophores of CQ or PQ.[127, 128] The CQ-quinoxaline series displayed more interesting activities against blood forms of *P. falciparum,* with conjugate **14** (**Figure 14**), being the most promising one (3D7: IC_{50} = 0.52 ± 0.11 μM; FCR-3: IC_{50} = 0.40 ± 0.23 μM; liver-stage: IC_{50} = 14.59, 10.13 and 6.39 μM against *P. yoelii*, *P. berghei*, and *P. falciparum*).[128] On the other hand, the PQ-quinoxaline series showed enhanced activity against liver forms of *P. yoelii*, *P. berghei*,

and *P. falciparum* infections, specially conjugates **15a** and **15b** (**Figure 14**), which displayed similar or better activities and selective index (SI) values than the parent drug PQ (3D7 and FCR-3: IC_{50} = 36 – 68 μM; liver-stage: IC_{50}(**15a**) = 1.39, 5.19 and 5.38 μM, IC_{50}(**15b**) = 5.71, 1.14 and 3.64 μM, IC_{50}(PQ) = 2.13, 3.65, and 0.40 against *P. yoelii*, *P. berghei*, and *P. falciparum*, respectively). Moreover, both compounds inhibited sporogony of *P. berghei*, with compound **15a** showing 92% blocking of transmission. *In vivo* efficacy against liver forms revealed that compound **15a** also showed causal prophylactic activity, reducing parasitemia by up to 95% on day 4, slightly less than PQ, and extending the prepatency period by approximately 24 h. Alongside these results, no signs of genotoxicity or *in vivo* acute toxicity were observed.[127, 128]



14 **15a:** R = H **15b:** R = Cl

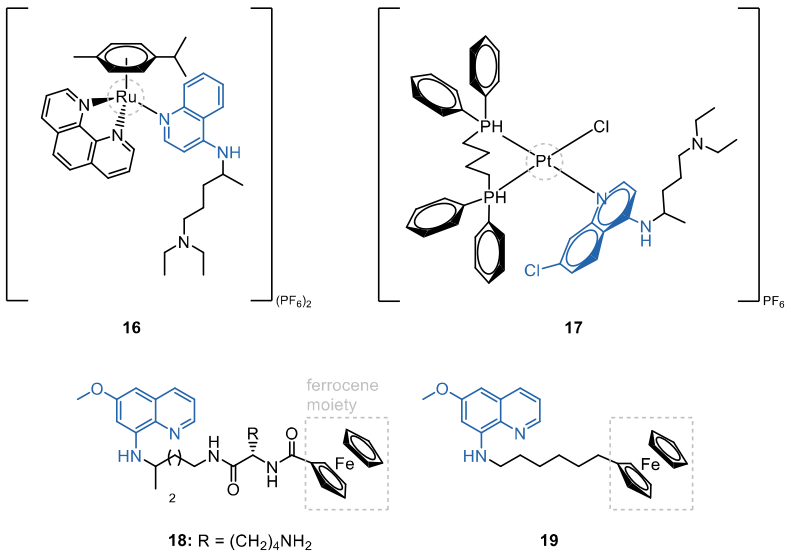
Figure 14. AQ-Quinoxaline conjugates developed by Bonilla-Ramirez *et al.* (**14-15**).[127, 128]

4.1.6. AQ-Organometallic conjugates

A substantial number of metal complexes containing AQs as a ligands have been investigated as antimalarial agents as well and, in most cases, an improvement in the potency against intraerythrocytic stages of *P. falciparum* was observed, in comparison to the relevant metal-free AQ derivative.[129, 130] In this context, Macedo *et al.* investigated the activity of AQs combining with ruthenium or platinum(II) complexes as potential conjugates with multi-stage activity.[131, 132] Indeed, the authors found that the best AQ-ruthenium conjugate, **16** (**Figure 15**), (i) possessed activity against all intraerythrocytic stages, (ii) exhibited fast parasiticidal activity against trophozoites by producing ROS, (iii) strongly reduced the viability of stage V gametocytes, and (iv) possessed moderate activity against liver forms of *P. berghei* (blood-stage, 3D7: IC_{50}(**16**) = 0.30 ± 0.03 μM, IC_{50}(CQ) = 0.11 ± 0.035 μM; W2: IC_{50}(**16**) = 0.31 ± 0.01 μM, IC_{50}(CQ) = 0.43 ± 0.09 μM; gametocytocidal-stage: IC_{50}(**16**) = 4.28 ± 1.05 μM, IC_{50}(CQ) > 20 μM). Noteworthy, the AQ of reference for the design of these conjugates, CQ, is devoid of activity against liver and sexual blood forms of *Plasmodium*, emphasizing the importance of its complexation with ruthenium.[131]

The best conjugate of the AQ-platinum set, complex **17** (**Figure 15**), also showed to act as a parasiticidal agent against trophozoites, with similar activities to those of CQ against the CQ-sensitive 3D7 and CQ-resistant W2 strains of *P. falciparum* (3D7: IC_{50}(**17**) = 0.32 ± 0.02 μM, IC_{50}(CQ) = 0.11 ± 0.035 μM; W2: IC_{50}(**17**) = 0.76 ± 0.10 μM, IC_{50}(CQ) = 0.43 ± 0.09 μM). Additionally, the activity against the hepatic stages of *P. berghei* was like that of reference PQ (IC_{50}(**17**) = 10.8 ± 0.68 μM; IC_{50}(PQ) = 10 μM).[132]

Ferrocene is another scaffold widely used in the preparation of bioactive organometallic structures.[133, 134] The most emblematic example of the contribution of the ferrocene moiety to the improvement of a drug is that of ferroquine.[135] Ferroquine was the first organometallic drug containing the ferrocenyl group covalently linked to an AQ, which was found to be remarkably effective against CQ-resistant strains of *P. falciparum*.[136] These interesting antimalarial properties of ferroquine stimulated extensive research studies where ferrocene was used to enhance the antimalarial activity to create novel dual-action hybrid drugs with highly promising results.[133-135] In this connection, Matos *et al.* reported the synthesis and antiplasmodial activity of novel conjugates linking PQ to ferrocene, designed with the purpose of displaying multi-stage action.[137] Only the conjugates containing a basic aliphatic amine group connected to a polymethylene chain exhibited both transmission-blocking and blood schizontocidal activities. This feature is not required for liver stage activity in which all conjugates showed comparable or better activities than the parent drug PQ. Overall, conjugate **18** (**Figure 15**) was the best one with *in vitro* activities comparable to PQ against erythrocytes of CQ-resistant *P. falciparum* W2 strain and liver forms of *P. berghei* (blood-stage: IC_{50}(**18**) = 3.48 μM; IC_{50}(PQ)= 3.3 μM; liver-stage: IC_{50}(**18**) = 6.46 μM; IC_{50}(PQ) = 7.50 μM). Additionally, this conjugate was able to almost completely inhibit the sporogonic cycle of *Plasmodium* at 10 μmol/kg *in vivo*, a concentration at which PQ only inhibited 45.7 %. Noteworthy, conjugate **19**, in which the PQ's aliphatic chain was replaced by hexylferrocene, was 38- and 45-fold more potent against liver stage parasitemia than the previous conjugate (**18**) and PQ, respectively (IC_{50}(**19**) = 0.17 μM).[137]



16 **17**

18: R = $(CH_2)_4NH_2$ **19**

Figure 15. AQ-Organometallic conjugates developed by Macedo *et al.*[131, 132] (**16**, **17**) and Matos *et al.* (**18**, **19**).[137]

4.1.7. Other AQ conjugates

N-heterocycles such as 1,3,5-triazines and pyrimidines are inhibitors of DHFR that prevent biosynthesis of DNA leading to the death of the malaria parasite. Therefore, their use as scaffolds for the conception of multi-stage hybrids containing AQs has been explored.[138-141] In this line of thought, Rodrigues *et al.* [142] developed conjugate **20** (**Figure 16**) that resulted from the direct linkage of 1,3,5-triazine with two PQ moieties and one chlorine atom. It emerged as the most potent compound against *P. berghei* liver-stage infection and blood forms of the CQ-resistant W2 *P. falciparum* strain (liver-stage: IC_{50}(**20**) = 27.5 ± 1.5 nM; IC_{50}(PQ) = 9500 ± 2300 nM; blood-stage: IC_{50}(**20**) = 0.60 ± 0.01 μM; IC_{50}(CQ) = 0.03 ± 0.009 μM). This was combined with good metabolic stability in rat liver microsomes.[142] On the other hand, based on reports of CQ-pyrimidine conjugates with enhanced activities against the blood stage of the parasite,[143, 144] Kaur *et al.* combined, for the first time, PQ with the pyrimidine-5-carboxylate scaffold.[145] Despite the moderate activities against blood forms of the CQ-sensitive *P. falciparum* NF54 strain, the conjugates showed good activities against the liver stages of the rodent parasite *P. berghei*, better than reference PQ. Conjugate **21** (**Figure 16**) stood out for its dual action, especially in the liver stage, and non-toxicity (blood-stage: IC_{50}(**21**) = 2.671 μM, IC_{50}(CQ) = 0.0125 μM; liver-stage: IC_{50} (**21**) = 1.500 ± 0.594 μM, IC_{50}(PQ) = 8.428 ± 3.389 μM; CC_{50} ≥ 100).[145]

Squaric acid is another pharmacophore gaining growing interest in this domain, primarily due to its function as a Michael acceptor that enables it to potentially inhibit falcipains, a group of parasitic cysteine proteases crucial in the metabolism of *P. falciparum*.[146] The potential of this scaffold as an antimalarial agent started being explored by Moreira and

co-workers, who demonstrated that squaric acids connected to AQs result in hybrids that are active *in vitro* against blood forms of the malaria pathogen.[147] Based on this, the authors linked PQ and squaramide scaffolds.[148] From this combination, resulted conjugates **22** and **23**, which were much more potent than PQ against liver-stage parasites and modestly active against the CQ-resistant W2 *P. falciparum* strain (liver-stage: IC_{50}(**22**) = 1.3 ± 0.1 μM; IC_{50}(**23**) = 1.3 ± 0.1 μM, IC_{50}(PQ) = 9.5 ± 2.3 μM; blood-stage: (IC_{50}(**22**) = 18.6 μM; IC_{50}(**23**) = 2.2 μM; IC_{50}(PQ) = 3.3 μM).[148]

The interest in using the adamantane moiety was raised in the ability of amantadine to block *N*-methyl-D-aspartate and calcium channels, which may enable the adamantane moiety to inhibit the *P. falciparum* CQ resistance transporter protein.[149] In this sense, Terzić *et al.* reported a new generation of AQs coupled with an adamantane moiety with dual action.[150] Despite the activities of conjugates against the blood forms of *P. falciparum* being quite modest (IC_{50}(**24**) = 135, 197 and 238 nM, IC_{50}(CQ) = 12, 139 and 456 nM against D6, C235 and W2 *P. falciparum* strains, respectively), the best compound (**24**, **Figure 16**), containing a fluorine atom in C(3) position of the 4-AQ, exhibited pronounced *in vitro* (IC_{50}(**24**) = 0.31 ± 0.14 μM) and *in vivo* activity against liver forms of *P. berghei* (*in vivo* 92% reduction of the *P. berghei* liver load at 80 mg/kg dose).[150]

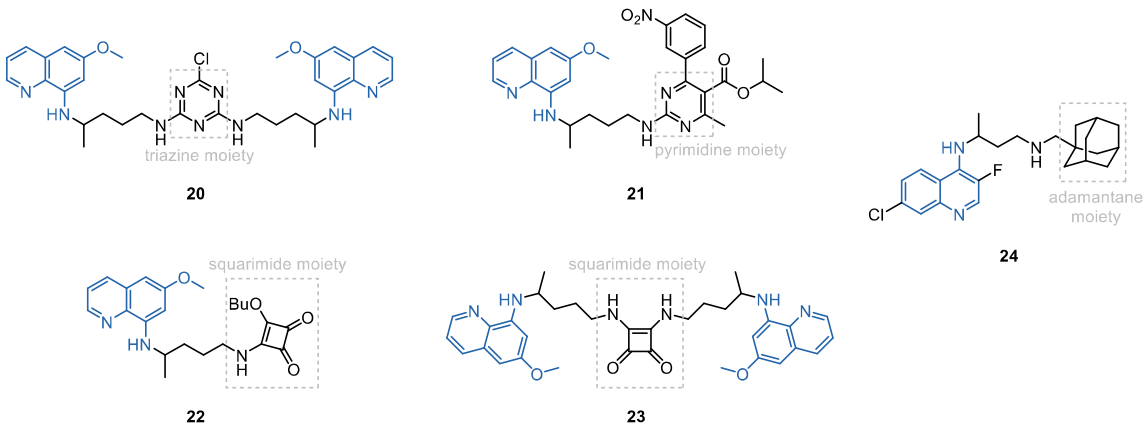


Figure 16. AQ-Triazine, AQ- pyrimidine, AQ-Squaramide, and AQ-adamantane conjugates developed by Rodrigues *et al.* (**20**),[142] Kaur *et al.* (**21**),[145] Ribeiro *et al.* (**22, 23**),[148] and Terzić *et al.* (**24**),[150] respectively.

4.2. Acridine-based conjugates

The interest in ACR-based structures as antimalarials occurred from early findings on QN. Since then, ACRs have been reported as possessing a broad spectrum of biological activities, which positions them as crucial components in the development of hybrids for combating malaria, alongside the AQs. However, the development of ACR-based

conjugates with multi-stage activity has not been an easy process, and typically results in hybrids that only target the blood stage of *Plasmodium* parasites.[32]

To the best of our knowledge, only Gomes and co-workers have previously described multi-stage ACR-based hybrids, the first of which were reported by Pérez *et al.* and resulted from the conjugation of the 9-aminoacridine heterocycle with CAs through a flexible aminobutyl chain.[151] The use of this specific spacer and of the cinnamoyl moiety were due to promising results obtained for AQ-derived hybrids, as already described in 4.1.3. The best ACR-cinnamoyl hybrid arising from this study, compound **25** (**Figure 17**), showed activity *in vitro* against both the liver and blood-stage of *Plasmodium* development, while being non-toxic to human hepatoma cells (Huh-7) at concentrations up to 5 μM. Specifically, hybrid **25** was equipotent to CQ against erythrocytic stages of the CQ-resistant W2 *P. falciparum* strain, and 2- and 5-fold more potent against liver stages of *P. berghei* than references PQ and CQ, respectively (W2: IC_{50}(**25**) = 138 ± 2 nM; liver-stage: IC_{50}(**25**) = 3.2 μM, IC_{50}(CQ) > 15 μM, IC_{50}(PQ) = 8 μM).[151] This was an unprecedented result, since QN and other ACR-based antimalarial compounds reported until that date were devoid of activity in the hepatic stage of the parasite.

Based on these promising results, years later, the same research group extended the study to ACR-based hybrids where the 9-aminoacridine moiety was replaced by the 9-amino-6-chloro-2-methoxyacridine core of QN, since the presence of both the 2-methoxy and the 6-chloro substituents was known as relevant for a potent action against CQ-resistant and CQ-sensitive strains of *P. falciparum*.[152] Compared to previous conjugates, these new hybrids were found to possess stronger dual-action against both the blood and liver stages of *Plasmodium*. Conjugate **26** (**Figure 17**), exhibiting a *para*-fluor substituent in the cinnamoyl moiety, exhibited the best profile of the series with activities (i) comparable to or higher than those of CQ against blood forms of 3D7, Dd2, and W2 *P. falciparum* parasites (3D7: IC_{50}(**26**) = 29.8 nM, IC_{50}(CQ) = 21.0 nM; Dd2: IC_{50}(**26**) = 131.0 nM, IC_{50}(CQ) = 107.5 nM; W2: IC_{50}(**26**) = 17.8 nM, IC_{50}(CQ) = 225.8 nM), and (ii) 5-fold higher than PQ against liver forms of *P. berghei* (IC_{50}(**26**) = 1.6 μM, IC_{50}(PQ) = 7.5 μM).[153] Moreover, this compound was the least cytotoxic of the set, which corroborates literature reports indicating that fluorinated compounds exhibit superior bioavailability, solubility, and metabolic stability when compared to their nonfluorinated counterparts.[154] ACR-derivatives like **25** or **26**, i.e., showing activity against hepatic forms of *Plasmodium* parasites and low cytotoxicity were unprecedented in the literature, and constituted an adequate starting point to advance QN-based hybrids with multi-stage action.

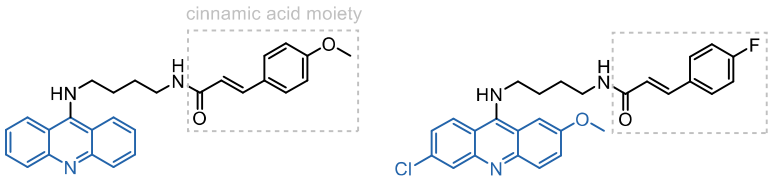


Figure 17. ACR-based conjugates developed by Gomes and co-workers (**25**, **26**).[151, 153]

4.3. Aminoquinoline-based merged hybrids

Interestingly, from a chemical point of view, the ACR core can be considered as a merge of the two well-known AQs - CQ and PQ. This feature triggered the interest of Gomes and co-workers towards the development on novel merged hybrids in which the two parent molecules are fused, instead of being connected by a linker; as such, this research group designed a 4,9-diaminoacridine structure (**27**, **Figure 18**) as a fusion of CQ and PQ, and hypothesized that the resulting merged hybrid would be active against the three stages of the *Plasmodium* life cycle inside the human host: liver-, blood-, and gametocyte stage.[102]

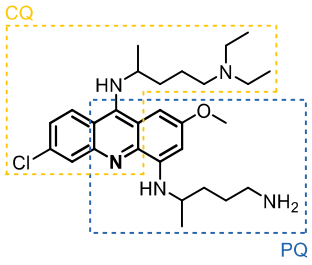
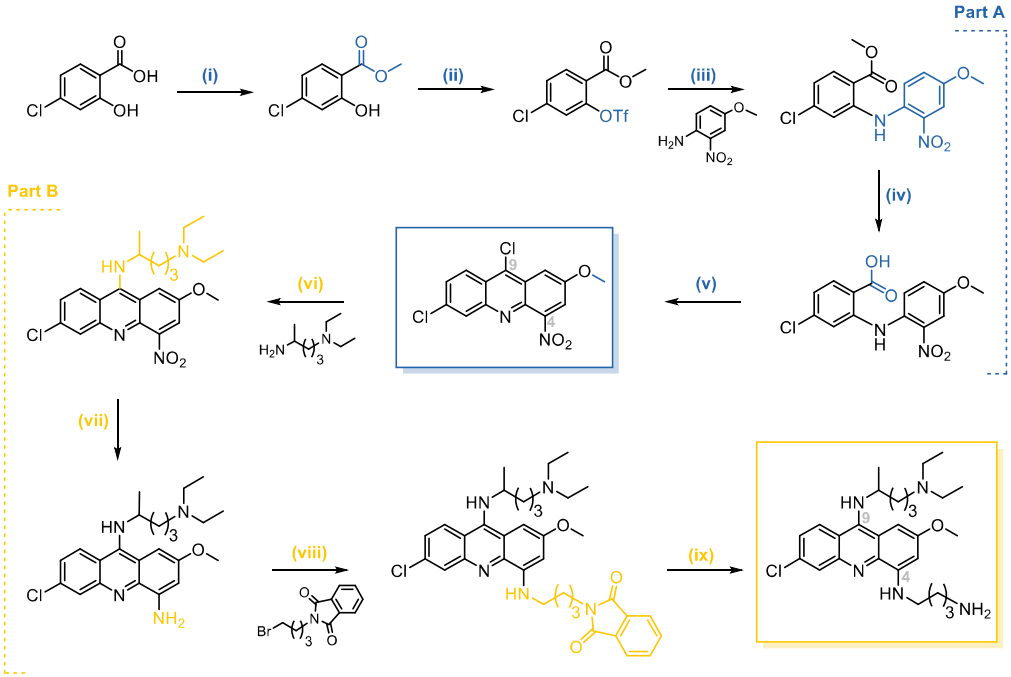


Figure 18. 4,9-diaminoacridine merged hybrid (**27**) recently developed by Gomes and co-workers as a potential multi-stage antiplasmodial,[102] which served as driving force for the doctoral research project herein reported.

To confirm the above hypothesis, the same research group pursued the chemical synthesis of 4,9-diaminoacridine **27**, which was accomplished by a 9-step synthesis divided in two main parts (**Scheme 1**): Part A - synthesis of 6,9-dichloro-2-methoxy-4-nitroacridine, the precursor of **27** and other future analogues/derivatives, and Part B - the introduction of the amino side chains in the desired C-9 and C-4 positions of the ACR aromatic ring. Briefly, Part A started with the esterification of the carboxylic group present in 4-chlorosalycilic acid (step i). The resulting ester was converted into a triflate (step ii), which then reacted with 4-methoxy-2-nitroaniline through a Buchwald-Hartwig amination (step iii). Next, the ester group was hydrolyzed to afford the corresponding carboxylic acid (step iv) that, after Friedel-Crafts intramolecular acylation, gave the desired 6,9-

dichloro-2-methoxy 4-nitroacridine (step v). Once this precursor was obtained, Part B started with the introduction of the same side chain that is present in CQ, in the acridine heterocycle, which was achieved by nucleophilic aromatic substitution (step vi). After reduction of the nitro group present in the C-4 of the acridine ring into the corresponding aniline (step vii), the *N*-phthalimide-protected amino butyl side chain was introduced in the aromatic system by bimolecular nucleophilic substitution (step viii). Finally, hydrazinolysis to remove the *N*-phthalimide protecting group delivered the target 4,9-diaminoacridine **27** (step ix).[102]



Scheme 1. Synthesis route developed by Fonte *et al.* for the obtention of 4,9-diaminoacridine derivative. Reagents and conditions: **Part A** (at blue) - **(i)** CH_3I, Cs_2CO_3, dimethylformamide (DMF), room temperature (rt), 90 min; **(ii)** Tf_2O, Et_3N, CH_2Cl_2, N_2 atmosphere, -25 °C, 30 min; **(iii)** 4-methoxy-2-nitroaniline, Cs_2CO_3, $Pd(OAc)_2$, *rac*-BINAP, toluene, N_2 atmosphere, 120 °C, 5 h; **(iv)** (1) $Ba(OH)_2{\cdot}8H_2O$, CH_3OH, 90 °C, 2 h; (2) 1 M aq. HCl; **(v)** $POCl_3$, 120 °C, 2.5 h; **Part B** (at yellow) – **(vi)** Phenol, Cs_2CO_3, dimethylsulfoxide (DMSO), 4 Å molecular sieves, 100 °C, 2 h, then *N,N*-diethylpentan-1,4-diamine, 100°C, 4 h; **(vii)** $SnCl_2$, 37% aq. HCl, 0→40 °C, 30 min; **(viii)** *N*-(4-bromobutyl)phthalimide, CH_3COONa, CH_3CH_2OH, microwave (MW) heating (100 W, 120°C) in a pressurized vial (100 psi), 2.5 h; **(ix)** NH_2NH_2, tetrahydrofuran (THF), 60°C, 72 h.[102]

Before the synthesis of **27** was achieved, most of the ACR-based compounds reported featured chemical alterations primarily at the C-9 and *N*-10 positions, which are the most reactive sites of the acridine heterocycle due to the presence of the pyridinic nitrogen. Hence, to the best of our knowledge, the synthesis of merged hybrids like **27** had not been previously achieved, since modifications on positions of the ACR core other than C-9 and *N*-10, are comparatively scarce. Therefore, the synthesis of **27** was an

unprecedented outcome in the organic chemistry field and opened the door towards development of new ACR-based constructs with multi-stage antiplasmodial activity, i.e., it set the foundations for the doctoral research project presented herein.

5. Overview of the present work

P. falciparum multi-drug resistance is the main obstacle hindering malaria eradication. Given the substantial decline in the effectiveness of the current first-line antimalarial treatment (ACTs), there is an urgent need for the development of new potent drugs, ideally having low tendency to induce resistance. Multi-stage drugs have emerged as a promising strategy in response to this yet unmet need. Targeting multiple processes in the parasite's life cycle with a single medication may provide greater efficacy by rapidly clearing parasites, while reducing the likelihood of viable resistant parasites to emerge.

In face of the above and driven by the results highlighted in section 4.3., the doctoral research project herein reported addressed the development of potential multi-stage antimalarials, by means of the covalent bitherapy approach, which, in this case, primarily consisted in merging the chemical structures of CQ and PQ into ACR-based constructs (**Figure 19**). Jointly, the antimalarial action of the two parent AQ drugs cover three distinct stages of the *Plasmodium* life cycle, thus we anticipated that the new hybrids - 4-aminoacridines and 4,9-diaminoacridines - would combine these different activities in a single molecular construct, resulting in a multi-stage antimalarial hit.

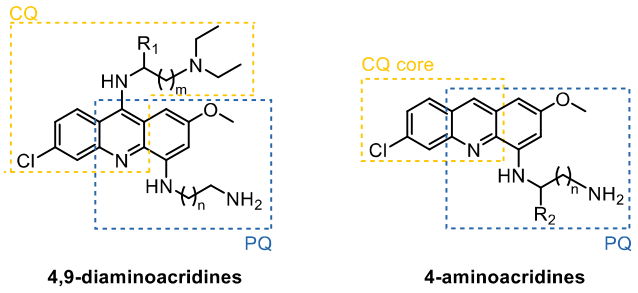


Figure 19. 4,9-diaminoacridines and 4-aminoacridines developed in this doctoral project as potential multi-stage antimalarial hits, resulting from the "merge" of the chemical structures of the antimalarial AQ drugs CQ and PQ.

To attain the global aim of this project, four experimental goals (**Figure 20**) were pursued and achieved, as follows.

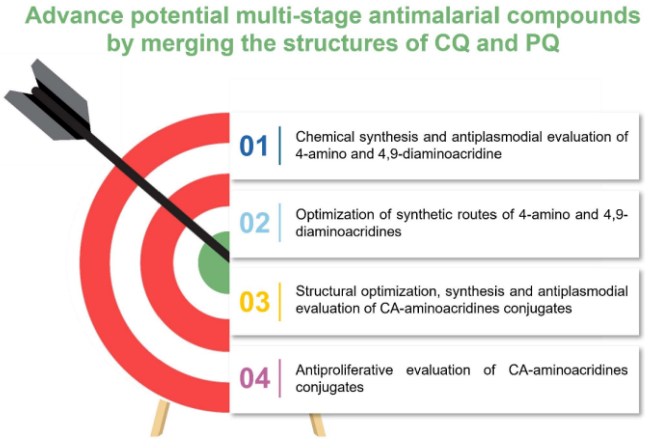


Figure 20. The four experimental goals set to achieve the global aim of this doctoral project (highlighted in green).

Goal 1. Chemical synthesis of 4-aminoacridines and 4,9-diaminoacridines and evaluation of their antiplasmodial activity *in vitro*

The synthesis of six new 4-aminoacridines and 4,9-diaminoacridines was pursued and accomplished, by use of the previously established synthetic route described in section 4.3. Their chemical structures were confirmed using proton and carbon nuclear mass resonance (^{1}H-NMR and ^{13}C-NMR, respectively) and electrospray ionization ion trap mass spectrometry (ESI-IT MS), and their purity degrees assessed by high-performance liquid chromatography (HPLC). The two families of ACR-based hybrids were next evaluated *in vitro* against the liver and blood stages of the malaria parasite and confirmed to possess dual action, as anticipated. These results and their discussion are described in detail in chapter II, specifically in article I.

Goal 2. Optimization of the synthesis route towards the target 4-aminoacridines and 4,9-diaminoacridines

Considering the low overall yield of the quite laborious synthesis route presented in section 4.3 (Scheme 1), it was also our intention to optimize this route. This was considered even more relevant once Goal 1 was achieved, thereby validating the working hypothesis that the merged hybrids would display multi-stage action. In this regard, several synthesis approaches were explored, and it was possible to establish an alternative route with fewer synthesis steps and a higher overall yield. This part of the work is described and discussed in article II of chapter II.

Goal 3. Taking the covalent bitherapy approach one step ahead: conjugation of CAs to the 4-aminoacridines and 4,9-diaminoacridines developed

Driven by the previous reports on the improvement of antiplasmodial activity of ACR-based compounds by their conjugation to CA, as already described in section 4.2., we also aimed at applying the same covalent bitherapy approach for the structural optimization of the 4-aminoacridines and 4,9-diaminoacridines initially developed in this doctoral project. To this end, different CAs were coupled to the compounds within each acridine family that had shown the best antiplasmodial profile. This resulted in 20 new conjugates that were evaluated against blood, liver, and gametocyte forms of the parasite, which allowed us to confirm that the antiplasmodial action was overall improved. These findings are reported and analyzed in chapter III, namely in articles III and IV.

Goal 4. Assessment of the antiproliferative action of the target ACR-based constructs *in vitro*

Many ACR-based molecules are well known for their strong DNA-binding character, which has been explored not only for their use as nucleic acid stains (e.g., acridine orange; ACMA - 9-amino-6-chloro-2-methoxyacridine), but also for their potential therapeutic value as antiproliferative agents. In view of this, the final goal of this doctoral project was to investigate whether the 4-aminoacridines and 4,9-diaminoacridines developed as potential multi-stage antimalarials could also be interesting templates for the future development of ACR-based antitumoral drugs. To this end, we evaluated their antiproliferative activity against three tumoral and one non-tumoral cell lines *in vitro*. Significant activity was selectively exerted by 4,9-diaminoacridines/CA conjugates against the tumoral lines, as detailed in article V of chapter III.

In summary, the research work conducted to attain each of the goals above is described and discussed in the following Chapters II (Goals 1 and 2) and III (Goals 3 and 4). The last chapter (Chapter IV) gathers the main conclusions of the overall doctoral project, as well as future perspectives in this specific area of research.

References

1. World Health Organization, *World Malaria Report 2023*; World Health Organization, **2023**. https://www.who.int/teams/global-malaria-programme/reports/world-malaria-report-2023 (accessed June 12, 2024).

2. Teklehaimanot, A.; Mejia, P., Malaria and poverty. *Annals of the New York Academy of Sciences* **2008**, *1136*, 32-7.

3. World Health Organization, *The Global Health Observatory*; World Health Organization, **2023**. https://www.who.int/data/gho/data/indicators/indicator-details/GHO/estimated-number-of-malaria-cases (accessed May 7, 2024).

4. González-Sanz, M. B., P.; Norman, F. F., Updates on Malaria Epidemiology and Prevention Strategies. *Current Infectious Disease Reports* **2023**, 1-9.

5. World Health Organization, *Global Technical Strategy for Malaria 2016-2030*; World Health Organization, **2021**. https://www.who.int/publications/i/item/9789240031357 (accessed May 28, 2024).

6. Mahase, E., Malaria: Climate change poses "substantial risk to progress", WHO warns. *British Medical Journal* **2023**, *383*, 2848.

7. World Health Organization, *World Malaria Report 2021*; World Health Organization, **2021**. https://www.who.int/teams/global-malaria-programme/reports/world-malaria-report-2021 (accessed June 12, 2024).

8. World Health Organization, *World Malaria Report 2022*; World Health Organization, **2022**. https://www.who.int/teams/global-malaria-programme/reports/world-malaria-report-2022 (accessed June 12, 2024).

9. World Health Organization, *World Malaria Report 2020*; World Health Organization, **2020**. https://www.who.int/teams/global-malaria-programme/reports/world-malaria-report-2020 (accessed June 12, 2024).

10. World Health Organization, *World Malaria Report 2019*; World Health Organization, **2019**. https://www.who.int/teams/global-malaria-programme/reports/world-malaria-report-2019 (accessed June 12, 2024).

11. Joste, V.; Kamaliddin, C.; Kendjo, E.; Hubert, V.; Argy, N.; Houzé, S., Distinction of *Plasmodium ovale wallikeri* and *Plasmodium ovale curtisi* using quantitative Polymerase Chain Reaction with High Resolution Melting revelation. *Scientific Reports* **2018**, *8* (1), 300.

12. Mahittikorn, A.; Masangkay, F. R.; Kotepui, K. U.; Milanez, G. J.; Kotepui, M., Comparison of *Plasmodium ovale curtisi* and *Plasmodium ovale wallikeri* infections by a meta-analysis approach. *Scientific Reports* **2021**, *11* (1), 6409.

13. Markus, M. B., Do hypnozoites cause relapse in malaria? *Trends in Parasitology* **2015**, *31* (6), 239-45.

14. Sato, S., *Plasmodium*—a brief introduction to the parasites causing human malaria and their basic biology. *Journal of Physiological Anthropology* **2021**, *40* (1), 1.

15. Venugopal, K.; Hentzschel, F.; Valkiūnas, G.; Marti, M., *Plasmodium* asexual growth and sexual development in the haematopoietic niche of the host. *Nature Reviews Microbiology* **2020**, *18* (3), 177-189.

16. Prudêncio, M.; Rodriguez, A.; Mota, M. M., The silent path to thousands of merozoites: the Plasmodium liver stage. *Nature Reviews Microbiology* **2006**, *4* (11), 849-856.

17. Hulden, L.; Hulden, L., Activation of the hypnozoite: a part of *Plasmodium vivax* life cycle and survival. *Malaria Journal* **2011**, *10* (1), 90.

18. Chahine, Z.; Le Roch, K. G., Decrypting the complexity of the human malaria parasite biology through systems biology approaches. *Frontiers in Systems Biology* **2022**, *2*, 940321.

19. Munro, B. A.; McMorran, B. J., Antimalarial Drug Strategies to Target *Plasmodium* Gametocytes. *Parasitologia* **2022**, *2* (2), 101-124.

20. Graumans, W.; Jacobs, E.; Bousema, T.; Sinnis, P., When Is a *Plasmodium*-Infected Mosquito an Infectious Mosquito? *Trends in Parasitology* **2020**, *36* (8), 705-716.

21. Blasco, B.; Leroy, D.; Fidock, D. A., Antimalarial drug resistance: linking *Plasmodium falciparum* parasite biology to the clinic. *Nature Medicine* **2017**, *23* (8), 917-928.

22. Lobo, N. F.; Achee, N. L.; Greico, J.; Collins, F. H., Modern Vector Control. *Cold Spring Harbor Perspectives in Medicine* **2018**, *8* (1), a025643.

23. Wang, S.; Jacobs-Lorena, M., Genetic approaches to interfere with malaria transmission by vector mosquitoes. *Trends in Biotechnology* **2013**, *31* (3), 185-93.

24. James, S.; Santos, M., The Promise and Challenge of Genetic Biocontrol Approaches for Malaria Elimination. *Tropical Medicine and Infectious Disease* **2023**, *8* (4), 201.

25. Laurens, M. B., RTS,S/AS01 vaccine (Mosquirix™): an overview. *Human Vaccines & Immunotherapeutics* **2020**, *16* (3), 480-489.

26. Datoo, M. S.; Dicko, A.; Tinto, H.; Ouédraogo, J. B.; Hamaluba, M.; Olotu, A.; Beaumont, E.; Ramos Lopez, F.; Natama, H. M.; Weston, S.; Chemba, M.; Compaore, Y. D.; Issiaka, D.; Salou, D.; Some, A. M.; Omenda, S.; Lawrie, A.; Bejon, P.; Rao, H.; Chandramohan, D.; Roberts, R.; Bharati, S.; Stockdale, L.; Gairola, S.; Greenwood, B. M.; Ewer, K. J.; Bradley, J.; Kulkarni, P. S.; Shaligram, U.; Hill, A. V. S., Safety and

efficacy of malaria vaccine candidate R21/Matrix-M in African children: a multicentre, double-blind, randomised, phase 3 trial. *Lancet* **2024**, *403* (10426), 533-544.

27. El-Moamly, A. A.; El-Sweify, M. A., Malaria vaccines: the 60-year journey of hope and final success—lessons learned and future prospects. *Tropical Medicine and Health* **2023**, *51* (1), 29.

28. Aderinto, N.; Olatunji, G.; Kokori, E.; Sikirullahi, S.; Aboje, J. E.; Ojabo, R. E., A perspective on Oxford's R21/Matrix-M™ malaria vaccine and the future of global eradication efforts. *Malaria Journal* **2024**, *23* (1), 16.

29. Van Schalkwyk, D. A., History of Antimalarial Agents. In *Encyclopedia of Life Sciences*, Ltd ed.; John Wiley & Sons, Ed. Nature: 2015; pp 1-5.

30. Schlitzer, M., Malaria Chemotherapeutics Part I: History of Antimalarial Drug Development, Currently Used Therapeutics, and Drugs in Clinical Development. *ChemMedChem* **2007**, *2* (7), 944-986.

31. Tse, E. G.; Korsik, M.; Todd, M. H., The past, present and future of anti-malarial medicines. *Malaria Journal* **2019**, *18* (1), 93.

32. Fonte, M.; Tassi, N.; Gomes, P.; Teixeira, C., Acridine-Based Antimalarials—From the Very First Synthetic Antimalarial to Recent Developments. *Molecules* **2021**, *26* (3), 600.

33. Prasher, P.; Sharma, M., Medicinal chemistry of acridine and its analogues. *MedChemComm* **2018**, *9* (10), 1589-1618.

34. Gensicka-Kowalewska, M.; Cholewiński, G.; Dzierzbicka, K., Recent developments in the synthesis and biological activity of acridine/acridone analogues. *RSC Advances* **2017**, *7* (26), 15776-15804.

35. Coronado, L. M.; Nadovich, C. T.; Spadafora, C., Malarial hemozoin: from target to tool. *Biochimica et Biophysica Acta* **2014**, *1840* (6), 2032-41.

36. Deshpande, S.; Kay, B., 4-aminoquinolines: An Overview of Antimalarial Chemotherapy. *Medicinal Chemistry* **2016**, *6* (1), 001-011.

37. Hawley, S. R.; Bray, P. G.; Park, B. K.; Ward, S. A., Amodiaquine accumulation in *Plasmodium falciparum* as a possible explanation for its superior antimalarial activity over chloroquine. *Molecular and Biochemical Parasitology* **1996**, *80* (1), 15-25.

38. Chu, W. Y.; Dorlo, T. P. C., Pyronaridine: a review of its clinical pharmacology in the treatment of malaria. *Journal of Antimicrobial Chemotherapy* **2023**, *78* (10), 2406-2418.

39. Davis, T. M.; Hung, T. Y.; Sim, I. K.; Karunajeewa, H. A.; Ilett, K. F., Piperaquine: a resurgent antimalarial drug. *Drugs* **2005**, *65* (1), 75-87.

40. Palmer, K. J.; Holliday, S. M.; Brogden, R. N., Mefloquine. *Drugs* **1993**, *45* (3), 430-475.

41. Group, W. A. R. N. L. P. K. P. D. S., Artemether-lumefantrine treatment of uncomplicated *Plasmodium falciparum* malaria: a systematic review and meta-analysis of day 7 lumefantrine concentrations and therapeutic response using individual patient data. *BMC Medicine* **2015**, *13* (1), 227.

42. Baird, J. K., 8-Aminoquinoline Therapy for Latent Malaria. *Clinical Microbiology Reviews* **2019**, *32* (4), e00011-19.

43. Ashley, E. A.; Recht, J.; White, N. J., Primaquine: the risks and the benefits. *Malaria Journal* **2014**, *13* (1), 418.

44. John, G. K.; Douglas, N. M.; von Seidlein, L.; Nosten, F.; Baird, J. K.; White, N. J.; Price, R. N., Primaquine radical cure of *Plasmodium vivax*: a critical review of the literature. *Malaria Journal* **2012**, *11* (1), 280.

45. Lu, K.-Y.; Derbyshire, E. R., Tafenoquine: A Step toward Malaria Elimination. *Biochemistry* **2020**, *59* (8), 911-920.

46. Mayence, A.; Vanden Eynde, J. J., Tafenoquine: A 2018 Novel FDA-Approved Prodrug for the Radical Cure of *Plasmodium vivax* Malaria and Prophylaxis of Malaria. *Pharmaceuticals* **2019**, *12* (3), 115.

47. Watson, J. A.; Commons, R. J.; Tarning, J.; Simpson, J. A.; Llanos Cuentas, A.; Lacerda, M. V. G.; Green, J. A.; Koh, G. C. K. W.; Chu, C. S.; Nosten, F. H.; Price, R. N.; Day, N. P. J.; White, N. J., The clinical pharmacology of tafenoquine in the radical cure of *Plasmodium vivax* malaria: An individual patient data meta-analysis. *eLife* **2022**, *11*, e83433.

48. Markus, M. B., Safety and Efficacy of Tafenoquine for *Plasmodium vivax* Malaria Prophylaxis and Radical Cure: Overview and Perspectives. *Therapeutics and Clinical Risk Management* **2021**, *17*, 989-999.

49. Starkl Renar, K.; Iskra, J.; Križaj, I., Understanding malarial toxins. *Toxicon* **2016**, *119*, 319-329.

50. Coban, C., The host targeting effect of chloroquine in malaria. *Current Opinion in Immunology* **2020**, *66*, 98-107.

51. Müller, I. B.; Hyde, J. E., Antimalarial drugs: modes of action and mechanisms of parasite resistance. *Future Microbiology* **2010**, *5* (12), 1857-1873.

52. Gorka, A. P.; de Dios, A.; Roepe, P. D., Quinoline drug-heme interactions and implications for antimalarial cytostatic versus cytocidal activities. *Journal of Medicinal Chemistry* **2013**, *56* (13), 5231-46.

53. Hoppe, H. C.; van Schalkwyk, D. A.; Wiehart, U. I.; Meredith, S. A.; Egan, J.; Weber, B. W., Antimalarial quinolines and artemisinin inhibit endocytosis in *Plasmodium falciparum*. *Antimicrobial Agents and Chemotherapy* **2004**, *48* (7), 2370-8.

54. Herraiz, T.; Guillén, H.; González-Peña, D.; Arán, V. J., Antimalarial Quinoline Drugs Inhibit β-Hematin and Increase Free Hemin Catalyzing Peroxidative Reactions and Inhibition of Cysteine Proteases. *Scientific Reports* **2019**, *9* (1), 15398.

55. Wong, W.; Bai, X. C.; Sleebs, B. E.; Triglia, T.; Brown, A.; Thompson, J. K.; Jackson, K. E.; Hanssen, E.; Marapana, D. S.; Fernandez, I. S.; Ralph, S. A.; Cowman, A. F.; Scheres, S. H. W.; Baum, J., Mefloquine targets the *Plasmodium falciparum* 80S ribosome to inhibit protein synthesis. *Nature Microbiology* **2017**, *2*, 17031.

56. Popovici, J.; Tebben, K.; Witkowski, B.; Serre, D., Primaquine for *Plasmodium vivax* radical cure: What we do not know and why it matters. *International Journal for Parasitology: Drugs and Drug Resistance* **2021**, *15*, 36-42.

57. Camarda, G.; Jirawatcharadech, P.; Priestley, R. S.; Saif, A.; March, S.; Wong, M. H. L.; Leung, S.; Miller, A. B.; Baker, D. A.; Alano, P.; Paine, M. J. I.; Bhatia, S. N.; O'Neill, P. M.; Ward, S. A.; Biagini, G. A., Antimalarial activity of primaquine operates via a two-step biochemical relay. *Nature Communications* **2019**, *10* (1), 3226.

58. Cui, L.; Su, X. Z., Discovery, mechanisms of action and combination therapy of artemisinin. *Expert Review of Anti-infective Therapy* **2009**, *7* (8), 999-1013.

59. O'Neill, P. M.; Barton, V. E.; Ward, S. A., The Molecular Mechanism of Action of Artemisinin—The Debate Continues. *Molecules* **2010**, *15* (3), 1705-1721.

60. Wang, J.; Huang, L.; Li, J.; Fan, Q.; Long, Y.; Li, Y.; Zhou, B., Artemisinin directly targets malarial mitochondria through its specific mitochondrial activation. *PLOS ONE* **2010**, *5* (3), e9582.

61. Bridgford, J. L.; Xie, S. C.; Cobbold, S. A.; Pasaje, C. F. A.; Herrmann, S.; Yang, T.; Gillett, D. L.; Dick, L. R.; Ralph, S. A.; Dogovski, C.; Spillman, N. J.; Tilley, L., Artemisinin kills malaria parasites by damaging proteins and inhibiting the proteasome. *Nature Communications* **2018**, *9* (1), 3801.

62. Peters, P. J.; Thigpen, M. C.; Parise, M. E.; Newman, R. D., Safety and toxicity of sulfadoxine/pyrimethamine: implications for malaria prevention in pregnancy using intermittent preventive treatment. *Drug Safety* **2007**, *30* (6), 481-501.

63. Tan, K. R.; Magill, A. J.; Parise, M. E.; Arguin, P. M., Doxycycline for malaria chemoprophylaxis and treatment: report from the CDC expert meeting on malaria chemoprophylaxis. *American Journal of Tropical Medicine and Hygiene* **2011**, *84* (4), 517-31.

64. Okada, M.; Guo, P.; Nalder, S. A.; Sigala, P. A., Doxycycline has distinct apicoplast-specific mechanisms of antimalarial activity. *eLife* **2020**, *9*.

65. World Health Organization, *WHO Model List of Essential Medicines – 23rd List (2023)*; World Health Organization, **2023**. https://www.who.int/publications/i/item/WHO-MHP-HPS-EML-2023.02 (accessed May 4, 2024).

66. World Health Organization, *Guidelines for the treatment of Malaria 2015*; World Health Organization, **2015**. https://iris.who.int/handle/10665/162441 (accessed May 25, 2024).

67. Eulambius Mathias, M., Malaria Treatment Landscape: Current Trends and Future Directions. In *Malaria*, Amoah Linda Eva; Acquah Festus Kojo; Asare Kwame Kumi, Eds. IntechOpen: Rijeka, 2023.

68. Chu, C. S.; White, N. J., The prevention and treatment of *Plasmodium vivax* malaria. *PLOS Medicine* **2021**, *18* (4), e1003561.

69. Nosten, F.; White, N. J., Artemisinin-based combination treatment of *falciparum* malaria. *American Journal of Tropical Medicine Hygiene* **2007**, *77* (6 Suppl), 181-92.

70. Ippolito, M. M.; Moser, K. A.; Kabuya, J.-B. B.; Cunningham, C.; Juliano, J. J., Antimalarial Drug Resistance and Implications for the WHO Global Technical Strategy. *Current Epidemiology Reports* **2021**, *8* (2), 46-62.

71. World Health Organization, *Strategy to respond to antimalarial drug resistance in Africa*; World Health Organization, **2022**. https://www.who.int/publications/i/item/9789240060265 (accessed May 3, 2024).

72. Shibeshi, M. A.; Kifle, Z. D.; Atnafie, S. A., Antimalarial Drug Resistance and Novel Targets for Antimalarial Drug Discovery. *Infection and Drug Resistance* **2020**, *13*, 4047-4060.

73. Payne, D., Spread of chloroquine resistance in *Plasmodium falciparum*. *Parasitology Today* **1987**, *3* (8), 241-6.

74. Hanboonkunupakarn, B.; White, N. J., The threat of antimalarial drug resistance. *Tropical Diseases, Travel Medicine and Vaccines* **2016**, *2* (1), 10.

75. Assefa, A.; Fola, A. A.; Tasew, G., Emergence of *Plasmodium falciparum* strains with artemisinin partial resistance in East Africa and the Horn of Africa: is there a need to panic? *Malaria Journal* **2024**, *23* (1), 34.

76. Müller, O.; Lu, G. Y.; von Seidlein, L., Geographic expansion of artemisinin resistance. *Journal of Travel Medicine* **2019**, *26* (4).

77. Nsanzabana, C., Resistance to Artemisinin Combination Therapies (ACTs): Do Not Forget the Partner Drug! *Tropical Medicine and Infectious Disease* **2019**, *4* (1), 26.

78. Ward, K. E.; Fidock, D. A.; Bridgford, J. L., *Plasmodium falciparum* resistance to artemisinin-based combination therapies. *Current Opinion in Microbiology* **2022**, *69*, 102193.

79. Chen, I.; Hsiang, M. S., Triple artemisinin-based combination therapies for malaria: a timely solution to counter antimalarial drug resistance. *The Lancet Infectious Diseases* **2022**, *22* (6), 751-753.

80. Nguyen, T. D.; Gao, B.; Amaratunga, C.; Dhorda, M.; Tran, T. N.-A.; White, N. J.; Dondorp, A. M.; Boni, M. F.; Aguas, R., Preventing antimalarial drug resistance with triple artemisinin-based combination therapies. *Nature Communications* **2023**, *14* (1), 4568.

81. Kokori, E.; Olatunji, G.; Akinboade, A.; Akinoso, A.; Egbunu, E.; Aremu, S. A.; Okafor, C. E.; Oluwole, O.; Aderinto, N., Triple artemisinin-based combination therapy (TACT): advancing malaria control and eradication efforts. *Malaria Journal* **2024**, *23* (1), 25.

82. Van der Pluijm, R. W.; Amaratunga, C.; Dhorda, M.; Dondorp, A. M., Triple Artemisinin-Based Combination Therapies for Malaria - A New Paradigm? *Trends in Parasitology* **2021**, *37* (1), 15-24.

83. Siqueira-Neto, J. L.; Wicht, K. J.; Chibale, K.; Burrows, J. N.; Fidock, D. A.; Winzeler, E. A., Antimalarial drug discovery: progress and approaches. *Nature Reviews Drug Discovery* **2023**, *22* (10), 807-826.

84. Burrows, J. N.; Duparc, S.; Gutteridge, W. E.; Hooft van Huijsduijnen, R.; Kaszubska, W.; Macintyre, F.; Mazzuri, S.; Möhrle, J. J.; Wells, T. N. C., New developments in anti-malarial target candidate and product profiles. *Malaria Journal* **2017**, *16* (1), 26.

85. Okombo, J.; Chibale, K., Recent updates in the discovery and development of novel antimalarial drug candidates. *MedChemComm* **2018**, *9* (3), 437-453.

86. Makhoba, X. H.; Viegas, C., Jr.; Mosa, R. A.; Viegas, F. P. D.; Pooe, O. J., Potential Impact of the Multi-Target Drug Approach in the Treatment of Some Complex Diseases. *Drug Design, Development and Therapy* **2020**, *14*, 3235-3249.

87. Tibon, N. S.; Ng, C. H.; Cheong, S. L., Current progress in antimalarial pharmacotherapy and multi-target drug discovery. *European Journal of Medicinal Chemistry* **2020**, *188*, 111983.

88. Flannery, E. L.; Chatterjee, A. K.; Winzeler, E. A., Antimalarial drug discovery - approaches and progress towards new medicines. *Nature Reviews Microbiology* **2013**, *11* (12), 849-62.

89. Pandey, S. K.; Anand, U.; Siddiqui, W. A.; Tripathi, R., Drug Development Strategies for Malaria: With the Hope for New Antimalarial Drug Discovery-An Update. *Advances in Medicine* **2023**, *2023*, 5060665.

90. Gupta, P.; Singh, L.; Singh, K., The hybrid antimalarial approach. In *Annual Reports in Medicinal Chemistry*, Kelly Chibale, Ed. Academic Press: 2019; Vol. 53, pp 73-105.

91. Njogu, P. M.; Okombo, J.; Chibale, K., Designed Hybrid Compounds for Tropical Parasitic Diseases. In *Design of Hybrid Molecules for Drug Development*, Michael Decker, Ed. Elsevier: 2017; pp 83-135.

92. Muregi, F. W.; Ishih, A., Next-Generation Antimalarial Drugs: Hybrid Molecules as a New Strategy in Drug Design. *Drug Development Research* **2010**, *71* (1), 20-32.

93. Meunier, B., Towards Antimalarial Hybrid Drugs. In *Polypharmacology in Drug Discovery*, Jens-Uwe Peters, Ed. 2012; pp 423-439.

94. Meunier, B., Hybrid Molecules with a Dual Mode of Action: Dream or Reality? *Accounts of Chemical Research* **2008**, *41* (1), 69-77.

95. Coslédan, F.; Fraisse, L.; Pellet, A.; Guillou, F.; Mordmüller, B.; Kremsner, P. G.; Moreno, A.; Mazier, D.; Maffrand, J. P.; Meunier, B., Selection of a trioxaquine as an antimalarial drug candidate. *Proceedings of the National Academy of Sciences of the United States of America* **2008**, *105* (45), 17579-84.

96. Dechy-Cabaret, O.; Benoit-Vical, F.; Loup, C.; Robert, A.; Gornitzka, H.; Bonhoure, A.; Vial, H.; Magnaval, J.-F.; Séguéla, J.-P.; Meunier, B., Synthesis and Antimalarial Activity of Trioxaquine Derivatives. *Chemistry – A European Journal* **2004**, *10* (7), 1625-1636.

97. Agarwal, D.; Gupta, R. D.; Awasthi, S. K., Are Antimalarial Hybrid Molecules a Close Reality or a Distant Dream? *Antimicrobial Agents and Chemotherapy* **2017**, *61* (5).

98. Oliveira, R.; Miranda, D.; Magalhães, J.; Capela, R.; Perry, M. J.; O'Neill, P. M.; Moreira, R.; Lopes, F., From hybrid compounds to targeted drug delivery in antimalarial therapy. *Bioorganic & Medicinal Chemistry* **2015**, *23* (16), 5120-5130.

99. Prasad Raiguru, B.; Panda, J.; Mohapatra, S.; Nayak, S., Recent developments in the synthesis of hybrid antimalarial drug discovery. *Bioorganic Chemistry* **2023**, *139*, 106706.

100. Lödige, M.; Hiersch, L., Design and Synthesis of Novel Hybrid Molecules against Malaria. *International Journal of Medicinal Chemistry* **2015**, *2015*, 458319.

101. Davioud-Charvet, E.; Delarue, S.; Biot, C.; Schwöbel, B.; Boehme, C. C.; Müssigbrodt, A.; Maes, L.; Sergheraert, C.; Grellier, P.; Schirmer, R. H.; Becker, K., A

Prodrug Form of a *Plasmodium falciparum* Glutathione Reductase Inhibitor Conjugated with a 4-Anilinoquinoline. *Journal of Medicinal Chemistry* **2001**, *44* (24), 4268-4276.

102. Fonte, M.; Fagundes, N.; Gomes, A.; Ferraz, R.; Prudêncio, C.; Araújo, M. J.; Gomes, P.; Teixeira, C., Development of a synthetic route towards N^4,N^9-disubstituted 4,9-diaminoacridines: On the way to multi-stage antimalarials. *Tetrahedron Letters* **2019**, *60* (17), 1166-1169.

103. Nqoro, X.; Tobeka, N.; Aderibigbe, B. A., Quinoline-Based Hybrid Compounds with Antimalarial Activity. *Molecules* **2017**, *22* (12), 2268.

104. Hu, Y.-Q.; Gao, C.; Zhang, S.; Xu, L.; Xu, Z.; Feng, L.-S.; Wu, X.; Zhao, F., Quinoline hybrids and their antiplasmodial and antimalarial activities. *European Journal of Medicinal Chemistry* **2017**, *139*, 22-47.

105. Lödige, M.; Lewis, M. D.; Paulsen, E. S.; Esch, H. L.; Pradel, G.; Lehmann, L.; Brun, R.; Bringmann, G.; Mueller, A.-K., A primaquine–chloroquine hybrid with dual activity against *Plasmodium* liver and blood stages. *International Journal of Medical Microbiology* **2013**, *303* (8), 539-547.

106. De Souza Pereira, C.; Costa Quadros, H.; Magalhaes Moreira, D. R.; Castro, W.; Santos De Deus Da Silva, R. I.; Botelho Pereira Soares, M.; Fontinha, D.; Prudêncio, M.; Schmitz, V.; Dos Santos, H. F.; Gendrot, M.; Fonta, I.; Mosnier, J.; Pradines, B.; Navarro, M., A Novel Hybrid of Chloroquine and Primaquine Linked by Gold(I): Multitarget and Multiphase Antiplasmodial Agent. *ChemMedChem* **2021**, *16* (4), 662-678.

107. De Souza Pereira, C.; Quadros, H. C.; Aboagye, S. Y.; Fontinha, D.; D'Alessandro, S.; Byrne, M. E.; Gendrot, M.; Fonta, I.; Mosnier, J.; Moreira, D. R. M.; Basilico, N.; Williams, D. L.; Prudêncio, M.; Pradines, B.; Navarro, M., A Hybrid of Amodiaquine and Primaquine Linked by Gold(I) Is a Multistage Antimalarial Agent Targeting Heme Detoxification and Thiol Redox Homeostasis. *Pharmaceutics* **2022**, *14* (6), 1251.

108. Peter, S.; Jama, S.; Alven, S.; Aderibigbe, B. A., Artemisinin and Derivatives-Based Hybrid Compounds: Promising Therapeutics for the Treatment of Cancer and Malaria. *Molecules* **2021**, *26* (24), 7521.

109. Capela, R.; Cabal, G. G.; Rosenthal, P. J.; Gut, J.; Mota, M. M.; Moreira, R.; Lopes, F.; Prudêncio, M., Design and evaluation of primaquine-artemisinin hybrids as a multistage antimalarial strategy. *Antimicrobial Agents and Chemotherapy* **2011**, *55* (10), 4698-706.

110. Miranda, D.; Capela, R.; Albuquerque, I. S.; Meireles, P.; Paiva, I.; Nogueira, F.; Amewu, R.; Gut, J.; Rosenthal, P. J.; Oliveira, R.; Mota, M. M.; Moreira, R.; Marti, F.; Prudêncio, M.; O'Neill, P. M.; Lopes, F., Novel Endoperoxide-Based Transmission-

Blocking Antimalarials with Liver- and Blood-Schizontocidal Activities. *ACS Medicinal Chemistry Letters* **2014**, *5* (2), 108-112.

111. Capela, R.; Magalhães, J.; Miranda, D.; Machado, M.; Sanches-Vaz, M.; Albuquerque, I. S.; Sharma, M.; Gut, J.; Rosenthal, P. J.; Frade, R.; Perry, M. J.; Moreira, R.; Prudêncio, M.; Lopes, F., Endoperoxide-8-aminoquinoline hybrids as dual-stage antimalarial agents with enhanced metabolic stability. *European Journal of Medicinal Chemistry* **2018**, *149*, 69-78.

112. Benoit-Vical, F.; Lelièvre, J.; Berry, A.; Deymier, C.; Dechy-Cabaret, O.; Cazelles, J.; Loup, C.; Robert, A.; Magnaval, J. F.; Meunier, B., Trioxaquines are new antimalarial agents active on all erythrocytic forms, including gametocytes. *Antimicrobial Agents and Chemotherapy* **2007**, *51* (4), 1463-72.

113. Pérez, B.; Teixeira, C.; Figueiras, M.; Gut, J.; Rosenthal, P. J.; Gomes, J. R. B.; Gomes, P., Novel cinnamic acid/4-aminoquinoline conjugates bearing non-proteinogenic amino acids: Towards the development of potential dual action antimalarials. *European Journal of Medicinal Chemistry* **2012**, *54*, 887-899.

114. Pérez, B.; Teixeira, C.; Gut, J.; Rosenthal, P. J.; Gomes, J. R. B.; Gomes, P., Cinnamic Acid/Chloroquinoline Conjugates as Potent Agents against Chloroquine-Resistant *Plasmodium falciparum*. *ChemMedChem* **2012**, *7* (9), 1537-1540.

115. Kanaani, J.; Ginsburg, H., Effects of cinnamic acid derivatives on *in vitro* growth of *Plasmodium falciparum* and on the permeability of the membrane of malaria-infected erythrocytes. *Antimicrobial Agents and Chemotherapy* **1992**, *36* (5), 1102-8.

116. Santos, M. M.; Moreira, R., Michael acceptors as cysteine protease inhibitors. *Mini-Reviews in Medicinal Chemistry* **2007**, *7* (10), 1040-50.

117. Pérez, B.; Teixeira, C.; Albuquerque, I. S.; Gut, J.; Rosenthal, P. J.; Gomes, J. R. B.; Prudêncio, M.; Gomes, P., *N*-Cinnamoylated Chloroquine Analogues as Dual-Stage Antimalarial Leads. *Journal of Medicinal Chemistry* **2013**, *56* (2), 556-567.

118. Pérez, B.; Teixeira, C.; Albuquerque, I. S.; Gut, J.; Rosenthal, P. J.; Prudêncio, M.; Gomes, P., PRIMACINS, *N*-cinnamoyl-primaquine conjugates, with improved liver-stage antimalarial activity. *MedChemComm* **2012**, *3* (9), 1170-1172.

119. Gomes, A.; Machado, M.; Lobo, L.; Nogueira, F.; Prudêncio, M.; Teixeira, C.; Gomes, P., *N*-Cinnamoylation of Antimalarial Classics: Effects of Using Acyl Groups Other than Cinnamoyl toward Dual-Stage Antimalarials. *ChemMedChem* **2015**, *10* (8), 1344-1349.

120. Chu, X. M.; Wang, C.; Wang, W. L.; Liang, L. L.; Liu, W.; Gong, K. K.; Sun, K. L., Triazole derivatives and their antiplasmodial and antimalarial activities. *European Journal of Medicinal Chemistry* **2019**, *166*, 206-223.

121. Abdul Rahman, S. M.; Bhatti, J. S.; Thareja, S.; Monga, V., Current development of 1,2,3-triazole derived potential antimalarial scaffolds: Structure- activity relationship (SAR) and bioactive compounds. *European Journal of Medicinal Chemistry* **2023**, *259*, 115699.

122. Ravindar, L.; Hasbullah, S. A.; Rakesh, K. P.; Hassan, N. I., Triazole hybrid compounds: A new frontier in malaria treatment. *European Journal of Medicinal Chemistry* **2023**, *259*, 115694.

123. Wadi, I.; Prasad, D.; Batra, N.; Srivastava, K.; Anvikar, A. R.; Valecha, N.; Nath, M., Targeting Asexual and Sexual Blood Stages of the Human Malaria Parasite *P. falciparum* with 7-Chloroquinoline-Based 1,2,3-Triazoles. *ChemMedChem* **2019**, *14* (4), 484-493.

124. Huang, G.; Solano, C. M.; Melendez, J.; Yu-Alfonzo, S.; Boonhok, R.; Min, H.; Miao, J.; Chakrabarti, D.; Yuan, Y., Discovery of fast-acting dual-stage antimalarial agents by profiling pyridylvinylquinoline chemical space via copper catalyzed azide-alkyne cycloadditions. *European Journal of Medicinal Chemistry* **2021**, *209*, 112889.

125. Pereira, J. A.; Pessoa, A. M.; Cordeiro, M. N.; Fernandes, R.; Prudêncio, C.; Noronha, J. P.; Vieira, M., Quinoxaline, its derivatives and applications: A State of the Art review. *European Journal of Medicinal Chemistry* **2015**, *97*, 664-72.

126. Suthar, S. K.; Chundawat, N. S.; Singh, G. P.; Padrón, J. M.; Jhala, Y. K., Quinoxaline: A comprehension of current pharmacological advancement in medicinal chemistry. *European Journal of Medicinal Chemistry Reports* **2022**, *5*, 100040.

127. Bonilla-Ramírez, L.; Galiano, S.; Quiliano, M.; Aldana, I.; Pabón, A., Primaquine–quinoxaline 1,4-di-*N*-oxide hybrids with action on the exo-erythrocytic forms of *Plasmodium* induce their effect by the production of reactive oxygen species. *Malaria Journal* **2019**, *18* (1), 201.

128. Bonilla-Ramirez, L.; Rios, A.; Quiliano, M.; Ramirez-Calderon, G.; Beltrán-Hortelano, I.; Franetich, J. F.; Corcuera, L.; Bordessoulles, M.; Vettorazzi, A.; López de Cerain, A.; Aldana, I.; Mazier, D.; Pabón, A.; Galiano, S., Novel antimalarial chloroquine- and primaquine-quinoxaline 1,4-di-*N*-oxide hybrids: Design, synthesis, *Plasmodium* life cycle stage profile, and preliminary toxicity studies. *European Journal of Medicinal Chemistry* **2018**, *158*, 68-81.

129. Kumar, R.; Thakur, A.; Sachin; Chandra, D.; Kumar Dhiman, A.; Kumar Verma, P.; Sharma, U., Quinoline-based metal complexes: Synthesis and applications. *Coordination Chemistry Reviews* **2024**, *499*, 215453.

130. Marcelino, P. R. F.; Moreira, M. B.; Lacerda, T. M.; da Silva, S. S., Metal-Based Drugs for Treatment of Malaria. In *Biomedical Applications of Metals*, Mahendra Rai; Avinash P. Ingle; Serenella Medici, Eds. Springer, Cham: 2018; pp 167-193.

131. Macedo, T. S.; Colina-Vegas, L.; M, D. A. P.; Navarro, M.; Barreto, B. C.; Oliveira, P. C.; Macambira, S. G.; Machado, M.; Prudêncio, M.; D'Alessandro, S.; Basilico, N.; Moreira, D. R.; Batista, A. A.; Soares, M. B., Chloroquine-containing organoruthenium complexes are fast-acting multistage antimalarial agents. *Parasitology* **2016**, *143* (12), 1543-56.

132. Macedo, T. S.; Villarreal, W.; Couto, C. C.; Moreira, D. R. M.; Navarro, M.; Machado, M.; Prudêncio, M.; Batista, A. A.; Soares, M. B. P., Platinum(ii)–chloroquine complexes are antimalarial agents against blood and liver stages by impairing mitochondrial function. *Metallomics* **2017**, *9* (11), 1548-1561.

133. Xiao, J.; Sun, Z.; Kong, F.; Gao, F., Current scenario of ferrocene-containing hybrids for antimalarial activity. *European Journal of Medicinal Chemistry* **2020**, *185*, 111791.

134. Nqoro, X.; Aderibigbe, B. A., 4-Aminoquinoline-ferrocene Hybrids as Potential Antimalarials. *Recent Patents on Anti-infective Drug Discovery* **2020**, *15* (2), 157-172.

135. Wani, W. A.; Jameel, E.; Baig, U.; Mumtazuddin, S.; Hun, L. T., Ferroquine and its derivatives: New generation of antimalarial agents. *European Journal of Medicinal Chemistry* **2015**, *101*, 534-551.

136. McCarthy, J. S.; Rückle, T.; Djeriou, E.; Cantalloube, C.; Ter-Minassian, D.; Baker, M.; O'Rourke, P.; Griffin, P.; Marquart, L.; Hooft van Huijsduijnen, R.; Möhrle, J. J., A Phase II pilot trial to evaluate safety and efficacy of ferroquine against early *Plasmodium falciparum* in an induced blood-stage malaria infection study. *Malaria Journal* **2016**, *15* (1), 469.

137. Matos, J.; Cruz, F. P. d.; Cabrita, É.; Gut, J.; Nogueira, F.; Rosário, V. E. d.; Moreira, R.; Rosenthal, P. J.; Prudêncio, M.; Gomes, P., Novel Potent Metallocenes against Liver Stage Malaria. *Antimicrobial Agents and Chemotherapy* **2012**, *56* (3), 1564-1570.

138. Singh, S.; Mandal, M. K.; Masih, A.; Saha, A.; Ghosh, S. K.; Bhat, H. R.; Singh, U. P., 1,3,5-Triazine: A versatile pharmacophore with diverse biological activities. *Archiv der Pharmazie* **2021**, *354* (6), 2000363.

139. Manohar, S.; Satya Pavan, V.; Taylor, D.; Kumar, D.; Ponnan, P.; Wiesner, L.; Rawat, D. S., Highly active 4-aminoquinoline–pyrimidine based molecular hybrids as potential next generation antimalarial agents. *RSC Advances* **2015**, *5* (36), 28171-28186.

140. Kumar, D.; Khan, S. I.; Tekwani, B. L.; Ponnan, P.; Rawat, D. S., Synthesis, antimalarial activity, heme binding and docking studies of 4-aminoquinoline–pyrimidine based molecular hybrids. *RSC Advances* **2014**, *4* (109), 63655-63669.

141. Maurya, S. S.; Bahuguna, A.; Khan, S. I.; Kumar, D.; Kholiya, R.; Rawat, D. S., *N*-Substituted aminoquinoline-pyrimidine hybrids: Synthesis, *in vitro* antimalarial activity evaluation and docking studies. *European Journal of Medicinal Chemistry* **2019**, *162*, 277-289.

142. Rodrigues, C. A.; Frade, R. F.; Albuquerque, I. S.; Perry, M. J.; Gut, J.; Machado, M.; Rosenthal, P. J.; Prudêncio, M.; Afonso, C. A.; Moreira, R., Targeting the erythrocytic and liver stages of malaria parasites with s-triazine-based hybrids. *ChemMedChem* **2015**, *10* (5), 883-90.

143. Singh, K.; Kaur, H.; Chibale, K.; Balzarini, J.; Little, S.; Bharatam, P. V., 2-Aminopyrimidine based 4-aminoquinoline anti-plasmodial agents. Synthesis, biological activity, structure–activity relationship and mode of action studies. *European Journal of Medicinal Chemistry* **2012**, *52*, 82-97.

144. Singh, K.; Kaur, H.; Smith, P.; de Kock, C.; Chibale, K.; Balzarini, J., Quinoline–Pyrimidine Hybrids: Synthesis, Antiplasmodial Activity, SAR, and Mode of Action Studies. *Journal of Medicinal Chemistry* **2014**, *57* (2), 435-448.

145. Kaur, H.; Machado, M.; de Kock, C.; Smith, P.; Chibale, K.; Prudêncio, M.; Singh, K., Primaquine–pyrimidine hybrids: Synthesis and dual-stage antiplasmodial activity. *European Journal of Medicinal Chemistry* **2015**, *101*, 266-273.

146. Kumar, S. P.; Glória, P. M. C.; Gonçalves, L. M.; Gut, J.; Rosenthal, P. J.; Moreira, R.; Santos, M. M. M., Squaric acid: a valuable scaffold for developing antimalarials? *MedChemComm* **2012**, *3* (4), 489-493.

147. Ribeiro, C. J. A.; Kumar, S. P.; Gut, J.; Gonçalves, L. M.; Rosenthal, P. J.; Moreira, R.; Santos, M. M. M., Squaric acid/4-aminoquinoline conjugates: Novel potent antiplasmodial agents. *European Journal of Medicinal Chemistry* **2013**, *69*, 365-372.

148. Ribeiro, C. J. A.; Espadinha, M.; Machado, M.; Gut, J.; Gonçalves, L. M.; Rosenthal, P. J.; Prudêncio, M.; Moreira, R.; Santos, M. M. M., Novel squaramides with *in vitro* liver stage antiplasmodial activity. *Bioorganic & Medicinal Chemistry* **2016**, *24* (8), 1786-1792.

149. Solaja, B. A.; Opsenica, D.; Smith, K. S.; Milhous, W. K.; Terzić, N.; Opsenica, I.; Burnett, J. C.; Nuss, J.; Gussio, R.; Bavari, S., Novel 4-aminoquinolines active against chloroquine-resistant and sensitive *P. falciparum* strains that also inhibit botulinum serotype A. *Journal of Medicinal Chemistry* **2008**, *51* (15), 4388-91.

150. Terzić, N.; Konstantinović, J.; Tot, M.; Burojević, J.; Djurković-Djaković, O.; Srbljanović, J.; Štajner, T.; Verbić, T.; Zlatović, M.; Machado, M.; Albuquerque, I. S.; Prudêncio, M.; Sciotti, R. J.; Pecic, S.; D'Alessandro, S.; Taramelli, D.; Šolaja, B. A., Reinvestigating Old Pharmacophores: Are 4-Aminoquinolines and Tetraoxanes Potential Two-Stage Antimalarials? *Journal of Medicinal Chemistry* **2016**, *59* (1), 264-281.

151. Pérez, B.; Teixeira, C.; Gomes, A. S.; Albuquerque, I. S.; Gut, J.; Rosenthal, P. J.; Prudêncio, M.; Gomes, P., *In vitro* efficiency of 9-(*N*-cinnamoylbutyl)aminoacridines against blood- and liver-stage malaria parasites. *Bioorganic & Medicinal Chemistry Letters* **2013**, *23* (3), 610-613.

152. Yu, X.-M.; Ramiandrasoa, F.; Guetzoyan, L.; Pradines, B.; Quintino, E.; Gadelle, D.; Forterre, P.; Cresteil, T.; Mahy, J.-P.; Pethe, S., Synthesis and Biological Evaluation of Acridine Derivatives as Antimalarial Agents. *ChemMedChem* **2012**, *7* (4), 587-605.

153. Gomes, A.; Pérez, B.; Albuquerque, I.; Machado, M.; Prudêncio, M.; Nogueira, F.; Teixeira, C.; Gomes, P., *N*-Cinnamoylation of Antimalarial Classics: Quinacrine Analogues with Decreased Toxicity and Dual-Stage Activity. *ChemMedChem* **2014**, *9* (2), 305-310.

154. Upadhyay, C.; Chaudhary, M.; De Oliveira, R. N.; Borbas, A.; Kempaiah, P.; S, P.; Rathi, B., Fluorinated scaffolds for antimalarial drug discovery. *Expert Opinion on Drug Discovery* **2020**, *15* (6), 705-718.

CHAPTER II

On the way to multi-stage antimalarials

This chapter describes the discovery of new 4-aminoacridine and 4,9-diaminoacridine derivatives as promising multi-stage antiplasmodial hits.

Contents:

Article I

4,9-Diaminoacridines and 4-Aminoacridines as Dual-Stage Antiplasmodial Hits

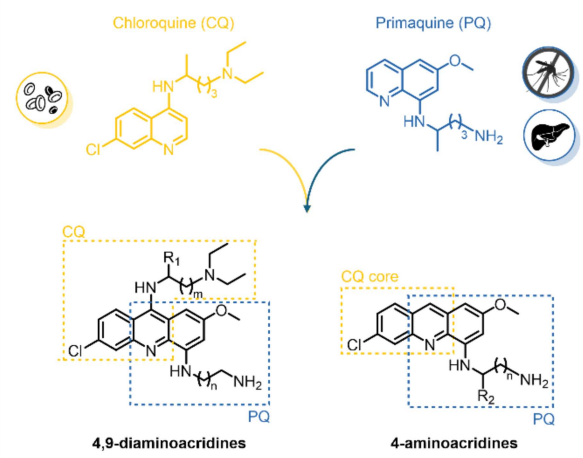
Article II

Improved synthesis of antiplasmodial 4-aminoacridines and 4,9-diaminoacridines

Article I

4,9-Diaminoacridines and 4-Aminoacridines as Dual-Stage Antiplasmodial Hits

Mélanie Fonte, Natália Tassi, Diana Fontinha, Inés Bouzón-Arnáiz, Ricardo Ferraz, Maria J. Araújo, Xavier Fernàndez-Busquets, Miguel Prudêncio, Paula Gomes, Cátia Teixeira.



ChemMedChem, **2021**, 16, 788–792 doi: 10.1002/cmdc.202000740

Summary

There has been growing interest in developing multi-target antimalarial drugs, since as targeting more than one process in the *Plasmodium* life cycle may potentially increase efficiency, while decreasing the chance for emergence of parasite resistance. In this connection, the work presented in the following article describes the initial phase of this doctoral project that consisted in the development of two novel ACR-based families of compounds - 4-aminoacridines and 4,9-diaminoacridines - which incorporate the structural features of PQ and CQ, as potential multi-stage antiplasmodial hits. Compounds were obtained in moderate to good yields through a synthetic pathway developed in-house, and their chemical structures and high purity were confirmed using spectroscopy and chromatography techniques, respectively. As predicted, the merge hybrids developed showed dual action against blood and liver forms of *Plasmodium*.

Declaration of authorship of published article I: 4,9-Diaminoacridines and 4-Aminoacridines as Dual-Stage Antiplasmodial Hits[1]

I, Mélanie Fonte, declare that the experimental design/methodology, laboratory work involving the synthesis and characterization of all compounds used in this study, and the data analysis and discussion were carried out by me, under the supervision of Prof. Paula Gomes, Dr. Cátia Teixeira and Dr. Miguel Prudêncio. I was also responsible for the writing of the article's original draft that was next corrected and validated by all the co-authors.

We, Cátia Teixeira, Paula Gomes, and Miguel Prudêncio, as Mélanie Fonte's supervisors, hereby confirm that the information above is correct.

Mélanie Fonte

Mélanie Fonte

Paula Gomes | Cátia Teixeira | Miguel Prudêncio

[1] Copyright Wiley-VCH GmbH. Reproduced with permission.

ChemMedChem
Communications
doi.org/10.1002/cmdc.202000740
Chemistry Europe
European Chemical Societies Publishing

Check for updates

4,9-Diaminoacridines and 4-Aminoacridines as Dual-Stage Antiplasmodial Hits

Mélanie Fonte[+],[a] Natália Tassi[+],[a] Diana Fontinha,[b] Inés Bouzón-Arnáiz,[c, d] Ricardo Ferraz,[a, e] Maria J. Araújo,[a] Xavier Fernàndez-Busquets,[c, d] Miguel Prudêncio,[b] Paula Gomes,[a] and Cátia Teixeira*[a]

Multi-stage drugs have been prioritized in antimalarial drug discovery, as targeting more than one process in the *Plasmodium* life cycle is likely to increase efficiency, while decreasing the chances of emergence of resistance by the parasite. Herein, we disclose two novel acridine-based families of compounds that combine the structural features of primaquine and chloroquine. Compounds prepared and studied thus far retained the *in vitro* activity displayed by the parent drugs against the erythrocytic stages of chloroquine-sensitive and -resistant *Plasmodium falciparum* strains, and against the hepatic stages of *Plasmodium berghei*, hence acting as dual-stage antiplasmodial hits.

The eradication of malaria, one of the deadliest infectious diseases in the world,[1] remains to be achieved. This is partly due to the emergence of parasite resistance to virtually all the antimalarial drugs introduced in the clinic over the last decades.[1,2] In endemic areas, where chloroquine-resistant *Plasmodium falciparum* prevails, artemisinin combination therapies (ACT) are the antimalarial treatment currently recommended by the WHO. However, reported resistance to ACT in western Cambodia and across the Greater Mekong subregion is threatening the efficacy of these first-line therapies, for which suitable alternatives remain unavailable.[1–3] Therefore, while an effective antimalarial vaccine remains elusive,[4] new efforts bend towards the discovery of multi-target antiplasmodials, capable of targeting more than one process in the malaria parasite's life cycle.[5] In the pursuit of such efforts, one must bear in mind that only cost-effective approaches towards affordable medicines will have a real impact in the fight against malaria, which mainly affects low to middle income countries. Thus, priority should be given to the repurposing of existing drugs for malaria,[6] or to the rescuing of antimalarial pharmacophores towards the development of new multi-target compounds.[7]

Quinacrine (QN, Figure 1) was the first clinically tested synthetic antimalarial drug;[8] it is a potent blood schizonticide, but its serious adverse effects led to its rapid replacement by chloroquine (CQ, Figure 1), whose efficiency, oral bioavailability, and safety were far superior to those of QN.[2] Interestingly, "disassembly" of the QN structure shows it as a "merge" of the structure of CQ with the heterocycle core of primaquine (PQ, Figure 1). PQ is another emblematic antiplasmodial, active against all liver forms of the parasite, and able to block parasite transmission from the human host to the mosquito vector.[2] In view of this, and based on previous promising results for similar compounds,[9] we hypothesized that 4,9-diaminoacridines (**1**) and 4-aminoacridines (**2**) might act as multi-target antiplasmodials, since compounds **1** embed the structures of both CQ and

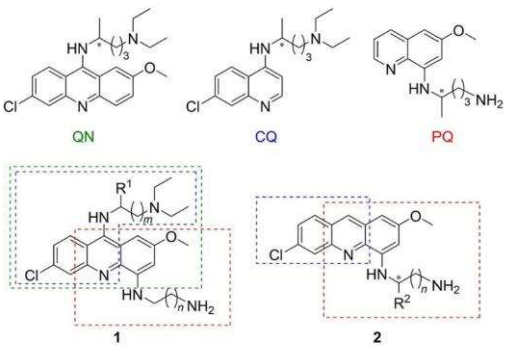


Figure 1. Structures of antimalarials quinacrine (QN), chloroquine (CQ), and primaquine (PQ), as well as the 4,9-diaminoacridines (1) and 4-aminoacridines (2) in this work.

[a] *M. Fonte,[+] N. Tassi,[+] Dr. R. Ferraz, Prof. M. J. Araújo, Prof. P. Gomes, Dr. C. Teixeira*
LAQV-REQUIMTE, Departamento de Química e Bioquímica
Faculdade de Ciências, Universidade do Porto
R. do Campo Alegre, 4169-007 Porto (Portugal)
E-mail: catia.teixeira@fc.up.pt
[b] *Dr. D. Fontinha, Dr. M. Prudêncio*
Instituto de Medicina Molecular João Lobo Antunes
Faculdade de Medicina, Universidade de Lisboa
Av. Prof. Egas Moniz, 1649-028 Lisboa (Portugal)
[c] *I. Bouzón-Arnáiz, Dr. X. Fernàndez-Busquets*
Nanomalaria Group, Institute for Bioengineering of Catalonia (IBEC)
The Barcelona Institute of Science and Technology
Baldiri Reixac, 10–12, 08028 Barcelona (Spain)
[d] *I. Bouzón-Arnáiz, Dr. X. Fernàndez-Busquets*
Barcelona Institute for Global Health (ISGlobal)
Hospital Clínic-Universitat de Barcelona
Carrer del Rosselló, 132, 08036 Barcelona (Spain)
[e] *Dr. R. Ferraz*
Ciências Químicas e das Biomoléculas
Escola Superior de Saúde, Politécnico do Porto
R. Dr. António Bernardino de Almeida 400
4200-072 Porto (Portugal)
[+] *These authors contributed equally to this work.*
Supporting information for this article is available on the WWW under https://doi.org/10.1002/cmdc.202000740

© 2020 Wiley-VCH GmbH

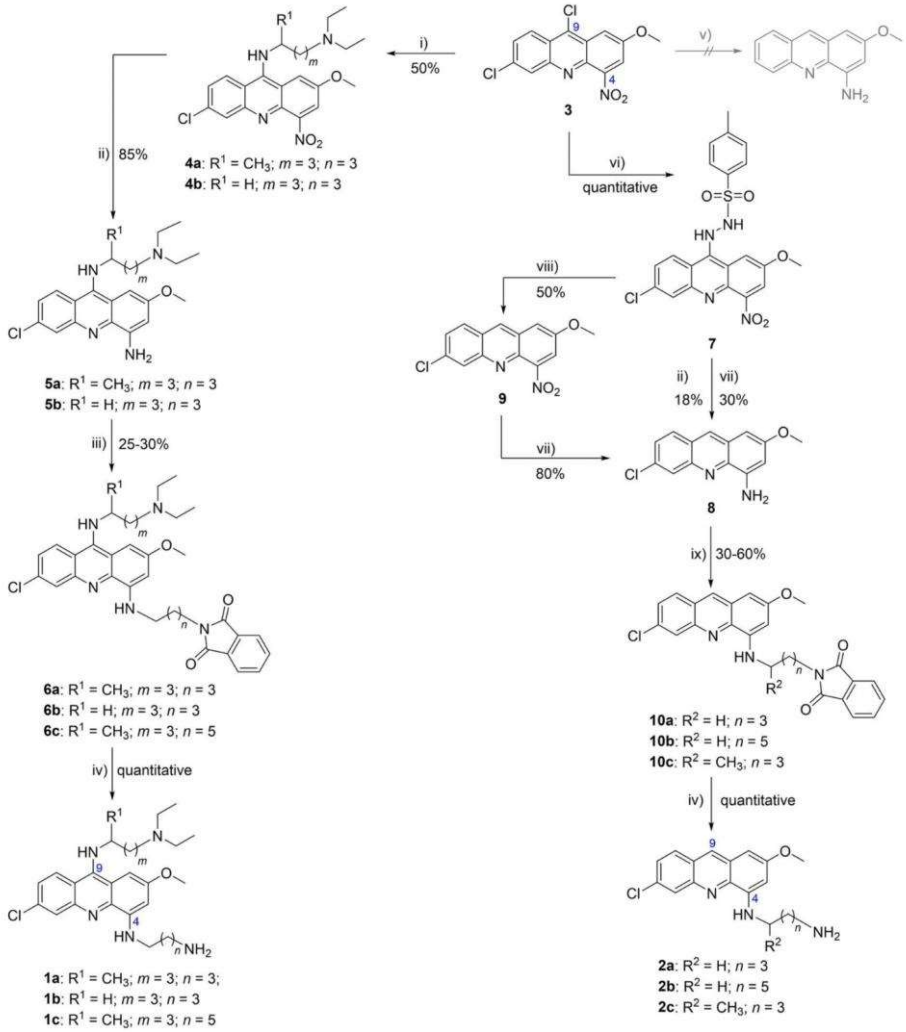
18607187, 2021, 5, Downloaded from https://chemistry-europe.onlinelibrary.wiley.com/doi/10.1002/cmdc.202000740 by Cochrane Portugal, Wiley Online Library on [10/11/2022]. See the Terms and Conditions (https://onlinelibrary.wiley.com/terms-and-conditions) on Wiley Online Library for rules of use; OA articles are governed by the applicable Creative Commons License

ChemMedChem
Communications
doi.org/10.1002/cmdc.202000740
Chemistry Europe
European Chemical Societies Publishing

18607187, 2021, 5, Downloaded from https://chemistry-europe.onlinelibrary.wiley.com/doi/10.1002/cmdc.202000740 by Cochrane Portugal, Wiley Online Library on [10/11/2022]. See the Terms and Conditions (https://onlinelibrary.wiley.com/terms-and-conditions) on Wiley Online Library for rules of use; OA articles are governed by the applicable Creative Commons License

PQ, and compounds **2** combine the heterocyclic core of CQ with PQ.

In view of the above, we have synthesized 4,9-diaminoacridines **1a–c** and 4-aminoacridines **2a–c**, as depicted in Scheme 1. The synthetic route towards 4,9-diaminoacridines **1** had been previously reported by us,[10] whereas the synthesis of 4-aminoacridines **2** starting from **3**, the common precursor to both compounds **1** and **2**, was established in the present work, as follows. The first step was the reduction of the nitro group, along with the removal of chlorine in position 9 of the acridine ring in 6,9-dichloro-2-methoxy-4-nitroacridine **3**; classical catalytic hydrogenation using H_2(g) and Pd/C (step v in Scheme 1) did not afford the desired compound, as nonselective removal of the two chlorine atoms occurred (data not shown). Alternatively, we applied a procedure early reported by Scovill et al.,[9] whereby **3** was converted into the *p*-toluene sulfonyl hydrazide (*p*-TSH) **7** (step vi). This intermediate was subsequently reduced to aniline **8**, for which either $SnCl_2$/HCl (step ii) or hydrazine hydrate and Pd/C (step vii) were used. In both cases, the desired product was obtained, at 18 and 30% yields,



Scheme 1. Synthetic routes towards 4,9-diaminoacridines **1** and 4-aminoacridines **2**. i) phenol (15 equiv.), Cs_2CO_3 (1 equiv.), anhydrous DMSO, 4 Å molecular sieves, 100 °C, 2 h, then diamine (4 equiv.), 100 °C, 4 h; ii) $SnCl_2$ (5 equiv.), 37% aq. HCl, 0→40 °C, 30 min; iii) *N*-(*n*-bromoalkyl)phthalimide (3 equiv.), CH_3COONa (3 equiv.), CH_3CH_2OH, microwave (MW) heating (100 W, 120 °C) in a pressurized vial (100 psi), 2.5 h; iv) hydrazine monohydrate (40 equiv.), tetrahydrofuran (THF), 60 °C, 72 h; v) H_2 (50 psi), Pd/C, CH_3OH, RT, 5 h; vi) *p*-TSH (1 equiv.), $CHCl_3$, RT, 24 h; vii) hydrazine monohydrate (10 equiv), Pd/C (10% wt), CH_3OH, 80 °C, 1–3 h; viii) ethylene glycol/H_2O (3:1), Na_2CO_3 (0.0625 M), 95 °C, 1.5 h; ix) *N*-(*n*-bromoalkyl)phthalimide (3 equiv.), Et_3N (3 equiv.), CH_3CH_2OH, MW heating (100 W, 120 °C) in a pressurized vial (100 psi), 3 h.

© 2020 Wiley-VCH GmbH

ChemMedChem
Communications
doi.org/10.1002/cmdc.202000740
Chemistry Europe
European Chemical Societies Publishing

18607187, 2021, 5, Downloaded from https://chemistry-europe.onlinelibrary.wiley.com/doi/10.1002/cmdc.202000740 by Cochrane Portugal, Wiley Online Library on [10/11/2022]. See the Terms and Conditions (https://onlinelibrary.wiley.com/terms-and-conditions) on Wiley Online Library for rules of use; OA articles are governed by the applicable Creative Commons License

respectively. An alternative two-step (steps viii and vii) procedure, via cleavage of the *p*-TSH moiety in **7** using Na_2CO_3 in aqueous ethylene glycol to give **9** and subsequent reduction of the latter with hydrazine hydrate and Pd/C to afford **8**, increased the overall yield to 40%. Aniline **8** was next alkylated with the appropriate *N*-(*N*-bromoalkyl)phthalimide, as previously reported by us.[10] This afforded compounds **10a–c** in moderate yields (30-60%), which were quantitatively converted into the respective final 4-aminoacridines **2a–c** by hydrazinolysis (step iv) using excess hydrazine monohydrate in refluxing tetrahydrofuran (THF). Detailed procedures and relevant spectroscopic data on intermediate and final compounds are given in the Supporting Information.

Target compounds **1a–c** and **2a–c**, as well as **4a**, **5a**, and **6a**, all of which are synthetic precursors of **1a**, were evaluated *in vitro* for their i) activity against erythrocytic forms of CQ-sensitive 3D7, and CQ-resistant W2 *P. falciparum* strains, ii) haemolytic effects, iii) activity against the hepatic stages of *Plasmodium berghei*, and iv) toxicity to human hepatic cells (Huh7 cell line). All the compounds exhibited antimalarial activity against blood forms of CQ-sensitive (3D7) and CQ-resistant (W2) *P. falciparum* parasites (Table 1), although those of 4-aminoacridines **2** were quite modest. Interestingly, the 4,9-diaminoacridines **1** showed better activity than compounds **2**, emphasizing the importance of the aminoalkyl chain in position 9 of the acridine ring, in close similarity to the structures of QN and CQ. Also, our data suggest that the length of the side chains at both positions 9 and 4 of the acridine ring influences the activity of 4,9-diaminoacridines **1**. Specifically, increasing the length of the side chain at position 4 from four (**1a**) to six (**1c**) carbons improved the activity against 3D7 and W2 strains of *P. falciparum* twofold and 12-fold, respectively. In turn, changes in the side chain at position 9 did not significantly affect activity against the 3D7 strain, but the IC_{50} value against the W2 strain decreased by nearly ten-fold when changing from four (**1a**) to three (**1b**) carbon atoms. Yet, as these two compounds also differ in R^1 (methyl in **1a** and hydrogen in **1b**), we cannot establish, at this stage, which of these two structural features, or both, lead to the observed difference, and why. Intermediates **4a**, **5a** and **6a** also showed interesting results, particularly against the CQ-sensitive 3D7 strain. Remarkably, neither any of these synthetic precursors of **1a**, nor any of the target compounds **1a–c** or **2a–c** were haemolytic up to 10 μM (Figure S1 in the Supporting Information).

Table 1. *In vitro* activity of **1a–c**, **2a–c**, and **9–11a**, against blood-stage *P. falciparum* (CQ-sensitive and -resistant strains 3D7 and W2, respectively) and liver-stage *P. berghei* parasites. Data for reference drugs are also included, for comparison.

Compound	IC_{50} [μM] blood-stage[c] *Pf* 3D7	*Pf* W2	IC_{50} [μM] liver-stage[c]
4a	0.28 ± 0.20	0.91 ± 0.23	ND[a]
5a	0.45 ± 0.22	0.49 ± 0.24	ND
6a	0.16 ± 0.22	0.98 ± 0.24	ND
1a	0.68 ± 0.24	6.17 ± 0.23	11.02 ± 0.44
1b	0.44 ± 0.21	0.66 ± 0.25	ND
1c	0.26 ± 0.35	0.49 ± 0.23	ND
2a	5.64 ± 0.22	5.14 ± 0.23	2.22 ± 0.51
2b	> 10	4.17 ± 0.23	1.64 ± 0.30
2c	> 10	2.39 ± 0.24	2.04 ± 0.38
CQ	0.02[b]	0.23[b]	–
QN	0.10[b]	0.16[b]	–
PQ	–	–	7.5[b]

[a] ND: Not determined; [b] Value taken from our previous work.[11]; [c] IC_{50} determination was carried out in two independent biological replicates. In each determination, all compound concentrations were tested in three technical replicates.

The effects of the compounds on hepatic *P. berghei* parasites and their host cells (Huh7) were further evaluated at 1 and 10 μM. As shown in Figure 2, 4-aminoacridines **2** appears to be slightly more active at 1 μM, except for **2b** that is inactive, than compounds **1** against liver stage *P. berghei*. On the other hand, at 10 μM both compounds **1** and **2** present similar activities, except for **1a** that is less active, but compounds **2** were not cytotoxic at that concentration unlike compounds **1**. The activities of compounds selected as most promising based on activity and cytotoxicity were quantitatively compared (Table 1). Relevantly, IC_{50} values of compounds **2** were roughly 3 to 5 times lower than that of the reference liver stage antiplasmodial drug, PQ. This indicates the relevance of having the side chain at position 4 of the acridine ring, in close similarity with the structure of PQ itself, to retain selective action against liver-stage forms of *Plasmodia*, and which should be further confirmed with a more complete structure-activity relationships (SAR) study. Moreover, these results suggest that fusion of the chlorobenzene ring (affording the 4-aminoacridine moiety) to the original 8-aminoquinoline ring of parent PQ is advantageous for liver stage activity, with no apparent increase in compound cytotoxicity (PQ vs. **2a–c**, Figure 2). Regarding compounds **1** and their respective precursors, all but **1a** were significantly active at 10 μM, although some 4,9-diaminoacridines (**1c, 5a** and **6a**) were highly cytotoxic at this concentration. Although the data set is not large enough to establish solid SAR, it seems that a decrease in length of the side chain at position 9 from **1a** to **1b** increases activity at the expense of a small increase in cytotoxicity. Interestingly, such small structural changes in the side chain at position 9, important to blood-stage activity, leads also to an increase in liver-stage activity (Figure 2). These results emphasize the importance of conducting an extensive SAR study to establish how liver stage activity can be modulated through structural changes at position 9. We also observed that increasing length of the side chain at position 4 (**1a** vs. **1c**) seems to improve liver stage activity and cause a significant increase in cytotoxicity.

Collectively, our findings show that the compounds reported herein, which can be regarded as a structural merge between classical antimalarial drugs PQ and CQ, and also as analogues of QN, define two novel classes of antimalarial hits. Logically, optimization of these structures is needed towards the development of more potent dual-stage antiplasmodial action and lower cytotoxicity. Yet, the robust synthetic routes now established for both families, and the *in vitro* data obtained thus far pave the way to the attainment of this goal. Also, the most promising compounds will be further evaluated for their gametocytocidal activity, which may hopefully establish them as triple-stage antimalarial hits.

© 2020 Wiley-VCH GmbH

ChemMedChem
Communications
doi.org/10.1002/cmdc.202000740
Chemistry Europe
European Chemical Societies Publishing

18607187, 2021, 5, Downloaded from https://chemistry-europe.onlinelibrary.wiley.com/doi/10.1002/cmdc.202000740 by Cochrane Portugal, Wiley Online Library on [10/11/2022]. See the Terms and Conditions (https://onlinelibrary.wiley.com/terms-and-conditions) on Wiley Online Library for rules of use; OA articles are governed by the applicable Creative Commons License

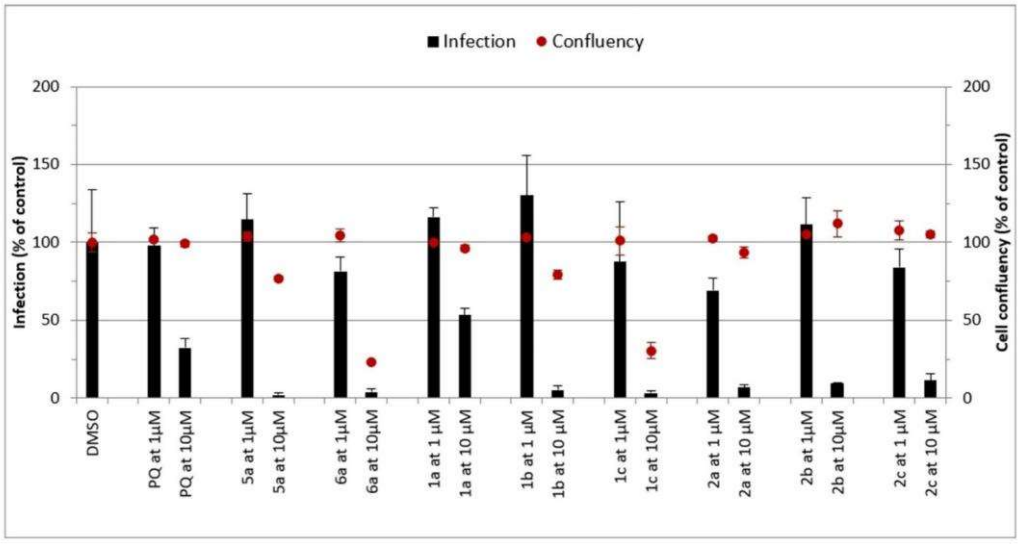


Figure 2. Activity of 1 a–c, 2 a–c, 5 a, and 6 a against liver forms of *P. berghei*, and toxicity towards human hepatocytes (Huh7 cell line). PQ used as reference drug.

Experimental Section

Compounds **1** and **3–6** were prepared as previously described, and their structural analyses (Supporting Information) agreed with formerly reported data.[10]

Synthesis of 6-chloro-2-methoxy-4-nitro-9-[(*p*–toluenesulfonyl) hydrazine]acridine (7): a solution of *p*-toluenesulfonyl hydrazide in $CHCl_3$ was added dropwise to a solution of compound **3** in $CHCl_3$. After stirring for 24 h, product **7** was precipitated with cold $CHCl_3$ and isolated in quantitative yield by vacuum filtration.

Synthesis of 6-chloro-2-methoxy-4-aminoacridine (8): compound **7** and Pd/C (10% wt) were suspended in CH_3OH and the mixture refluxed at 80 °C. Hydrazine hydrate (10 equiv.) was then added and the reaction mixture kept in reflux for 3 or 1 h (step xiii or step xv, respectively). Pd/C was next removed by filtration through Celite, and the filtrate evaporated to dryness. The residue obtained was dissolved in CH_2Cl_2 and the solution obtained was washed with saturated aq. $NaCO_3$ (3×50 mL) followed by saturated aq. NaCl (1× 50 mL). The organic layer was isolated and next dried over anhydrous $NaSO_4$, filtered, and the filtrate evaporated to dryness under reduced pressure. The crude product thus obtained was further purified by column chromatography on silica gel, using CH_2Cl_2 as mobile phase, affording **8**.

Synthesis of 6-chloro-2-methoxy-4-nitroacridine (9): compound 7 and Na_2CO_3 (6.25×10^{-2} M) were dissolved in ethylene glycol/water (18/9 mL). The reaction mixture was kept under reflux at 95 °C for 1,5 h. Next, the mixture was poured onto cold water, and the resulting black precipitate was isolated by vacuum filtration and next dissolved in CH_2Cl_2. The resulting solution was washed with saturated aq. $NaHCO_3$ (3×50 mL) followed by saturated aq. NaCl (1×50 mL). The organic layer was isolated and then dried over anhydrous Na_2SO_4, and the filtrate evaporated to dryness under reduced pressure. The crude product thus obtained was purified by column chromatography on silica gel, using CH_2Cl_2 as mobile phase, affording **9**.

Synthesis of compounds 10 a–c: triethylamine (3 equiv.) and the relevant *N*-(*n*-bromoalkyl)phthalimide (3 equiv.) were added to a solution of **8** in CH_3CH_2OH. The reaction mixture was transferred into a reaction vial that was next sealed and subjected to microwave (MW) irradiation (100 W); the reaction proceeded under MW heating for 3 h at 120 °C and 100 psi. Aliquots of triethylamine (3 equiv.) and the relevant *N*-(*n*-bromoalkyl)phthalimide (3 equiv.) were added to the reaction vial every 30 min. Once the reaction was halted, the solvent was removed under reduced pressure and the residue was next dissolved in CH_2Cl_2. The resulting solution was washed with saturated aq. $NaHCO_3$ (3×50 mL) and then with saturated aq. NaCl (1×50 mL). The organic layer was collected, dried over anhydrous Na_2SO_4 and filtered. The filtrate was next evaporated to dryness under reduced pressure, to afford the crude product that was partially purified by column chromatography on silica gel using hexane/ethyl acetate (4:1 *v/v*) as mobile phase. Fractions containing the target product were pooled and the solvent removed under reduced pressure. The residue was dissolved in CH_2Cl_2, 85.5% aq. H_3PO_4 was added dropwise, and the solution stirred for approximately 30 min. The liquid phase was removed by decantation and the precipitate formed, and it was washed three times with CH_2Cl_2, every time discarding the solvent also by decantation. Aq. 2 M NaOH was then added to the solid residue and the resulting solution was extracted with CH_2Cl_2 (3× 50 mL). The organic layer was collected, dried over anhydrous Na_2SO_4 and filtered. The filtrate was next evaporated to dryness under reduced pressure to afford compounds **10 a–c**.

Synthesis of compounds 2 a–c:To a solution of the relevant compound **15** in THF, $NH_2NH_2.H_2O$ (40 equiv.) was added. The reaction mixture was left under stirring at 60 °C until the reaction was completed, according to TLC analysis (ca. 48 h). The solvent was removed by evaporation under reduced pressure, the residue dissolved in CH_2Cl_2, and washed with saturated aq. $NaHCO_3$ (3× 50 mL) and saturated aq. NaCl (1×50 mL). The organic layer was collected and dried over anhydrous Na_2SO_4, filtered, and the filtrate evaporated to dryness under reduced pressure to afford the target

© 2020 Wiley-VCH GmbH

ChemMedChem
Communications
doi.org/10.1002/cmdc.202000740
Chemistry Europe
European Chemical Societies Publishing

compounds **2a–c**. The compounds used in biological assays were confirmed to have at least 95% purity, based on peak areas obtained through HPLC analyses that were run as detailed in the Supporting Information.

***In vitro* liver-stage assays**: *In vitro* inhibition of liver-stage infection by test compounds was determined by measuring the luminescence intensity in Huh7 cells infected with a firefly luciferase-expressing *P. berghei* line, PbGFP-Luccon, as previously described.[12] Huh7 cells were cultured in RPMI 1640 medium supplemented with 10% *v/v* fetal calf serum, 1% *v/v* nonessential amino acids, 1% *v/v* penicillin/streptomycin, 1% *v/v* glutamine, and 10 mM 4-(2-hydroxyethyl)-1-piperazineethanesulfonic acid (HEPES), pH 7, and maintained at 37 °C with 5% CO_2. For infection assays, Huh7 cells were seeded in 96-well plates the day before drug treatment and infection. Culture medium in the wells was replaced by infection medium (culture medium supplemented with 50 μg/mL gentamicin and 0.8 μg/mL amphotericin B) containing the appropriate concentration of each compound approximately 1 h prior to infection with sporozoites freshly obtained through disruption of salivary glands of infected female *Anopheles stephensi* mosquitoes. For control cells, culture medium was replaced by medium containing equivalent amounts of DMSO, the compounds solvent. After 48 h of infection, inhibition of infection was measured and the effect of the compounds on the viability of Huh7 cells was assessed by the AlamarBlue assay (Invitrogen) using the manufacturer's protocol. Nonlinear regression analysis was employed to fit the normalized results of the dose-response curves, and IC_{50} values were determined using Prism 8.0 (GraphPad software, La Jolla California USA).

Cytotoxicity was inferred from the cell confluency data. As a control, Huh7 cells were infected in the presence of a percentage of DMSO that mimics that of compound samples (0.01%), and that is known to not be cytotoxic. All compound data was then normalized to the DMSO control. Therefore, a reduction in cell confluency, as compared to the DMSO control, is indicative of cytotoxicity.

Ethics statement: The human blood used in this work was commercially obtained from the *Banc de Sang i Teixits* (www.bancsang.net). Blood was not specifically collected for this research; the purchased units had been discarded for transfusion, usually because of an excess of blood relative to anticoagulant solution. Prior to their use, blood units underwent the analytical checks specified in the current legislation. Before being delivered to us, unit data were anonymized and irreversibly dissociated, and any identification tag or label had been removed in order to guarantee the non-identification of the blood donor. No blood data were or will be supplied, in accordance with the current Spanish *Ley Orgánica de Protección de Datos* and *Ley de Investigación Biomédica*. The blood samples will not be used for studies other than those made explicit in this research. The studies reported here were performed in accordance with the current Spanish *Ley Orgánica de Protección de Datos* and *Ley de Investigación Biomédica* and under protocols reviewed and approved by the Ethical Committee on Clinical Research from the *Hospital Clínic de Barcelona* (Reg. HCB/2018/1223, January 23, 2019).

Acknowledgements

This work was developed within scope of projects UIDB/50006/2020, PTDC/BTM-SAL/29786/2017 and PTDC/SAU-INF/29550/2017, funded by Fundação para a Ciência e Tecnologia (FCT, Portugal). X.F.-B. was funded by i) The Spanish Ministry of Science, Innovation and Universities (http://www.ciencia.gob.es/), grant no. RTI2018-094579-B–I00 (which included FEDER funds), and ii) Generalitat de Catalunya, Spain (http://agaur.gencat.cat/), grant no. 2017-SGR-908. M.F. thanks FCT for doctoral grant SFRH/BD/147345/2019.

Conflict of Interest

The authors declare no conflict of interest.

Keywords: acridines · antimalarial activity · blood-stage · liver-stage · malaria · Plasmodium · synthesis

[1] *World Malaria Report 2019, World Health Organization*, https://www.who.int/publications/i/item/world-malaria-report-2019 (accessed on 10th september 2020).
[2] C. Teixeira, N. Vale, B. Pérez, A. Gomes, J. R. B. Gomes, P. Gomes, *Chem. Rev.* **2014**, *114*, 11164–11220.
[3] Artemisinin resistance and artemisinin-based combination therapy efficacy - status report **2018**, World Health Organization, https://apps.who.int/iris/handle/10665/274362 (accessed on 10th september 2020).
[4] S. J. Draper, B. K. Sack, C. R. King, C. M. Nielsen, J. C. Rayner, M. K. Higgins, C. A. Long, R. A. Seder, *Cell Host Microbe* **2018**, *24*, 43–56.
[5] a) D. Agarwal, R. D. Gupta, S. K. Awasthi, *Antimicrob. Agents Chemother.* **2017**, *61*, e00249–00217; b) G. Bérubé, *Expert Opin. Drug Discovery* **2016**, *11*, 281–305; c) B. Meunier, *Acc. Chem. Res.* **2008**, *41*, 69–77.
[6] D. Fontinha, I. Moules, M. Prudêncio, *Molecules* **2020**, *25*, 3409.
[7] L.-S. Feng, Z. Xu, L. Chang, C. Li, X.-F. Yan, C. Gao, C. Ding, F. Zhao, F. Shi, X. Wu, *Med. Res. Rev.* **2020**, *40*, 931–971.
[8] E. G. Tse, M. Korsik, M. H. Todd, *Malar. J.* **2019**, *18*, 93.
[9] J. P. Scovill, D. L. Klayman, T. S. Woods, T. R. Sweeney, *J. Med. Chem.* **1979**, *22*, 1164–1167.
[10] M. Fonte, N. Fagundes, A. Gomes, R. Ferraz, C. Prudêncio, M. J. Araújo, P. Gomes, C. Teixeira, *Tetrahedron Lett.* **2019**, *60*, 1166–1169.
[11] A. Gomes, B. Pérez, I. Albuquerque, M. Machado, M. Prudêncio, F. Nogueira, C. Teixeira, P. Gomes, *ChemMedChem* **2014**, *9*, 305–310.
[12] I. H. Ploemen, M. Prudencio, B. G. Douradinha, J. Ramesar, J. Fonager, G. J. van Gemert, A. J. Luty, C. C. Hermsen, R. W. Sauerwein, F. G. Baptista, M. M. Mota, A. P. Waters, I. Que, C. W. Lowik, S. M. Khan, C. J. Janse, B. M. Franke-Fayard, *PLoS One* **2009**, *4*, e7881.

Manuscript received: September 18, 2020
Revised manuscript received: November 13, 2020
Accepted manuscript online: November 20, 2020
Version of record online: December 7, 2020

© 2020 Wiley-VCH GmbH

18607187, 2021, 5, Downloaded from https://chemistry-europe.onlinelibrary.wiley.com/doi/10.1002/cmdc.202000740 by Cochrane Portugal, Wiley Online Library on [10/11/2022]. See the Terms and Conditions (https://onlinelibrary.wiley.com/terms-and-conditions) on Wiley Online Library for rules of use; OA articles are governed by the applicable Creative Commons License

ChemMedChem

Supporting Information

4,9-Diaminoacridines and 4-Aminoacridines as Dual-Stage Antiplasmodial Hits

Mélanie Fonte[+], Natália Tassi[+], Diana Fontinha, Inés Bouzón-Arnáiz, Ricardo Ferraz, Maria J. Araújo, Xavier Fernàndez-Busquets, Miguel Prudêncio, Paula Gomes, and Cátia Teixeira*

Supporting Information

Table of Content:

1. Detailed synthetic procedures and analytical/spectral data for compounds 1-2 and 3-10 **2**

2. Procedure and results of *in vitro* haemolytic assays **10**

1. Detailed synthetic procedures and analytical/spectral data for compounds 1-2 and 3-10

Chemistry. All solvents and commercial chemicals were purchased from Sigma-Aldrich (Phenol, $Pd(OAc)_2$, $NH_2NH_2.H_2O$, *N,N*-diethylpentan-1,4-diamine, and *N*-(4-bromobutyl)phthalimide, 4-methoxy-2-nitroaniline, ethylene glycol anhydrous 99,8%, Pd-C, and *p*-toluenesulfonyl hydrazide), FluoroChem (*N*-6-(bromohexyl)phthalimide), Fluka ($SnCl_2$), Biochem Chemopharma ($NaHCO_3$), VWR international (Et_3N, HCl 37 %, *HPLC gradient grade* or *LC-MS grade*, according to the application, and *p.a.* quality solvents of Merck as DMSO), LabChem (CH_3OH, CH_3CH_2OH, dimethylformamide (DMF), CH_2Cl_2, hexane, AcOEt, tetrahydrofuram (THF), diethyl ether), Fisher Scientific (*N,N*-diethylprop-1,3-diamine and NaOH), and CortecNet (deuterated solvents). Aluminium foils coated with silica-gel 60 F254 from Merck were used for TLC analysis (retention factor, R_f), and TLC chromatograms obtained were revealed with ultra-violet light (254 nm), using a Viber Lourmat lamp, model CN-6. For purification of compounds **4**, **6**, **8-10**, normal phase liquid chromatography was used, utilizing silica gel 60, from Sigma-Aldrich, as solid-phase. A mixture of solvents (identified in each case) was used as the mobile phase (eluent). The synthesis of compounds **6a-c** and **10a-c** was carried out in a CEM microwave model *Discovery S*. ESI-IT MS analyses (direct injection mode) were performed with solutions of the pure products in methanol, using a Finnigan Surveyor LCQ DECA XP MAX spectrometer, at the Department of Chemistry and Biochemistry of the Faculty of Sciences of the University of Porto. Analyses of the target compounds **1a-c** and **2a-c** (determination of the retention time (RT) and purity degree) were carried out by analytical HPLC, using a Hitachi-Merck Elite LaChrom system equipped with an L-2130 quaternary pump, an L-2200 thermostatted (Peltier effect) automated sampler, and an L-2455 diode-array detector (DAD). Samples were prepared by dissolution of compounds in acetonitrile and injected in a reverse phase column (C18) Purospher star RP-C18 of 125 × 4.0 mm and 5 µm pore size. A gradient elution (1 to 100 % of acetonitrile in acidified H_2O (with 0.05% of TFA)) was carried out for 30 minutes, at a flow rate of 1 mL/min, and detection was set at 220 nm (**2a-c**) or 290 nm (**1a-c**). ^{1}H-NMR and ^{13}C-NMR spectra were acquired on a Bruker Avance III spectrometer at frequencies of 400 mHz and 100 mHz, respectively, and samples were prepared in DMSO-d_6 and $CDCl_3$ with tetramethylsilane (TMS) as an internal reference.

General procedure for the synthesis of compounds 4a-b. In the presence of 4 Å molecular sieves and at N_2 atmosphere, compound **3**, phenol (15 equiv.), and Cs_2CO_3 (1 equiv.) were dissolved in anhydrous DMSO and stirred at 100 °C for 2 h. *N,N*-diethylalkyl-n,n-diamine (4 equiv.) was next added to the mixture. After 4 h of reaction, the mixture was cooled down to rt, diluted with CH_2Cl_2, and the molecular sieves removed by vacuum filtration. The filtrate was washed with 2 M aq. NaOH (25 mL), and next acidified with 10% aq. CH_3COOH (3 × 50 mL). The resulting aqueous phase was basified using 25% aq. NH_3 (3 × 50 mL) and the organic layer was isolated, dried over anhydrous Na_2SO_4, filtered, and the filtrate evaporated to dryness under reduced pressure. The crude was next purified by column

chromatography on silica gel using CH_2Cl_2/CH_3OH (4:1 v/v) as mobile phase. Fractions containing the pure compound were pooled and the solvent removed under reduced pressure to afford compounds **4a-c**, whose analytical and spectral data were as follows.

6-chloro-9-[*N*-(4-(diethylamino)pent-2-yl]amino-2-methoxy-4-nitroacridine (4a): red oil (50% yield); R_f: 0.45 in CH_2Cl_2/CH_3OH (4:1 v/v); $^m/_z$ $(M+H)^+$ 445.47, $(M+2H)^{2+}$ 223.38 ($C_{23}H_{30}ClN_4O_3$ requires 444.19); RT (HPLC-DAD) 11.913 min.; Grade purity (HPLC-DAD) 95%; δ_H/ppm (400 MHz; DMSO-d_6): 0.74 (t, *J* = 7.1 Hz; 6H), 1.15 – 1.36 (m; 2H), 1.44 (d, *J* = 6.4 Hz; 3H), 1.55 – 1.64 (m; 1H), 1.71 – 1.82 (m, 1H), 2.12 - 2.17 (m, 2H), 2.20 (q, *J* = 7.1 Hz; 4H), 3.98 (s, 3H), 4.03 – 4.14 (m; 1H), 6.87 (d; *J* = 9.76 Hz; 1H;), 7.43 (dd, *J* = 9.3 Hz; J= 2.2 Hz; 1H), 7.85 (d, *J* = 2.2 Hz; 1H), 7.86 (d, *J* = 2.6 Hz; 1H), 8.05 (d, *J* = 2.6 Hz; 1H), 8.32 (d, *J* = 9.32 Hz; 1H); δ_C/ppm (100 MHz; DMSO-d_6): 11.30, 21.85, 23.36, 36.10, 46.07, 51.69, 56.14, 56.41, 104.78, 115.51, 117.34, 118.22, 124.04, 126.42, 127.30, 135.10, 137.10, 148.54, 149.15, 151.62, 152.82.

6-chloro-9-[*N*-(3-(diethylamino)prop-1-yl]amino-2-methoxy-4-nitroacridine (4b): red oil (50% yield); R_f: 0.44 in CH_2Cl_2/CH_3OH (4:1 v/v); $^m/_z$ $(M+H)^+$ 417.80 ($C_{21}H_{25}ClN_4O_3$ requires 416.16); δ_H/ppm (400 MHz; DMSO-d_6): 1.07 - 1.19 (m, 6H), 2.05 – 2.15 (m, 2H), 3.33 (bs, 6H), 3.90 – 3.94 (m, 2H), 4.00 (s, 3H), 7.38 (d, *J* = 9.4 Hz, 1H), 7.63 (bs, 1H), 7.82 (bs, 1H), 7.96 (bs, 1H), 8.04 (bs, 1H), 8.39 (d, *J* = 9.3 Hz, 1H); δ_C/ppm (100 MHz; DMSO-d_6): 8.68, 24.69, 46.32, 48.28, 56.59, 104.95, 114.12, 117.13, 117.23, 123.46, 126.85, 127.19, 135.00, 136.85, 148.78, 149.04, 150.61, 152.70.

General procedure for the synthesis of compounds 5a-b and 8. A solution of the relevant compound **4** in 37% aq. HCl was cooled to 0 ºC with an ice bath. Next, $SnCl_2$ (3 equiv.) dissolved in 37% aq. HCl was dropwise added to the mixture. After the addition, the reaction mixture was slowly heated at 40 ºC and left under stirring for 30 min. Then, 25% aq. NH_3 was added, and the mixture was extracted with CH_2Cl_2 (3 × 50 mL). The organic layer was dried over anhydrous Na_2SO_4, filtered, and the filtrate evaporated to dryness under reduced pressure. Ethyl ether was added to precipitate impurities that were removed by vacuum filtration, followed by evaporation of the filtrate to dryness to afford the target compounds **5a-b** and **8**, whose analytical and spectral data were as follows.

4-amino-6-chloro-9-[*N*-(4-(diethylamino)pent-2-yl]amino-2-methoxyacridine (5a): yellow oil (85% yield); R_f: 0.25 in CH_2Cl_2/CH_3OH 4:1 (v/v); $^m/_z$ $(M+H)^+$ 415.40, $(M+2H)^{2+}$ 208.47 ($C_{23}H_{32}ClN_4O$ requires 414.22); RT (HPLC-DAD) 11.640 min.; Grade purity (HPLC-DAD) >99%; δ_H/ppm (400 MHz; DMSO-d_6): 0.77 (t; *J* = 7.1 Hz; 6H), 1.19 – 1.27 (m; 1H), 1.31 (d; *J* = 6.4 Hz; 3H), 1.37 – 1.43 (m; 1H), 1.49 – 1.59 (m; 1H), 1.65 – 1.75 (m; 1H), 2.17 (t; *J* = 7.9 Hz; 2H), 2.24 (q; *J* = 7.1 Hz; 4H), 3.85 (s; 3H), 3.89 – 4.00 (m; 1H), 5.98 (d; *J* = 10.2 Hz; 1H), 6.05 (s; 2H); 6.49 (d; *J* = 2.4 Hz; 1H), 6.79 (d; *J* = 2.5 Hz; 1H), 7.34 (dd; *J* = 9.2 Hz; *J* = 2.2 Hz; 1H), 7.91 (d; *J* = 2.2 Hz; 1H), 8.26 (d; *J* = 9.3 Hz; 1H); δ_C/ppm (100 MHz; DMSO-d_6): 11.95, 21.91, 23.60, 36.16, 46.12, 52.02, 55.03, 55.44, 87.90, 99.61, 116.73, 119.02, 123.30, 126.02, 127.54, 138.17, 145.65, 146.02, 150.21, 156.95.

4-amino-6-chloro-9-[*N*-(3-(diethylamino)prop-1-yl]amino-2-methoxyacridine (5b): yellow oil (85% yield); R_f: 0.24 in CH_2Cl_2/CH_3OH 4:1 (v/v); $^m/_z$ $(M+H)^+$ 387.73 ($C_{21}H_{27}ClN_4O$ requires 386.19); δ_H/ppm (400 MHz; DMSO-d_6): 0.85 (t, *J* = 7.1 Hz, 6H), 1.75 – 1.82 (m, 2H), 2.36 – 2.43 (m, 6H), 3.71 – 3.79 (m, 2H), 3.84 (s, 3H), 6.03 (s, 2H), 6.49 (d, *J* = 2.5 Hz, 1H), 6.77 – 6.80 (m, 1H), 6.79 (d, *J* = 2.5 Hz, 1H), 7.27 (dd, *J* = 2.3 Hz, *J* = 9.3 Hz, 1H), 7.86 (d, *J* = 2.2 Hz, 1H), 8.28 (d, *J* = 9.3 Hz, 1H). δC/ppm (100 MHz; DMSO-d_6): 11.49, 27.94, 46.39, 48.15, 49.98, 55.04, 87.74, 99.48, 114.84, 117.34, 122.37, 126.40, 127.42, 132.39, 137.65, 145.94, 145.99, 149.93, 156.64.

6-chloro-2-methoxy-4-aminoacridine (8): yellow oil (18% yield); R_f: 0.38 in hexane/AcOEt 4:1; $^m/_z$ $(M+H)^+$ 259.40 ($C_{14}H_{11}ClN_2O$ requires 258.06); δ_H/ppm (400 MHz; DMSO-d_6): 3.86 (s, 3), 6.20 (s, 2H), 6.57 (d, *J* = 2.6 Hz, 1H), 6.65 (d, *J* = 2.6 Hz, 1H), 7.55 (dd, *J* = 8.9 Hz, *J* = 2.1 Hz, 1H), 8.11-8.08 (m, 2H), 8.75 (s, 1H); δ_C/ppm (100 MHz; DMSO-d_6): 55.08, 91.18, 100.29, 125.36, 126.53, 127.24, 128.01, 129.74, 132.80, 133.35, 138.34, 144.34, 145.69, 158.74.

General procedure for the synthesis of compounds 6a-c. A mixture of the relevant compound **5**, sodium acetate (3 equiv.), and the relevant *N*-(n-bromoalkyl)phthalimide (3 equiv.) in CH_3CH_2OH was transferred into a reaction vial that was next sealed and submitted to MW irradiation (100 W); the reaction proceeded under MW heating for 2.5 h, at 120 °C and 100 psi. Then, the solvent was removed by evaporation under reduced pressure, and the residue dissolved in CH_2Cl_2 and washed with saturated aq. $NaHCO_3$ (3 × 50 mL) and saturated aq. NaCl (1 × 50 mL). The resulting organic layer was dried over anhydrous Na_2SO_4, filtered, and the filtrate evaporated to dryness under reduced pressure. The residue was submitted to column flash chromatography on silica gel, using CH_2Cl_2/CH_3OH (8:1 v/v) as mobile phase, to afford the target compounds **6a-c**, whose analytical and spectral data were as follows.

6-chloro-9-[*N*-(4-(diethylamino)pent-2-yl]amino-4-(4-phthalimidobutyl)amino-2-methoxy-acridine (6a): orange oil (30% yield); R_f: 0.46 in CH_2Cl_2/CH_3OH 8:1 (v/v); $^m/_z$ $(M+H)^+$ 616.60, $(M+2H)^{2+}$ 308.93 ($C_{35}H_{42}ClN_5O_3$ requires 615.30); RT (HPLC-DAD) 15.347 min.; Grade purity (HPLC-DAD) 95%; δ_H/ppm (400 MHz; DMSO-d_6): 1.03 (t; *J* = 7.1 Hz; 6H), 1.32 (d; *J* = 6.4 Hz; 3H), 1.51 – 1.64 (m; 3H), 1.66 – 1.79 (m; 5H), 2.74 – 2.91 (m; 6H), 3.24 – 3.30 (m; 2H), 3.65 (t; *J* = 6.6 Hz; 2H), 3.88 (s; 3H), 3.91 – 4.00 (m, 1H), 6.04 (d; *J* = 10.5 Hz; 1H), 6.21 (d; *J* = 2.3 Hz; 1H), 6.66 (t; *J* = 9.3; 1H), 6.74 (d; *J* = 2.3 Hz; 1H), 7.38 (dd; *J* = 9.3 Hz; *J* = 2.0 Hz; 1H), 7.84 (m; 4H), 7.93 (d; *J* = 2.2 Hz; 1H), 8.28 (d; *J* = 9.3 Hz; 1H); δ_C/ppm (100 MHz; DMSO-d_6): 8.62, 21.62, 25.71, 25.76, 34.92, 37.27, 42.05, 46.05, 50.68, 55.15, 86.78, 95.76, 117.20, 118,98, 122.97, 123.71, 125.93, 127.51, 131.60, 132.57, 134.35, 138.12, 145.24, 145.37, 149.85, 157.46, 168.01.

6-chloro-9-[*N*-(3-(diethylamino)prop-1-yl]amino-4-(4-phthalimidobutyl)amino-2-methoxy-acridine (6b): orange oil (30 % yield); R_f: 0.45 in CH_2Cl_2/CH_3OH 8:1 (v/v); $^m/_z$ $(M+H)^+$ 588.47 ($C_{33}H_{38}ClN_5O_3$ requires 587.27); δ_H/ppm (400 MHz; $CDCl_3$): 1.20 (t; *J* = 7.2 Hz; 6H), 1.78 – 1.93 (m; 4H), 2.02 – 2.09 (m; 2H), 2.85 (t; *J* = 6.8 Hz; 2H), 2.91 (q; *J* = 7.2 Hz; 4H), 3.24 – 3.37 (m; 2H), 3.76 (t; *J* = 6.7 Hz; 2H); 3.83 – 3.90 (m; 2H), 3.94 (s; 3H), 4.56 – 4.73 (bs; 1H), 6.22 (d; *J* = 2.2 Hz; 1H), 6.52 – 6.62 (m; 1H);

6.65 (d; *J* = 2.2 Hz; 1H); 7.17 (dd; *J* = 9.3 Hz; *J* = 2.1 Hz; 1H), 7.67 – 7.69 (m; 2H); 7.80 – 7.82 (m; 2H), 8.01 – 8.08 (m; 2H); δC/ppm (100 MHz; $CDCl_3$): 9.33, 25.92, 26.35, 26.57, 29.80, 37.84, 43.12, 46.71, 47.53, 50.28, 55.85, 86.83, 97.19, 123.31, 124.17, 124.96, 129.59, 132.19, 134.02, 158.16, 168.56.

6-chloro-9-[*N*-(4-(diethylamino)pent-2-yl]amino-4-(6-phthalimidohexyl)amino-2-methoxy-acridine (6c): orange oil (30% yield); R_f: 0.47 in CH_2Cl_2/CH_3OH 8:1 (v/v); $^m/_z$ $(M+H)^+$ 644.60, ($[M+2H]^{2+}$) 323.33 ($C_{37}H_{46}ClN_5O_3$ requires 643.33); δ_H/ppm (400 MHz; $CDCl_3$): 1.19 (t; *J* = 7.2 Hz; 6H), 1.27 (d; *J* = 6.1 Hz; 3H), 1.38 –1.90 (m; 13H), 2.77 – 2.85 (m; 2H), 2.89 (q; *J* = 7.2 Hz, 4H), 3.18 – 3.30 (m; 2H), 3.68 (t; *J* = 7.2 Hz; 2H), 3.94 (s; 3H), 3.97 – 4.03 (m; 1H); 4.59 – 4.97 (m; 1H), 6.22 (d; *J* = 2.2 Hz; 1H), 6.52 – 6.62 (m; 1H), 6.65 (d; *J* = 2.2 Hz; 1H); 7.17 (dd; *J* = 9.3 Hz; *J* = 2.1 Hz; 1H), 7.67 – 7.69 (m; 2H); 7.80 – 7.82 (m; 2H), 8.01 – 8.08 (m; 2H); δC/ppm (100 MHz; $CDCl_3$): 8.57, 20.96, 22.31, 26.77, 26.98, 28.61, 28.97, 35.54, 37.98, 43.41, 46.68, 51.76, 55.27, 55.64, 123.24, 124.46, 125.09, 132.19, 133.95, 158.63, 168.54.

General procedure for the synthesis of compounds 1a-c and 2a-c. To a solution of the relevant compound **6** or **10** in THF, $NH_2NH_2.H_2O$ (40 equiv.) was added. The reaction mixture was left under stirring at 60 °C until the reaction was completed, according to TLC analysis (approximately 48 h). The solvent was removed by evaporation under reduced pressure, the residue dissolved in CH_2Cl_2, and washed with saturated aq. $NaHCO_3$ (3 × 50 mL) and saturated aq. NaCl (1 × 50 mL). The organic layer was collected and dried over anhydrous Na_2SO_4, filtered, and the filtrate evaporated to dryness under reduced pressure to afford the target compounds **1a-c** and **2a-c**, whose analytical and spectral data follow.

4-(4-aminobutyl)amino-6-chloro-9-[*N*-(4-(diethylamino)pent-2-yl]amino-2-methoxy-acridine (1a): orange oil (100% yield); R_f: 0.02 in CH_3OH; $^m/_z$ $(M+H)^+$ 486.80, $(M+2H)^{2+}$ 244.53 ($C_{27}H_{40}ClN_5O$ requires 485.29); RT (HPLC-DAD) 10.587 min.; Grade purity (HPLC-DAD) >99%; δ_H/ppm (400 MHz; DMSO-d_6): 0.77 (t; *J* = 7.1 Hz; 6H), 1.31 (d; *J* = 6.4 Hz; 3H), 1.75 – 1.19 (m; 10H), 2.16 (t; *J* = 7.3 Hz; 2H), 2.24 (q; *J* = 7.1 Hz; 4H), 2.62 (t; *J* = 7.0 Hz; 1H), 3.25 (m; 2H), 3.87 (s; 3H), 3.95 (m; 1H), 6.01 (d; *J* = 10.1 Hz; 1H), 6.20 (d; *J* = 2.3 Hz; 1H), 6.63 (m; 1H), 6.75 (d; *J* = 2.3 Hz; 1H), 7.36 (dd; *J* = 9.3 Hz; *J* = 2.2 Hz; 1H), 7.94 (d; *J* = 2.1 Hz; 1H), 8.27 (d; *J* = 9.3 Hz; 1H); δC/ppm (100 MHz; DMSO-d_6): 11.55, 21.89, 23.63, 25.81, 30.47, 36.15, 41.24, 42.51, 46.11, 52.02, 55.03, 55.41, 95.70, 116.96, 118.69, 123.40, 125.94, 127.47, 132.50, 138.09, 145.27, 150.19, 157.28.

4-(4-aminobutyl)amino-6-chloro-9-[*N*-(3-(diethylamino)prop-1-yl]amino-2-methoxy-acridine (1b): orange oil (100% yield); R_f: 0.02 in CH_3OH; $^m/_z$ $(M+H)^+$ 458.53 ($C_{25}H_{36}ClN_5O$ requires 457.26); RT (HPLC-DAD) 9.653 min.; Grade purity (HPLC-DAD) 96%; δ_H/ppm (400 MHz; $CDCl_3$): 1.09 (t; *J* = 7.2 Hz; 6H), 1.39 – 1.50 (m; 2H), 1.68 – 1.63 (m; 2H), 1.92 – 1.80 (m; 4H), 2.62 – 2.69 (m; 6H), 2.78 (t; *J* = 7.0 Hz; 2H), 3.32 (t; *J* = 7.0 Hz; 2H), 3.84 – 3.86 (m; 2H), 3.89 – 3.91 (m; 1H), 3.92 (s; 3H), 6.25 (d; *J* = 2.3 Hz; 1H), 6.53 (d; *J* = 2.4 Hz; 1H), 6.48 – 6.57 (m; 1H), 7.20 (dd; *J* = 9.3 Hz; *J* = 2.2 Hz; 1H), 7.98 (d; *J* = 2.1 Hz; 1H), 8.06 (d; *J* = 9.3 Hz; 1H); δC/ppm (100 MHz; $CDCl_3$): 11.42, 14.16, 23.09, 24.12, 26.58,

27.80, 29.11, 29.83, 30.70, 31.58, 39.04, 42.14, 43.41, 47.33, 50.63, 52.22, 55.35, 67.91, 86.71, 96.05, 115.89, 117.33, 123.57, 124.95, 128.37, 129.61, 133.65, 138.66, 145.93, 146.60, 150.01, 157.48, 166.16.

4-(6-aminohexyl)amino-6-chloro-9-[*N*-(4-(diethylamino)pent-2-yl]amino-2-methoxy-acridine (1c): orange oil (100% yield); R_f: 0.02 in CH_3OH; $^m/_z$ $(M+H)^+$ 514.93, $(M+2H)^{2+}$ 258.53 ($C_{29}H_{44}ClN_5O$ requires 513.32); RT (HPLC-DAD) 11.140 min.; Grade purity (HPLC-DAD) 98%; δ_H/ppm (400 MHz; $CDCl_3$): 0.97 (t; *J* = 7.2 Hz; 6H), 1.25 (d; *J* = 2.6 Hz; 3H), 1.29 – 1.87 (m; 16H), 2.37 – 2.40 (m; 2H), 2.48 (q; *J* = 7.2 Hz; 4H), 2.70 (t; *J* = 6.6 Hz; 1H), 3.29 (q; 2H), 3.93 (s; 3H), 3.97 – 4.02 (m; 1H), 6.25 (d; *J* = 2.3 Hz; 1H), 6.43 (d; *J* = 2.3 Hz; 1H), 6.52 (t; *J* = 5.2 Hz, 1H), 7.29 (dd; *J* = 9.2 Hz; *J* = 2.1 Hz; 1H), 7.97 (d; *J* = 9.2 Hz; 1H), 8.04 (d; *J* = 2.1 Hz; 1H); δC/ppm (100 MHz; $CDCl_3$): 11.45, 22.31, 23.89, 26.86, 27.35, 29.15, 29.82, 30.44, 33.66, 37.00, 43.49, 46.88, 52.84, 55.30, 55.71, 85.70, 96.10, 118.23, 119.93, 124.20, 124.96, 128.68, 129.60, 133.68, 139.00, 146.18, 148.62, 158.48.

4-(4-aminobutyl)amino-6-chloro-2-methoxy-acridine (2a): orange oil (quantitative, 100%); R_f: 0.02 in CH_3OH; $^m/_z$ $(M+H)^+$ 330.56 ($C_{18}H_{20}ClN_3O$ requires 329.13); RT (HPLC-DAD): 17.153 min.; Grade purity (HPLC-DAD) >99%; δ_H/ppm (400 MHz; DMSO-d_6): 1.55-1.47 (m, 2H), 1.77-1.70 (m, 2H), 2.62 (t, *J* = 6.9 Hz, 2H), 3.29 – 3.39 (m, 4H), 3.88 (*s*, 3H), 6.27 (d, *J* = 2.4 Hz, 1H), 6.61 (d, *J* = 2.4 Hz, 1H), 6.72 (t, *J* = 5.6 Hz, 1H), 7.56 (dd, *J* = 9.0 Hz, *J* = 2.1 Hz, 1H), 8.09 (d, *J* = 9.0 Hz, 1H), 8.14 (d, *J* = 2.0 Hz, 1H), 8.75 (s, 1H); δ_C/ppm (100 MHz; DMSO-d_6): 29.88, 31.19, 41.96, 55.20, 90.39, 111.02, 113.89, 116.77, 119.65, 127.14, 129.82, 133.03, 133.51, 157.89, 158.27, 158.64, 159.02, 159.14.

4-(6-aminohexyl)amino-6-chloro-2-methoxy-acridine (2b): orange oil (quantitative, 100%); R_f: 0.02 in CH_3OH; $^m/_z$ $(M+H)^+$ 359.05 ($C_{20}H_{24}ClN_3O$ requires 357.16); RT (HPLC-DAD): 18.827 min.; Grade purity (HPLC-DAD) >99%; δH/ppm (400 MHz; $CDCl_3$): 1.42-1.56 (m; 6H), 1.80-1.87 (m; 4H), 2.72 (t, 2H), 3.31 (q; 2H), 3.93 (s; 3H), 6.27 (d; *J* = 2.4 Hz, 1H), 6.42-6.39 (m; 1H), 6.44 (d; *J* = 2.4 Hz; 1H), 7.40 (dd; *J* = 8.9 Hz; *J* = 2.0 Hz; 1H), 7.81 (d; *J* = 9.0 Hz; 1H), 8.14 (d; *J* = 1.8 Hz; 1H), 8.40 (s; 1H); δC/ppm (100 MHz; $CDCl_3$): 159.60, 145.51, 145.11, 139.13, 133.85, 132.99, 128.74, 128.26, 128.18, 127.10, 125.96, 97.03, 90.25, 55.39, 43.47, 42.20, 33.60, 29.15, 27.36, 26.88.

4-(2-aminopentyl)amino-6-chloro-2-methoxy-acridine (2c): orange oil (quantitative, 100%); R_f: 0.02 in CH_3OH; $^m/_z$ $(M+H)^+$ 344.67 ($C_{19}H_{22}ClN_3O$ requires 343.15); RT (HPLC-DAD): 17.767 min.; Grade purity (HPLC-DAD) >99%; δ_H/ppm (400 MHz; $CDCl_3$): 1.32 – 1.36 (m; 3H), 1.40 – 1.54 (m; 2H), 1.69 – 1.78 (m; 2H), 2.02 – 2.05 (m; 2H), 3.58 – 3.70 (m; 3H), 3.92 (s; 3H), 6.25 – 6.30 (m; 1H), 6.26 (d; *J* = 2.1 Hz; 1H), 6.42 (d; *J* = 2.2 Hz; 1H), 7.40 (dd; *J* = 8.9 Hz; *J* = 1.8 Hz; 1H), 7.81 (d; *J* = 8.8 Hz; 1H), 8.14 - 8.17 (m; 1H), 8.40 (s, 1H); δ_C/ppm (100 MHz; $CDCl_3$): 11.24, 14.18, 23.12, 24.15, 29.14, 29.85, 30.73, 39.07, 55.39, 67.03, 97.20, 128.22, 129.64, 133.03, 134.40, 159.56, 166.12.

Synthesis of 6-chloro-2-methoxy-4-nitro-9-[(*p*-toluenesulfonyl)hydrazine]acridine (7): to a solution of compound **3** at 42.8 g/L in $CHCl_3$ was added dropwise a solution of *p*-toluenesulfonyl hydrazide in $CHCl_3$ at 27.6 g/L. After stirring for approximately 24 h, the precipitate colour changed from purple to

orange, indicative that the reaction was completed. The precipitate was isolated by vacuum filtration and washed with cold chloroform, to afford compound **7** as an orange solid, in quantitative yield and without further purification. mp = 181 °C; R_f: 0.12 in hexane/AcOEt 9:1 (v/v). $^m/_z$ $(M+H)^+$ 473.60 ($C_{21}H_{17}ClN_4O_5S$ requires 472.06).

Synthesis of 6-chloro-2-methoxy-4-aminoacridine (8): compound **7** or **9** and Pd-C (10% wt) were suspended in CH_3OH and put under reflux at 80 ºC. Then, hydrazine hydrate (10 equiv.) was added dropwise, and the reaction mixture was left under reflux for 1 h - 3 h. Pd-C was next removed by filtration through Celite, and the solvent removed under reduced pressure. The residue was dissolved in CH_2Cl_2 and treated with saturated aq. $NaCO_3$ (3 × 50 mL) and saturated aq. NaCl (1 × 50 mL). The obtained organic layer was next dried over anhydrous $NaSO_4$, filtered, and the filtrate evaporated evaporated to dryness to give the crude product, which was further purified by column chromatography on silica gel using CH_2Cl_2 as mobile phase. Compound **8** was thus isolated as a yellow oil (30% and 80% yield if the starting reagent are compounds **7** and **9**, respectively); R_f: 0.38 in hexane/AcOEt 4:1; $^m/_z$ $(M+H)^+$ 259.40 ($C_{14}H_{11}ClN_2O$ requires 258.06); δ_H/ppm (400 MHz; DMSO-d_6): 3.86 (s, 3H); 6.20 (s, 2H), 6.57 (d, J = 2.6 Hz, 1H), 6.65 (d, J = 2.6 Hz, 1H), 7.55 (dd, J = 8.9 Hz, J = 2.1 Hz, 1H), 8.11-8.08 (m, 2H), 8.75 (s, 1H); δ_C/ppm (100 MHz; DMSO-d_6): 55.08, 91.18, 100.29, 125.36, 126.53, 127.24, 128.01, 129.74, 132.80, 133.35, 138.34, 144.34, 145.69, 158.74.

Synthesis of 6-chloro-2-methoxy-4-nitroacridine (9): compound **7** was dissolved in ethylene glycol/ water (18/9 mL), and after Na_2CO_3 (6.25×10^{-2} M) was added. The reaction mixture still on reflux at 95 ºC for 1,5 h (follow by TLC). Next, cold water was poured onto the crude product, and the resulting black precipitate was next dissolved in CH_2Cl_2, and washed with saturated aq. $NaHCO_3$ (3 × 50 mL) and saturated aq. NaCl (1 × 50 mL). The organic layer was collected and dried over anhydrous Na_2SO_4, filtered, and the filtrate evaporated to dryness under reduced pressure. The crude product was purified by column chromatography on silica gel using CH_2Cl_2 as mobile phase, to afford the target compound **9** as a Light-yellow solid (50% yield); mp > 260 ºC; R_f: 0.77 in CH_2Cl_2; $^m/_z$ $(M+H)^+$ 289.95 ($C_{14}H_9ClN_2O_3$ requires 288.03); δ_H/ppm (400 MHz; DMSO-d_6): 4.01 (s, 3H), 7.70 (dd, J = 9.0 Hz, J = 2.0 Hz, 1H), 7,80 (d, J = 2.6 Hz, 1H), 8.16 (d, J = 2.6 Hz, 1H), 8.24 – 8.27 (m, 2H), 9.18 (s, 1H); δ_C/ppm (100 MHz; DMSO-d_6): 56.50, 108.10, 119.68, 125.46, 127.21, 127.27, 128.07, 130.39, 135.59, 135.82, 136.54, l148.29, 154.76.

General procedure for the synthesis of compounds 10a-c. Triethylamine (3 equiv.) and the relevant *N*-(n-bromoalkyl)phthalimide (3 equiv.) were added to a solution of compound **8** in CH_3CH_2OH. The reaction mixture was transferred into a reaction vial that was next sealed and submitted to MW irradiation (100 W); the reaction proceeded under MW heating for 30 min, at 120 °C and 100 psi. Then, aliquots of triethylamine (3 equiv.) and the relevant *N*-(n-bromoalkyl)phthalimide (3 equiv.) were added to the reaction vial, which was again sealed and submitted to MW irradiation in the same conditions previous described. This process was repeated each 30 minutes, for a total of 3 h of reaction. The solvent was next removed by evaporation under reduced pressure, the residue dissolved in CH_2Cl_2, and washed with

saturated aq. $NaHCO_3$ (3 × 50 mL) and saturated aq. NaCl (1 × 50 mL). The organic layer collected was dried over anhydrous Na_2SO_4, filtered, and the filtrate evaporated to dryness under reduced pressure. The crude product obtained was partially purified by column chromatography on silica gel using hexane/AcOEt (4:1 v/v) as mobile phase. After pooling the fractions containing the target product and removing the solvent under reduced pressure, the residue was dissolved in CH_2Cl_2 and 85.5% aq. H_3PO_4 was added dropwise. The resulting solution was stirred for approximately 30 min, and the precipitate formed was isolated by decanting the liquid phase. The precipitate was then washed three times with CH_2Cl_2, which was every time removed by decantation. Aq. 2 M NaOH was then added to the solid residue and the resulting solution was extracted with CH_2Cl_2 (3 × 50 mL). The organic layer was collected, dried over anhydrous Na_2SO_4 and filtered. The filtrate was next evaporated to dryness under reduced pressure to afford compounds **10a-c**.

6-chloro-4-(4-phthalimidobutyl)amino-2-methoxy-acridine (10a): orange oil (52% yield); R_f: 0.39 in hexane/AcOEt 9:1 (v/v); $^m/_z$ $(M+H)^+$ 460.40 ($C_{26}H_{22}ClN_3O_3$ requires 459.13); δ_H/ppm (400 MHz; $CDCl_3$): 1.94-1.83 (m, 4H), 3.41-3.33 (m, 2H), 3.79 (t, *J* = 6.6 Hz; 2H), 3.91 (s, 3H), 6.26 (d, *J* = 2.3 Hz, 1H), 6.40 (d, *J* = 2.3 Hz, 1H), 6.47-6.40 (m, 1H), 7.38 (dd, *J* = 8.9 Hz, *J* = 2.0 Hz, 1H), 7.69-7.67 (m, 2H), 7.77 (d, *J* = 8.9 Hz, 1H), 7.84-7.81 (m, 2H), 8.12 (d, *J* = 1.5 Hz; 1H), 8.35 (s, 1H); δ_C/ppm (100 MHz; $CDCl_3$): 26.46, 26.57, 29.82, 37.84, 43.00, 55.35, 90.41, 97.16, 123.32, 125.89, 127.04, 127.96, 128.14, 128.68, 132.22, 132.94, 133.80, 134.01, 138.99, 145.05, 145.24, 159.48, 168.55.

6-chloro-4-(6-phthalimidohexyl)amino-2-methoxy-acridine (10b): orange oil (60% yield); R_f: 0.43 in hexane/AcOEt 4:1 (v/v); $^m/_z$ $(M+H)^+$ 489.07 ($C_{28}H_{26}ClN_3O_3$ requires 487.17); δ_H/ppm (400 MHz; $CDCl_3$): 1.59-1.42 (m, 4H), 1.83-1.74 (m, 4H), 3.31 (q, 2H), 3.71 (t, *J* = 7.2 Hz, 2H), 3.93 (s, 3H), 6.26 (d, *J* = 2.4 Hz, 1H), 6.42-6.39 (m, 1H), 6.43 (d, *J* = 2.4 Hz, 1H), 7.40 (dd, *J* = 8.9 Hz, *J* = 2.1 Hz, 1H), 7.71-7.68 (m, 2H), 7.81 (d, *J* = 8.9 Hz, 1H), 7.85-7.83 (m, 2H), 8.15 (d, *J* = 2.0 Hz, 1H), 8.40 (s, 1H); δ_C/ppm (100 MHz; $CDCl_3$): 26.59, 26.86, 27.06, 28.70, 29.06, 38.07, 43.41, 55.38, 90.27, 97.03, 123.32, 125.96, 127.08, 128.22, 128.72, 132.32, 132.96, 133.81, 133.99, 139.12, 145.11, 145.48, 159.59, 168.61.

6-chloro-4-(2-aminophthalimidopentyl)amino-2-methoxy-acridine (10c): orange oil (30% yield); R_f: 0.28 in hexane/AcOEt 4:1 (v/v); $^m/_z$ $(M+H)^+$ 474.40 ($C_{27}H_{24}ClN_3O_3$ requires 473.15); δ_H/ppm (400 MHz; $CDCl_3$): 1.35 (d, *J* = 6.4 Hz, 3H), 1.92-1.68 (m, 4H), 3.72-3.67 (m, 1H), 3.75 (t, *J* = 6.7 Hz, 2H), 3.92 (s, 3H), 6.27 (d, *J* = 2.3 Hz, 1H), 6.34 (d, *J* = 8.3 Hz, 1H), 6.41 (d, *J* = 2.3 Hz, 1H), 7.40 (dd, *J* = 8.9 Hz, *J* = 2.0 Hz, 1H), 7.71-7.68 (m, 2H), 7.83-7.79 (m, 3H), 8.15 (d, *J* = 1.5 Hz, 1H), 8.38 (s, 1H); δ_C/ppm (100 MHz; $CDCl_3$): 20.55, 25.57, 29.84, 33.98, 38.12, 48.04, 55.36, 55.36, 90.12, 97.22, 123.33, 125.95, 127.09, 128.26, 128.33, 128.68, 132.25, 132.97, 133.79, 134.00, 139.09, 144.44, 145.04, 159.53, 168.57.

***N*-(4-bromopentyl)phthalimide**

Phthalimide potassium salt was dissolved in acetone followed by the addition of 1,4-dibromopentane. The reaction mixture was under stirring at 60 ºC for 24 h. Finished this time, the white precipitate formed was eliminated by filtration and the resulting filtrate was evaporated to dryness under reduced pressure

affording **16**. Light-yellow oil (quantitative, 100 % yield); R_f: 0.80 in CH_2Cl_2 (v/v); δH/ppm (400 MHz; DMSO – d_6): 1.64 (d; J = 6.6 Hz; 3H), 1.66 – 1.72 (m; 2H), 1.75 – 1.82 (m; 2H), 3.54 – 3.71 (m; 2H), 4.28 - 4.36 (m; 1H), 7.80 – 7.89 (m; 4H).

2. Procedures of *in vitro* hemolytic assays

Human RBCs were diluted to a final 2% hematocrit in RPMIc (Roswell Park Memorial Institute complete medium containing 5 mg/mL Albumax II (Life Technology, Auckland, New Zealand) and supplemented with 2 mM L-glutamine), plated in micro-titer plates and incubated at 37 °C for 48 h in the presence of two-fold serial dilutions of compounds **1a-c**, **2a-c**, **9a**, **10a** and **11a** (2.5 – 10 µM). For positive and negative controls, Triton X-100 detergent and RPMIc medium alone were added, respectively. After this period, the plates were centrifuged and supernatants transferred to another plate. Supernatant absorbance at 540 nm was assessed in a multi-mode microplate reader and values were treated using the following equation (1):[1]

$$\%\ Hemolysis\ = \frac{Abs - Abs\ (negative\ control)}{Abs\ (positive\ control) - Abs\ (negative\ control)}$$

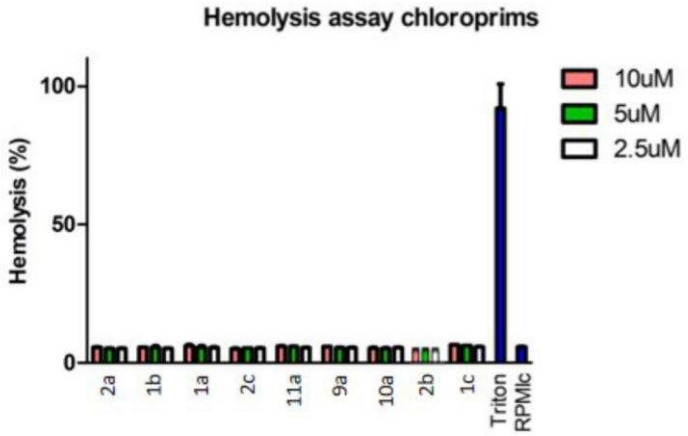


Figure S1: Hemolysis assay of compounds **1a-c**, **2a-c** and **9-11a**, and references Triton X-100 and RPMIc.

Ethics statement

The human blood used in this work was commercially obtained from the *Banc de Sang i Teixits* (www.bancsang.net). Blood was not specifically collected for this research; the purchased units had been discarded for transfusion, usually because of an excess of blood relative to anticoagulant solution. Prior to their use, blood units underwent the analytical checks specified in the current legislation. Before being delivered to us, unit data were anonymized and irreversibly dissociated, and any identification tag or label had been removed in order to guarantee the non-identification of the blood donor. No blood data were or will be supplied, in accordance with the current Spanish *Ley Orgánica de Protección de Datos* and *Ley de Investigación Biomédica*. The blood samples will not be used for studies other than those made explicit in this research. The studies reported here were performed in accordance with the current Spanish *Ley Orgánica de Protección de Datos* and *Ley de Investigación Biomédica* and under protocols reviewed and

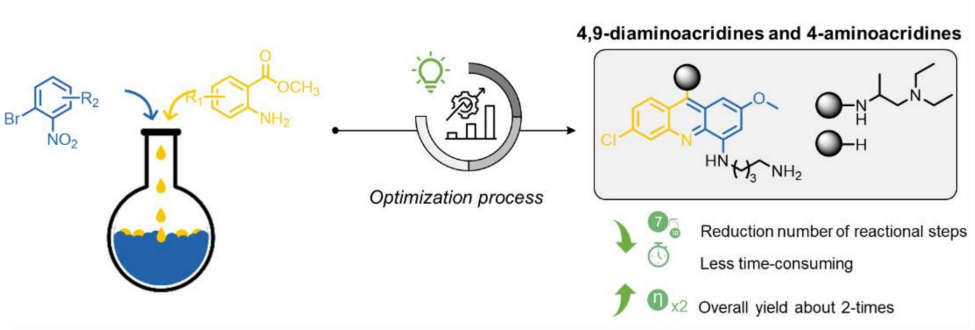
approved by the Ethical Committee on Clinical Research from the *Hospital Clínic de Barcelona* (Reg. HCB/2018/1223, January 23, 2019).

[1] K. Amin, R.-M. Dannenfelser, *Journal of Pharmaceutical Sciences* **2006**, *95*, 1173-1176.

Article II

Improved synthesis of antiplasmodial 4-aminoacridines and 4,9-diaminoacridines

Mélanie Fonte, Cátia Teixeira, Paula Gomes



RSC Adv., **2024**, 14, 6253-6261 doi: 10.1039/d4ra00091a

Summary

ACRs are one of the most important nitrogen-containing heterocycle systems owing to their biological properties. We have previously established and reported two unprecedented multi-step synthesis routes towards 4,9-diaminoacridines and 4-aminoacridines. Although we were successful in addressing such challenging syntheses, the global moderate yields obtained alongside the harsh and time-consuming procedures involved, prompted us to work on the optimization of the synthetic routes. The following article outlines the efforts that led to significant advancements in the synthesis scheme. These improvements include greener, simpler, and more efficient methods, resulting in fewer reaction steps and better overall yields, which doubled in some cases.

Declaration of authorship of published article II: Improved synthesis of antiplasmodial 4-aminoacridines and 4,9-diaminoacridines[2]

I, Mélanie Fonte, declare that the all the organic synthesis and laboratory work involved in this study, and the data analysis and discussion were carried out by me, under the supervision of Prof. Paula Gomes and Dr. Cátia Teixeira. I was also responsible for the writing of the article's original draft that was next corrected and validated by all the co-authors.

We, Cátia Teixeira, Paula Gomes, and Miguel Prudêncio, as Mélanie Fonte's supervisors, hereby confirm that the information above is correct.

Mélanie Fonte

Mélanie Fonte

Paula Gomes

Cátia Teixeira

Miguel Prudêncio

[2] Reproduced with permission from the Royal Society of Chemistry.

RSC Advances

PAPER

View Article Online
View Journal | View Issue

Check for updates

Cite this: *RSC Adv.*, 2024, **14**, 6253

Improved synthesis of antiplasmodial 4-aminoacridines and 4,9-diaminoacridines†

Mélanie Fonte,* Cátia Teixeira‡ and Paula Gomes *

Received 4th January 2024
Accepted 7th February 2024

DOI: 10.1039/d4ra00091a

rsc.li/rsc-advances

Acridines are one of the most important nitrogen-containing heterocycle systems and have many applications in the therapeutic field. However, the synthesis of acridine-based scaffolds is not always straightforward. Herein, we report the optimization of two multi-step synthetic routes towards 4,9-diaminoacridines and 4-aminoacridines, which have shown promising antiplasmodial properties. The improved synthesis pathways make use of greener, simpler, and more efficient methods, with less reaction steps and increased overall yields, which were doubled in some cases. These are impactful results towards future approaches to the chemical synthesis of acridine-based compounds.

Open Access Article. Published on 19 February 2024. Downloaded on 5/7/2024 9:52:29 PM.
This article is licensed under a Creative Commons Attribution 3.0 Unported Licence.

Introduction

Acridine (Fig. 1) was initially extracted by Grabe and Caro from the anthracene fraction of coal tar in 1870.[1,2] Due to its unique physical and chemical properties, biological activities, and industrial applications, it represents one of the most important nitrogen-containing heterocycle systems. Acridines were first used as dyes in fabrics, but their fluorescence properties soon after triggered their wide application in several cellular investigations such as cell cycle determination, nucleic acid staining, and flow cytometry. The therapeutic potential of aminoacridines, owing to their antimicrobial properties, was recognized as soon as in 1912 and underpinned the use of acridines as antiseptics during World War I. The therapeutic relevance of acridine-based compounds was further consolidated in World War II, when mepacrine, a 9-aminoacridine, was widely employed as an antimalarial drug to compensate for the ongoing chloroquine shortage. Since then, both mepacrine and other acridine derivatives have been reported with antitumoral, antibacterial, anthelmintic, antiviral, antifungal, antitubercular, and antileishmanial activities, among other potential therapeutic uses, including for neurodegenerative diseases.[1–6]

There is no general method for the synthesis of acridine derivatives. Direct functionalization of the acridine ring is a most interesting method, since it reduces the number of synthetic steps required, facilitating the synthesis of complex polycyclic structures. However, these approaches have a limited range of applications, as classic electrophilic substitutions on the acridine ring are usually not regioselective and produce many polyfunctionalized products. In this sense, the most widely applied syntheses of acridines involve, as a first step, ring closure through the condensation of adequately functionalized anilines and *o*-halobenzoic acids. The Bernthsen reaction was one of the earliest methods to obtain the acridine core and consists in mixing an aromatic or aliphatic carboxylic acid with a diphenylamine in the presence of zinc chloride and heating at high temperature (200–270 °C) for several hours.[7] Due to these harsh conditions and to the limited variety of substrates available, this method was quickly superseded by copper- or palladium-catalyzed methods, namely, Ulmann and Buchwald–Hartwig cross-coupling reactions, respectively, followed by dehydrogenation.[1,6,8,9] The acridine core obtained *via* the aforementioned methods is a versatile scaffold that can undergo many further modifications, mainly in the C-9 and N-10 positions, which are the most reactive sites due to the presence of the pyridinic nitrogen in the heterocycle. The reactivity of these positions is obviously modulated by the electron-donating or withdrawing properties of the substituents on the phenyl rings of the acridine scaffold.[6,10,11] The N-10 position is the main nucleophilic site of the acridine core, in which *N*-alkylations can easily occur, with the formation of acridinium salts under strongly acidic conditions. On the other hand, due to the strong electron deficiency caused by the pyridinic nitrogen on the C-9 position, this is the most electrophilic site of the acridine system, allowing for nucleophilic reactions to take place there.[10] For these reasons, most of the acridine-based

LAQV-REQUIMTE, Departamento de Química e Bioquímica, Faculdade de Ciências, Universidade do Porto, Portugal. E-mail: pgomes@fc.up.pt

† Electronic supplementary information (ESI) available: ^{1}H-NMR and ^{13}C-NMR spectra, ESI-MS and HPLC chromatograms shown in the ESI only refer to compounds that were synthesized using an improved protocol. See DOI: https://doi.org/10.1039/d4ra00091a

‡ Current affiliation: Gyros Protein Technologies Inc., Tucson, Arizona, USA.

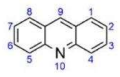
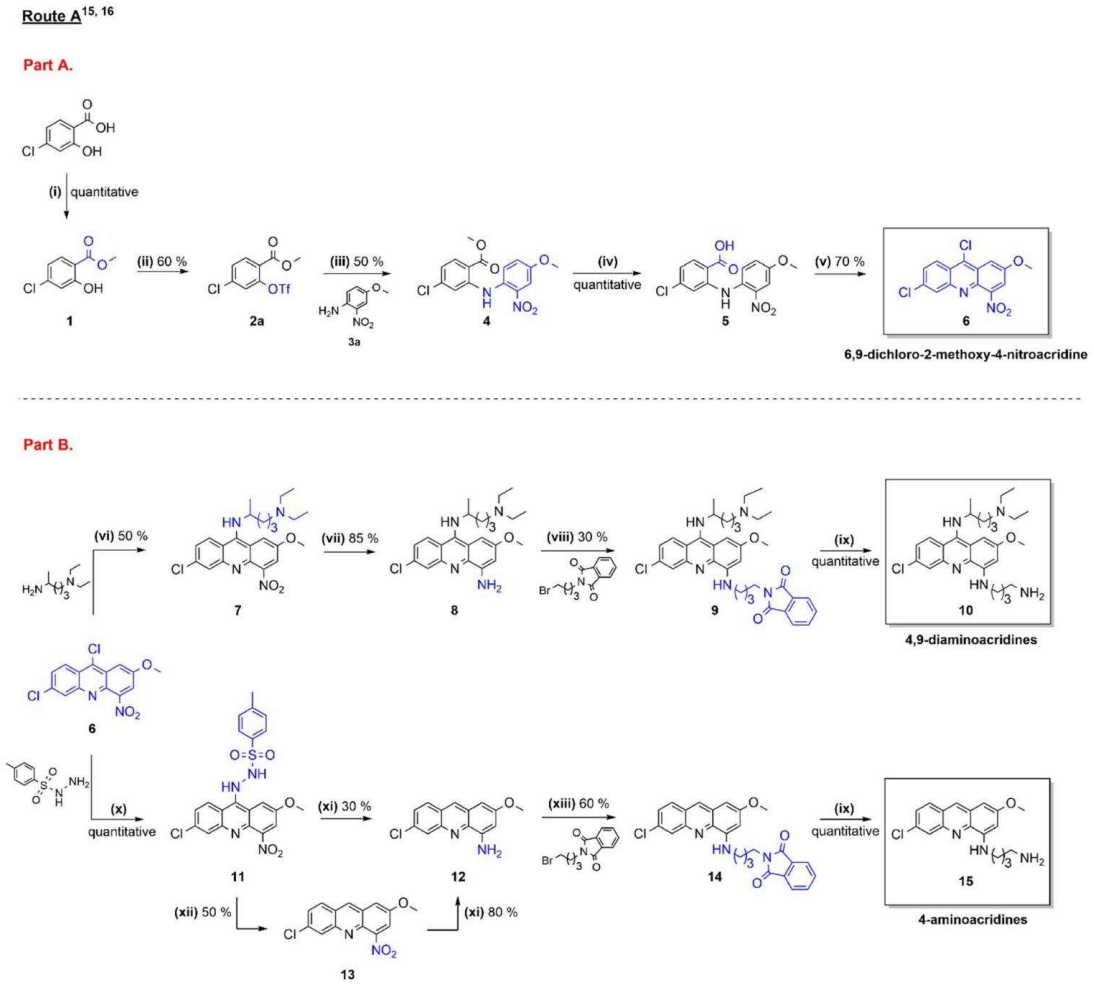


Fig. 1 Acridine structure and its numbering as defined by the International Union of Pure and Applied Chemistry (IUPAC).

© 2024 The Author(s). Published by the Royal Society of Chemistry

Open Access Article. Published on 19 February 2024. Downloaded on 5/7/2024 9:52:29 PM.
This article is licensed under a Creative Commons Attribution 3.0 Unported Licence.



Scheme 1 Synthetic route A towards 6,9-dichloro-2-methoxy-4-nitroacridine (**6**), 4,9-diaminoacridines (**10**) and 4-aminoacridines (**15**), as previously reported by Fonte M. *et al.*[15,16] Reagents and conditions: (i) CH_3I (5 molar equivalents, equiv.), Cs_2CO_3 (0.5 equiv.), dimethylformamide (DMF), room temperature (rt), 1.5 h; (ii) Tf_2O (1.5 equiv.), Et_3N (2 equiv.), CH_2Cl_2, N_2 atmosphere, −25 °C, 30 min; (iii) 4-methoxy-2-nitroaniline (**3a**, 1.2 equiv.), Cs_2CO_3 (1.4 equiv.), $Pd(OAc)_2$ (0.05 equiv.), *rac*-BINAP (0.08 equiv.), toluene, N_2 atmosphere, 120 °C, 5 h; (iv) (1) $Ba(OH)_2 \cdot 8H_2O$ (1.5 equiv.), CH_3OH, 90 °C, 2 h; (2) 1 M aq. HCl; (v) $POCl_3$ (34 equiv.), 120 °C, 2.5 h; (vi) (1) phenol (15 equiv.), Cs_2CO_3 (1 equiv.), anhydrous dimethyl sulfoxide (DMSO), 4 Å molecular sieves, 100 °C, 2 h; (2) *N*′,*N*′-diethylpentan-1,4-diamine (4 equiv.), 100 °C, 4 h; (vii) $SnCl_2$ (5 equiv.), 37% aq. HCl, 0 → 40 °C, 30 min; (viii) *N*-(4-bromobutyl)phthalimide (3 equiv.), CH_3COONa (3 equiv.), CH_3CH_2OH, microwave (MW) heating (100 W, 120 °C) in a pressurized vial (100 psi), 2.5 h; (ix) hydrazine monohydrate (40 equiv.), tetrahydrofuran (THF), 80 °C, 24–48 h; (x) *p*-toluenesulfonyl hydrazide (*p*-TSH, 1 equiv.), $CHCl_3$, rt, 24–48 h; (xi) NH_2NH_2 (10 equiv.), Pd/C (10% wt), CH_3OH, 80 °C, 1–3 h; (xii) $HOCH_2CH_2OH/H_2O$ (2 : 1), Na_2CO_3 (0.0625 M), 95 °C, 1.5 h; (xiii) *N*-(4-bromobutyl)phthalimide (3 equiv.), Et_3N (3 equiv.), CH_3CH_2OH, MW heating (100 W, 120 °C) in a pressurized vial (100 psi), 3 h.

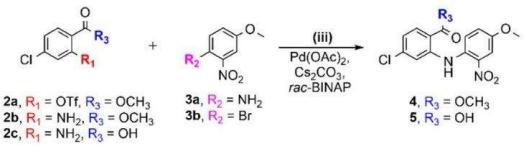
compounds developed so far display chemical modifications in those two positions,[12,13] while modifications elsewhere in the acridine ring remain limited.[13]

Based on the well-known therapeutic potential of aminoacridines,[14–17] our research group recently developed two unprecedented synthesis routes towards 4,9-diaminoacridines and 4-aminoacridines (Scheme 1).[15,16] These routes comprise two main parts: (a) production of the 6,9-dichloro-2-methoxy-4-nitroacridine precursor common to both 4,9-diaminoacridine and 4-aminoacridine target families (Scheme 1, part A), and (b) further modifications in C-9 and/or C-4 positions of the acridine ring (Scheme 1, part B).[15,16] Both are extensive and laborious synthetic routes that involve several steps featuring harsh reactional conditions and low yields. Based on this, and further motivated by the fact that these families of aminoacridines have shown interesting antiplasmodial properties,[16] we have now investigated whether simpler, more selective, and less time-consuming

 © 2024 The Author(s). Published by the Royal Society of Chemistry

Open Access Article. Published on 19 February 2024. Downloaded on 5/7/2024 9:52:29 PM.
This article is licensed under a Creative Commons Attribution 3.0 Unported Licence.

Table 1 Optimization of step iii (Scheme 1, part A) in the synthesis route to 6,9-dichloro-2-methoxy-4-nitroacridine **6**



2a, R_1 = OTf, R_3 = OCH_3
2b, R_1 = NH_2, R_3 = OCH_3
2c, R_1 = NH_2, R_3 = OH

3a, R_2 = NH_2
3b, R_2 = Br

4, R_3 = OCH_3
5, R_3 = OH

Entry	Amine (equiv.)	Halogen (equiv.)	Product	Time/h, *T*/°C	Yield/%
1	**3a** (1.2)	**2a** (1.0)	**4**	5, 120	50[b]
2	**2c** (1.2)	**3b** (1.0)	**5**	5, 120	45[a]
3	**2c** (1.2)	**3b** (1.0)	**5**	24, 120	70[a] (<50)[b]
4	**2b** (1.2)	**3b** (1.0)	**4**	1, 120	75[b]
5	**2b** (1.0)	**3b** (1.0)	**4**	2, 120	90[b]

[a] Synthesis at the 100 mg scale. [b] Synthesis at the 1.5 g scale.

methods could be used to synthesize the same target aminoacridines in fewer reactional steps and with improved yields. Successful improvement of the synthesis routes was achieved, as herein reported.

Results and discussion

Optimization of the synthesis route to 6,9-dichloro-2-methoxy-4-nitroacridine (6)

6,9-Dichloro-2-methoxy-4-nitroacridine (**6**) is the main synthetic precursor of acridines modified in the C-4 and C-9 positions. We have previously achieved the synthesis of **6**, starting from commercial 4-chlorosalicylic acid that was first protected by conversion into its methyl ester (**1**, Scheme 1, step i), then activated by conversion of the alcohol into a triflate (**2a**, Scheme 1, step ii), which was next reacted with 4-methoxy-2-nitroaniline (**3a**) *via* the Buchwald–Hartwig coupling reaction (Scheme 1, step iii). The product obtained (**4**) was next submitted to basic hydrolysis (Scheme 1, step iv) to afford the carboxylic acid **5**, and this was then treated $POCl_3$ (Scheme 1, step v) to promote the desired cyclization into 6,9-dichloro-2-methoxy-4-nitroacridine **6** (Scheme 1, part A).[15] This synthetic route was adapted from the literature,[18] and was the only one that, in our hands, successfully led to the target precursor **6**, which we recurrently failed to produce by means of Ulmann-type reactions.[15] Still, this synthetic route to **6** posed a few challenges, mainly due to the strong electron-withdrawing effect of the nitro group that significantly decreased the reactivity of the aniline **3a** in the Buchwald–Hartwig coupling. While this was compensated by use of an excellent leaving group such as triflate, triflate **2a** is not commercially available, which added three more steps to the synthesis route (Scheme 1, steps i, ii and iv).

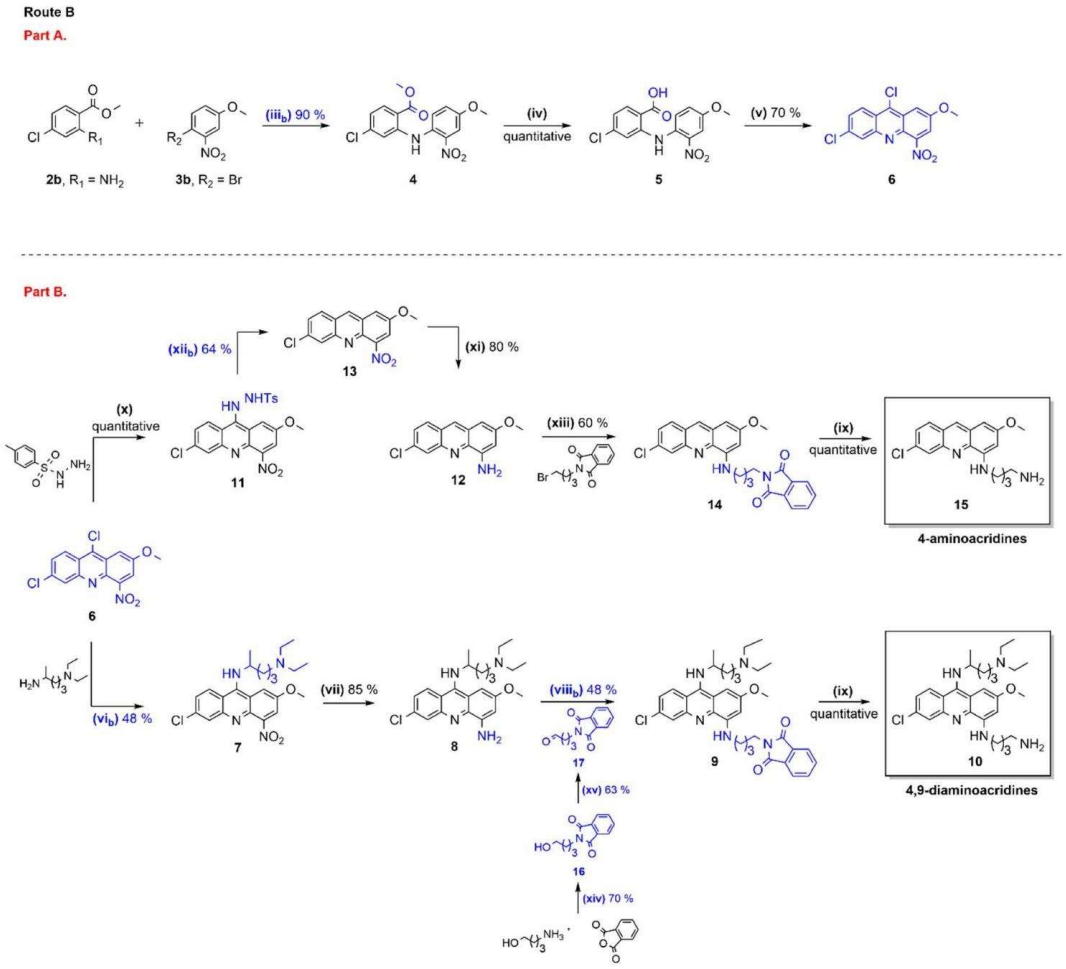
In face of the above, we decided to work on the optimization of the synthesis route to **6**. Therefore, we opted to take advantage of the properties of the nitro group, and replaced **2a** and **3a** (Table 1, entry 1) by reagents **2c** and **3b** (Table 1, entry 2). In this case, the nucleophilicity of **2c** is not affected by the nitro group that, in turn, makes the bromine in *ortho* position of **3b** very electrophilic, which favors the cross-coupling reaction. This led to successful synthesis of **5** in moderate yield (Table 1, entry 2; η = 45%) and without the need for steps i, ii and iv shown in Scheme 1. Additionally, the increase of the reaction time from 5 h to 24 h considerably improved the yield (Table 1, entry **3a**; η = 70%). Despite this clear improvement, the low solubility of **5** makes scale-up challenging, especially concerning its isolation by column chromatography on silica, which reduces the overall yield to below 50% (Table 1, entry **3b**). An attempt to overcome this obstacle, by carrying out both the cross-coupling and cyclization steps in a one-pot procedure, avoiding the purification step, was not successful. In view of this, we next tested replacement of the carboxylic acid **2c** by the corresponding methyl ester **2b**; this allowed production and isolation of **4** in very good overall yield (75%), without any purification issues (Scheme 2, step iii and Table 1, entry 4). Relevantly, the yield was significantly improved by not using any excess of **2b** (Table 1, entry 5).

The optimization efforts above targeted production of **6**, which bears a chlorine substituent in C-9. Yet, production of the acridine derivative devoid of chlorine in this position is also of great interest for the synthesis of the 4-aminoacridines **15**, as it will turn the two reduction steps in Scheme 1 (step x and xii) unnecessary. As such, we addressed the partial reduction of ester **4** into the corresponding aldehyde, which after cyclization using a strong acid like trifluoracetic acid could directly afford compound **13**. Therefore, we adopted the methodology reported by Na and co-workers,[19,20] which makes use of a DIBALH/morpholine system to produce a morpholine amide intermediate that, in the presence of an hydride source, leads to aldehyde formation in mild conditions, short reaction times (<60 min), and almost quantitative yields. Unfortunately, this approach was not successful in our case. Likewise, the reduction of ester **4** to the corresponding alcohol using a sodium borohydride–methanol system, followed by oxidation to the aldehyde,[21–23] equally failed.

One last optimization effort for the synthesis of **6** regarded the cyclization by dehydrogenation (Scheme 1, step v). Replacement of $POCl_3$ by $POBr_3$ to produce the Br-substituted

© 2024 The Author(s). Published by the Royal Society of Chemistry

Open Access Article. Published on 19 February 2024. Downloaded on 5/7/2024 9:52:29 PM.
This article is licensed under a Creative Commons Attribution 3.0 Unported Licence.



Scheme 2 Synthetic route B towards 6,9-dichloro-2-methoxy-4-nitroacridine (**6**), 4,9-diaminoacridines (**10**) and 4-aminoacridines (**15**). Reagents and conditions: (iii$_b$) **2b** (1 equiv.), **3b** (1 equiv.), Cs_2CO_3 (1.4 equiv.), $Pd(OAc)_2$ (0.05 equiv.), *rac*-BINAP (1.8 equiv.), toluene, 120 °C, 2 h; (iv) (1) $Ba(OH)_2 \cdot 8H_2O$ (1.5 equiv.), CH_3OH, 90 °C, 2 h; (2) 1 M aq. HCl; (v) $POCl_3$ (34 equiv.), 120 °C, 2.5 h. (vi$_b$) Phenol (15 equiv.), Cs_2CO_3 (1 equiv.), *N*′,*N*′-diethylpentan-1,4-diamine (4 equiv.), anhydrous DMSO, MW heating (100 W, 100 °C) in a pressurized vial (100 psi), 40 min; (vii) $SnCl_2$ (5 equiv.), 37% aq. HCl, 0 °C → 40 °C, 0.5 h; (viii$_b$) **17** (1.1 equiv.), $NaBH(OAc)_3$ (2 equiv.), 1,2-dichloroethane (DCE), rt, 4 h or 72 h; (ix) hydrazine monohydrate (40 equiv.), THF, 80 °C, 24–48 h; (x) *p*-TSH (1 equiv.), $CHCl_3$, rt, 24 h; (xi) NH_2NH_2 (10 equiv.), Pd/C (10% wt), CH_3OH, 80 °C, 1–3 h; (xii$_b$) $NaBH_4$ (10 equiv.), CH_3OH, 80 °C, 24 h; (xiii) *N*-(4-bromobutyl)phthalimide (3 equiv.), Et_3N (3 equiv.), CH_3CH_2OH, MW heating (100 W, 120 °C) in a pressurized vial (100 psi), 3 h; (xiv) phthalic anhydride (1 equiv.), 4-aminobutan-1-ol (1 equiv.), dioxane, 100 °C, overnight; (xv) **16** (1 equiv.), Dess–Martin periodinane (DMP, 1.1 equiv.), CH_2Cl_2, rt, 24 h.

acridine in C-9 was attempted, given the fact that bromine is a better leaving group than chlorine which could improve the ensuing aromatic substitutions (Scheme 1, steps vi and x). Unfortunately, these conditions led to a complex mixture of products, amongst which the desired one could not be detected by mass spectrometry (MS) or thin layer chromatography (TLC).

Overall, and regardless of obstacles found, the synthesis route to **6** depicted in Scheme 2 allowed to produce the target compound, 6,9-dichloro-2-methoxy-4-nitroacridine, in only three steps and with an overall yield of 63% (Scheme 2, part B). This is clearly a significant improvement over the previously reported route, where **6** was produced in 5 steps (Scheme 1, part A) with an overall 21% yield.[15,16]

Optimization of the synthesis route to 4,9-diaminoacridines (10)

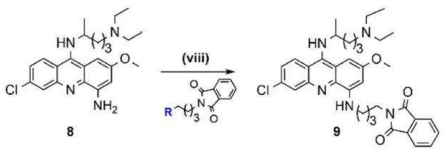
The chemical synthesis of 4,9-diaminoacridines **10** had been previously achieved *via* four reaction steps (Scheme 1, steps vi–ix),[15] starting with a nucleophilic aromatic substitution (S_NAr) on **6** using *N*′,*N*′-diethylpentan-1,4-diamine; this was a time-consuming (6 h) procedure comprising activation of **6** by formation of an aryl ether intermediate at C-9, and the

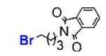
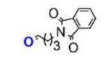
 © 2024 The Author(s). Published by the Royal Society of Chemistry

Open Access Article. Published on 19 February 2024. Downloaded on 5/7/2024 9:52:29 PM.
This article is licensed under a Creative Commons Attribution 3.0 Unported Licence.

subsequent nucleophilic attack by the amine to this intermediate (Scheme 1, step vi). The rate and regioselectivity of this reaction is strongly dependent on acridine substituents, and the presence of the nitro group in the C-4 position of **6** significantly increases its reactivity, which results in the formation of multiple by-products.[10,11] For this reason, our first optimization attempt consisted in first reducing **6** into 6,9-dichloro-2-methoxy-4-aminoacridine, by use of $SnCl_2$, and then perform the S_NAr reaction. However, 6,9-dichloro-2-methoxy-4-aminoacridine failed to undergo the desired S_NAr, probably due to the electron-donating effect of the amine group in C-4. Therefore, we alternatively focused our optimization efforts on the steps carried out under microwave (MW) heating, as this has very well-known advantages, such as reducing the reaction times, improving yields and purity of the target compounds, and overall simplifying work-up procedures.[24] As such, we adapted the procedure reported by Staderini and co-workers,[25] to produce compound **7** using MW microwave heating at 100 °C (Scheme 2, step vi_b); this reaction showed to be quite time-dependent, since an increase of reaction time from 40 minutes to 1 h about halved the yield from 46% to 24%. Relevantly, conventional heating led to similar yields, but use of MW heating notably reduced the reaction time from 6 h to 40 minutes, and simplified the overall procedure and work-up, by obviating the need for an initial phenol-activation step. We next addressed optimization of the introduction of the aminoalkyl side chain in the C-4 position of the acridine ring of aniline **8**; we had previously started by reducing the nitro group in **7** with $SnCl_2$/HCl, to produce **8** in 85% yield (Scheme 1, step vii), and next alkylated **8** with *N*-(4-bromobutyl)phthalimide using CH_3COONa as base (Scheme 1, step viii and Table 2, entry 1). However, this approach required high temperature (120 °C) and excess of the alkylating agent (3 equiv.), which allowed the formation of the di-alkylated product. As such, we started by testing whether reducing the amount of alkylating agent from 3 to 1 molar equivalents could reduce the amount of di-alkylated product and consequently increase the yield of the desired mono-alkylated product, **9**. However, although this change did decrease the extension of the side-reaction, it also lowered the yield of formation of **9** from 30% to 10% (Table 2, entry 2). Alternatively, compound **9** was synthesized *via* reductive amination of aldehyde **17**, which was first produced by reaction of phthalic anhydride with 4-aminobutan-1-ol (Scheme 2, step xiv; $\eta = 70\%$) followed by selective oxidation with Dess–Martin periodinane (DMP) (Scheme 2, step xv; $\eta = 63\%$).[26] This method, which uses milder conditions and avoids di-alkylated by-products, successfully afforded **9** in 48% yield, thus offering a significant improvement over our initial approach (Table 2, entry 3 and Scheme 2, step $viii_b$). The increase of reaction time and of the amount of aldehyde to 24 h and 3 molar equivalents, respectively, favored formation of by-products with a consequent decrease in the reaction yield to 10% (Table 2, entry 4).

Table 2 Optimization of step viii (Scheme 1, part B) in the synthesis route to 4,9-diaminoacridines **10**



Entry	Phthalimide	Phthalimide equiv.	Time/h	*T*/°C	Yield/%
1[a]		3.0	2.5	120	30
2[a]		1.0	2.5	120	10
3[b]		1.1	4.0	rt	48
4[b]		3.0	24	rt	10

[a] Reaction performed in a MW reactor (100 psi, 100 W) using CH_3CH_2OH as solvent. [b] Reaction performed at rt using DCE and $NaBH(OAc)_3$ as solvent and reducing agent, respectively.

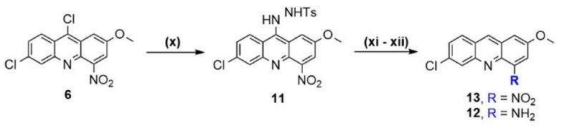
Optimization of the synthesis route to 4-aminoacridines (15)

Our initial synthesis route to 4-aminoacridines **15** comprised five reactional steps starting from **6**, in which reduction of the chlorine and nitro groups in C-9 and C-4, respectively, led to the 4-aminoacridine **12** that was next *N*-alkylated to afford the *N*-phthalimide **14**, which was finally converted into **15** by removal of the phthaloyl *N*-protecting group (Scheme 1, steps x–ix).[16] Our efforts to improve the synthesis of the target 4-aminoacridines **15**, which are summarized in Table 3, first focused on the reduction steps. Initial attempts involved the selective remotion of the chlorine in C-9 by reduction with H_2/Pd–C or with Et_3SiH/$Pd(PPh_3)_2Cl_2$; these attempts led to the loss the two chlorines in the acridine systems (Table 3, entry 1 and 2). In view of this, we redirected our focus to the reduction of intermediate **11** that is produced by reacting **6** with *p*-toluenesulfonyl hydrazide (*p*-TSH). The cleavage of the *p*-TSH group and the reduction of the nitro group can be simultaneously achieved by treatment with hydrazine (Table 3, entry 3) or $SnCl_2$ (Table 3, entry 4). Alternatively, a two-step procedure can be employed using Na_2CO_3 in aqueous ethylene glycol (Table 3, entry 5) followed by reduction with hydrazine (Table 3, entry 7).[16] As a way of enhancing the yield, we next tested the stepwise reduction of **11** into **13**, by use of $NaBH_4$ in refluxing CH_3OH (Scheme 2, step xii_b and Table 3, entry 6), which afforded the desired compound in 65% yield, higher than that previously achieved (50%). Encouraged by this result, we next tried once more to improve the conditions for simultaneous reduction of the two groups of interest, *i.e.*, chlorine in C-9 and nitro in C-4. To this end, different combinations of $NaBH_4$ with transition-metal salts, such as $NiCl_2 \cdot 6H_2O$, $CuBr_2$, $Fe(OTf)_3$, $Cu(NO_3)_2 \cdot 3H_2O$, $CuSO_4/CoCl_2$, $Ni(OAc)_2 \cdot 4H_2O$, $Cu(acac)_2$, $SnCl_2 \cdot 2H_2O$, have been reported in the literature as being capable of reducing nitro groups as well.[27–31] Therefore, we tested the use of $NaBH_4/Cu(NO_3)_2 \cdot 3H_2O$, $NaBH_4/CuBr_2$ and $NaBH_4/SnCl_2 \cdot 2H_2O$ combinations, but these failed to promote reduction of the nitro group, thus affording **13** (Table 3, entries 8, 9 and 10). Another three one-pot reactions were attempted whereby other combinations of reducing agents were used, namely, Na_2CO_3 in aqueous ethylene glycol followed

© 2024 The Author(s). Published by the Royal Society of Chemistry

Open Access Article. Published on 19 February 2024. Downloaded on 5/7/2024 9:52:29 PM.
This article is licensed under a Creative Commons Attribution 3.0 Unported Licence.

Table 3 Optimization of steps x–xii (Scheme 1, part B) in the synthesis route to 4-aminoacridines **15**



Entry	Starting reagent	Product	Reducing agent (equiv.)	Catalyst	T/°C, time/h	Solvent	Yield/%
1[a]	**6**	**13**	H_2	Pd–C (10 wt%)	rt, 5	CH_3OH	—
2	**6**	**13**	Et_3Si (1.4)	$Pd(PPh_3)_2Cl_2$ (1 mol%)	70, 3	CH_3CN	—
3	**11**	**12**	NH_2NH_2 (10)	Pd–C (10 wt%)	80, 5	CH_3OH	30
4	**11**	**12**	$SnCl_2$ (3.0)	—	40, 0.5	Aq. HCl 37%	18
5	**11**	**13**	Na_2CO_3	—	95, 1.5	$HOCH_2CH_2OH/H_2O$ (2 : 1)	50
6	**11**	**13**	$NaBH_4$ (20)	—	80, 24	CH_3OH	65
7	**13**	**12**	NH_2NH_2 (10)	Pd–C (10 wt%)	80, 1	CH_3OH	80
8[b]	**11**	**12**	$NaBH_4$ (3.0)	$Cu(NO_3)_2 \cdot 3H_2O$ (15 mol%)	80, 24	CH_3OH	—
9[c]	**11**	**12**	$NaBH_4$ (10)	$CuBr_2$ (10 mol%)	80, 28	CH_3OH	—
10[d]	**11**	**12**	(1) $NaBH_4$ (10) (2) $SnCl_2 \cdot 2H_2O$ (10)	—	80, 28	CH_3OH	—
11[e,h]	**11**	**12**	(1) Na_2CO_3 (2) NH_2NH_2 (10)	Pd–C (10 wt%)	(1) 95, 1.5 (2) 80, 1	$HOCH_2CH_2OH/H_2O$ (2 : 1)	6
12[f,h]	**11**	**12**	(1) Na_2CO_3 (2) $SnCl_2$ (3.0)	—	(1) 95, 1.5 (2) 40, 0.5	(1) $HOCH_2CH_2OH/H_2O$ (2 : 1) (2) HCl	13
13[g,h]	**11**	**12**	(1) $NaBH_4$ (20) (2) NH_2NH_2 (10)	Pd–C (10 wt%)	80, 25	CH_3OH	15
14	**13**	**12**	$SnCl_2$ (3)	—	40, 0.5	Aq. HCl 37%	27

[a] Reaction conditions: H_2 (50 psi). [b] $NaBH_4$, $Cu(NO_3)_2 \cdot 3H_2O$, CH_3OH, 80 °C, 24 h. [c] $NaBH_4$, $CuBr_2$, CH_3OH, 80 °C, 28 h. [d] $NaBH_4$, CH_3OH, 80 °C, 24 h, followed by addition of $SnCl_2 \cdot 2H_2O$, 4 h. [e] Na_2CO_3 (0.0625 M), $HOCH_2CH_2OH/H_2O$ (2 : 1), 95 °C, 1.5 h, followed by addition of NH_2NH_2 and Pd–C, 80 °C, 1 h. [f] Na_2CO_3 (0.0625 M), $HOCH_2CH_2OH/H_2O$ (2 : 1), 95 °C, 1.5 h, filtration of the black precipitate followed by its dissolution in aqueous HCl 37% → anhydrous $SnCl_2$, 40 °C, 0.5 h. [g] $NaBH_4$, CH_3OH, 80 °C, 24 h, followed by addition of NH_2NH_2 and Pd–C, 80 °C, 1 h. [h] One-pot reaction; without isolation of intermediate **13**.

by hydrazine hydrate (Table 3, entry 11; $\eta = 6\%$); Na_2CO_3 in aqueous ethylene glycol followed by $SnCl_2$/HCl (Table 3, entry 12; $\eta = 13\%$); and $NaBH_4$ followed by hydrazine hydrate (Table 3, entry 13; $\eta = 15\%$). Again, none of these attempts gave better yields than the previous methods for concomitant reduction of both groups, *i.e.*, direct conversion of **11** into **12**. As one last attempt to improve production of aminoacridine **12**, $SnCl_2$ was used to reduce the nitro group (Scheme 2, step xi_b and Table 3, entry 14), similarly to what had been carried out in the synthesis route to 4,9-diaminoacridines **10**. However, results were not so good in this case, since compound **12** was obtained in only 27% yield; mass spectrometry analysis (data not shown) revealed that reduction of the nitro group into the corresponding aniline was accompanied by the entry of a chlorine atom in C-9. Altogether, this optimization effort enabled us to conclude that the best option to produce **12** is by a two-step procedure where the *p*-TSH group in **11** is first removed by reduction with $NaBH_4$ followed by reduction of the nitro group with hydrazine, which allows an improvement of the overall yield from 40% to 52% (Scheme 2, steps xi and xii_b).

Finally, we addressed the improvement of the alkylation of **12** with *N*-(4-bromobutyl)phthalimide to produce **14** (Scheme 1, step xiii). Based on the good results obtained in the optimized synthesis route to 4,9-diaminoacridines **10**, we applied reductive amination to obtain **14**. However, a significant amount of **12** remained unreacted even after 72 h, probably due to the lowered reactivity of its aniline group, as compared to that in compound **8**, its counterpart in the synthesis of 4,9-diaminoacridines **10**. This translated into a 30% yield, lower than the 60% achieved *via* bimolecular nucleophilic substitution in the presence of triethylamine (Scheme 1, step xiii). As a very last effort, we still tested the use of acetic acid as catalyst under MW heating,[32] but these conditions failed to deliver the desired product.

The highest scale attempt for the synthesis of 4-aminoacridine (**15**) was about 2 g, *i.e.*, starting from approximately 1.8 g of 6,9-dichloroaminoacridine (**6**). Under these conditions, we were able to obtain 0.5 g of 4-aminoacridine (**15**). No further scale-up attempts have been performed, but we trust that at least a doubled scale (starting from 4 g) is feasible without significantly affecting the yield.

Experimental section

Synthetic procedures§

All chemicals were purchased from Sigma-Aldrich, Abcr, Fluorochem, Fluka, Biochem, Chemopharma, Alfa Aesar, Merck or PanReac AppliChem and used without further purification. The

§ The procedures described in the Experimental section only refer to the new procedures that led to an improvement on the overall synthesis routes, as depicted in the synthetic route B (Scheme 2).

© 2024 The Author(s). Published by the Royal Society of Chemistry

Open Access Article. Published on 19 February 2024. Downloaded on 5/7/2024 9:52:29 PM.
This article is licensed under a Creative Commons Attribution 3.0 Unported Licence.

solvents were all of p.a. quality and purchased from VWR International, Carlo Erba, LabChem or Honeywell Riedel-de-Haën. When needed, anhydrous solvents were purchased as such, *i.e.*, not requiring any additional treatment (apart from the use of inert reaction conditions that are identified whenever applicable). Information about the specific brand of each reagent and solvent used is given in detail in the ESI.† Similarly, detailed information about the type of equipments used (such as NMR and mass spectrometers, rotary evaporator, microwave, *etc.*) is included in the ESI.†

Route A¶. Compounds **1–15** were prepared following the procedures previously described, and their structural analyses agreed with formerly reported data.[15,16]

Route B

*Synthesis of compound **4** (step iii$_b$).* In a 250 mL glass round-bottom flask charged with a magnetic stir bar, 4-bromo-3-nitroanisole (1 equiv., 4.36 mmol, 1.0117 g) was dissolved in toluene (50 mL). Then, Cs_2CO_3 (1.4 equiv., 6.10 mmol, 1.9875 g), $Pd(OAc)_2$ (0.05 equiv., 0.22 mmol, 0.0494 g) and *rac*-BINAP (0.08 equiv., 0.35 mmol, 0.2179 g) were added. After about 5 min, methyl 2-amino-4-chlorobenzoate (1 equiv., 4.36 mmol, 0.8093 g) was added, and the mixture was heated to 120 °C in an oil bath for 2 h until the starting material disappeared (monitored by TLC). After cooling the mixture to rt, CH_2Cl_2 was added (50 mL) and a grey precipitate was collected by gravity filtration and discarded. The filtrate collected in a 250 mL glass round-bottom flask was then evaporated to dryness under reduced pressure and purified by liquid chromatography on a silica gel column using CH_2Cl_2/hexane (3 : 1 v/v) as eluent. Orange solid, $\eta = 90\%$ (1.3213 g, 3.92 mmol); ^{1}H-NMR (400 MHz, DMSO-d$_6$) δ_H 3.85 (3H, s); 3.88 (3H, s); 6.98 (1H, dd, J = 8.6 Hz, J = 2.0 Hz); 7.20 (1H, d, J = 2.0 Hz); 7.36 (1H, dd, J = 9.1 Hz, J = 3.0 Hz); 7.61 (1H, d, J = 3.0 Hz); 7.64 (1H, d, J = 9.1 Hz); 7.92 (1H, d, J = 8.6 Hz); 10.48 (1H, bs s); ^{13}C-NMR (100 MHz, DMSO-d$_6$) δ_C 52.35; 55.97; 109.09; 113.18; 115.17; 119.57; 122.67; 124.32; 128.90; 133.15; 139.01; 140.79; 145.75; 154.56; 166.84; *m*/*z* (ESI-IT MS, +) 337.07 (M + H$^+$), M$^+$ ($C_{15}H_{13}ClN_2O_5$) requires 336.05; retention factor (R_f), 0.46 in CH_2Cl_2/hexane 3 : 1 (v/v); HPLC-DAD: retention time (RT), 25.620 min, purity degree (peak relative area) 100%.

*Synthesis of compound **7** (step vi$_b$).* A suspension of phenol (15 equiv., 3.81 mmol, 0.3586 g), Cs_2CO_3 (1 equiv., 0.25 mmol, 0.0828 g), *N*,*N*-diethylpentane-1,4-diamine (4 equiv., 1.02 mmol, 0.20 mL) and compound **6** (1 equiv., 0.25 mmol, 0.0820 g) in anhydrous DMSO (15 mL) was prepared in a 50 mL glass round-bottom flask. Then, the mixture was transferred to a 35 mL reaction glass vessel, sealed, and submitted to MW heating (100 W) for 40 minutes, at 120 °C. Finished this time, the mixture was cooled to rt, diluted with CH_2Cl_2 (25 mL), and, washed with a 2 M aqueous NaOH solution (3 × 50 mL) in a 100 mL glass separatory funnel. The organic layer was collected into a 250 mL Erlenmeyer flask, dried over anhydrous Na_2SO_4, filtered by gravity, and evaporated to dryness under reduced pressure to yield the crude product. This was next purified by liquid chromatography on a silica gel column, using CH_2Cl_2/CH_3OH (4 : 1 v/v) as eluent. Red oil, $\eta = 48\%$ (51.5 mg, 0.12 mmol); ^{1}H-NMR (400 MHz, DMSO-d$_6$) δ_H 0.74 (6H, t, J = 7,1 Hz), 1.15–1.36 (2H, m), 1.44 (3H, d, J = 6.4 Hz), 1.55–1.64 (1H, m), 1.73–1.82 (1H, m), 2.12–2.17 (2H, m), 2.20 (4H, q, J = 7.1 Hz), 3.98 (3H, s), 4.03–4.14 (1H, m), 6.87 (1H, d, J = 9.76 Hz), 7.43 (1H, dd, J = 9.3 Hz; J = 2.2 Hz), 7.85 (1H, d, J = 2.2 Hz), 7.86 (1H, d, J = 2.6 Hz), 8.05 (1H, d, J = 2.6 Hz), 8.32 (1H, d, J = 9.32 Hz); ^{13}C-NMR (100 MHz, DMSO-d$_6$) δ_C 11.30, 21.85, 23.36, 36.10, 46.07, 51.69, 56.14, 56.41, 104.78, 115.51, 117.34, 118.22, 124.04, 126.42, 127.30, 135.10, 137.10, 148.54, 149.15, 151.62, 152.82; *m*/*z* (ESI-IT MS, +) 445.47 (M + H$^+$), M$^+$ ($C_{23}H_{30}ClN_4O_3$) requires 444.19; R_f, 0.45 in CH_2Cl_2/CH_3OH 4 : 1 (v/v); HPLC-DAD: RT, 11.913 min, purity degree (peak relative area) 96%.

*Synthesis of compound **9** (step viii$_b$).* In a 25 mL glass round-bottom flask charged with a magnetic stir bar and put under inert conditions (argon atmosphere), compound **8** (1 equiv., 0.10 mmol, 0.0424 g) was dissolved in DCE (10 mL) and then, compound **17** (1.1 equiv., 0.11 mmol, 0.0239 g) and $NaBH(OAc)_3$ (2 equiv., 0.20 mmol, 0.0424 g) were added. After stirring at rt for 4 h, CH_2Cl_2 (25 mL) was added and the mixture was washed with a saturated aqueous $NaHCO_3$ solution (3 × 25 mL) in a 100 mL glass separatory funnel, dried with anhydrous Na_2SO_4, filtered by gravity, and concentrated by evaporation under reduced pressure. Purification by liquid chromatography on a silica gel column using CH_2Cl_2/CH_3OH (4 : 1 v/v) as eluent delivered the target compound; Orange oil, $\eta = 48\%$ (30.5 mg, 0.05 mmol); ^{1}H-NMR (400 MHz, $CDCl_3$) δ_H 1.19 (6H, t, J = 7.6 Hz), 1.32 (3H, d, J = 6.3 Hz), 1.60–1.77 (2H, m), 1.80–1.91 (6H, m), 2.85 (2H, t, J = 7.5 Hz), 2.93 (4H, q, J = 7.1 Hz), 3.31 (2H, t, J = 6.1 Hz), 3.76 (2H, t, J = 6.6 Hz), 3.93 (3H, s), 3.99–4.08 (1H, m), 6.24 (1H, d, J = 2.2 Hz), 6.59 (1H, m), 7.26 (1H, dd), 7.67–7.69 (2H, m), 7.79–7.81 (2H, m), 8.00 (1H, d, J = 9.2 Hz), 8.07 (1H, d, J = 1.8 Hz); ^{13}C-NMR (100 MHz, $CDCl_3$) δ_C 168.53, 158.54, 134.03, 132.17, 125.01, 124.72, 123.29, 55.69, 55.34, 51.77, 46.67, 43.11, 37.80, 35.37, 29.78, 26.55, 26.29, 22.29, 20.94, 8.48, 0.08; *m*/*z* (ESI-IT MS, +) 616.73 (M + H$^+$), M$^+$ ($C_{35}H_{42}ClN_5O_3$) requires 615.30; R_f, 0.46 in CH_2Cl_2/CH_3OH 8 : 1 (v/v); HPLC-DAD: RT, 15.347 min, purity degree (peak relative area) 89%.

*Synthesis of compound **13** (step xii$_b$).* A suspension of **11** (1 equiv., 3.75 mmol, 1.7749 g) in CH_3OH (50 mL) was prepared in a 250 mL glass round-bottom flask charged with a magnetic stir bar, and after that, $NaBH_4$ (10 equiv., 37.5 mmol, 1.4186 g) was carefully and slowly added using a spatula during 30 min (paying attention to the exothermic reaction; as during the addition the mixture heats up to boiling). Finished the addition, the mixture was left under stirring until all the starting reagent was consumed (monitored by TLC, approximately 24 h) at 80 °C in an oil bath. After that, the mixture was cooled to rt and CH_3OH was eliminated by evaporation under reduced pressure. Next, the resulting residue was dissolved in CH_2Cl_2 (50 mL) and transferred to a 250 mL glass separatory funnel where it was washed with a saturated aqueous $NaHCO_3$ solution (3 × 50 mL). The organic layer was collected in a 250 mL Erlenmeyer flask, dried over anhydrous Na_2SO_4, filtered by gravity, and concentrated under reduced pressure. The residue was incorporated in the silica (1 g) and then purified by liquid chromatography on a silica gel column using CH_2Cl_2 as eluent. Light-yellow solid, $\eta = 64\%$ (0.6914 g, 2.39 mmol); ^{1}H-NMR (400 MHz, DMSO-d$_6$) δ_H 4.01 (3H, s), 7.70 (1H, dd, J = 9.0 Hz, J = 2.1 Hz), 7,80 (1H, d, J =

¶ The procedures employed in the synthetic route A (Scheme 1) have been already described in detail in ref. 15 and 16.

Open Access Article. Published on 19 February 2024. Downloaded on 5/7/2024 9:52:29 PM.
This article is licensed under a Creative Commons Attribution 3.0 Unported Licence.

2.7 Hz), 8.16 (1H, d, $J = 2.0$ Hz), 8.24–8.27 (2H, m), 9.18 (1H, s); ^{13}C-NMR (100 MHz, DMSO-d_6) δ_C 56.49, 108.10, 119.68, 125.46, 127.21, 127.27, 128.07, 130.39, 135.59, 135.82, 136.54, 148.29, 154.76; *m/z* (ESI-IT MS, +) 289.53 (M + H^+), M^+ ($C_{14}H_9ClN_2O_3$) requires 288.03; R_f, 0.77 in CH_2Cl_2; HPLC-DAD: RT, 23.817 min, purity degree (peak relative area) 96.4%.

Synthesis of compound ***16*** *(step xiv).* In a 250 mL glass round-bottom flask charged with a magnetic stir bar, 4-aminobutan-1-ol (1 equiv., 6.93 mmol, 0.64 mL) and phthalic anhydride (1 equiv., 6.93 mmol, 1.0270 g) were dissolved in dioxane (100 mL) and left under stirring overnight at 100 °C in an oil bath. Then, dioxane was removed under reduced pressure and 50 mL of CH_2Cl_2 was added to the flask. The mixture was transferred to a 250 mL glass separating funnel and washed with a saturated aqueous NaCl solution (3 × 50 mL). The resulting organic phase was collected in a 250 mL Erlenmeyer flask, dried over anhydrous Na_2SO_4, filtered by gravity, and evaporated to dryness under reduced pressure. The residue was then purified by liquid chromatography on a silica gel column using CH_2Cl_2/CH_3OH (4 : 1 v/v) as eluent. Yellowish solid, η = 70% (1.0633 g, 4.85 mmol); ^{1}H-NMR (400 MHz, DMSO-d_6) δ_H 1.44–1.37 (2H, m), 1.66–1.58 (2H, m), 3.39 (2H, q, $J = 2.0$ Hz), 3.57 (2H, t, $J = 7.1$ Hz), 4.38 (1H, t, $J = 5.2$ Hz), 7.88–7.81 (4H, m); ^{13}C-NMR (100 MHz, DMSO-d_6) δ_C 24.71, 29.77, 37.37, 60.15, 122.96, 131.58, 134.34, 167.93; R_f, 0.86 in CH_2Cl_2/CH_3OH 4 : 1 (v/v); HPLC-DAD: RT, 12.280 min, purity degree (peak relative area) 99.8%.

Synthesis of compound ***17*** *(step xv).* In a 250 mL glass round-bottom flask charged with a magnetic stir bar and placed under inert conditions (argon atmosphere), compound **16** (1 equiv., 4.51 mmol, 0.9892 g) was dissolved in anhydrous CH_2Cl_2 (100 mL) followed by the addition of DMP (1.1 equiv., 4.96 mmol, 2.1037 g). The mixture reacted at rt for 1 h and a white precipitate was formed, which was collected by gravity filtration and discarded. The filtrate was evaporated to dryness under reduced pressure and purified by liquid chromatography on a silica gel column using hexane/AcOEt (1 : 1 v/v) as eluent. Yellowish oil, η = 63% (0.6169 g, 2.84 mmol); ^{1}H-NMR (400 MHz, DMSO-d_6) δ_H 1.84 (2H, p, $J = 7.0$ Hz), 2.54–2.51 (2H, m), 3.59 (2H, t, $J = 6.8$ Hz), 7.88–7.81 (4H, m), 9.64 (1H, t, $J = 1.1$ Hz); ^{13}C-NMR (100 MHz, DMSO-d_6) δ_C 20.61, 36.77, 122.96, 131.65, 134.30, 167.97, 200.46; R_f, 0.61 in hexane/AcOEt 1 : 1 (v/v).

Concluding remarks

Acridine-based compounds have for long attracted the interest of researchers across disciplines, and such interest endures due to the unique chemical, physical, and biological properties of those heterocyclic molecules. Our research group makes no exception to this rule, very much driven by our long-term interest in anti-infective agents, including antimalarials inspired in mepacrine.[14–17,33–38] This led us to advance, in recent years, new 4-aminoacridines (**15**) and 4,9-diaminoacridines (**10**) as multi-stage antiplasmodial hits.[15,16] Although we were successful in addressing their quite challenging synthesis, the overall modest yields obtained as well as harsh and/or time-consuming procedures involved prompted us to work on the optimization of the synthetic routes. The efforts undertaken are herein described and allowed us to make significant progress on several parts of the overall synthesis scheme. As such, the synthesis of compound **6**, a common precursor to both families of the target amino-acridines, can now be achieved in three (Scheme 2, part A) instead of five (Scheme 1, part A) steps, using two commercially available reagents and offering an overall yield of 63%, which more than doubles that of the previous approach (24%). Also, the introduction of side chains in the C-9 and C-4 positions of the acridine ring in the route to 4,9-diaminoacridines **10** (Scheme 1, steps vi and viii) could be significantly improved by, respectively, use of MW heating in step vi, and change from a bimolecular nucleophilic substitution into a reductive amination in step viii (Scheme 2, part B, steps vi_b and $viii_b$); overall, this simplified experimental procedures and considerably reduced reaction time and the need to use high temperatures, while improving yield. Finally, the synthesis route to 4-aminoacridines **15** could also be improved, mainly by a fine tuning of experimental conditions of the reduction steps leading to the 4-aminoacridine intermediate **12** (Scheme 2, part B, steps xi_b and xii_b).

To sum up, after these efforts, 4,9-diaminoacridines **15** can be produced from **6** by four reactional steps (S_NAr in C-9, reduction in C-4, reductive amination in C-4, and hydrazinolysis) in 21% overall yield that is about 2-fold higher than that previously reported (13%).[15] Likewise, 4-aminoacridines **10** can be now delivered from **6** by five reactional steps (S_NAr in C-9, reduction in C-9 and C-4, S_N2 in C-4 and hydrazinolysis) with an overall yield of 34%, also superior to that afforded by the previous synthetic route (21%).[15,16] Overall, this translates into a more convenient and sustainable production of functionalized acridines, paving the way towards future synthetic approaches targeting acridine-based compounds.

Conflicts of interest

There are no conflicts to declare.

Acknowledgements

This work received financial support from PT national funds (FCT/MCTES, Fundação para a Ciência e Tecnologia and Ministério da Ciência, Tecnologia e Ensino Superior) through project CIRCNA/BRB/0281/2019. The authors further thank FCT/MCTES for supporting Research Unit LAQV-REQUIMTE (10.54499/LA/P/0008/2020; 10.54499/UIDP/50006/2020; 10.54499/UIDB/50006/2020) and for the Doctoral Grant to MF (SRFH/BD/147354/2019). MP further acknowledges the "la Caixa" Foundation for Grant HR21-848.

Notes and references

1 N. R. Raulins, Acridines, in *Chemistry of Heterocyclic Compounds*, ed. R. M. Acheson, John Wiley & Sons, Inc., 2nd edn, 1973, ch. 1, pp. 9–108.
2 R. M. Acheson, Nomenclature and Numbering System, in *Chemistry of Heterocyclic Compounds*, ed. R. M. Acheson, John Wiley & Sons, Inc., 2nd edn, 1973, vol. 9, pp. 1–8.

© 2024 The Author(s). Published by the Royal Society of Chemistry

Open Access Article. Published on 19 February 2024. Downloaded on 5/7/2024 9:52:29 PM.
This article is licensed under a Creative Commons Attribution 3.0 Unported Licence.

3 P. Prasher and M. Sharma, *MedChemComm*, 2018, **9**, 1589–1618.
4 M. Gensicka-Kowalewska, G. Cholewiński and K. Dzierzbicka, *RSC Adv.*, 2017, **7**, 15776–15804.
5 R. Kumar, S. Sharma and D. Prasad, Acridones: A Relatively Lesser Explored Heterocycle for Multifactorial Diseases, in *Key Heterocycle Cores for Designing Multitargeting Molecules*, ed. O. Silakari, Elsevier, 1st edn, 2018, ch. 3, pp. 53–132.
6 R. Kumar, M. Kaur and M. Kumari, *Acta Pol. Pharm.*, 2012, **69**, 3–9.
7 A. Bernthsen, *Justus Liebigs Ann. Chem.*, 1884, **224**, 1–56.
8 J. Ježek, J. Hlaváček and J. Šebestík, Syntheses, in *Biomedical Applications of Acridines: Derivatives, Syntheses, Properties and Biological Activities with a Focus on Neurodegenerative Diseases*, ed. J. Ježek, J. Hlaváček and J. Šebestík, Springer International Publishing, Cham, 2017, vol. 72, pp. 9–45.
9 A. Schmidt and M. Liu, Recent Advances in the Chemistry of Acridines, in *Advances in Heterocyclic Chemistry*, ed. E. F. V. Scriven and C. A. Ramsden, Academic Press, 2015, ch. 4, vol. 115, pp. 287–353.
10 J. Chiron and J.-P. Galy, *Synthesis*, 2004, 313–325.
11 Z. Zawada, J. Šebestík, M. Šafařík and P. Bouř, *Eur. J. Org Chem.*, 2011, 6989–6997.
12 M. Kozurkova, D. Sabolova and P. Kristian, *J. Appl. Toxicol.*, 2021, **41**, 175–189.
13 M. Fonte, N. Tassi, P. Gomes and C. Teixeira, *Molecules*, 2021, **26**, 600.
14 A. Gomes, B. Pérez, I. Albuquerque, M. Machado, M. Prudêncio, F. Nogueira, C. Teixeira and P. Gomes, *ChemMedChem*, 2014, **9**, 305–310.
15 M. Fonte, N. Fagundes, A. Gomes, R. Ferraz, C. Prudêncio, M. J. Araújo, P. Gomes and C. Teixeira, *Tetrahedron Lett.*, 2019, **60**, 1166–1169.
16 M. Fonte, N. Tassi, D. Fontinha, I. Bouzón-Arnáiz, R. Ferraz, M. J. Araújo, X. Fernàndez-Busquets, M. Prudêncio, P. Gomes and C. Teixeira, *ChemMedChem*, 2021, **16**, 788–792.
17 B. Pérez, C. Teixeira, A. S. Gomes, I. S. Albuquerque, J. Gut, P. J. Rosenthal, M. Prudêncio and P. Gomes, *Bioorg. Med. Chem. Lett.*, 2013, **23**, 610–613.
18 M. O. Anderson, J. Sherrill, P. B. Madrid, A. P. Liou, J. L. Weisman, J. L. DeRisi and R. K. Guy, *Bioorg. Med. Chem.*, 2006, **14**, 334–343.
19 S. Young Kim, Y. Ri Kim, H. Tae Kim, A. Kumar Jaladi and D. Keun An, *ChemistrySelect*, 2022, **7**, e202202351.
20 A. R. Jeon, M. E. Kim, J. K. Park, W. K. Shin and D. K. An, *Tetrahedron*, 2014, **70**, 4420–4424.
21 N. Boechat, J. C. S. da Costa, J. de Souza Mendonça, P. S. M. de Oliveira and M. V. N. D. Souza, *Tetrahedron Lett.*, 2004, **45**, 6021–6022.
22 C. P. Prasanth, E. Joseph, A. Abhijith, D. S. Nair, I. Ibnusaud, J. Raskatov and B. Singaram, *J. Org. Chem.*, 2018, **83**, 1431–1440.
23 A. Saeed and Z. Ashraf, *J. Chem. Sci.*, 2006, **118**, 419–423.
24 A. de la Hoz, A. Díaz-Ortiz and P. Prieto, Microwave-Assisted Green Organic Synthesis, in *Alternative Energy Sources for Green Chemistry*, ed. G. Stefanidis and A. Stankiewicz, The Royal Society of Chemistry, 23rd edn, 2016, ch. 1, pp. 1–33.
25 M. Staderini, N. Cabezas, M. L. Bolognesi and J. C. Menéndez, *Tetrahedron*, 2013, **69**, 1024–1030.
26 S. D. Meyer and S. L. Schreiber, *J. Org. Chem.*, 1994, **59**, 7549–7552.
27 D. Setamdideh and B. Khezri, *Asian J. Chem.*, 2010, **22**, 5575–5580.
28 H. K. Kadam and S. G. Tilve, *RSC Adv.*, 2012, **2**, 6057–6060.
29 A. J. MacNair, M.-M. Tran, J. E. Nelson, G. U. Sloan, A. Ironmonger and S. P. Thomas, *Org. Biomol. Chem.*, 2014, **12**, 5082–5088.
30 M. Ficker, J. F. Petersen, J. S. Hansen and J. B. Christensen, *Org. Prep. Proced. Int.*, 2014, **46**, 176–182.
31 K. Hanaya, T. Muramatsu, H. Kudo and Y. L. Chow, *J. Chem. Soc., Perkin Trans. 1*, 1979, 2409–2410.
32 H. Bailey, W. Heaton, N. Vicker and B. Potter, *Synlett*, 2006, **2006**, 2444–2448.
33 B. Pérez, C. Teixeira, J. Gut, P. J. Rosenthal, J. R. B. Gomes and P. Gomes, *ChemMedChem*, 2012, **7**, 1537–1540.
34 B. C. Pérez, C. Teixeira, I. S. Albuquerque, J. Gut, P. J. Rosenthal, J. R. B. Gomes, M. Prudêncio and P. Gomes, *J. Med. Chem.*, 2013, **56**, 556–567.
35 B. C. Pérez, C. Teixeira, M. Figueiras, J. Gut, P. J. Rosenthal, J. R. B. Gomes and P. Gomes, *Eur. J. Med. Chem.*, 2012, **54**, 887–899.
36 B. Pérez, C. Teixeira, I. S. Albuquerque, J. Gut, P. J. Rosenthal, M. Prudêncio and P. Gomes, *MedChemComm*, 2012, **3**, 1170–1172.
37 A. Gomes, I. Fernandes, C. Teixeira, N. Mateus, M. J. Sottomayor and P. Gomes, *ChemMedChem*, 2016, **11**, 2703–2712.
38 A. Gomes, M. Machado, L. Lobo, F. Nogueira, M. Prudêncio, C. Teixeira and P. Gomes, *ChemMedChem*, 2015, **10**, 1344–1349.

© 2024 The Author(s). Published by the Royal Society of Chemistry

Electronic Supporting Information

Improved synthesis of antiplasmodial 4-aminoacridines and 4,9-diaminoacridines

Mélanie Fonte,*[a] Cátia Teixeira[a,†] and Paula Gomes*[a]

[a] LAQV-REQUIMTE, Departamento de Química e Bioquímica, Faculdade de Ciências, Universidade do Porto, Portugal;

† Current affiliation: Gyros Protein Technologies Inc., Tucson, Arizona, USA.

Contents:

General information 2

Spectral and chromatographic traces for compounds 4, 7, 9, 13, 16, 17 (Figures S1-S21) 3

General information.

All solvents and commercial chemicals were purchased from Sigma-Aldrich (phenol, $Pd(OAc)_2$, *N,N*-diethylpentan-1,4-diamine, $NH_2NH_2.2H_2O$, Pd-C, Cs_2CO_3, 2-amino-4-chlorobenzoic acid, phthalic anhydride, $SnCl_2.2H_2O$, $Pd(PPh_3)_2Cl_2$, 4-bromo-3-nitroanisole, $Cu(NO_3)_2.3H_2O$, $CuBr_2$, and $NaBH(OAc)_3$), Fluorochem (Dess-Martin periodiane and *N*-(4-bromobutyl)-phthalimide), Fluka (4-aminobutanol, $NaBH_4$, Et_3SiH, and anhydrous $SnCl_2$), Biochem Chemopharma ($NaHCO_3$), Abcr (*rac*-BINAP), VWR international (HCl 37 %; HPLC gradient grade, LC-MS grade, and p.a. quality solvents), Merck (CH_3COONa), Fisher Chemical (glacial acetic acid), Alfa Aesar (methyl 2-amino-4-chlorobenzoate), PanReac AppliChem (Na_2SO_4 and NH_3 25 %), Carlo Erba (toluene), LabChem (CH_3OH, CH_2Cl_2, hexane, AcOEt, diethyl ether), Honeywell Riedel-de-Haën (dioxane and dichloroethane), and CortecNet (deuterated solvents).

Aluminium foils coated with silica-gel 60 F254 from Merck were used for TLC analysis (retention factor, R_f). TLC chromatograms obtained were revealed with ultra-violet light (254 nm), using a Viber Lourmat lamp, model CN-6 and/or using a phosphomolybdic acid stain (15 mL of phosphomolybdic acid solution (20% wt in ethanol) and 85 mL of ethanol).

The purification of the compounds was carried out via normal phase liquid chromatography in glass columns charged with silica gel 60, from Sigma Aldrich, as solid phase. A mixture of solvents (identified in each case) was used as the mobile phase (eluent).

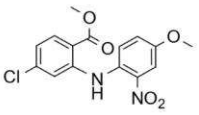
The synthesis of compound **7** was carried out in a CEM microwave model Discovery S.

Electrospray ionization-ion trap mass spectrometry (ESI-IT MS) analyses (direct injection with detection in positive mode) were performed with solutions of the pure products in p.a. methanol, using a Finnigan Surveyor LCQ DECA XP MAX spectrometer, at the Department of Chemistry and Biochemistry of the Faculty of Sciences of the University of Porto.

The determination of the retention time (RT) and purity degree of the compounds was carried out by analytical reverse-phase high-performance liquid chromatography (RP-HPLC), using a Hitachi-Merck Elite LaChrom system equipped with an L-2130 quaternary pump, an L-2200 thermostatted (Peltier effect) automated sampler, and an L-2455 diode-array detector (DAD). Samples were prepared by dissolution of compounds in acetonitrile and injected in an end-capped octadecylsilane (C18) column Purospher star RP-C18 of 125 × 4.0 mm and 5 µm pore size. A gradient elution (1 to 100 % of acetonitrile in 0.05% aqueous trifluoroacetic acid) was carried out for 30 minutes, at a flow rate of 1 mL/min, and detection was set at 290 nm.

^{1}H-NMR and ^{13}C-NMR spectra were acquired on a Bruker Avance III spectrometer at frequencies of 400 mHz and 100 mHz, respectively, and samples were prepared in either DMSO-d_6 or $CDCl_3$, using tetramethylsilane (TMS) as an internal reference. Chemical shifts for protons and carbon are reported in parts per million (ppm) downfield and are referenced to residual protium in the NMR solvent. Data are represented as follows: chemical shift, integration, multiplicity (br = broad, s = singlet, d = double, t = triplet, q = quartet, m = multiplet), coupling constants in Hertz (Hz).

Methyl 4-chloro-2-[(4-methoxy-2-nitrophenyl)amino]benzoate (4)



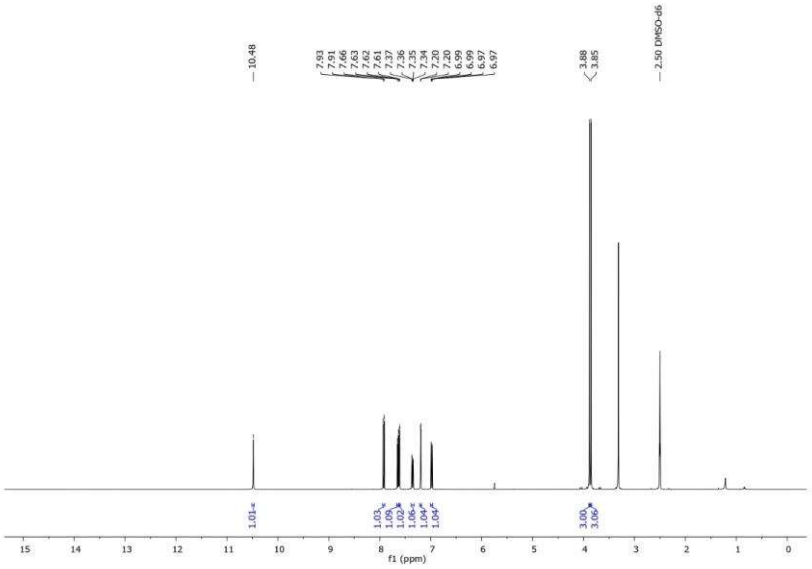


Figure S1. ^{1}H-NMR spectrum (400 MHz, DMSO-d_6) of **4**.

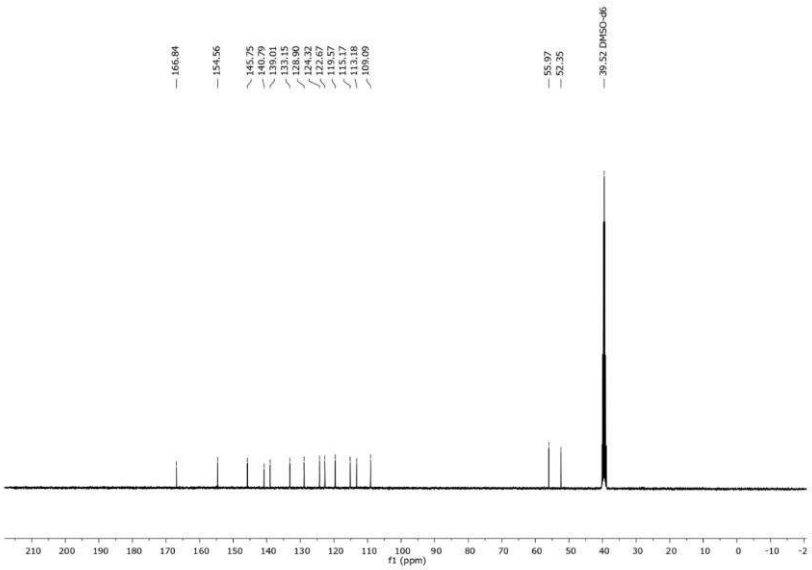


Figure S2. ^{13}C- NMR spectrum (100 MHz, DMSO-d_6) of **4**.

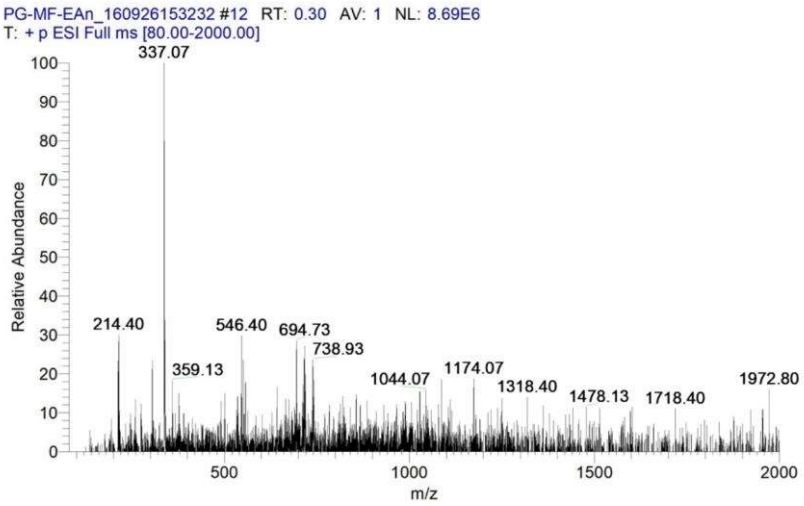


Figure S3. ESI-IT (+) mass spectrum of **4**.

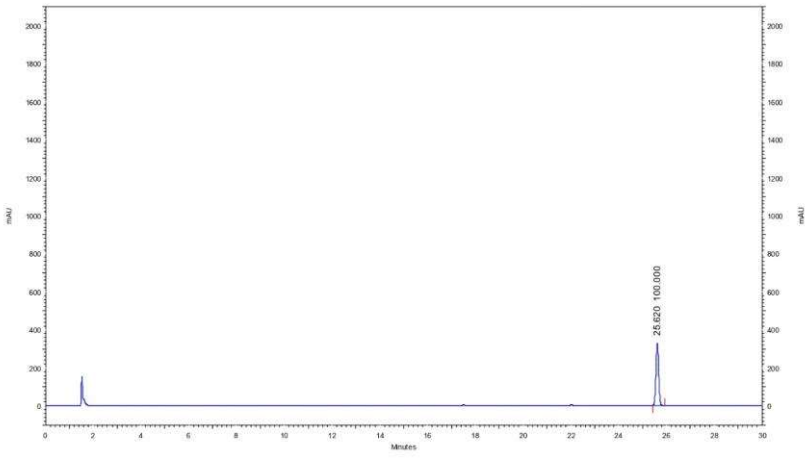
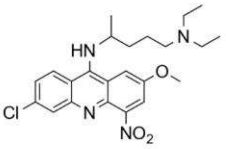


Figure S4. HPLC trace of **4**.

6-chloro-9-[*N*-(4-(diethylamino)pent-2-yl]amino-2-methoxy-4-nitroacridine (7)



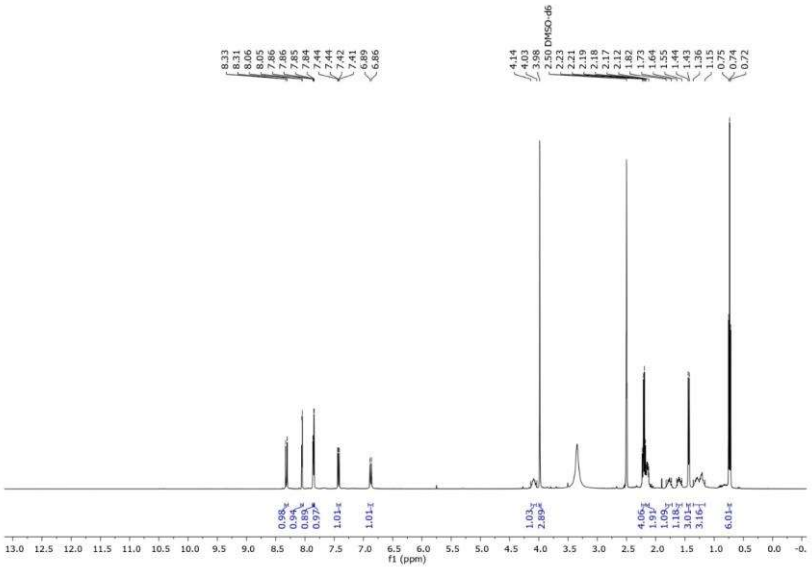


Figure S5. ^{1}H-NMR spectrum (400 MHz, DMSO-d_6) of **7**.

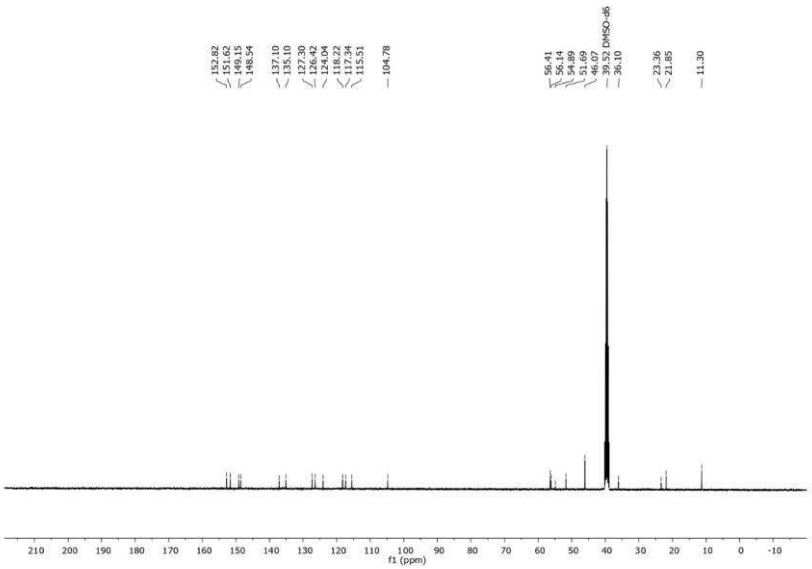


Figure S6. ^{13}C-NMR spectrum (100 MHz, DMSO-d_6) of **7**.

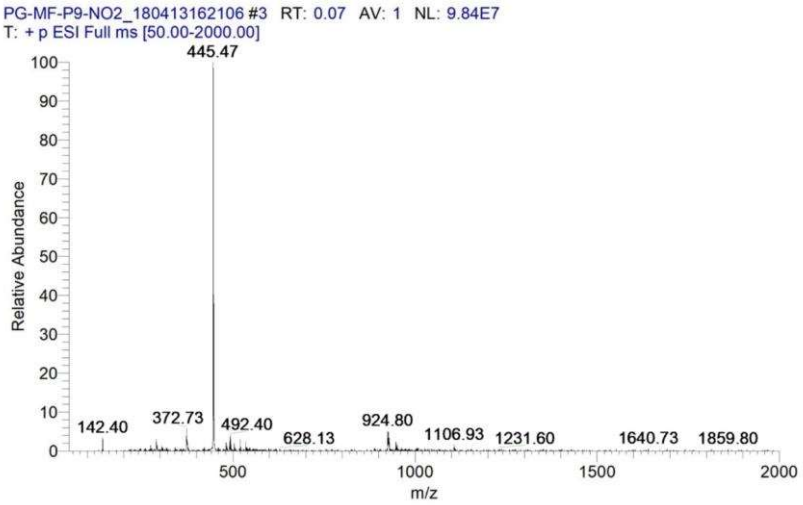


Figure S7. ESI-IT (+) mass spectrum of **7**.

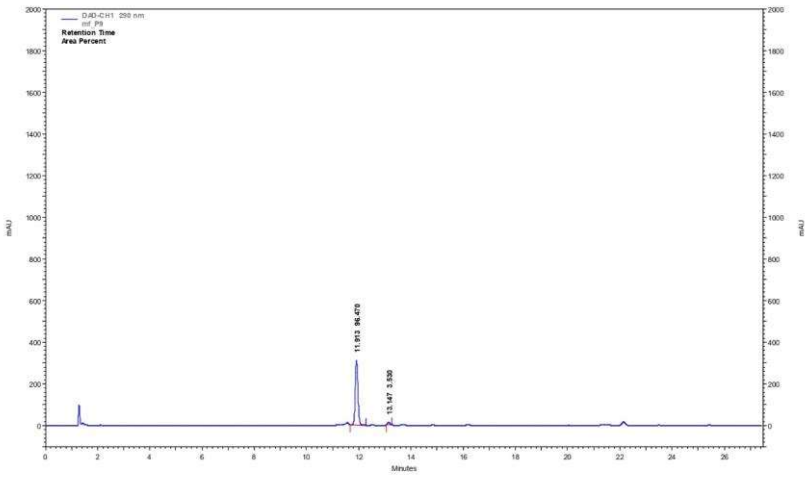
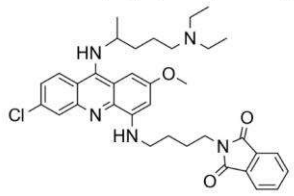


Figure S8. HPLC trace of **7**.

6-chloro-9-[*N*-(4-(diethylamino)pent-2-yl]amino-4-(4-phthalimidobutyl)amino-2-methoxy-acridine (9)



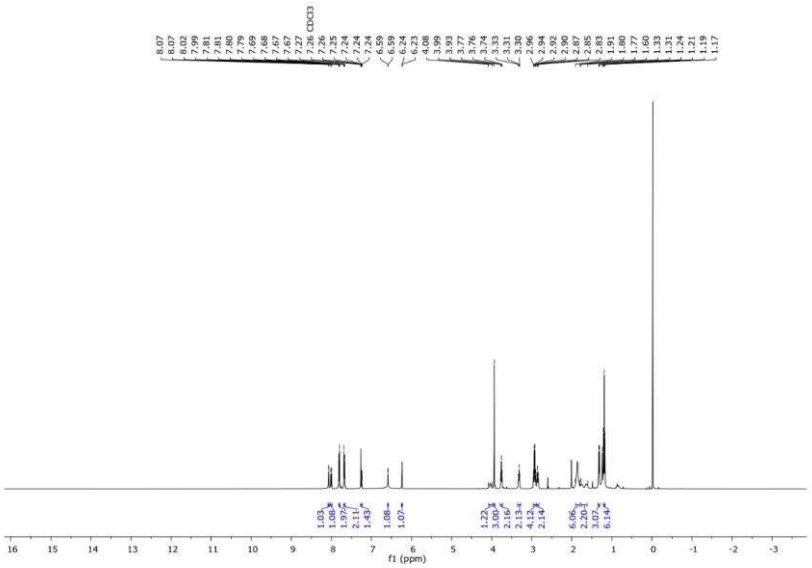


Figure S9. ^{1}H-NMR spectrum (400 MHz, $CDCl_3$) of **9**.

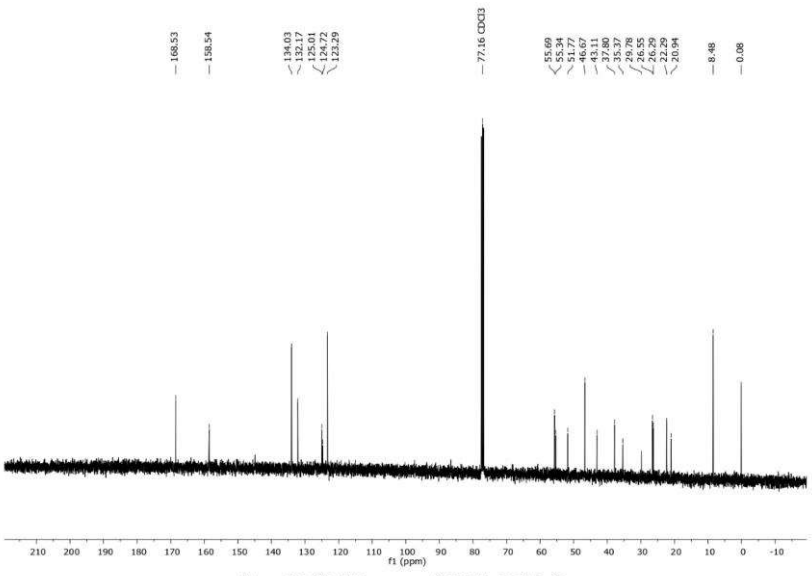


Figure S10. ^{13}C-NMR spectrum (100 MHz, $CDCl_3$) of **9**.

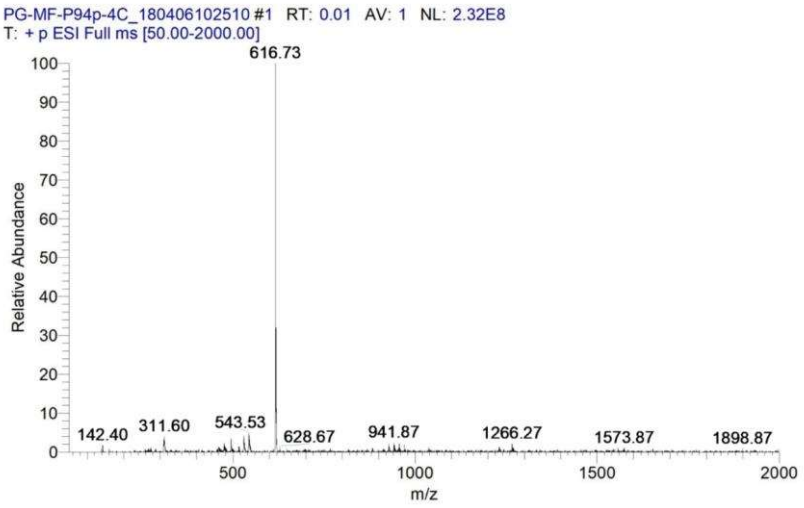


Figure S11. ESI-IT (+) mass spectrum of **9**.

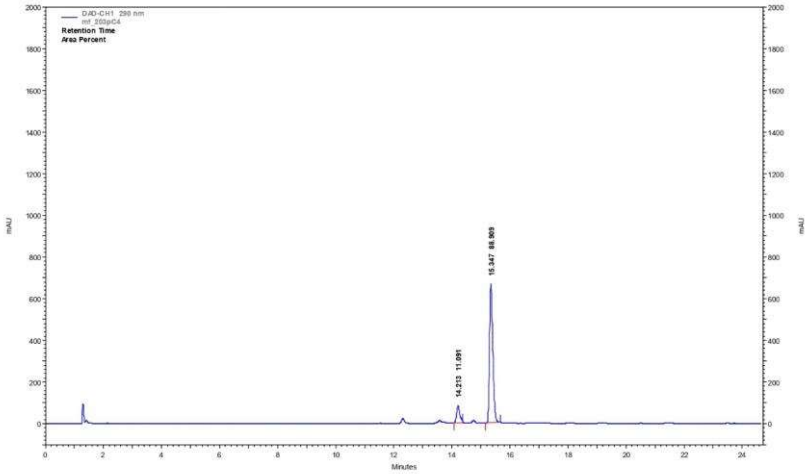
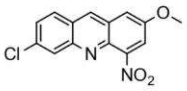


Figure S12. HPLC trace of **9**.

6-chloro-2-methoxy-4-nitroacridine (13)



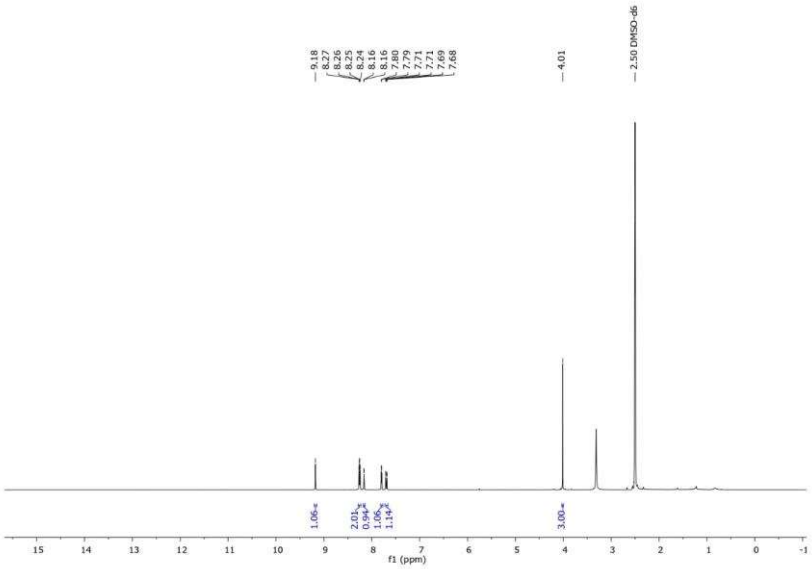


Figure S13. ^{1}H-NMR spectrum (400 MHz, DMSO-d_6) of **13**.

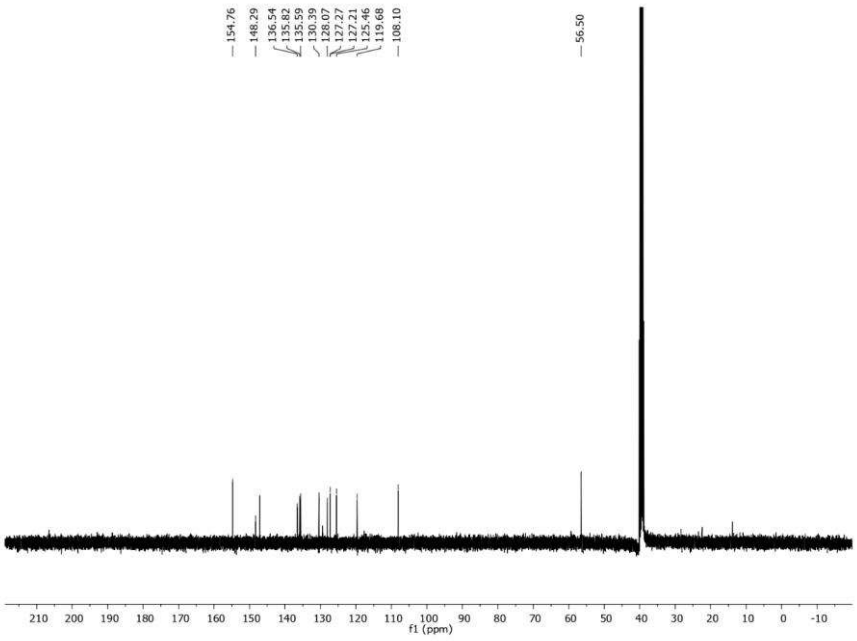


Figure S14. ^{13}C-NMR spectrum (100 MHz, DMSO-d_6) of **13**.

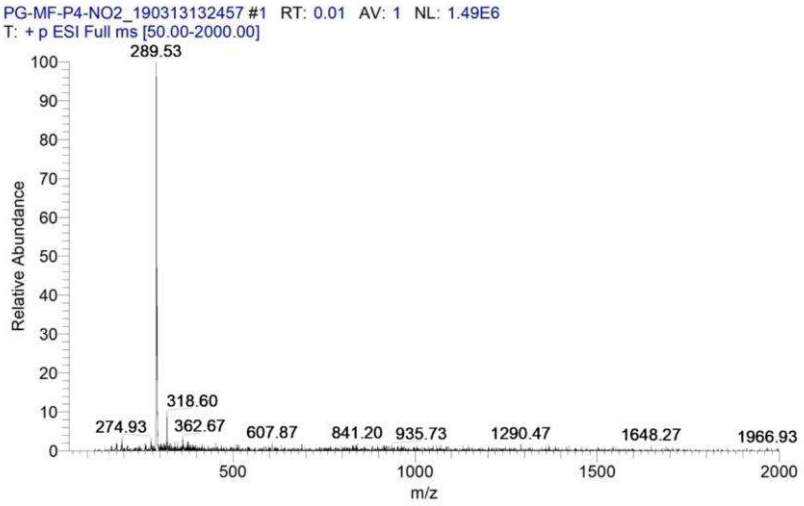


Figure S15. ESI-IT (+) mass spectrum of **13**.

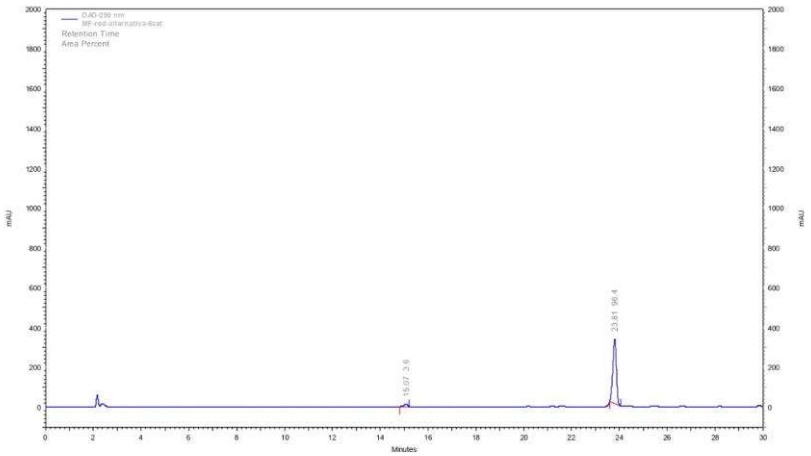
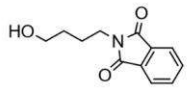


Figure S16. HPLC trace of **13**.

***N*-(4-hydroxybutyl)phthalimide (16)**



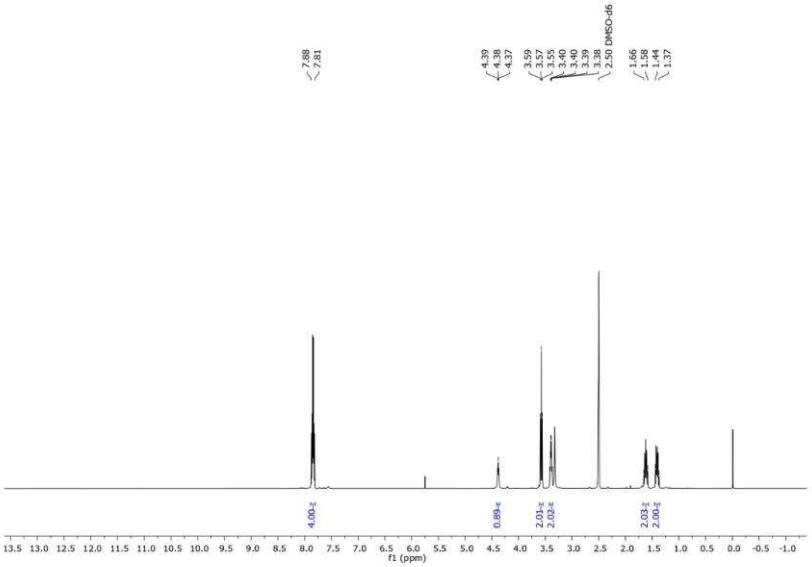


Figure S17. ^{1}H-NMR spectrum (400 MHz, DMSO-d_6) of **16**.

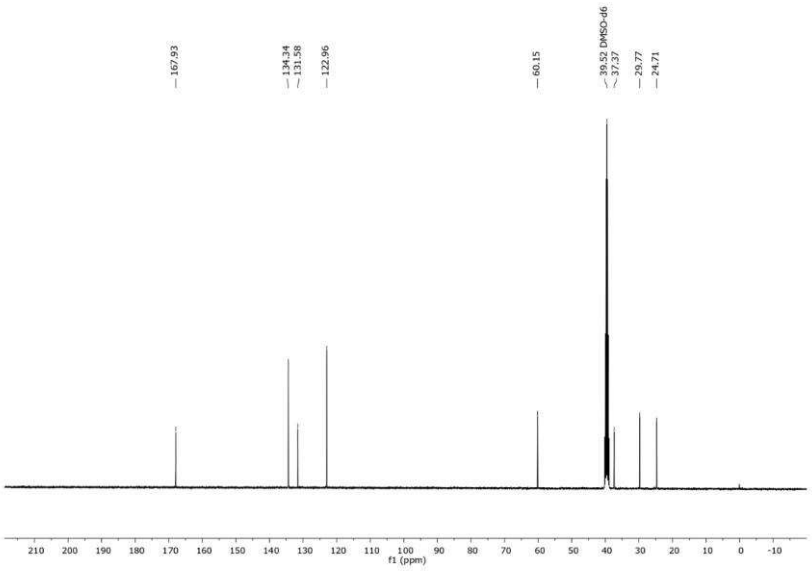


Figure S18. ^{13}C- NMR spectrum (100 MHz, DMSO-d_6) of **16**.

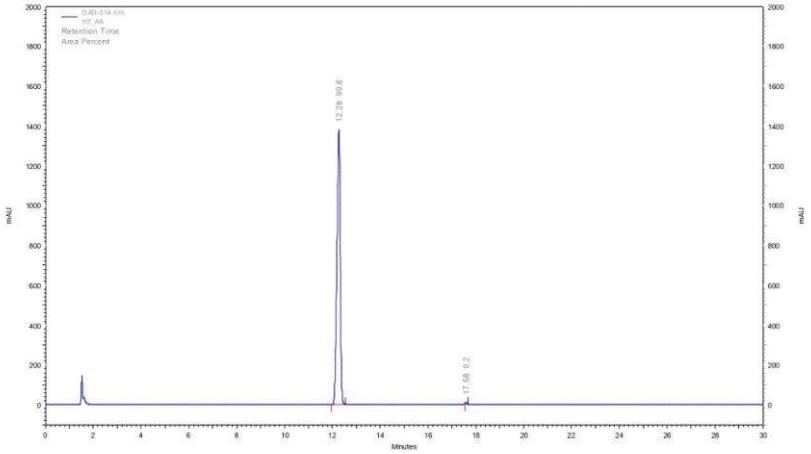
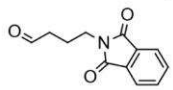


Figure S19. HPLC trace of **16**.

Y-Phthalimidobutyraldehyde (17)



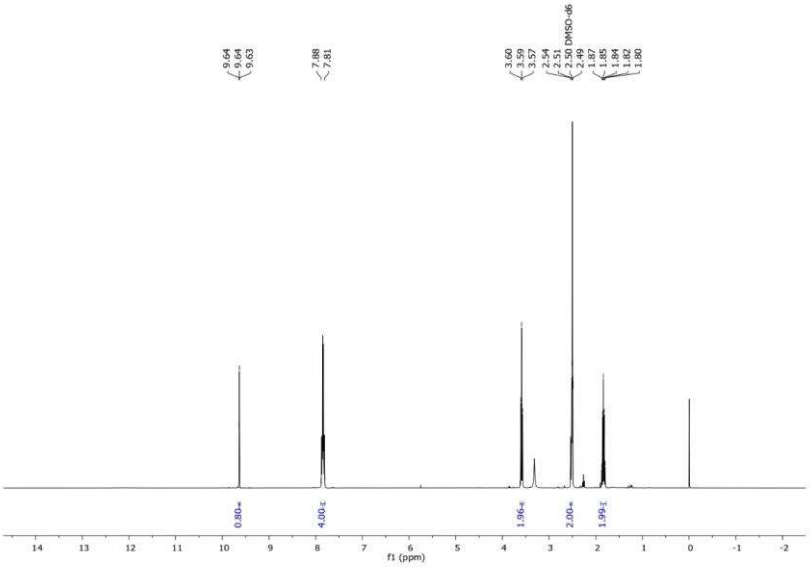


Figure S20. ^{1}H-NMR spectrum (400 MHz, DMSO-d_6) of **17**.

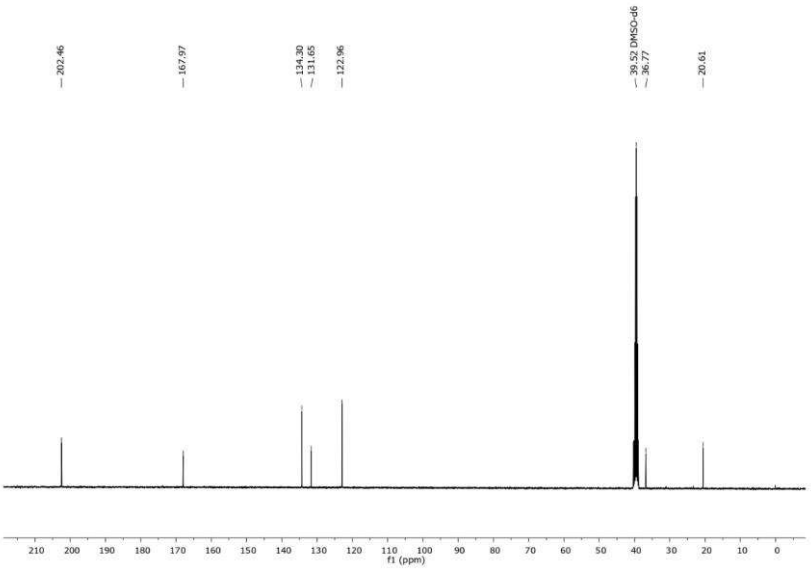


Figure S21. ^{13}C-NMR spectrum (100 MHz, DMSO-d_6) of **17**.

CHAPTER III

Aminoacridine-cinnamic acid hybrids

This chapter describes the synthesis and *in vitro* evaluation of the antiplasmodial and antiproliferative properties of cinnamic acid conjugates of 4-aminoacridines and 4,9-diaminoacridines.

Contents:

Article III

New 4-(*N*-cinnamoylbutyl)aminoacridines as potential multi-stage antiplasmodial leads

Article IV

Disclosure of cinnamic acid/4,9-diaminoacridine conjugates as multi-stage antiplasmodial hits

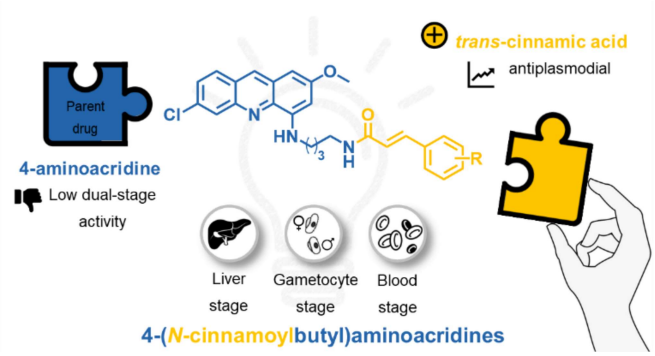
Article V

Repurposing antiplasmodial leads for cancer: exploring the antiproliferative effects of *N*-cinnamoyl-aminoacridines

Article III

New 4-(*N*-cinnamoylbutyl)aminoacridines as potential multi-stage antiplasmodial leads

Mélanie Fonte, Diana Fontinha, Diana Moita, Omar Caño-Prades, Yunuen Avalos-Padilla, Xavier Fernàndez-Busquets, Miguel Prudêncio, Paula Gomes, Cátia Teixeira



Eur. J. Med. Chem., **2023**, *258, 115575* doi: 10.1016/j.ejmech.2023.115575

Summary

Following the findings reported in Chapter II (Article I), where PQ-CQ merge hybrids, namely, 4-aminoacridines and 4,9-diaminoacridines, were confirmed to display moderate dual antiplasmodial action, we addressed the optimization of this action by producing second-generation compounds, firstly by conjugation of CAs to 4-aminoacridines. Twelve new conjugates were synthesized and further evaluated against blood, liver, and gametocyte forms of the malarial parasite. The results confirmed the positive impact of such conjugation in the overall antiplasmodial activity *in vitro*, but especially in liver and gametocyte stages, with no observable increase in cytotoxicity.

Declaration of authorship of published article III: New 4-(*N*-cinnamoylbutyl)aminoacridines as potential multi-stage antiplasmodial leads[3]

I, Mélanie Fonte, declare that the experimental design, laboratory work involving the synthesis, purification, and characterization of all compounds used in this study, and the data analysis and discussion were carried out by me, under the supervision of Prof. Paula Gomes, Dr. Cátia Teixeira and Dr. Miguel Prudêncio. Additionally, I participated in the *in vitro* assays of all the tested compounds in *Instituto de Medicina Molecular João de Lobo Antunes – Faculdade de Medicina da Universidade de Lisboa,* under the guidance of Dr. Miguel Prudêncio, and carried out the hemolysis assays performed in *Faculdade de Ciências da Universidade do Porto*. I was also responsible for the writing of the article's original draft that was next corrected and validated by all the co-authors.

We, Cátia Teixeira, Paula Gomes, and Miguel Prudêncio, as Mélanie Fonte's supervisors, hereby confirm that the information above is correct.

Mélanie Fonte

Mélanie Fonte

Paula Gomes | Cátia Teixeira | Miguel Prudêncio

[3] Copyright Elsevier 2023. Reproduced with permission.

European Journal of Medicinal Chemistry 258 (2023) 115575

Contents lists available at ScienceDirect

European Journal of Medicinal Chemistry

journal homepage: www.elsevier.com/locate/ejmech

Research paper

New 4-(*N*-cinnamoylbutyl)aminoacridines as potential multi-stage antiplasmodial leads

Mélanie Fonte [a,*], Diana Fontinha [b], Diana Moita [b], Omar Caño-Prades [c], Yunuen Avalos-Padilla [c], Xavier Fernàndez-Busquets [c,d,e], Miguel Prudêncio [b], Paula Gomes [a,**], Cátia Teixeira [a,f]

[a] LAQV-REQUIMTE, Departamento de Química e Bioquímica, Faculdade de Ciências, Universidade do Porto, Portugal
[b] Instituto de Medicina Molecular, Faculdade de Medicina, Universidade de Lisboa, Portugal
[c] Nanomalaria Group, Institute for Bioengineering of Catalonia (IBEC), The Barcelona Institute of Science and Technology, Barcelona, Spain
[d] Barcelona Institute for Global Health (ISGlobal, Hospital Clínic-Universitat de Barcelona), Spain
[e] Nanoscience and Nanotechnology Institute (IN2UB), University of Barcelona, Spain
[f] Gyros Protein Technologies Inc., Tucson, AZ, USA

ARTICLE INFO

Handling Editor: Dr. Z Liu

Keywords:
Acridine
Antimalarial
Blood-stage
Cinnamic acid
Gametocyte
Hybrid
Liver-stage
Multi-target

ABSTRACT

A novel family of 4-aminoacridine derivatives was obtained by linking this heteroaromatic core to different *trans*-cinnamic acids. The 4-(*N*-cinnamoylbutyl)aminoacridines obtained exhibited *in vitro* activity in the low- or sub-micromolar range against (i) hepatic stages of *Plasmodium berghei*, (ii) erythrocytic forms of *Plasmodium falciparum*, and (iii) early and mature gametocytes of *Plasmodium falciparum*. The most active compound, having a *meta*-fluorocinnamoyl group linked to the acridine core, was 20- and 120-fold more potent, respectively, against the hepatic and gametocyte stages of *Plasmodium* infection than the reference drug, primaquine. Moreover, no cytotoxicity towards mammalian and red blood cells at the concentrations tested was observed for any of the compounds under investigation. These novel conjugates represent promising leads for the development of new multi-target antiplasmodials.

1. Introduction

Malaria is an infectious disease caused by protozoan parasites of the genus *Plasmodium* that remains a major concern in low-income tropical and sub-tropical countries. Despite the steady decrease in the malaria burden during the first decade of the 21st century, progress has stalled in the past five years. Moreover, global warming may favor the migration of the *Anopheles* mosquitoes, the disease's main vector, to currently malaria-free regions [1]. Among the reasons for malaria's ongoing burden are (i) the complex life cycle of the *Plasmodium* parasite, which hampers the swift and successful development of effective drugs and vaccines, and (ii) the fast selection and spread of drug-resistant parasite strains to all the drugs developed so far [2]. In fact, the world is now facing a concerning decline in the effectiveness of the frontline artemisinin-based combination therapies (ACT), as signs of resistance to this therapy has transposed the borders of Southeast Asia and has spread even to Africa [3–7]. This highlights the pressing need to discover new potent and safe antimalarial drugs, ideally, cost-effective since malaria mostly affects low-income populations, and actives against multiple stages of the life cycle of different *Plasmodium* species to decrease the probability of resistance appearance [8].

One cost-effective strategy towards affordable medicines is based on rescuing old antimalarial pharmacophores, through chemical modifications, aiming at their re-introduction in the antimalarial chemotherapy arsenal [9,10]. In this regard, our research group have been working on the rescuing of classical antimalarial drugs like quinacrine (QN), chloroquine (CQ), and primaquine (PQ), which their use has been limited due to toxicity and resistance issues [11–18]. QN, an acridine-based compound, was the first synthetic antimalarial drug and its potent blood-schizonticidal activity turned it into a promising substitute for quinine, the first effective therapy used against malaria [10,19]. However, the serious side effects of QN led to its rapid replacement

* Corresponding author.
** Corresponding author.
E-mail addresses: up201305020@edu.fc.up.pt (M. Fonte), pgomes@fc.up.pt (P. Gomes).

https://doi.org/10.1016/j.ejmech.2023.115575
Received 14 April 2023; Received in revised form 9 June 2023; Accepted 14 June 2023
Available online 22 June 2023
0223-5234/© 2023 The Authors. Published by Elsevier Masson SAS. This is an open access article under the CC BY license (http://creativecommons.org/licenses/by/4.0/).

by CQ, which displayed higher efficiency, oral bioavailability and safety. Still, the use of CQ to treat malaria has been gradually abandoned due to the emergence and spread of CQ-resistant strains of *P. falciparum*, the most lethal agent of human malaria [19,20]. While most antimalarial agents available, such as the case of QN and CQ, target blood-stage parasites, PQ remained, for many years, the only drug in clinical use that (i) acts against liver forms of all *Plasmodium* species, including the latent hypnozoites of *P. vivax* and *P. ovale* that can cause malaria relapses, and (ii) efficiently eliminates gametocytes, the mosquito vector-infective forms of malaria parasites [21]. Nevertheless, PQ also presents significant downsides that limit its clinical application, including its high hemotoxicity and low oral bioavailability [22,23]. Recently, in 2018, the Food and Drug Administration approved tafenoquine (TQ), which has higher efficacy due to its superior pharmacokinetic properties, but is also hemotoxic and, like PQ, cannot be used in G6PD-unknown or -deficient patients [24]. Thus, our latest efforts focused on the development of novel QN analogues merging both the CQ and the PQ cores in a single structure (**1a-c**, Fig. 1), as potential multi-stage antiplasmodials [17,18]. Multi-target drugs have raised considerable interest in the last decade owing to their advantages in the treatment of complex diseases such as malaria and drug resistance issues [25,26]. 4-*N*-butylaminoacridine (**1a**), the best derivative from this family, displayed promising results since the compounds retained the activity of the parent drugs, CQ and PQ, showing significant *in vitro* activity against both liver and blood stages malaria parasites. Based on this and inspired by the "covalent bitherapy" concept first advanced by Meunier [27,28], which advocates the combination of two pharmacophores in one molecule, our working hypothesis was that conjugation of 4-*N*-butylaminoacridine (**1a**) to bioactive *trans*-cinnamic acids would afford new constructs (**2a-l**) with improved efficacy and safety in multiple stages of malaria parasite life cycle while being less likely to elicit resistance. This "covalent bitherapy" approach has already been successfully employed in the preparation of compounds with pronounced antimalarial activity [29,30]. Cinnamic acid derivatives, due to their α,β-unsaturated carbonyl moiety, can act as Michael acceptors and inhibit cysteine proteases, especially falcipain-2 and falcipain-3, involved in hemoglobin degradation and thus vital for the intraerythrocytic stage of the parasite [31–36]. In this sense, we choose *trans*-cinnamic acids not only to introduce the α,β-vinylcarbonyl moiety (Michael acceptor), but also because of their antimalarial potential that was advanced by Kanaani and Ginsburg in 1992, based on cinnamic acids' ability to inhibit lactate transport, the major product of parasite energy metabolism and, thus, vital for the survival and growth of intraerythrocytic parasites. These authors also confirmed that cinnamic acid derivatives hampered the production of ATP by the parasite and inhibited the transport of glucose, glycine, and sorbitol by *Plasmodium*-infected erythrocytes [37,38]. Since then, conjugation of cinnamic acids with classical antimalarials such as CQ, QN and PQ has been studied by different groups [39,40], including ours [15,16,41,42], and has delivering promising *in vitro* antiplasmodial results [39,43]. In view of this, we have coupled a series of twelve different *trans*-cinnamoyl moieties to the aliphatic amino group of **1a**, and evaluated their *in vitro* activity against the liver, blood and gametocyte stages of *Plasmodium* parasites, aiming at the establishment of relevant structure-activity relationship (SAR). The data herein obtained demonstrated that the new conjugates preserved and, in some cases, improved multi-stage activity *in vitro* and that this activity is very dependent of the *trans*-cinnamoyl moiety coupled to the aliphatic amino group of **1a**.

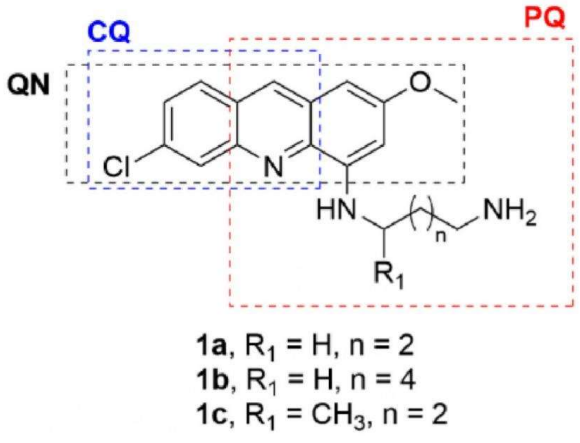


Fig. 1. QN analogues with dual-stage antiplasmodial activity previously reported by Fonte *et al.* [18].

2. Results and discussion

2.1. Chemistry

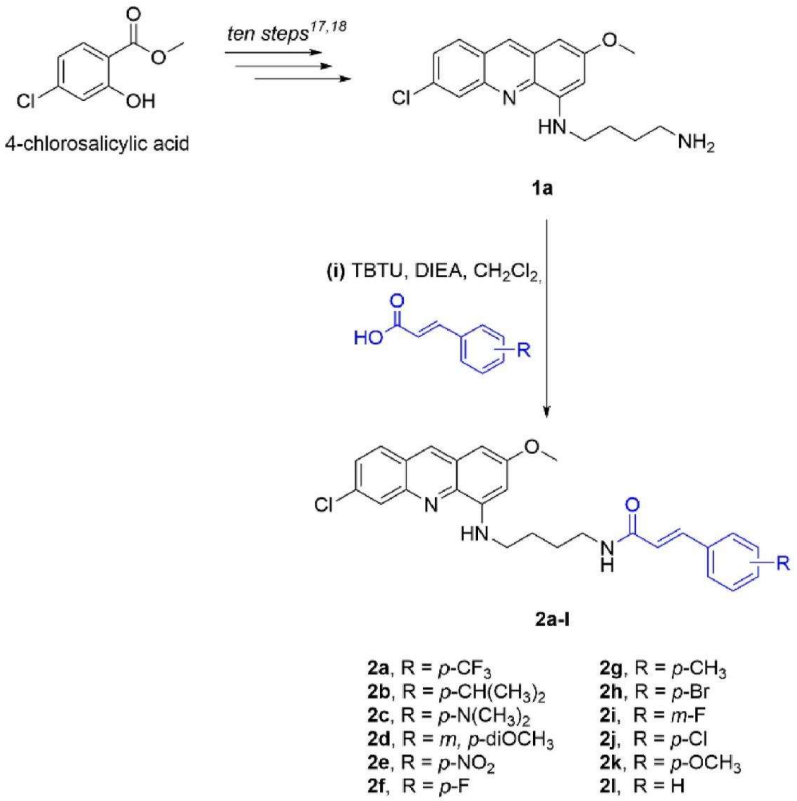
The chemical synthesis of target compounds **2a-l** was carried out *via* the synthetic route presented in Scheme 1. Detailed procedures and relevant spectroscopic data of the final compounds are provided in Section 4 and in Supplementary Information (SI).

The QN analogue 4-(4-aminobutyl)amino-6-chloro-2-methoxy-acridine (**1a**) was first obtained by a ten-step synthetic route starting from the commercial compound 4-chlorosalicylic acid, as previously reported [17,18]. Compound **1a** was then coupled to a series of *trans*-cinnamic acids by a standard *in situ* amide coupling method, using O-(Benzotriazol-1-yl)-*N,N,N′,N′*-tetramethyluronium tetrafluoroborate (TBTU) and *N,N*-diisopropylethylamine (DIEA) as a coupling agent and base, respectively, to afford the target compounds **2a-l**. To this end, the carboxylic acid group in the *trans*-cinnamic acid was first activated for 1 h with TBTU and DIEA, in dichloromethane (DCM); after the activation period, **1a** was added to the mixture and the reaction allowed to proceed at room temperature (r.t.). The crude products were purified by liquid chromatography on silica-gel columns, to obtain the target compounds in 95–99% purity, as confirmed by high-performance liquid chromatography (HPLC). Structural analyses by electrospray ionization-ion trap mass spectrometry (ESI-IT MS), and by proton (^{1}H) and carbon-13 (^{13}C) nuclear magnetic resonance (NMR) confirmed the expected structures for all target compounds **2a-l**, which were obtained in moderate to excellent overall yields (33–95%).

2.2. Biological assays

2.2.1. Hepatic stage activity

The *in vitro* activity previously observed for QN analogue **1a** against hepatic forms of *P. berghei* parasites revealed the importance of including the aminoalkyl side chain in position 4 of the acridine ring, since, according to the literature, QN has poor activity against liver stage parasites and a low selectivity index [16]; moreover, such modification did not abolish the blood stage activity typical of QN and related compounds [18]. Advancing drug candidates that eliminate liver stage parasites is highly relevant, as they are not only scarce [22], but may also hamper the development of thousands of erythrocyte-infective merozoites responsible for disease symptoms [44,45]. Therefore, based on our previous studies showing that *N*-cinnamoylation of the classical antimalarial drugs CQ, PQ and QN led to an improvement of liver stage activity, we hypothesized that a similar benefit might result from coupling **1a** to *trans*-cinnamic acids to produce conjugates **2a-l**. Hence, *in vitro* activity of 1 and 10 μM **2a-l** against the hepatic stage of *P. berghei* infection was evaluated using a previously described bioluminescence-based method to quantify the parasite load of human hepatoma (Huh-7) cells [18]. The toxicity of the compounds to this human cell line was also assessed through the fluorescence measurement of cell confluency (Fig. 2), as described in detail in Section 4. Our



Scheme 1. Synthetic route to target compounds **2a-l**[a]
[a]The QN analogue **1a** was first obtained in ten steps as previously described [17,18], and subsequently coupled to different *trans*-cinnamic acids (highlighted in blue) under the following conditions: respective *trans*-cinnamic acid (1.1 equiv), TBTU (1.1 equiv), DIEA (2 equiv) and DCM at r.t.

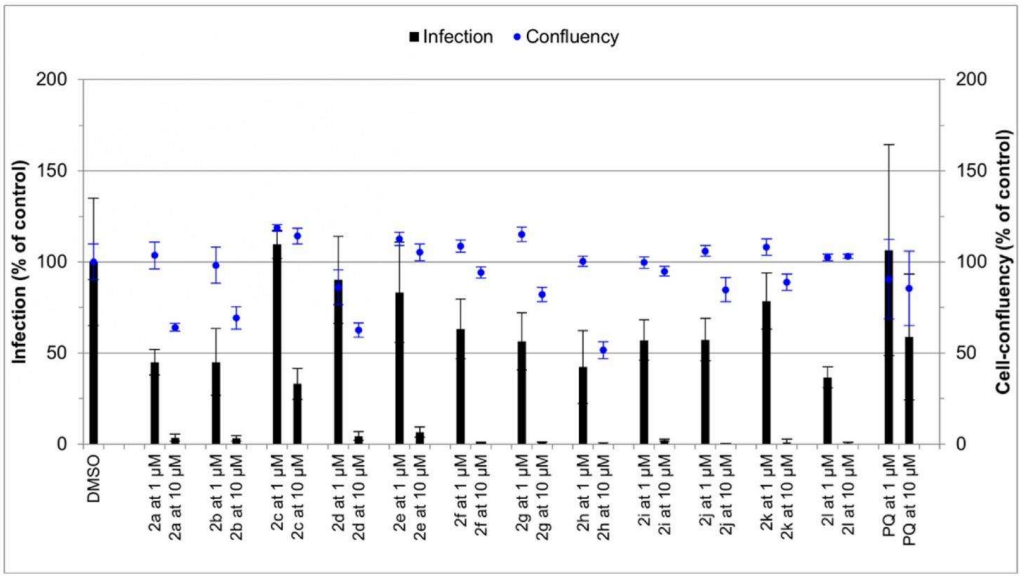


Fig. 2. *In vitro* activity of compounds **2a-l** and PQ, at 1 and 10 µM, against liver forms of *P. berghei*. Cytotoxicity to Huh7 cells (cell confluency scale, blue circles) are also shown.

results show that all the compounds **2a-l** were more active than the reference drug PQ against hepatic forms of *P. berghei* (Fig. 2).

IC_{50} values were then determined for the most active and least cytotoxic (above ~75% confluency relative to control) compounds at the highest concentration tested, 10 μM (**2e-f, i-l**). All IC_{50} values obtained were in the low- or sub-micromolar range ($0.496 < IC_{50} < 1.189$ μM) (Table 1). All *N*-cinnamoyl conjugates **2a-l** were more active than their parent compound **1a** ($IC_{50} = 2.22$ μM), which is in support of our initial hypothesis. The IC_{50} values were dependent on the substituent of the aryl ring in the cinnamoyl building block (R), and the following observations can be made in this regard.

(i) adding a substituent to the aryl ring of the cinnamoyl moiety seems to be slightly deleterious for liver stage activity, as compound **2l** (R=H) was the most active of the set ($IC_{50} = 0.496$ μM);
(ii) amongst the aryl substituents (i.e., R ≠ H, **2a-k**), the halogens led to higher activities, which seemed to increase with the size of the halogen atom, i.e., follow the order **2f** (R = *p*-F; $IC_{50} = 0.884$ μM) > **2j** (R = *p*-Cl; $IC_{50} = 0.998$ μM) > **2h** (R = *p*-Br); however, the *p*-bromine-substituted compound, **2h**, was significantly toxic to Huh-7 cells, hence its IC_{50} against hepatic stage parasites could not be reliably determined;
(iii) changing the position of the aryl substituent from *para* to *meta*, as in **2f** (R = *p*-F; $IC_{50} = 0.884$ μM) *versus* **2i** (R = *m*-F; $IC_{50} = 0.561$ μM), increased slightly the *in vitro* activity;
(iv) compared to all the previously mentioned ones, and regardless of their electron-withdrawing or -donating nature, polyatomic R groups, as in **2a** (R = *p*-CF_3), **2b** (R = *p*-$CH(CH_3)_2$; 0.129 μM), **2c** (R = *p*-$N(CH_3)_2$), **2e** (R = *p*-NO_2; $IC_{50} = 1.189$ μM), or **2k** (R = *p*-OMe; 1.182 μM), were not advantageous, as they led to either a decrease in liver stage activity (**2c,e,k**) or a clear increase in cytotoxicity at 10 μM (**2a,b**); insertion of a second substituent, as in **2d** (R = *o,m*-di(OMe)) further aggravated the latter.

Overall, conjugates **2i** and **2l** stood out for their higher activity against hepatic forms of *P. berghei*, being approximately 25-fold more potent than the reference drug PQ, while not showing any significant toxicity to Huh-7 cells up to 10 μM.

2.2.2. Gametocytocidal activity

Like antiplasmodials targeting liver stage *Plasmodium* parasites, those that are able to kill gametocytes are also highly important, but scarce. Since gametocytes are the only forms of *Plasmodium* that are infective to the mosquito vector, their elimination hampers the host-to-vector transmission, therefore blocking the dissemination of the disease. As such, the gametocytocidal activity of compounds **2a-l** was also assessed *in vitro* against early gametocytes of *P. falciparum* (3D7 strain) using the test compounds at 5 μM, which is the IC_{10} value for the reference drug PQ. Results depicted in Fig. 3 are expressed as % of inhibition of gametocyte growth and show that the inhibitory activity of conjugates **2a-l** is comparable to (**2a, 2c, 2d, 2f, 2h** and **2j**, 15–30%

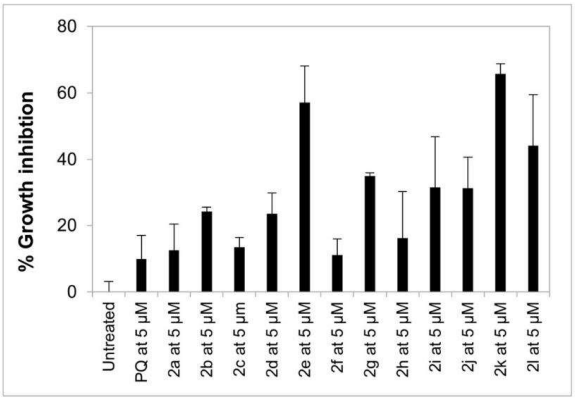
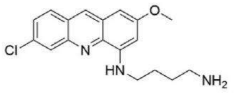
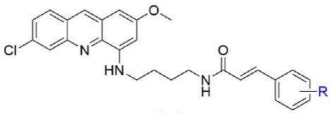


Fig. 3. *In vitro* growth inhibition of early *P. falciparum* 3D7 gametocytes upon incubation with test compounds **2a-l** at 5 μM; PQ was included as the reference gametocytocidal drug.

Table 1
In vitro activity of compounds **2a-l** against liver forms of *P. berghei*, as well as early gametocytes and ring stages of *P. falciparum* 3D7.



1a



2a-l

Compound	R	Liver stage[a] (IC_{50} ± SD, μM)	Gametocyte stage[b] (IC_{50} ± SD, μM)	Blood stage[c] (IC_{50} ± SD, μM)
1a	–	2.22 ± 0.51[d]	–	5.64 ± 0.22[d]
2a	*p*-CF_3	ND[b]	–	–
2b	*p*-$CH(CH_3)_2$	0.129 ± 0.063	–	–
2c	*p*-$N(CH_3)_2$	–	–	–
2d	*m, p*-diOCH_3	–	–	–
2e	*p*-NO_2	1.189 ± 0.163	16.33 ± 1.29	3.82
2f	*p*-F	0.884 ± 0.046	–	5.83
2g	*p*-CH_3	ND[e]	0.63 ± 0.35	10.82
2h	*p*-Br	ND[e]	–	–
2i	*m*-F	0.561 ± 0.179	0.14 ± 0.43	4.34
2j	*p*-Cl	0.998 ± 0.103	–	–
2k	*p*-OCH_3	1.182 ± 0.115	0.52 ± 0.38	10.30
2l	H	0.496 ± 0.230	6.66 ± 1.54	>70
PQ	–	12.255 ± 2.001	17.66 ± 2.31	–
CQ	–	–	–	0.02[d]

[a] Liver-stage antiplasmodial activity was determined against *P. berghei*, using PQ as reference drug.
[b] Gametocytocidal activity was determined in *P. falciparum* NF54-gexp02-Tom strain, using PQ as reference drug.
[c] Blood-stage antiplasmodial activity was determined against the CQ-sensitive *P. falciparum* 3D7 strain, using CQ as reference drug.
[d] Value taken from Ref. [18].
[e] Not determined due to its high toxicity to Huh-7 cells.

inhibition) or higher than (**2e, 2g, 2i, 2k** and **2l**, >40% inhibition) that of PQ. IC_{50} values were determined for the top-five compounds (Table 1), which revealed that 2e (IC_{50} = 16.33 μM) was comparable to PQ (IC_{50} = 17.66 μM), while the remaining four compounds displayed stronger gametocytocidal activity (6.66 > IC_{50} > 0.14 μM) than the reference drug. The influence of substituent R on the gametocytocidal activity of conjugates **2a-l** was perceptible, but clear SAR could not be drawn, as the three best compounds, 2g (R = *p*-CH_3; IC_{50} = 0.63 μM), 2i (R = *m*-F; 0.14 μM) and 2k (R = *p*-OCH_3; IC_{50} = 0.52 μM) have R groups with quite distinct stereo-electronic properties and even occupy different positions in the aryl ring.

2.2.3. Blood stage activity

Motivated by the encouraging results obtained for the activity of the compounds against both liver and gametocyte stages of *Plasmodium* parasites, we further tested the blood stage activity of **2e, 2g, 2i, 2k** and **2l**, i.e., the top-five gametocytocidals, which includes the top-two compounds against liver forms of the parasite. The *P. falciparum* 3D7 strain was used to assess the effect of the compounds *in vitro* against blood stage parasites by means of flow cytometry, employing the SYTO 11 green-fluorescent nucleic acid stain. The hemolytic activity of the compounds at 20 μM was assessed in parallel, and none was found significantly hemolytic at this concentration. As for blood antiplasmodial activity (Table 1), except for the unsubstituted (R=H) derivative **2l** (IC_{50} > 70 μM), all other compounds displayed IC_{50} values in the low micromolar range. Still, none of them could match the potent activity of the reference drug CQ against the same *P. falciparum* 3D7 strain (IC_{50} = 0.02). As described for the gametocytocidal activity, no clear SAR could be drawn in regard to blood stage activity because the set of compounds tested was not large enough to allow withdrawing any meaningful conclusions. Nevertheless, it appears that electron-withdrawing R groups, such as *p*-NO_2 in **2e** (IC_{50} = 3.82 μM), *p*-F in **2f** (IC_{50} = 5.827 μM) and *m*-F in **2i** (IC_{50} = 4.34 μM), lead to higher activity than electro-donating ones, as in **2g** (R = *p*-CH_3; IC_{50} = 10.82 μM) and **2k** (R = *p*-OCH_3; IC_{50} = 10.3 μM).

The data compiled in Table 1 proves the validity of our working hypothesis, since the second-generation compounds (**2a-l**) herein reported display the expected multi-stage activity *in vitro* of with no increase in cytotoxicity, as compared to the parent compound **1a**. Actually, the new compounds are more active against liver and gametocyte stages of parasite development than the reference drug, PQ, and more active than the parent drug **1a** against the erythrocytic stage. Therefore, the moiety newly introduced clearly has a positive impact on overall antiplasmodial activity. Ongoing studies *in vitro* (undisclosed data) will allow us to check whether falcipain inhibition may play a role in the slight increase in blood-stage activity of the 2nd generation compounds reported.

The exact mechanism of QN's antimalarial action remains unclear, but it has been demonstrated that QN can interact with β-hematin, consequently inhibiting hemozoin formation and the development of intraerythrocytic parasites. However, other mechanisms of action have been suggested to elucidate the antimalarial activity of QN derivatives, such as (i) inhibition of: the parasite's NF-κB pathway, the mitochondrial bc1 complex, and/or the parasitic DNA topoisomerases II; (ii) activation of the p53 pathway; and/or (iii) binding to DNA, either by intercalation or by groove binding [46,47]. On the other hand, as mentioned above, cinnamic acids are reported as inhibitors of lactate, glucose, glycine, and sorbitol transport by *Plasmodium*-infected erythrocytes and as being able to hinder the production of ATP by the parasite [37]. Therefore, both QN and cinnamic acid derivatives are reported to affect crucial pathways in the growth and survival of *Plasmodium*-infected erythrocytes. Yet, the new compounds herein reported are new molecular entities that may owe their multi-stage antiplasmodial action by effects other than those described to their separate building blocks, or by a combination of (a few) of them. Previous studies in our group focused on similar chloroquine-cinnamic acid conjugates demonstrated their ability to strongly interact with DNA [48], and preliminary studies (undisclosed data) on the compounds now reported point to a similar direction. Further studies will be conducted to deliver conclusive data on mode of action and possible off-target effect. Still, the lack of significant toxicity of the new compounds to either hepatocytes or erythrocytes are suggestive of a selective action.

3. Concluding remarks

Herein, we report the synthesis and *in vitro* evaluation of a new family of compounds **2a-l**, as promising multi-stage antiplasmodial leads obtained through the coupling of a series of *trans*-cinnamic acids to the aliphatic amine of the 4-aminoacridine **1a**, which we previously found to present dual-stage antiplasmodial activity *in vitro* [18]. Our working hypothesis was that the antimalarial activity of **1a** might be improved via such *N*-cinnamoylation procedure, in light of our earlier findings showing that a similar modification was applied to the classical antimalarial drugs PQ, CQ and QN [15,16,41,42]. This hypothesis was confirmed by the data obtained, as they demonstrate that the new conjugates preserve multi-stage activity *in vitro*, being more active against liver and gametocyte stages of parasite development than the reference drug, PQ. In fact, one compound (**2i**) showed a 20- and 120-fold higher activity than PQ against liver and gametocyte stages, respectively, alongside low micromolar activity against blood stage *P. falciparum* parasites. Blood-stage activity of the new compounds is not spectacular; still, some of them represent an improvement over the first-generation compound **1a**, while preserving relevant activity against other stages of parasite development. This provides confirmation of our working hypothesis and, together with results from ongoing mechanistic studies, offers an important advance towards the fine tuning of this type of molecular scaffolds envisaging their improvement as multi-stage antiplasmodial leads. These findings are in line with previous reports by other authors on the beneficial role not only of conjugation to *trans*-cinnamic acids, but also of fluorination in antimalarial drug discovery [49]. Moreover, none of the new compounds reported herein showed significant toxicity to either hepatic Huh-7 cells or erythrocytes. The fact that no compound at 20 μM was found to be significantly hemolytic is very important since the main problem associated to drugs active in liver stages, as PQ, is the hemolytic toxicity in G6PD-unknown or -deficient patients.

Altogether, these are encouraging results highlight scaffolds like **2i** as novel potential multi-stage antiplasmodial leads. Considering the importance of halting progression of infection at its very onset in the host, i.e., during the liver stage of the parasite's life cycle, and of avoiding its vector-mediated dissemination from infected to healthy people, these findings are a promising starting point that may have a relevant impact in the future development of antimalarial candidates.

4. Experimental Section

4.1. Chemistry

4.1.1. Chemicals and instrumentation

The chemicals and solvents used in this study were purchased from Sigma-Aldrich (*trans*-4-(trifluoromethyl)cinnamic acid, *trans*-4-nitrocinnamic acid, *trans*-3-fluorocinnamic acid and *trans*-4-(dimethylamino) cinnamic acid), Bachem (TBTU), Alfa Aesar (DIEA, *trans*-4-isopropylcinnamic acid), Acros organics (*trans*-cinnamic acid, *trans*-4-chlorocinnamic acid, *trans*-4-methoxycinnamic acid and *trans*-4-methylcinnamic acid), PanReac AppliChem (anhydrous Na_2SO_4), Biochem Chemopharma ($NaHCO_3$), VWR international (HPLC gradient grade, LC-MS grade and p.a. grade solvents, i.e., acetonitrile and methanol), LabChem (synthesis grade solvents, i.e., DMF, DCM, hexane and ethyl acetate), and CortecNet (deuterated solvents for NMR analysis). Aluminium foils coated with silica-gel 60 F254 from Merck were used for monitoring reaction progress, purification steps, and determination

of compound retention factors (R_f) by thin-layer chromatography (TLC). TLC chromatograms were revealed with ultra-violet light (254 nm), using a Viber Lourmat lamp, model CN-6. The purifications of compounds were performed by normal phase liquid chromatography using silica gel 60 from Sigma-Aldrich as solid-phase and a mixture of hexane and ethyl acetate 1:1 (v/v) as mobile-phase. ESI-IT MS analyses (positive mode) were achieved with solutions of the pure products in methanol, using a Finnigan Surveyor LCQ DECA XP MAX spectrometer, at the Department of Chemistry and Biochemistry of the Faculty of Sciences of the University of Porto. ^{1}H NMR and ^{13}C NMR spectra were recorded on a Bruker Avance III spectrometer at frequencies of 400 mHz and 100 mHz, respectively, and samples were prepared in hexadeuterated dimethylsulfoxide (DMSO-d_6) and deuterated chloroform ($CDCl_3$) with tetramethylsilane (TMS) as an internal reference. The determination of the retention times (RT) and purity degrees of compounds n was carried out by analytical HPLC, using a Hitachi-Merck Elite LaChrom system equipped with an L-2130 quaternary pump, an L-2200 thermostatted (Peltier effect) automated sampler, and an L-2455 diode-array detector (DAD). The compounds were dissolved in acetonitrile and injected in a reverse phase column (C18) Purospher star RP-C18 of 125 × 4.0 mm and 5 μm pore size. A gradient elution from 1 to 100% of acetonitrile in 0.05% aqueous (aq.) trifluoroacetic acid (TFA) was carried out for 30 min, at a flow rate of 1 mL min^{-1}, and detection was set at 220 nm.

4.1.2. General procedures. Compound 1a

The 4-(4-aminobutyl)amino-6-chloro-2-methoxy-acridine (**1a)** was prepared by a 10-step route previously described by us, and its structural data agreed with those earlier reported [18]. **Compounds 2a-l.** TBTU (1.1 equiv) and DIEA (2 equiv) were added to a solution of the *trans*-cinnamic acid of interest (1 equiv) in DCM. After 1 h of activation, a solution of 1a (1 equiv) in DCM was added to the mixture, and the reaction allowed to proceed at r.t. until no further progress could be observed by TLC (1–3 h). The mixture was then washed with saturated aq. $NaHCO_3$ (3 x 50 mL) and saturated aq. NaCl (3 x 50 mL), and the organic layer was collected and dried over anhydrous Na_2SO_4. The resulting suspension was filtered by gravity, and the filtrate evaporated to dryness under reduced pressure. The crude product thus obtained was purified by column chromatography on silica gel using hexane/ethyl acetate 1:1 (v/v) as eluent to afford compounds **2a-l** with purity degrees between 94.8 and 99.8% (HPLC) and correct structural data (NMR and ESI-IT-MS), as given in detail below. Chromatographic and spectral traces are provided in the SI.

4.1.2.1. (E)-N-(4-((6-chloro-2-methoxyacridin-4-yl)amino)butyl)-3-(4-(trifluoromethyl)phenyl)acrylamide (2a). Yellow solid, η = 67%; ^{1}H NMR (400 MHz, DMSO-d_6) δ 8.75 (s, 1H), 8.26 (t, *J* = 5.7 Hz, 1H), 8.13 (d, *J* = 2.1 Hz, 1H), 8.09 (d, *J* = 9.0 Hz, 1H), 7.76 (s, 4H), 7.55 (dd, *J* = 8.9, 2.1 Hz, 1H), 7.49 (d, *J* = 15.8 Hz, 1H), 6.76 (d, *J* = 15.9 Hz, 1H), 6.71–6.74 (m, 1H), 6.61 (d, *J* = 2.5 Hz, 1H), 6.30 (d, *J* = 2.5 Hz, 1H), 3.87 (s, 3H), 3.35–3.37 (m, 2H), 3.26–3.31 (m, 2H), 1.72–1.80 (m, 2H), 1.60–1.67 (m, 2H); ^{13}C NMR (100 MHz, DMSO-d_6) δ 164.88, 159.58, 145.33, 144.59, 139.55, 138.82, 137.27, 133.79, 133.33, 130.18, 128.57, 128.44, 127.67, 127.13, 126.26, 126.23, 126.00, 125.62, 97.01, 90.66, 55.60, 42.64, 39.01, 27.35, 26.26; $^m/_z$ (ESI-IT MS, +) 528.47 (M + H$^+$); M$^+$ ($C_{28}H_{25}ClF_3N_3O_2$) requires 527.16; HPLC-DAD: RT, 28.2 min; purity degree (peak relative area), 99.7%.

4.1.2.2. (E)-N-(4-((6-chloro-2-methoxyacridin-4-yl)amino)butyl)-3-(4-isopropylphenyl)acrylamide (2b). Orange solid, η = 63%; ^{1}H NMR (400 MHz, DMSO-d_6) δ 8.75 (s, 1H), 8.16–8.08 (m, 3H), 7.56 (dd, *J* = 9.0, 2.1 Hz, 1H), 7.49–7.44 (m, 2H), 7.38 (d, *J* = 15.8 Hz, 1H), 7.30–7.25 (m, 2H), 6.72 (t, *J* = 5.8 Hz, 1H), 6.61 (d, *J* = 2.4 Hz, 1H), 6.57 (d, *J* = 15.8 Hz, 1H), 6.30 (d, *J* = 2.5 Hz, 1H), 3.87 (s, 3H), 3.41–3.34 (m, 2H), 3.26 (q, *J* = 6.6 Hz, 2H), 1.82–1.71 (m, 2H), 1.69–1.56 (m, 2H); ^{13}C NMR (100 MHz, DMSO-d_6) δ 164.99, 159.09, 149.88, 144.84, 144.10, 138.34, 133.29, 132.83, 132.61, 129.68, 127.94, 127.51, 127.19, 126.83, 126.64, 125.51, 121.36, 96.51, 90.17, 55.10, 42.17, 38.44, 33.26, 26.94, 25.79, 23.65; $^m/_z$ (ESI-IT MS, +) 502.52 (M + H$^+$); M$^+$ ($C_{30}H_{32}ClN_3O_2$) requires 501.22; HPLC-DAD: RT, 29.3 min; purity degree (peak relative area), 99.5%.

4.1.2.3. (E)-N-(4-((6-chloro-2-methoxyacridin-4-yl)amino)butyl)-3-(4-(dimethylamino)phenyl)acrylamide (2c). Orange solid, η = 71%; ^{1}H NMR (400 MHz, DMSO-d_6) δ 8.75 (s, 1H), 8.15–8.13 (m, 1H), 8.10 (d, *J* = 9.0 Hz, 1H), 7.94 (t, *J* = 5.7 Hz, 1H), 7.56 (dd, *J* = 9.0, 2.1 Hz, 1H), 7.39–7.34 (m, 2H), 7.30 (d, *J* = 15.6 Hz, 1H), 6.74–6.68 (m, 3H), 6.61 (d, *J* = 2.5 Hz, 1H), 6.35 (d, *J* = 15.7 Hz, 1H), 6.29 (d, *J* = 2.5 Hz, 1H), 3.87 (s, 3H), 3.38–3.33 (m, 2H), 3.28–3.21 (m, 2H), 2.94 (s, 6H), 1.80–1.70 (m, 2H), 1.61 (m, 2H); ^{13}C NMR (100 MHz, DMSO-d_6) δ 165.59, 159.09, 151.00, 144.85, 144.10, 138.86, 138.33, 133.29, 132.83, 129.67, 128.73, 127.94, 127.19, 126.64, 125.51, 122.42, 116.83, 111.97, 96.50, 90.16, 55.11, 42.19, 38.35, 27.05, 25.80; $^m/_z$ (ESI-IT MS, +) 503.67 (M + H$^+$); M$^+$ ($C_{29}H_{31}ClN_4O_2$) requires 502.21; HPLC-DAD: RT, 24.6 min; purity degree (peak relative area), 94.8%.

4.1.2.4. (E)-N-(4-((6-chloro-2-methoxyacridin-4-yl)amino)butyl)-3-(3,4-dimethoxyphenyl)acrylamide (2d). Roasted yellow solid, η = 90%; ^{1}H NMR (400 MHz, DMSO-d_6) δ 8.75 (s, 1H), 8.14 (d, *J* = 2.0 Hz, 1H), 8.12–8.08 (m, 1H), 8.05 (t, *J* = 5.7 Hz, 1H), 7.56 (dd, *J* = 9.0, 2.1 Hz, 1H), 7.35 (d, *J* = 15.6 Hz, 1H), 7.14 (d, *J* = 2.0 Hz, 1H), 7.10 (dd, *J* = 8.3, 2.0 Hz, 1H), 6.99–6.94 (m, 1H), 6.72 (t, *J* = 5.8 Hz, 1H), 6.62 (d, *J* = 2.5 Hz, 1H), 6.51 (d, *J* = 15.7 Hz, 1H), 6.30 (d, *J* = 2.4 Hz, 1H), 3.87 (s, 3H), 3.78 (d, *J* = 3.6 Hz, 6H), 3.41–3.31 (m, 2H), 3.26 (q, *J* = 6.7 Hz, 2H), 1.81–1.69 (m, 2H), 1.68–1.56 (m, 2H); ^{13}C NMR (100 MHz, DMSO-d_6) δ 165.16, 159.09, 150.01, 148.87, 144.85, 144.11, 138.47, 138.33, 133.30, 132.84, 129.69, 127.95, 127.76, 127.19, 126.65, 125.52, 121.26, 120.06, 111.74, 109.94, 96.51, 90.17, 55.52, 55.39, 55.11, 42.18, 38.42, 31.13, 29.81, 26.97, 25.79; $^m/_z$ (ESI-IT MS, +) 520.54 (M + H$^+$); M$^+$ ($C_{29}H_{30}ClN_3O_4$) requires 519.19; HPLC-DAD: RT, 25.0 min; purity degree (peak relative area), 99.5%.

4.1.2.5. (E)-N-(4-((6-chloro-2-methoxyacridin-4-yl)amino)butyl)-3-(4-nitrophenyl)acrylamide (2e). Dark red solid, η = 70%; ^{1}H NMR (400 MHz, DMSO-d_6) δ 8.75 (s, 1H), 8.31 (t, *J* = 5.7 Hz, 1H), 8.28–8.22 (m, 2H), 8.13 (d, *J* = 2.2 Hz, 1H), 8.10 (d, *J* = 9.0 Hz, 1H), 7.84–7.80 (m, 2H), 7.58–7.50 (m, 2H), 6.81 (d, *J* = 15.8 Hz, 1H), 6.72 (t, *J* = 5.8 Hz, 1H), 6.61 (d, *J* = 2.4 Hz, 1H), 6.30 (d, *J* = 2.5 Hz, 1H), 3.87 (s, 3H), 3.41–3.33 (m, 2H), 3.30–3.25 (m, 2H), 1.82–1.70 (m, 2H), 1.70–1.59 (m, 2H); ^{13}C NMR (100 MHz, DMSO-d_6) δ 164.66, 159.58, 147.93, 145.33, 144.59, 142.10, 138.82, 136.64, 133.79, 133.33, 130.18, 129.00, 128.44, 127.67, 127.10, 126.00, 124.56, 97.02, 90.67, 55.61, 42.64, 39.06, 27.32, 26.25; $^m/_z$ (ESI-IT MS, +) 505.47 (M + H$^+$); M$^+$ ($C_{27}H_{25}ClN_4O_4$) requires 504.16; HPLC-DAD: RT, 26.4 min; purity degree (peak relative area), 97.7%.

4.1.2.6. (E)-N-(4-((6-chloro-2-methoxyacridin-4-yl)amino)butyl)-3-(4-fluorophenyl)acrylamide (2f). Orange solid, η = 92%; ^{1}H NMR (400 MHz, DMSO-d_6) δ 8.75 (s, 1H), 8.18–8.12 (m, 2H), 8.10 (d, *J* = 9.0 Hz, 1H), 7.65–7.58 (m, 2H), 7.56 (dd, *J* = 9.0, 2.1 Hz, 1H), 7.41 (d, *J* = 15.8 Hz, 1H), 7.29–7.19 (m, 2H), 6.72 (t, *J* = 5.8 Hz, 1H), 6.61 (d, *J* = 2.5 Hz, 1H), 6.57 (d, *J* = 15.8 Hz, 1H), 6.30 (d, *J* = 2.5 Hz, 1H), 3.87 (s, 3H), 3.42–3.34 (m, 2H), 3.29–3.23 (m, 2H), 1.81–1.70 (m, 2H), 1.67–1.59 (m, 2H); ^{13}C NMR (100 MHz, DMSO-d_6) δ 164.79, 159.09, 144.85, 144.11, 138.34, 137.23, 133.31, 132.84, 129.62, 129.54, 127.95, 127.19, 126.65, 125.52, 122.25, 115.96, 115.74, 96.52, 90.19, 55.11, 42.17, 38.46, 31.13, 29.82, 26.92, 25.78; $^m/_z$ (ESI-IT MS, +) 478.93 (M + H$^+$); M$^+$ ($C_{27}H_{25}ClFN_3O_2$) requires 477.16; HPLC-DAD: RT, 26.6 min; purity degree (peak relative area), 98.8%.

4.1.2.7. (E)-N-(4-((6-chloro-2-methoxyacridin-4-yl)amino)butyl)-3-(p-tolyl)acrylamide (2g). Orange solid, η = 98%; ^{1}H NMR (400 MHz, DMSO-d_6) δ 8.75 (s, 1H), 8.16–8.07 (m, 3H), 7.56 (dd, J = 8.9, 2.1 Hz, 1H), 7.47–7.41 (m, 2H), 7.38 (d, J = 15.7 Hz, 1H), 7.24–7.17 (m, 2H), 6.72 (t, J = 5.8 Hz, 1H), 6.61 (d, J = 2.5 Hz, 1H), 6.57 (d, J = 15.8 Hz, 1H), 6.29 (d, J = 2.5 Hz, 1H), 3.87 (s, 3H), 3.40–3.34 (m, 2H), 3.26 (q, J = 6.6 Hz, 2H), 2.31 (s, 2H), 1.80–1.70 (m, 1H), 1.67–1.57 (m, 1H); ^{13}C NMR (100 MHz, DMSO-d_6) δ 164.99, 159.08, 144.84, 144.10, 139.03, 138.35, 138.33, 133.29, 132.83, 132.20, 129.68, 129.48, 127.94, 127.41, 127.19, 126.64, 125.51, 121.29, 96.51, 90.16, 55.10, 42.17, 38.42, 31.13, 29.81, 26.95, 25.78, 20.90; $^{m}/_{z}$ (ESI-IT MS, +) 474.20 (M + H$^+$); M$^+$ ($C_{28}H_{28}ClN_3O_2$) requires 473.19; HPLC-DAD: RT, 27.5 min; purity degree (peak relative area), 96.9%.

4.1.2.8. (E)-3-(4-bromophenyl)-N-(4-((6-chloro-2-methoxyacridin-4-yl)amino)butyl)acrylamide (2h). Brown solid, η = 52%; ^{1}H NMR (400 MHz, DMSO-d_6) δ 8.75 (s, 1H), 8.17 (t, J = 5.7 Hz, 1H), 8.14 (d, J = 2.2 Hz, 1H), 8.10 (d, J = 9.0 Hz, 1H), 7.58–7.62 (m, 2H), 7.56 (dd, J = 8.9, 2.1 Hz, 1H), 7.49–7.52 (m, 2H), 7.39 (d, J = 15.8 Hz, 1H), 6.72 (t, J = 5.8 Hz, 1H), 6.64 (d, J = 15.8 Hz, 1H), 6.62 (d, J = 2.4 Hz, 1H), 6.30 (d, J = 2.5 Hz, 1H), 3.87 (s, 3H), 3.24–3.36 (m, 4H), 1.72–1.79 (m, 2H), 1.59–1.66 (m, 2H); ^{13}C NMR (100 MHz, DMSO-d_6) δ 165.13, 159.58, 145.33, 144.60, 138.82, 137.65, 134.76, 133.79, 133.33, 132.34, 130.18, 129.89, 128.44, 127.68, 127.14, 126.01, 123.70, 122.95, 97.01, 90.66, 55.60, 42.65, 38.97, 27.39, 26.26; $^{m}/_{z}$ (ESI-IT MS, +) 540.64 (M + H$^+$); M$^+$ (C27$H_{25}BrClN_3O_3$) requires 537.08; HPLC-DAD: RT, 28.3 min; purity degree (peak relative area), 99.7%.

4.1.2.9. (E)-N-(4-((6-chloro-2-methoxyacridin-4-yl)amino)butyl)-3-(3-fluorophenyl)acrylamide (2i). Yellow solid, η = 84%; ^{1}H NMR (400 MHz, DMSO-d_6) δ 8.75 (s, 1H), 8.19 (t, J = 5.6 Hz, 1H), 8.14 (d, J = 2.2 Hz, 1H), 8.10 (d, J = 9.0 Hz, 1H), 7.56 (dd, J = 8.9, 2.1 Hz, 1H), 7.37–7.47 (m, 4H), 6.72 (t, J = 5.9 Hz, 1H), 6.67 (d, J = 15.8 Hz, 1H), 6.61 (d, J = 2.5 Hz, 1H), 6.30 (d, J = 2.5 Hz, 1H), 3.87 (s, 3H), 3.35–3.37 (m, 2H), 3.25–3.29 (m, 2H), 1.72–1.79 (m, 2H), 1.60–1.67 (m, 2H); ^{13}C NMR (100 MHz, DMSO-d_6) δ 165.05, 159.58, 145.33, 144.59, 138.82, 137.63, 137.61, 133.79, 133.33, 131.37, 131.29, 130.18, 128.44, 127.68, 127.13, 126.01, 124.40, 124.07, 114.43, 114.22, 97.01, 90.66, 55.60, 42.65, 38.98, 27.38, 26.26; $^{m}/_{z}$ (ESI-IT MS, +) 478.73 (M + H$^+$); M$^+$ ($C_{27}H_{25}ClFN_3O_2$) requires 477.16; HPLC-DAD: RT, 26.8 min; purity degree (peak relative area), 95.1%.

4.1.2.10. (E)-N-(4-((6-chloro-2-methoxyacridin-4-yl)amino)butyl)-3-(4-chlorophenyl)acrylamide (2j). Orange solid, η = 25%; ^{1}H NMR (400 MHz, DMSO-d_6) δ 8.75 (s, 1H), 8.17 (t, J = 5.7 Hz, 1H), 8.13 (d, J = 2.1 Hz, 1H), 8.10 (d, J = 9.0 Hz, 1H), 7.59–7.56 (m, 2H), 7.49–7.44 (m, 2H), 7.40 (d, J = 15.8 Hz, 1H), 6.72 (t, J = 5.9 Hz, 1H), 6.67–6.59 (m, 2H), 6.29 (d, J = 2.4 Hz, 1H), 3.87 (s, 3H), 3.35 (d, J = 6.8 Hz, 2H), 3.32–3.22 (m, 2H), 1.81–1.70 (m, 2H), 1.68–1.58 (m, 2H); ^{13}C NMR (100 MHz, DMSO-d_6) δ 164.65, 159.09, 144.84, 144.10, 138.33, 137.07, 133.94, 133.73, 133.30, 132.84, 129.69, 129.14, 128.92, 127.95, 127.19, 126.64, 125.51, 123.15, 96.52, 90.17, 55.11, 42.16, 38.47, 26.90, 25.77; $^{m}/_{z}$ (ESI-IT MS, +) 494.40 (M + H$^+$); M$^+$ ($C_{27}H_{25}Cl_2N_3O_2$) requires 493.13; HPLC-DAD: RT, 28.0 min; purity degree (peak relative area), 99.5%.

4.1.2.11. (E)-N-(4-((6-chloro-2-methoxyacridin-4-yl)amino)butyl)-3-(4-methoxyphenyl)acrylamide (2k). Roasted yellow solid, η = 28%; ^{1}H NMR (400 MHz, $CDCl_3$) δ 8.39 (s, 1H), 8.13 (d, J = 1.7 Hz, 1H), 7.80 (d, J = 8.9 Hz, 1H), 7.56 (d, J = 15.6 Hz, 1H), 7.44–7.34 (m, 3H), 6.91–6.81 (m, 2H), 6.44 (d, J = 2.4 Hz, 2H), 6.28 (d, J = 2.4 Hz, 1H), 6.21 (d, J = 15.6 Hz, 1H), 5.77 (t, J = 5.2 Hz, 1H), 3.91 (s, 3H), 3.81 (s, 3H), 3.47 (q, J = 6.7 Hz, 2H), 3.41–3.32 (m, 2H), 1.93–1.84 (m, 2H), 1.84–1.71 (m, 2H); ^{13}C NMR (100 MHz, $CDCl_3$) δ 166.44, 160.96, 159.51, 145.28, 145.11, 140.69, 139.05, 133.93, 133.06, 129.43, 128.76, 128.23, 128.13, 127.71, 127.13, 125.96, 118.45, 114.33, 97.31, 90.50, 55.46, 55.39, 43.11, 39.60, 27.70, 26.57; $^{m}/_{z}$ (ESI-IT MS, +) 490.80 (M + H$^+$); M$^+$ ($C_{28}H_{28}ClN_3O_3$) requires 489.18; HPLC-DAD: RT, 26.2 min; purity degree (peak relative area), 99.8%.

4.1.2.12. N-(4-((6-chloro-2-methoxyacridin-4-yl)amino)butyl)-cinnamamide (2l). Orange solid, η = 35%; ^{1}H NMR (400 MHz, $CDCl_3$) δ 8.37 (s, 1H), 8.12 (d, J = 1.8 Hz, 1H), 7.78 (d, J = 8.9 Hz, 1H), 7.61 (d, J = 15.6 Hz, 1H), 7.47–7.41 (m, 2H), 7.39 (dd, J = 8.9, 2.0 Hz, 1H), 7.34–7.29 (m, 2H), 6.42 (d, J = 2.4 Hz, 1H), 6.35 (d, J = 15.6 Hz, 1H), 6.27 (d, J = 2.4 Hz, 1H), 5.92 (t, J = 5.3 Hz, 1H), 3.91 (s, 3H), 3.47 (q, J = 6.7 Hz, 2H), 3.35 (t, J = 6.7 Hz, 2H), 1.91–1.83 (m, 2H), 1.81–1.73 (m, 2H); ^{13}C NMR (100 MHz, $CDCl_3$) δ 166.13, 159.47, 145.23, 145.06, 141.03, 138.98, 134.98, 133.94, 133.06, 129.70, 128.88, 128.74, 128.19, 128.06, 127.87, 127.11, 125.92, 120.85, 97.32, 90.50, 55.37, 43.07, 39.64, 27.61, 26.55; $^{m}/_{z}$ (ESI-IT MS, +) 460.67 (M + H$^+$); M$^+$ ($C_{27}H_{26}ClN_3O_2$) requires 459.17; HPLC-DAD: RT, 26.4 min; purity degree (peak relative area), 99.6%.

4.2. In vitro assays

4.2.1. Hepatic stage activity

The *in vitro* inhibition of hepatic infection by the test compounds was determined by measuring the luminescence intensity in lysates of Huh7 cells infected with a firefly luciferase-expressing *P. berghei* line, *PbGFP*-Luccon, as previously described [50]. Huh7 cells were cultured in Roswell Park Memorial Institute 1640 medium (RPMI) supplemented with 10% v/v fetal calf serum, 1% v/v penicillin/streptomycin, 1% v/v nonessential amino acids, 1% v/v glutamine, and 10 mM 4-(2-hydroxyethyl)-1-piperazine ethanesulfonic acid (HEPES), pH 7, and maintained at 37 °C with 5% CO_2. For infection assays, Huh7 cells were seeded in 96-well plates the day before drug treatment and infection. Approximately 1 h prior to infection with sporozoites freshly obtained through disruption of salivary glands of infected female *Anopheles stephensi* mosquitoes, the culture medium in the wells was replaced by infection medium (culture medium supplemented with 50 μg/mL gentamicin and 0.8 μg/mL amphotericin B) containing the appropriate concentration of each compound. In control cells, culture medium was replaced by medium containing the same percentage of DMSO used in compound solutions (0.01%), which is not cytotoxic. After 48 h of infection, inhibition of infection was measured and the effect of the compounds on the viability of Huh7 cells was assessed by the AlamarBlue assay (Invitrogen, UK) using the manufacturer's protocol. Nonlinear regression analysis was employed to fit the normalized results of the dose-response curves, and IC_{50} values were determined using GraphPad Prism 8.0 (GraphPad software, La Jolla, CA, USA). Cytotoxicity was extrapolated from the cell confluency data. All data was then normalized to the DMSO control. Therefore, a decrease in cell confluency, as compared to the DMSO control, was indicative of cytotoxicity.

4.2.2. Gametocytocidal activity

P. falciparum parasites of the high-gametocyte productive NF54-gexp02-Tom line [51] (kindly provided by Prof. Alfred Cortés), which has a genome-integrated tandem Tomato (tdTomato) fluorescent marker gene controlled by an early gametocyte promoter, were used. Parasites were grown in group B human erythrocytes at 3% hematocrit in RPMI-based standard medium supplemented with 10% human plasma and 2 mM choline chloride, and incubated at 37 °C under hypoxia (5% O_2, 5% CO_2, and 90% N_2 at 37 °C). To induce sexual conversion, choline was removed from the medium, in combination with synchronization by sorbitol lysis. Induced cultures were then maintained without choline until the end of the experiment. The effect on gametocyte development was assessed in two independent replicas by adding growing concentrations (0.0048–100 μM) of each compound to the culture. The appearance of stage V gametocytes was daily monitored by light

microscopy. Fifteen days after choline removal, ~80% of gametocytes reached stages IV and V (mature forms). After this time, Giemsa-stained blood smears were prepared and at least 10,000 cells were counted for each condition. A negative control culture without drugs and a positive control treated with the IC_{90} of chloroquine and primaquine, where no gametocytes were observed at the end of the experiment, were also included. Growth inhibition data was transformed through sigmoidal fitting and used to determine the compounds' concentrations required for the reduction of *P. falciparum* viability by 50% (IC_{50}), using the GrapPhad Prism 9 software.

4.2.3. Blood stage activity

Asexual stages of the *P. falciparum* 3D7 strain were grown in group B human erythrocytes at 3% hematocrit using RPMI supplemented with 0.5% (w/v) Albumax II (Life Technologies, New Zealand) and 2 mM L-glutamine. Throughout the whole experiment, parasites were maintained in standard culturing conditions (37 °C, 5% O_2, 5% CO_2, and 90% N_2). Before starting the blood stage activity assays, parasites were synchronized in the ring stage with a 5% sorbitol lysis as described in Ref. [52]. Afterwards, growing concentrations of the different 4-(N-cinnamoylbutyl)aminoacridines (0.0000256–10 μM) were incubated with the parasite culture during 48 h. Finally, cultures were diluted to ca. 1 to 10×10^6 cells/mL and incubated with Syto11 to stain the nuclei. Parasitemia was analyzed by flow cytometry using a LSRFortessa flow cytometer (BD Biosciences, USA) set up with the 4 lasers, 20 parameters standard configuration. The single-cell population was selected on a forward-side scattergram. Syto 11 fluorescence signal was detected by exciting samples at 488 nm and collecting the emission with a 530/30-nm bandpass filter. Growth inhibition was calculated taking as reference values the growth rates of an untreated culture (0% inhibition) and of a chloroquine-treated culture (100% inhibition). Growth inhibition data was transformed through sigmoidal fitting and used to determine the compounds' concentrations required for the reduction of *P. falciparum* viability by 50% (IC_{50}) using the GraphPad Prism 9 software.

4.2.4. Hemolytic activity

Human blood samples were first centrifuged (Centurion scientific Ltd centrifuge with a BRK1001 rotor) at 2500 rpm for 5 min at 4 °C to remove the plasma. The red blood cells (RBC) thus collected were then washed three times with 0.01 M phosphate-buffered saline, pH 7.4 (PBS, Sigma-Aldrich) and diluted to a final 6% hematocrit in PBS. In a 96-well plate, 100 μL of RBCs at 6% hematocrit were plated in the presence of 100 μL of a solution of each compound at 40 μM in 1% DMSO in PBS, and next incubated at 37 °C for 1 h. 1% Triton X-100 in PBS and 1% DMSO in PBS were used as positive and negative controls, respectively. After the 1-h incubation period, the plates were centrifuged (Sigma® 3–30K centrifuge from Sigma Centrifuges GmbH with a swing-out 11222 rotor) at 860×*g* (2500 rpm), for 10 min at 25 °C. Finally, 80 μL of the supernatants were transferred to a new 96-well plate and absorbance (A) at 450 nm was measured in a microplate reader (Multiskan GO, Thermo Scientific). The percentage of hemolysis was calculated for each test compound using the following equation:

$$Hemolysis = \frac{A\ (peptide) - A\ (negative\ control)}{A\ (positive\ control) - A\ (negative\ control)}$$

Ethics statement

The human blood used in this work was obtained from Centro Hospitalar Universitário do Porto (CHUP) under a collaboration protocol with our group. Prior to being delivered to us, the blood units collected go through analytical checks specified in the current legislation. Each unit data was anonymized and permanently dissociated to ensure the non-identification of the blood donor, and only an identification label with the gender and type of blood was attached to the samples. The blood samples have been used only for the research purpose herein described.

Funding

This work received financial support from PT national funds (FCT/MCTES, Fundação para a Ciência e Tecnologia and Ministério da Ciência, Tecnologia e Ensino Superior) through the project CIRCNA/BRB/0281/2019.

Declaration of competing interest

The authors declare that they have no known competing financial interests or personal relationships that could have appeared to influence the work reported in this paper.

Data availability

Data will be made available on request.

Acknowledgment

The authors further thank FCT/MCTES for supporting Research Units LAQV-REQUIMTE (UIDB/50006/2020) and for the Doctoral Grant to MF (SRFH/BD/147354/2019). MP further acknowledges the "la Caixa" Foundation for Grant HR21-848. ISGlobal and IBEC are members of the CERCA Programme, Generalitat de Catalunya. We acknowledge support from the Ministerio de Ciencia e Innovación/Agencia Estatal de Investigación (MCIN/AEI/ 10.13039/501100011033) through the "Centro de Excelencia Severo Ochoa 2019-2023" Program (CEX2018-000806-S). This research is part of ISGlobal's Program on the Molecular Mechanisms of Malaria which is partially supported by the Fundación Ramón Areces.

Appendix A. Supplementary data

Supplementary data to this article can be found online at https://doi.org/10.1016/j.ejmech.2023.115575.

Abbreviations

ACT	artemisinin-based combination therapies
CQ	chloroquine
DIEA	*N,N*-diisopropylethylamine
ESI-IT MS	electrospray ionization-ion trap mass spectrometry
HEPES	4-(2-hydroxyethyl)-1-piperazine ethanesulfonic acid
P	*Plasmodium*
PQ	primaquine
QN	quinacrine
RPMI	roswell Park Memorial Institute 1640 medium
RT	retention time
SAR	structure and activity relationship
SD	standard deviation
TBTU	O-(Benzotriazol-1-yl)-N,N,N′,N′-tetramethyluronium tetrafluoroborate
TQ	Tafenoquine

References

[1] World Health Organization, World Malaria Report, 2022.
[2] D. Menard, A. Dondorp, Antimalarial drug resistance: a threat to malaria elimination, Cold Spring Harb. Perspect Med. 7 (2017).
[3] World Health Organization, Artemisinin Resistance and Artemisinin-Based Combination Therapy Efficacy, 2018.
[4] C. Nsanzabana, Resistance to artemisinin combination therapies (ACTs): do not forget the partner drug, Trav. Med. Infect. Dis. 4 (2019) 26.
[5] P.J. Rosenthal, Has artemisinin resistance emerged in Africa? Lancet Infect. Dis. 21 (2021) 1056–1057.

[6] N. Noreen, A. Ullah, S.M. Salman, Y. Mabkhot, A. Alsayari, S.L. Badshah, New insights into the spread of resistance to artemisinin and its analogues, J. Glob. Antimicrobial Resist. 27 (2021) 142–149.
[7] B. Balikagala, N. Fukuda, M. Ikeda, O.T. Katuro, S.-I. Tachibana, M. Yamauchi, W. Opio, S. Emoto, D.A. Anywar, E. Kimura, N.M.Q. Palacpac, E.I. Odongo-Aginya, M. Ogwang, T. Horii, T. Mita, Evidence of artemisinin-resistant malaria in Africa, N. Engl. J. Med. 385 (2021) 1163–1171.
[8] N.S. Tibon, C.H. Ng, S.L. Cheong, Current progress in antimalarial pharmacotherapy and multi-target drug discovery, Eur. J. Med. Chem. 188 (2020), 111983.
[9] V. Parvathaneni, N.S. Kulkarni, A. Muth, V. Gupta, Drug repurposing: a promising tool to accelerate the drug discovery process, Drug Discov. Today 24 (2019) 2076–2085.
[10] C. Teixeira, N. Vale, B. Pérez, A. Gomes, J.R.B. Gomes, P. Gomes, "Recycling" classical drugs for malaria, Chem. Rev. 114 (2014) 11164–11220.
[11] M.J. Araújo, J. Bom, R. Capela, C. Casimiro, P. Chambel, P. Gomes, J. Iley, F. Lopes, J. Morais, R. Moreira, E. de Oliveira, V. do Rosário, N. Vale, Imidazolidin-4-one derivatives of primaquine as novel transmission-blocking antimalarials, J. Med. Chem. 48 (2005) 888–892.
[12] N. Vale, F. Nogueira, V.E. do Rosário, P. Gomes, R. Moreira, Primaquine dipeptide derivatives bearing an imidazolidin-4-one moiety at the N-terminus as potential antimalarial prodrugs, Eur. J. Med. Chem. 44 (2009) 2506–2516.
[13] N. Vale, M. Prudêncio, C.A. Marques, M.S. Collins, J. Gut, F. Nogueira, J. Matos, P. J. Rosenthal, M.T. Cushion, V.E. do Rosário, M.M. Mota, R. Moreira, P. Gomes, Imidazoquines as antimalarial and antipneumocystis agents, J. Med. Chem. 52 (2009) 7800–7807.
[14] J. Matos, F.P.d. Cruz, É. Cabrita, J. Gut, F. Nogueira, V.E.d. Rosário, R. Moreira, P. J. Rosenthal, M. Prudêncio, P. Gomes, Novel potent metallocenes against liver stage malaria, Antimicrob. Agents Chemother. 56 (2012) 1564–1570.
[15] B.C. Pérez, C. Teixeira, I.S. Albuquerque, J. Gut, P.J. Rosenthal, J.R.B. Gomes, M. Prudêncio, P. Gomes, N-cinnamoylated chloroquine analogues as dual-stage antimalarial leads, J. Med. Chem. 56 (2013) 556–567.
[16] A. Gomes, B. Pérez, I. Albuquerque, M. Machado, M. Prudêncio, F. Nogueira, C. Teixeira, P. Gomes, N-cinnamoylation of antimalarial classics: quinacrine analogues with decreased toxicity and dual-stage activity, ChemMedChem 9 (2014) 305–310.
[17] M. Fonte, N. Fagundes, A. Gomes, R. Ferraz, C. Prudêncio, M.J. Araújo, P. Gomes, C. Teixeira, Development of a synthetic route towards N4,N9-disubstituted 4,9-diaminoacridines: on the way to multi-stage antimalarials, Tetrahedron Lett. 60 (2019) 1166–1169.
[18] M. Fonte, N. Tassi, D. Fontinha, I. Bouzón-Arnáiz, R. Ferraz, M.J. Araújo, X. Fernàndez-Busquets, M. Prudêncio, P. Gomes, C. Teixeira, 4,9-Diaminoacridines and 4-aminoacridines as dual-stage antiplasmodial hits, ChemMedChem 16 (2021) 788–792.
[19] M. Fonte, N. Tassi, P. Gomes, C. Teixeira, Acridine-based antimalarials—from the very first synthetic antimalarial to recent developments, Molecules 26 (2021) 600.
[20] C. Rasmussen, P. Alonso, P. Ringwald, Current and emerging strategies to combat antimalarial resistance, Expert Rev. Anti-infect. Ther. 20 (2022) 353–372.
[21] N. Vale, R. Moreira, P. Gomes, Primaquine revisited six decades after its discovery, Eur. J. Med. Chem. 44 (2009) 937–953.
[22] T. Rodrigues, M. Prudêncio, R. Moreira, M.M. Mota, F. Lopes, Targeting the liver stage of malaria parasites: a yet unmet goal, J. Med. Chem. 55 (2012) 995–1012.
[23] E.A. Ashley, J. Recht, N.J. White, Primaquine: the risks and the benefits, Malar. J. 13 (2014) 418.
[24] A. Mayence, J.J. Vanden Eynde, A. Tafenoquine, Novel FDA-approved prodrug for the radical cure of Plasmodium vivax malaria and prophylaxis of malaria, Pharmaceuticals 12 (2019) (2018) 115.
[25] A. Talevi, Multi-target pharmacology: possibilities and limitations of the "skeleton key approach" from a medicinal chemist perspective, Front. Pharmacol. 6 (2015).
[26] X.H. Makhoba, C. Viegas Jr., R.A. Mosa, F.P.D. Viegas, O.J. Pooe, Potential impact of the multi-target drug approach in the treatment of some complex diseases, Drug Des. Dev. Ther. 14 (2020) 3235–3249.
[27] B. Meunier, Towards antimalarial hybrid drugs, in: Polypharmacology in Drug Discovery, 2012, pp. 423–439.
[28] B. Meunier, Hybrid molecules with a dual mode of action: dream or reality? Acc. Chem. Res. 41 (2008) 69–77.
[29] Y. Li, A. Loureiro, M. Nguyen, M. Laurent, C. Bijani, F. Benoit-Vical, A. Robert, Y. Liu, B. Meunier, Synthesis and antimalarial activities of new hybrid atokel molecules, ChemistryOpen 11 (2022), e202200064.
[30] M. Ouji, G. Barnoin, Á. Fernández Álvarez, J.-M. Augereau, C. Hemmert, F. Benoit-Vical, H. Gornitzka, Hybrid gold(I) NHC-artemether complexes to target falciparum malaria parasites, Molecules 25 (2020) 2817.
[31] M.M. Santos, R. Moreira, Michael acceptors as cysteine protease inhibitors, Mini Rev. Med. Chem. 7 (2007) 1040–1050.
[32] B.R. Shenai, B.J. Lee, A. Alvarez-Hernandez, P.Y. Chong, C.D. Emal, R.J. Neitz, W. R. Roush, P.J. Rosenthal, Structure-activity relationships for inhibition of cysteine protease activity and development of Plasmodium falciparum by peptidyl vinyl sulfones, Antimicrob. Agents Chemother. 47 (2003) 154–160.
[33] I.D. Kerr, J.H. Lee, C.J. Farady, R. Marion, M. Rickert, M. Sajid, K.C. Pandey, C. R. Caffrey, J. Legac, E. Hansell, J.H. McKerrow, C.S. Craik, P.J. Rosenthal, L. S. Brinen, Vinyl sulfones as antiparasitic agents and a structural basis for drug design, J. Biol. Chem. 284 (2009) 25697–25703.
[34] P.J. Rosenthal, J.E. Olson, G.K. Lee, J.T. Palmer, J.L. Klaus, D. Rasnick, Antimalarial effects of vinyl sulfone cysteine proteinase inhibitors, Antimicrob. Agents Chemother. 40 (1996) 1600–1603.
[35] P.M.C. Glória, J. Gut, L.M. Gonçalves, P.J. Rosenthal, R. Moreira, M.M.M. Santos, Aza vinyl sulfones: synthesis and evaluation as antiplasmodial agents, Bioorg. Med. Chem. 19 (2011) 7635–7642.
[36] S. Previti, R. Ettari, S. Cosconati, G. Amendola, K. Chouchene, A. Wagner, U. A. Hellmich, K. Ulrich, R.L. Krauth-Siegel, P.R. Wich, I. Schmid, T. Schirmeister, J. Gut, P.J. Rosenthal, S. Grasso, M. Zappalà, Development of novel peptide-based Michael acceptors targeting rhodesain and falcipain-2 for the treatment of neglected tropical diseases (NTDs), J. Med. Chem. 60 (2017) 6911–6923.
[37] J. Kanaani, H. Ginsburg, Effects of cinnamic acid derivatives on in vitro growth of Plasmodium falciparum and on the permeability of the membrane of malaria-infected erythrocytes, Antimicrob. Agents Chemother. 36 (1992) 1102–1108.
[38] B.-B. F, V.-B. C, M. B, Prithwiraj De, Cinnamic acid derivatives in tuberculosis, malaria and cardiovascular diseases - a review, Curr. Org. Chem. 16 (2012) 747–768.
[39] A.T. Silva, C.M. Bento, A.C. Pena, L.M. Figueiredo, C. Prudêncio, L. Aguiar, T. Silva, R. Ferraz, M.S. Gomes, C. Teixeira, P. Gomes, Cinnamic acid conjugates in the rescuing and repurposing of classical antimalarial drugs, Molecules 25 (2020) 66.
[40] J. Wiesner, A. Mitsch, P. Wißner, H. Jomaa, M. Schlitzer, Structure–activity relationships of novel anti-malarial agents. Part 2: cinnamic acid derivatives, Bioorg. Med. Chem. Lett 11 (2001) 423–424.
[41] B. Pérez, C. Teixeira, A.S. Gomes, I.S. Albuquerque, J. Gut, P.J. Rosenthal, M. Prudêncio, P. Gomes, In vitro efficiency of 9-(N-cinnamoylbutyl)aminoacridines against blood- and liver-stage malaria parasites, Bioorg. Med. Chem. Lett 23 (2013) 610–613.
[42] B. Pérez, C. Teixeira, J. Gut, P.J. Rosenthal, J.R.B. Gomes, P. Gomes, Cinnamic acid/chloroquinoline conjugates as potent agents against chloroquine-resistant Plasmodium falciparum, ChemMedChem 7 (2012) 1537–1540.
[43] N. Ruwizhi, B.A. Aderibigbe, Cinnamic acid derivatives and their biological efficacy, Int. J. Mol. Sci. 21 (2020) 5712.
[44] M. Prudêncio, A. Rodriguez, M.M. Mota, The silent path to thousands of merozoites: the Plasmodium liver stage, Nat. Rev. Microbiol. 4 (2006) 849–856.
[45] Â.F. Chora, M.M. Mota, M. Prudêncio, The reciprocal influence of the liver and blood stages of the malaria parasite's life cycle, Int. J. Parasitol. 52 (2022) 711–715.
[46] K. Van Dyke, C. Lantz, C. Szustkiewicz, Quinacrine: mechanisms of antimalarial action, Science 169 (1970) 492–493.
[47] R. Ehsanian, C. Van Waes, S.M. Feller, Beyond DNA binding - a review of the potential mechanisms mediating quinacrine's therapeutic activities in parasitic infections, inflammation, and cancers, Cell Commun. Signal. 9 (2011) 13.
[48] A. Gomes, I. Fernandes, C. Teixeira, N. Mateus, M.J. Sottomayor, P. Gomes, A quinacrine analogue selective against gastric cancer cells: insight from biochemical and biophysical studies, ChemMedChem 11 (2016) 2703–2712.
[49] C. Upadhyay, M. Chaudhary, R.N. De Oliveira, A. Borbas, P. Kempaiah, P. S, B. Rathi, Fluorinated scaffolds for antimalarial drug discovery, Expet Opin. Drug Discov. 15 (2020) 705–718.
[50] I.H.J. Ploemen, M. Prudêncio, B.G. Douradinha, J. Ramesar, J. Fonager, G.-J. van Gemert, A.J.F. Luty, C.C. Hermsen, R.W. Sauerwein, F.G. Baptista, M.M. Mota, A. P. Waters, I. Que, C.W.G.M. Lowik, S.M. Khan, C.J. Janse, B.M.D. Franke-Fayard, Visualisation and quantitative analysis of the rodent malaria liver stage by real time imaging, PLoS One 4 (2009), e7881.
[51] H.P. Portugaliza, O. Llorà-Batlle, A. Rosanas-Urgell, A. Cortés, Reporter lines based on the gexp02 promoter enable early quantification of sexual conversion rates in the malaria parasite Plasmodium falciparum, Sci. Rep. 9 (2019), 14595.
[52] C. Lambros, J.P. Vanderberg, Synchronization of Plasmodium falciparum erythrocytic stages in culture, J. Parasitol. 65 (1979) 418–420.

Supporting Information

New 4-(*N*-cinnamoylbutyl)aminoacridines as potential multi-stage antiplasmodial leads

Mélanie Fonte,*[a] Diana Fontinha,[b] Diana Moita,[b] Omar Prades,[c] Yunuen Padilla,[c] Xavier Fernàndez-Busquets,[c],[d],[e] Miguel Prudêncio,[b] Paula Gomes**,[a] Cátia Teixeira[a], [f]

[a] LAQV-REQUIMTE, Departamento de Química e Bioquímica, Faculdade de Ciências, Universidade do Porto, Portugal;

[b] Instituto de Medicina Molecular, Faculdade de Medicina, Universidade de Lisboa, Portugal;

[c] Nanomalaria Group, Institute for Bioengineering of Catalonia (IBEC), The Barcelona Institute of Science and Technology, Spain;

[d] Barcelona Institute for Global Health (ISGlobal), Barcelona Center for International Health Research (CRESIB), Hospital Clínic-Universitat de Barcelona, Spain;

[e] Nanoscience and Nanotechnology Institute (IN2UB), University of Barcelona, Spain;

[f] current affiliation: Gyros Protein Technologies Inc., Tucson, Arizona, USA.

Contents:

Spectral and chromatographic traces for compounds 2a-l (Figures S1-S72)

Compound 2a

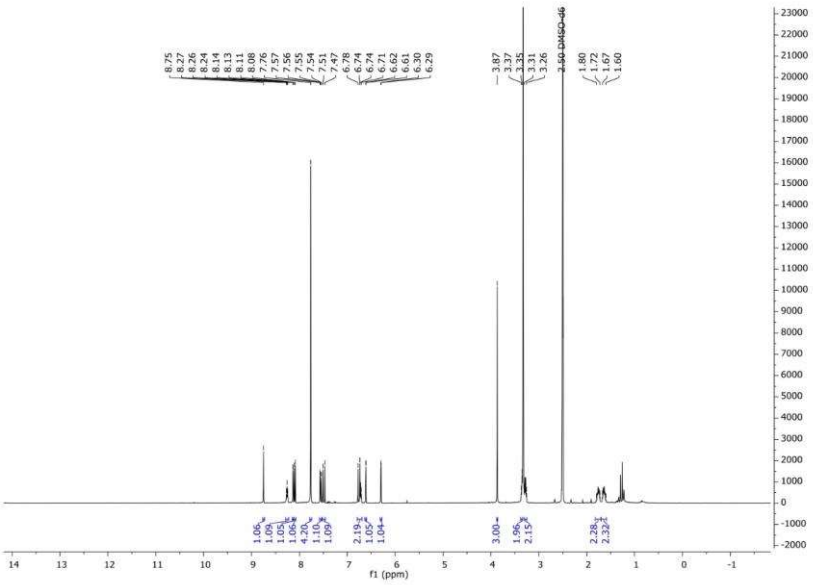


Figure S1. ^{1}H-RMN full spectrum (400 MHz, DMSO-d_6) of **2a**.

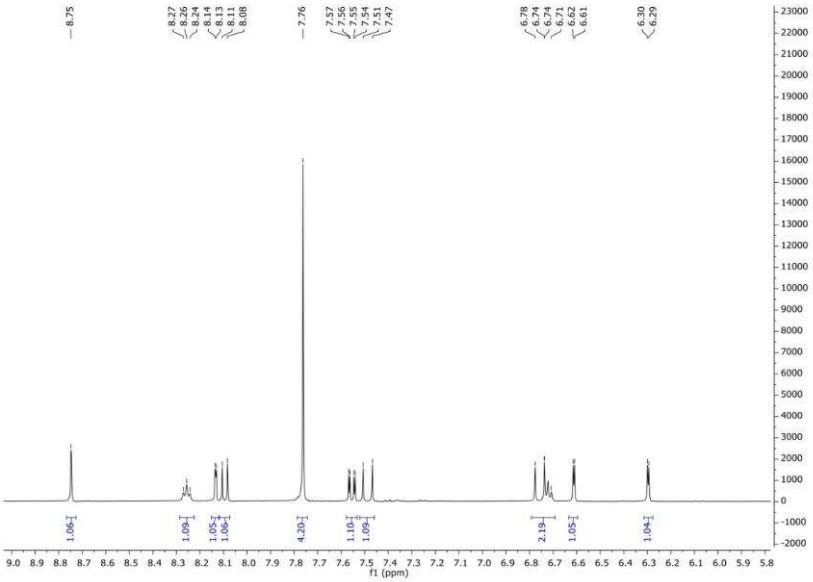


Figure S2. Aromatic region in the ^{1}H-RMN spectrum (400 MHz, DMSO-d_6) of **2a**.

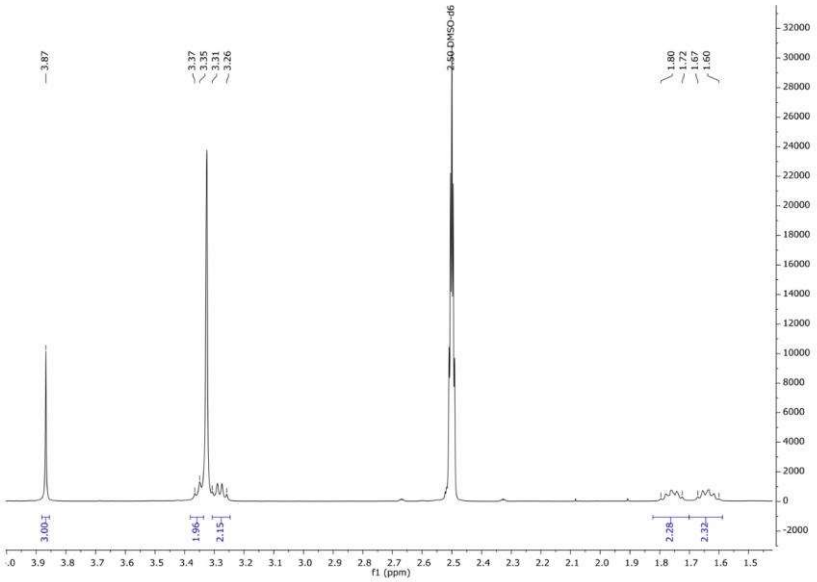


Figure S3. Aliphatic region in the ^{1}H-RMN spectrum (400 MHz, DMSO-d_6) of **2a**.

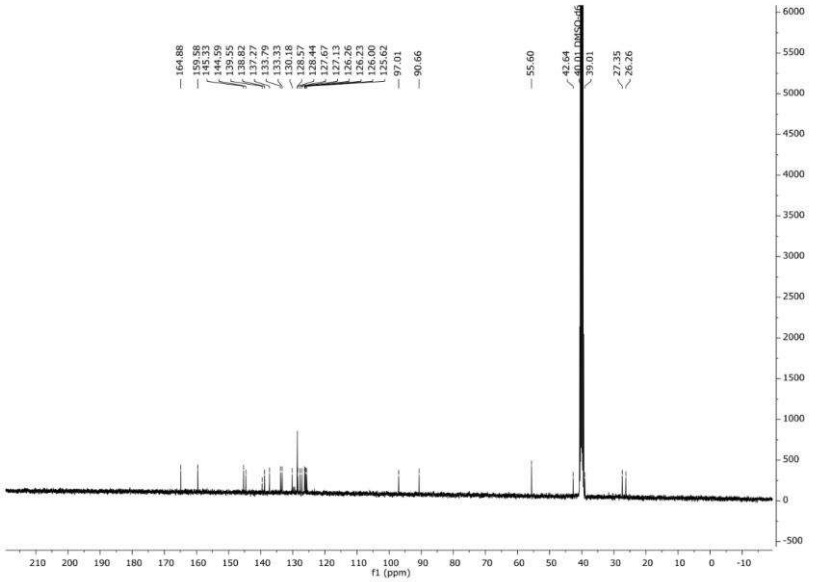


Figure S4. ^{13}C-RMN spectrum (100 MHz, DMSO-d_6) of **2a**.

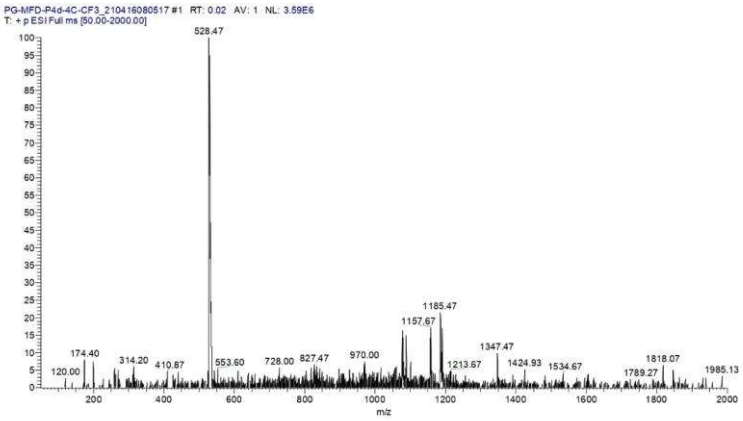


Figure S5. ESI-IT (+) spectrum of **2a**.

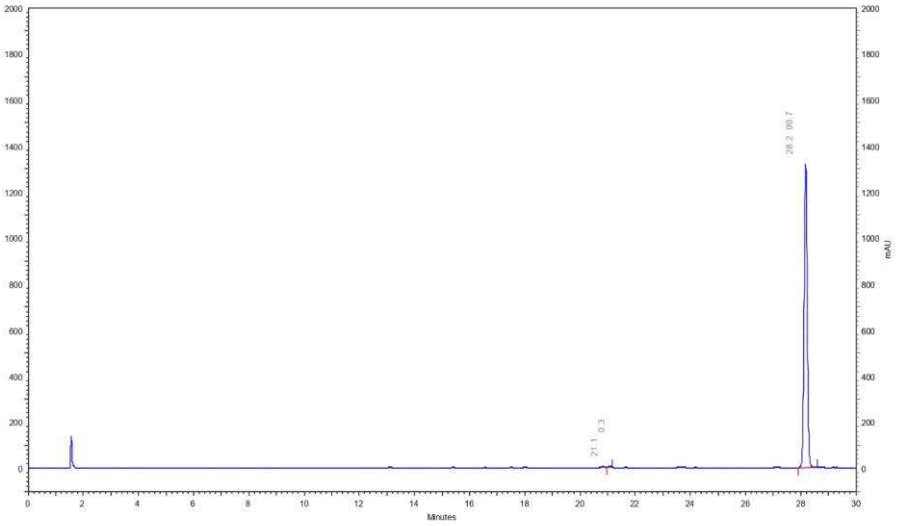


Figure S6. HPLC trace of **2a**.

Compound 2b

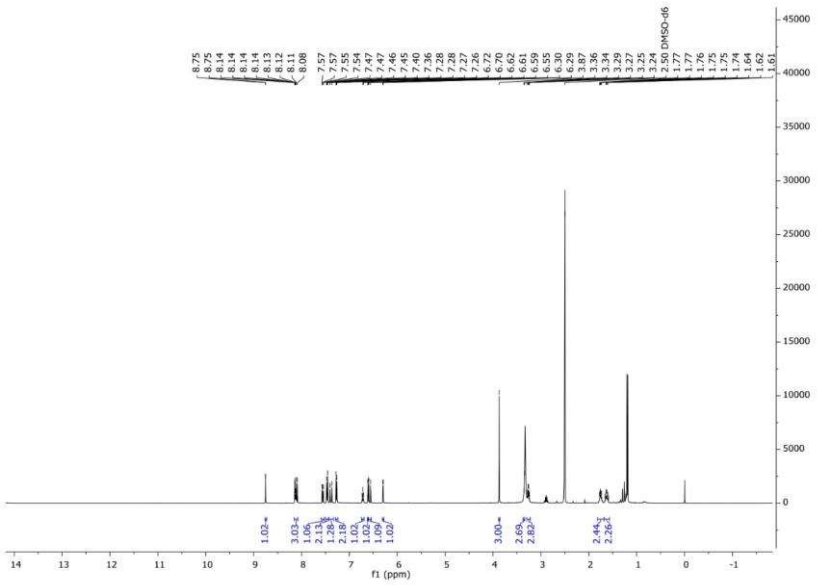


Figure S7. ^{1}H-RMN full spectrum (400 MHz, DMSO-d_6) of **2b**.

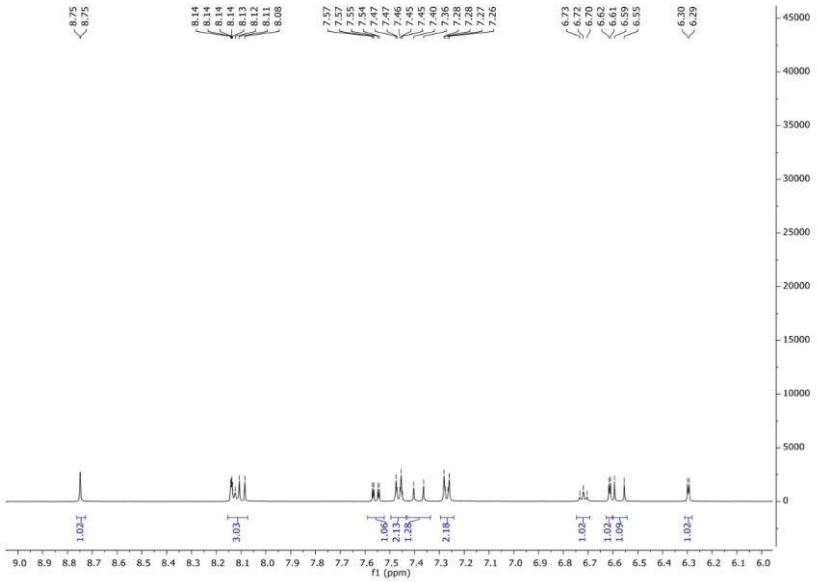


Figure S8. Aromatic region in the ^{1}H-RMN spectrum (400 MHz, DMSO-d_6) of **2b**.

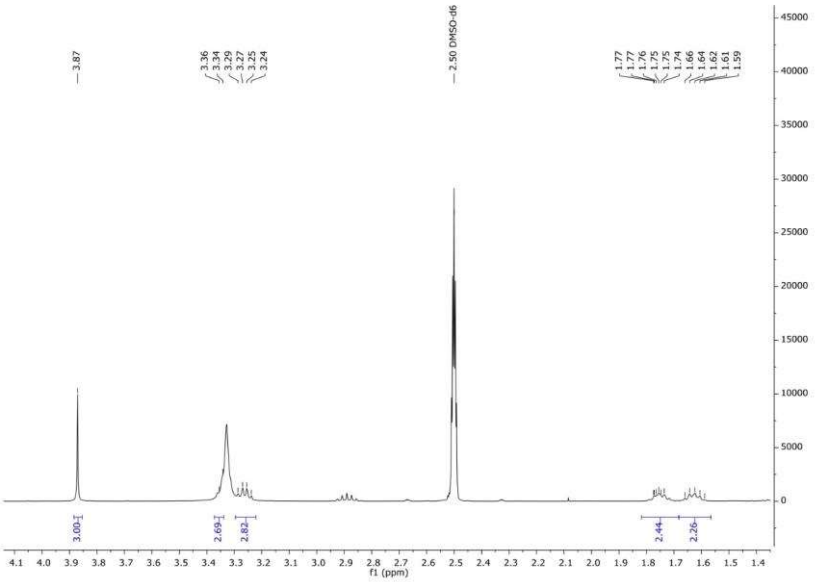


Figure S9. Aliphatic region in the ^{1}H-RMN spectrum (400 MHz, DMSO-d_6) of **2b**.

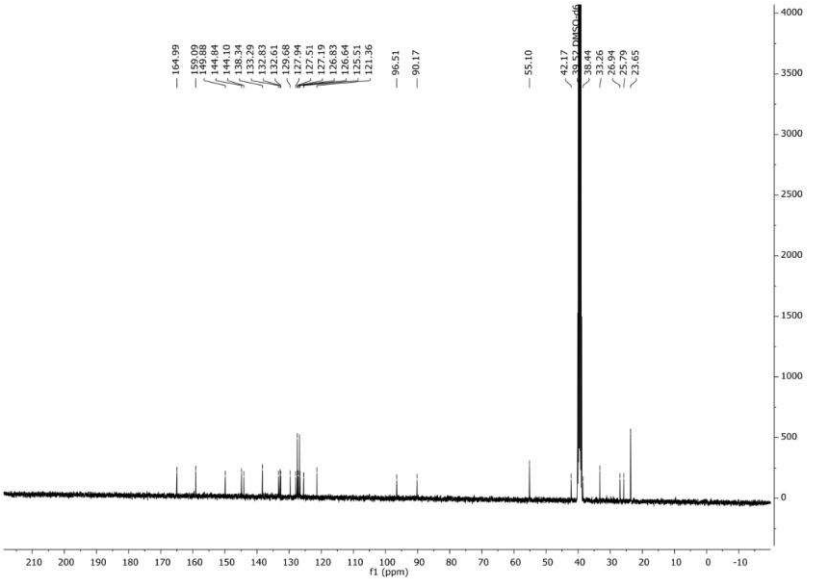


Figure S10. ^{13}C-RMN spectrum (100 MHz, DMSO-d_6) of **2b**.

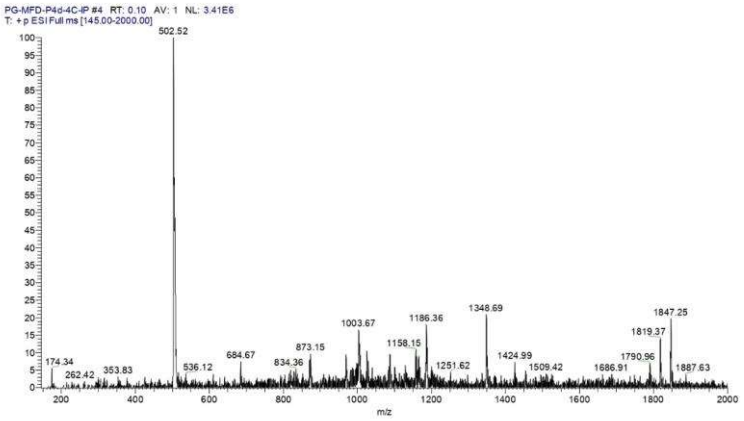


Figure S11. ESI-IT (+) spectrum of **2b**.

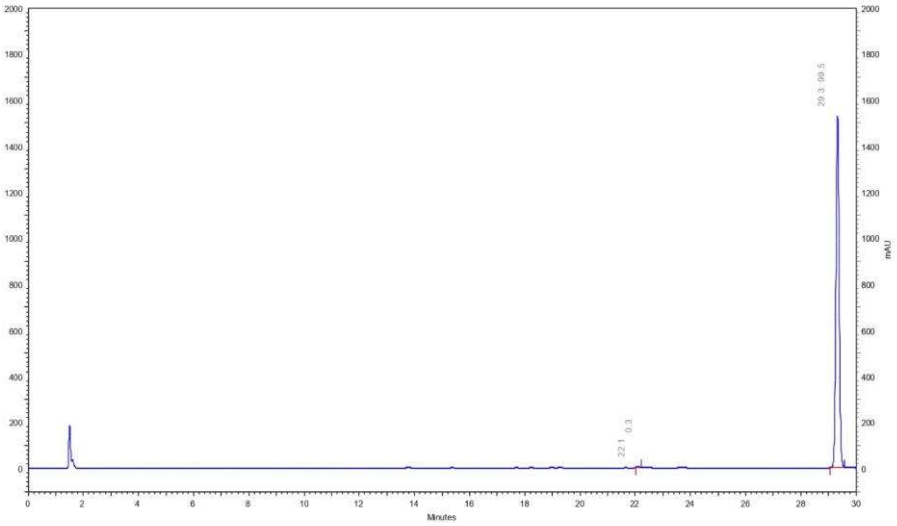


Figure S12. HPLC trace of **2b**.

Compound 2c

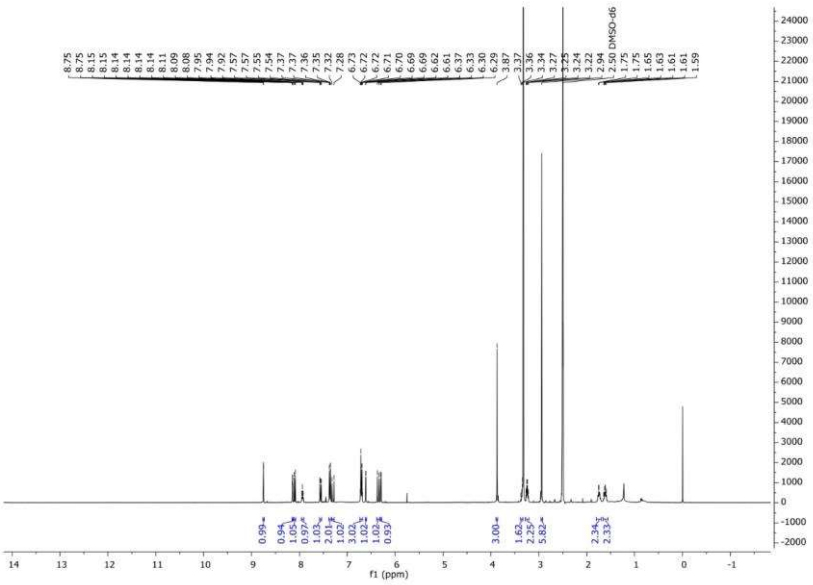


Figure S13. ^{1}H-RMN full spectrum (400 MHz, DMSO-d_6) of **2c**.

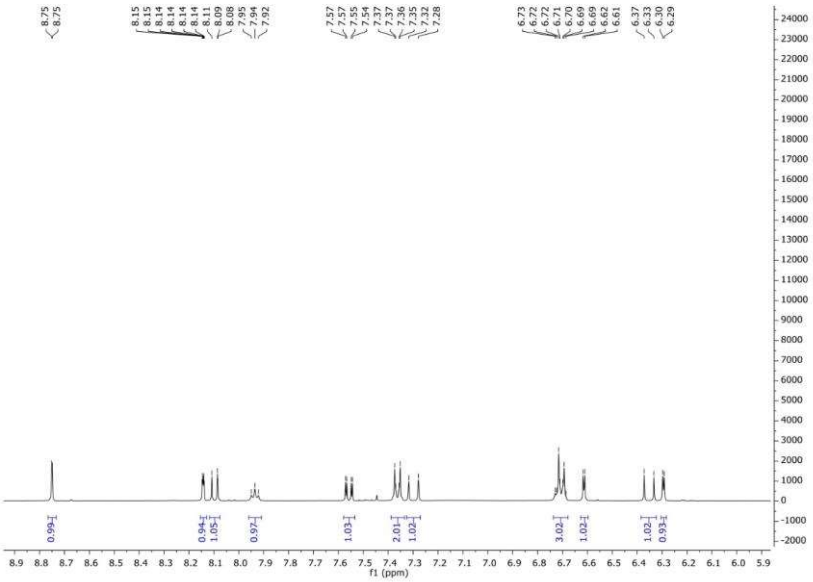


Figure S14. Aromatic region in the ^{1}H-RMN spectrum (400 MHz, DMSO-d_6) of **2c**.

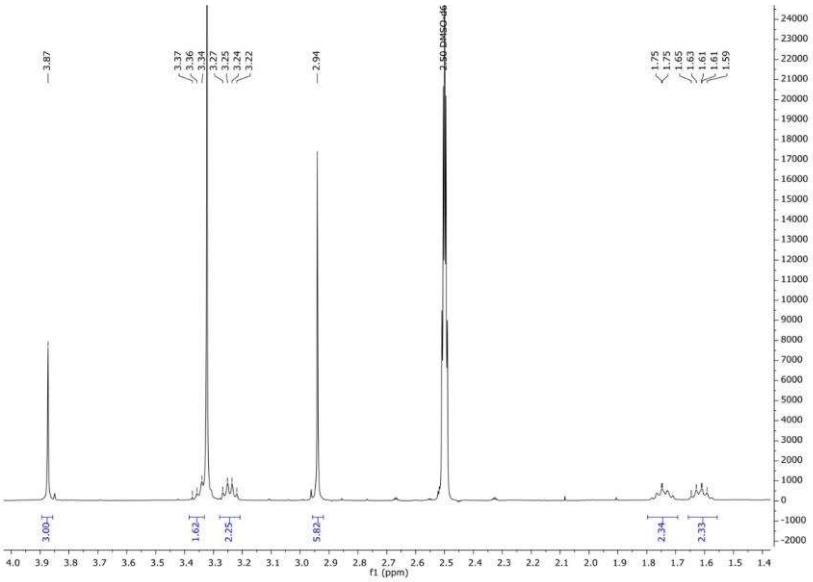


Figure S15. Aliphatic region in the ^{1}H-RMN spectrum (400 MHz, DMSO-d_6) of **2c**.

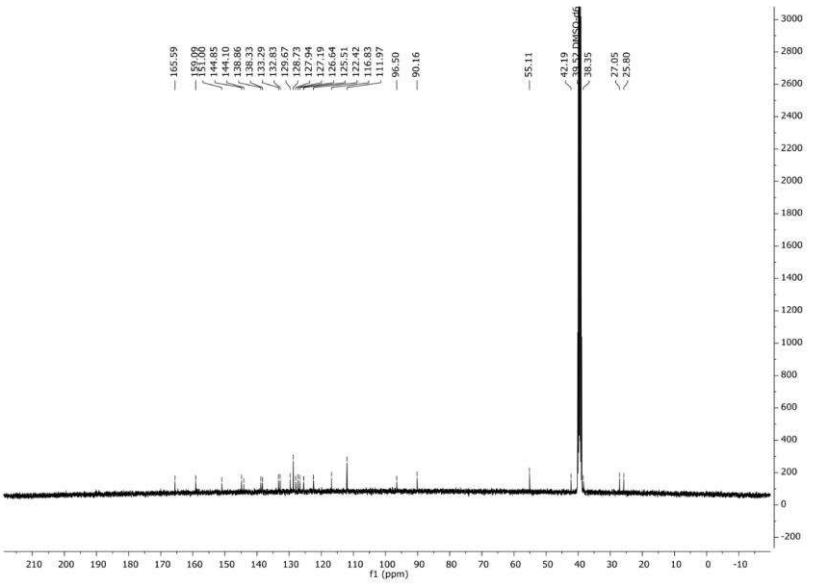


Figure S16. ^{13}C-RMN spectrum (100 MHz, DMSO-d_6) of **2c**.

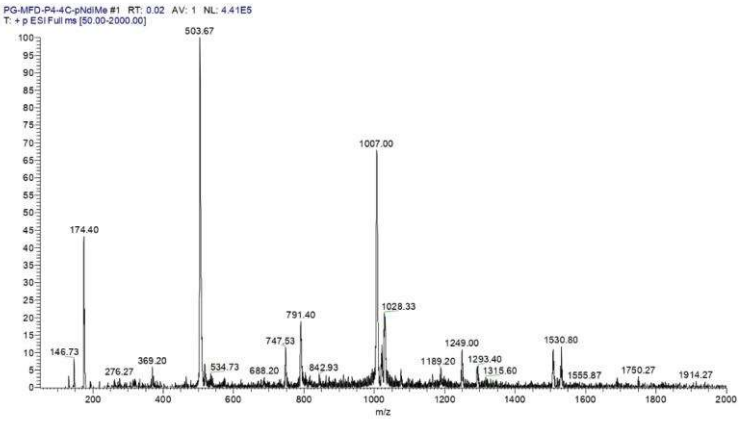


Figure S17. ESI-IT (+) spectrum of **2c**.

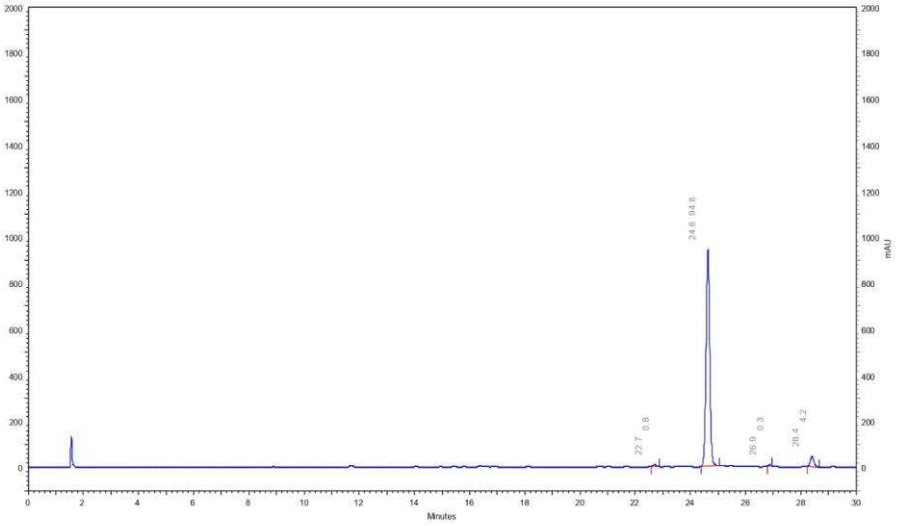


Figure S18. HPLC trace of **2c**.

Compound 2d

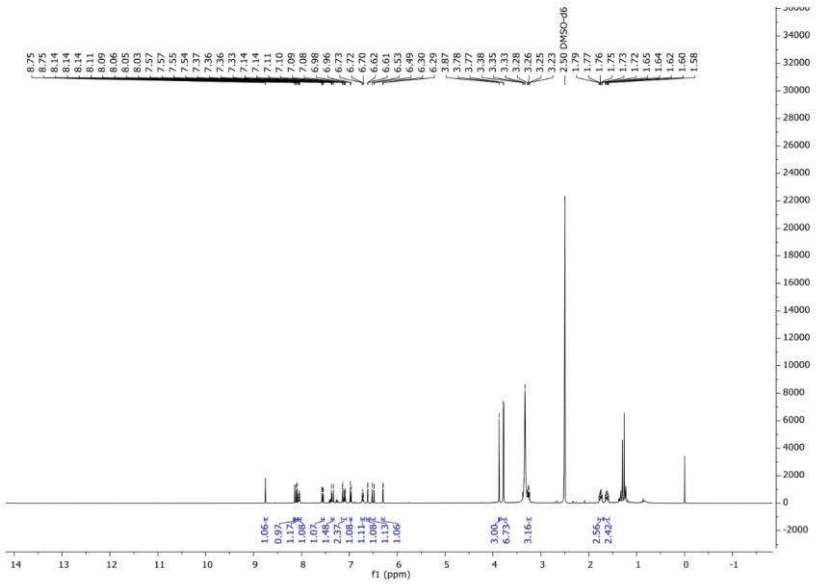


Figure S19. ^{1}H-RMN full spectrum (400 MHz, DMSO-d_6) of **2d.**

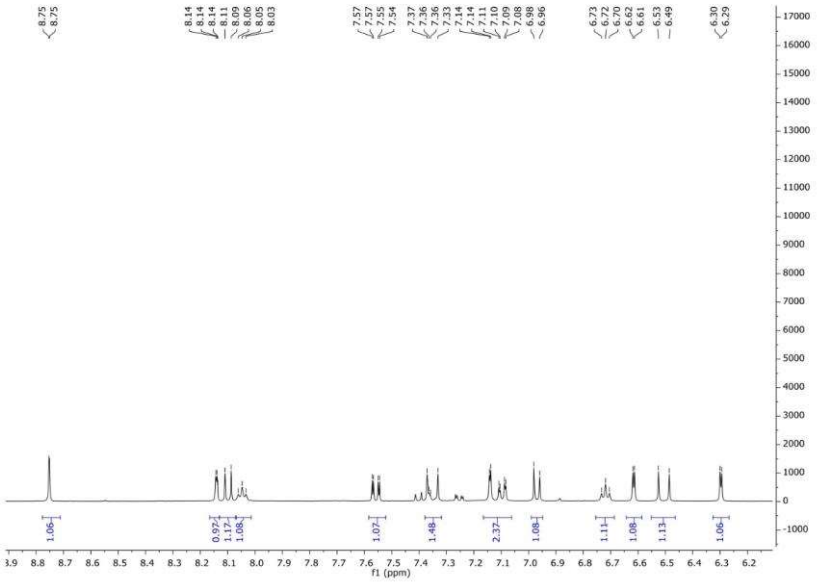


Figure S20. Aromatic region in the ^{1}H-RMN spectrum (400 MHz, DMSO-d_6) of **2d**.

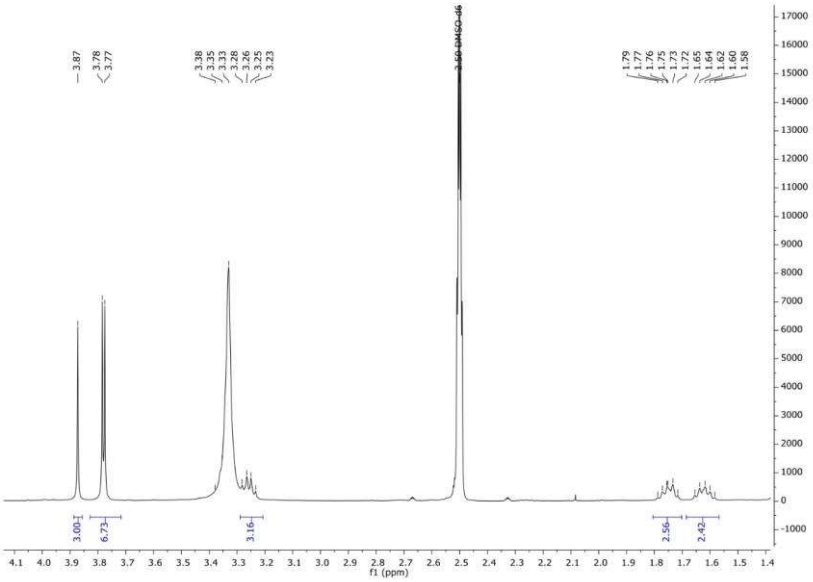


Figure S21. Aliphatic region in the ^{1}H-RMN spectrum (400 MHz, DMSO-d_6) of **2d**.

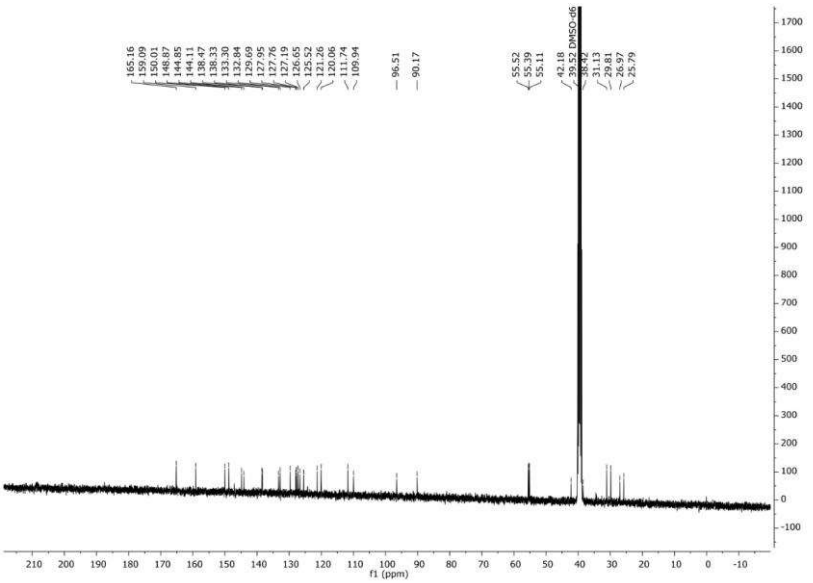


Figure S22. ^{13}C-RMN spectrum (100 MHz, DMSO-d_6) of **2d**.

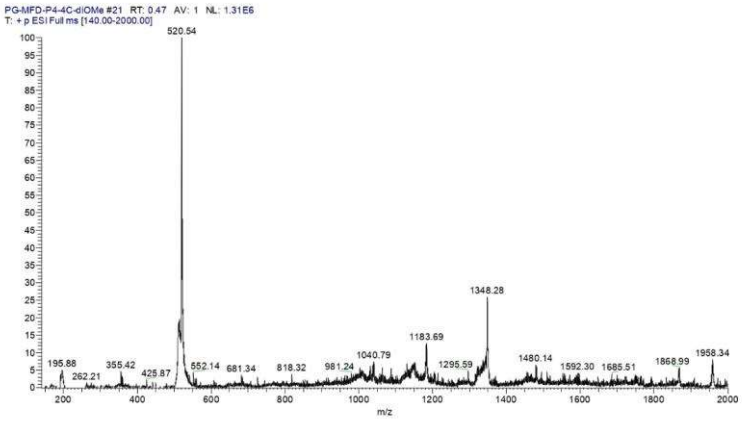


Figure S23. ESI-IT (+) spectrum of **2d**.

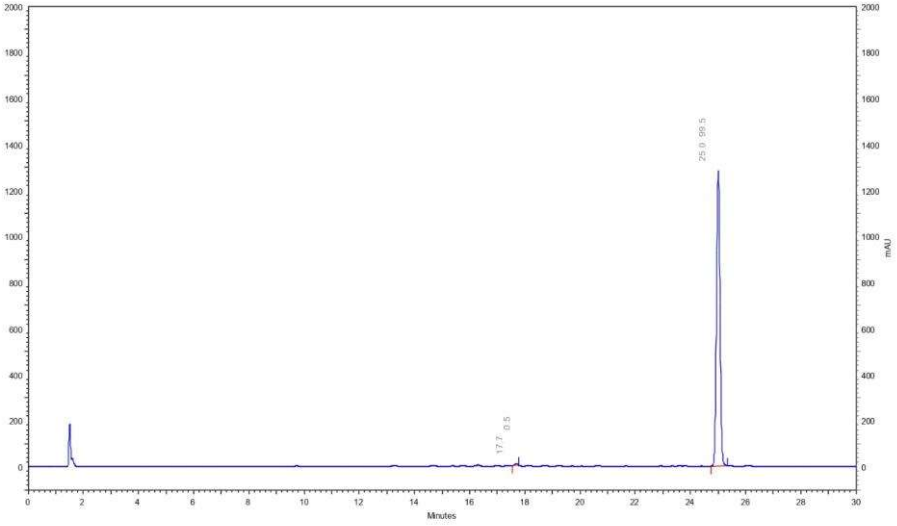


Figure S24. HPLC trace of **2d**.

Compound 2e

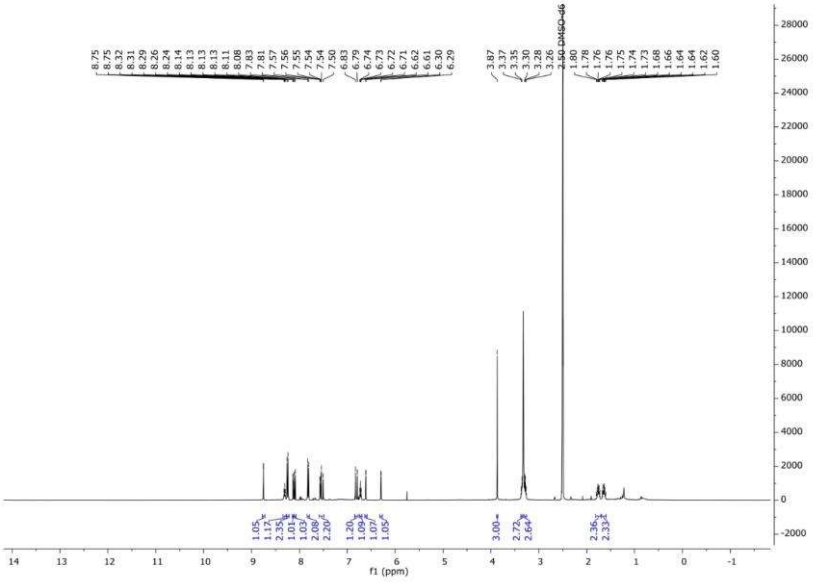


Figure S25. ^{1}H-RMN full spectrum (400 MHz, DMSO-d_6) of **2e**.

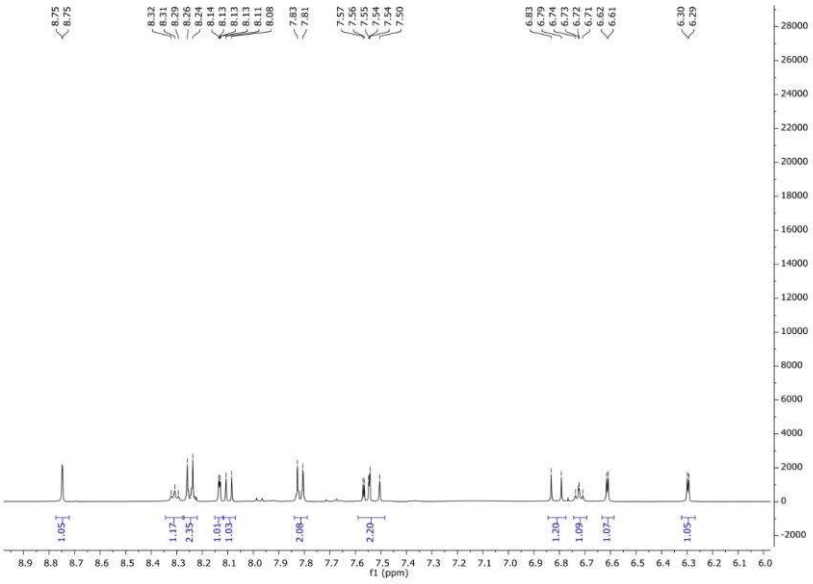


Figure S26. Aromatic region in the ^{1}H-RMN spectrum (400 MHz, DMSO-d_6) of **2e**.

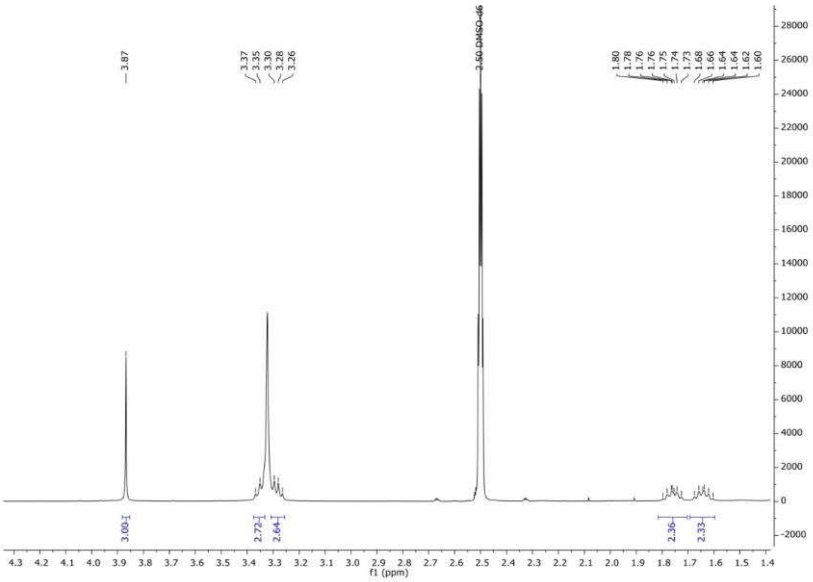


Figure S27. Aliphatic region in the ^{1}H-RMN spectrum (400 MHz, DMSO-d_6) of **2e**.

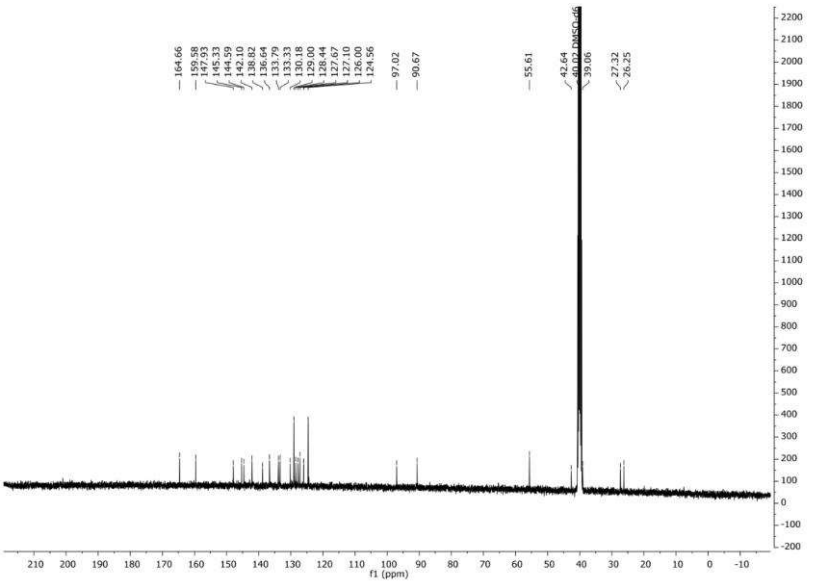


Figure S28. ^{13}C-RMN spectrum (100 MHz, DMSO-d_6) of **2e**.

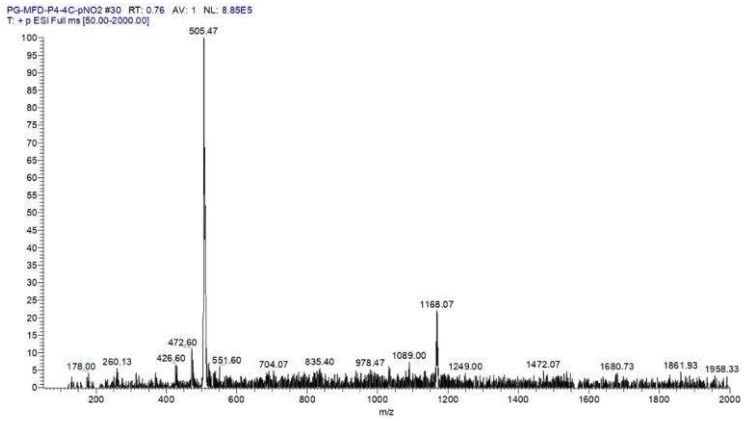


Figure S29. ESI-IT (+) spectrum of **2e**.

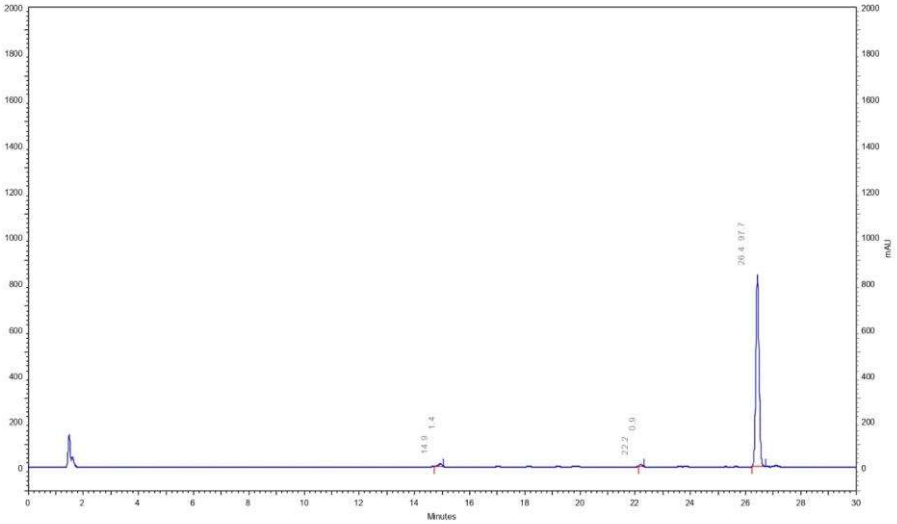


Figure S30. HPLC trace of **2e**.

Compound 2f

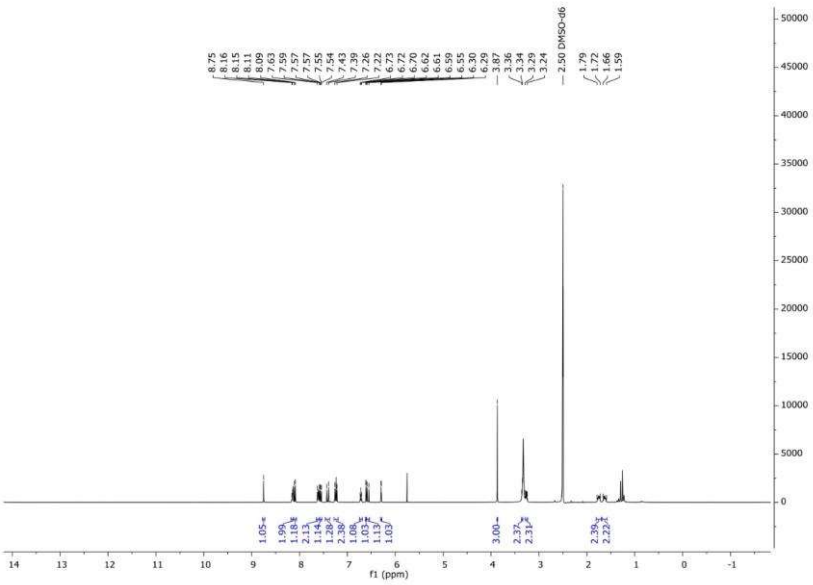


Figure S31. ^{1}H-RMN full spectrum (400 MHz, DMSO-d_6) of **2f**.

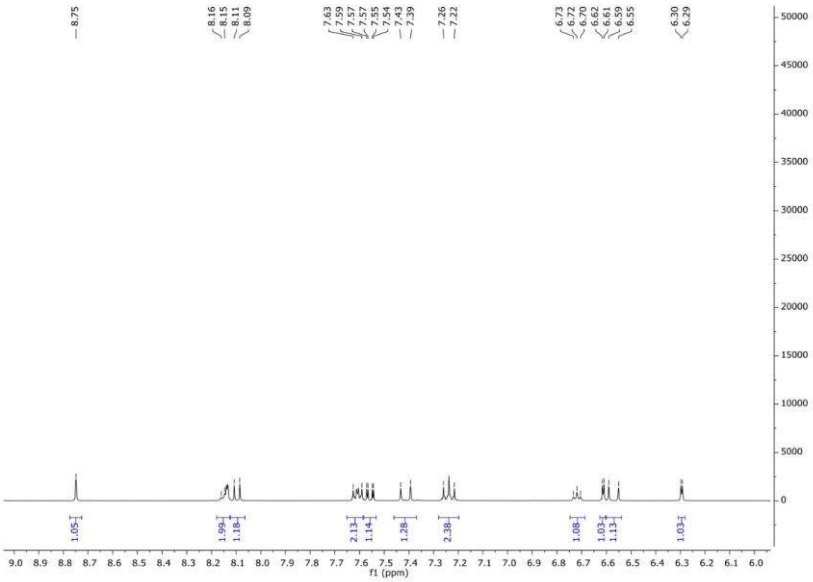


Figure S32. Aromatic region in the ^{1}H-RMN spectrum (400 MHz, DMSO-d_6) of **2f**.

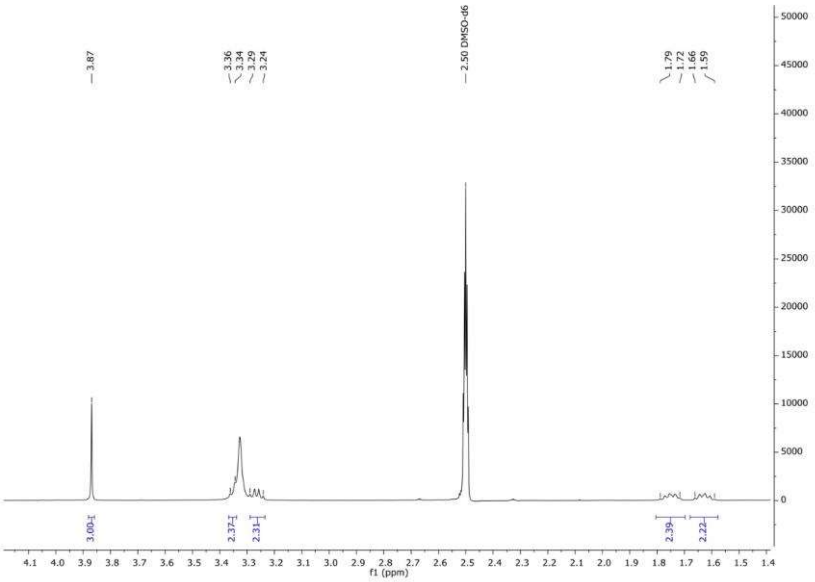


Figure S33. Aliphatic region in the ^{1}H-RMN spectrum (400 MHz, DMSO-d_6) of **2f**.

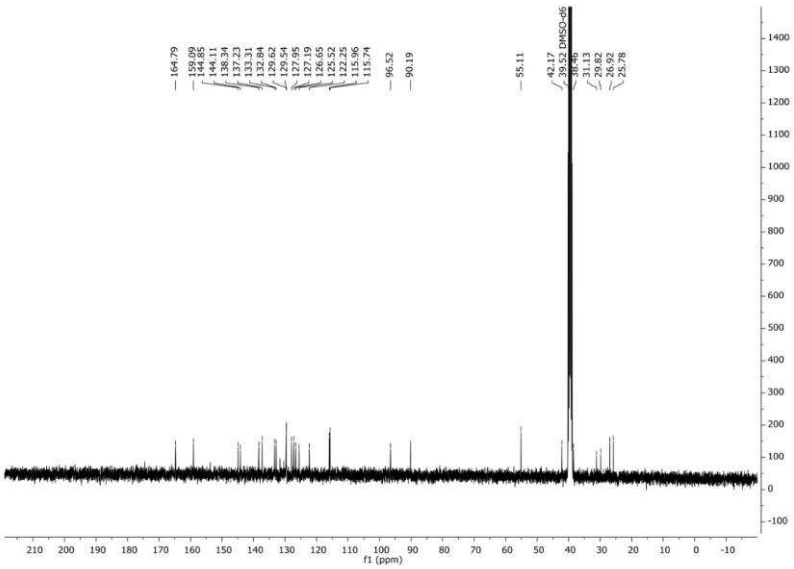


Figure S34. ^{13}C-RMN spectrum (100 MHz, DMSO-d_6) of **2f**.

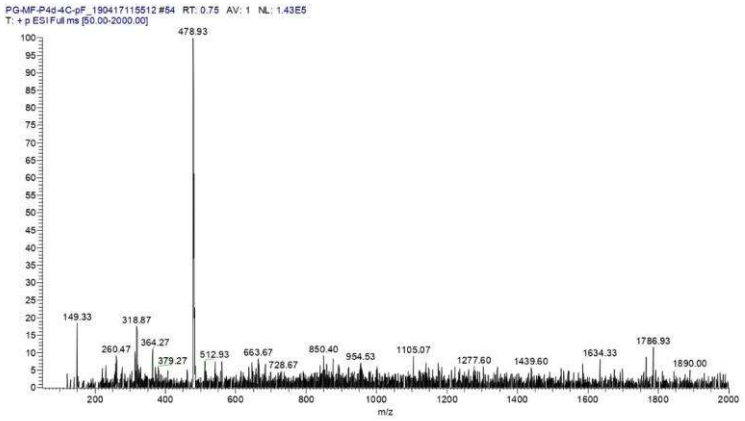


Figure S35. ESI-IT (+) spectrum of **2f**.

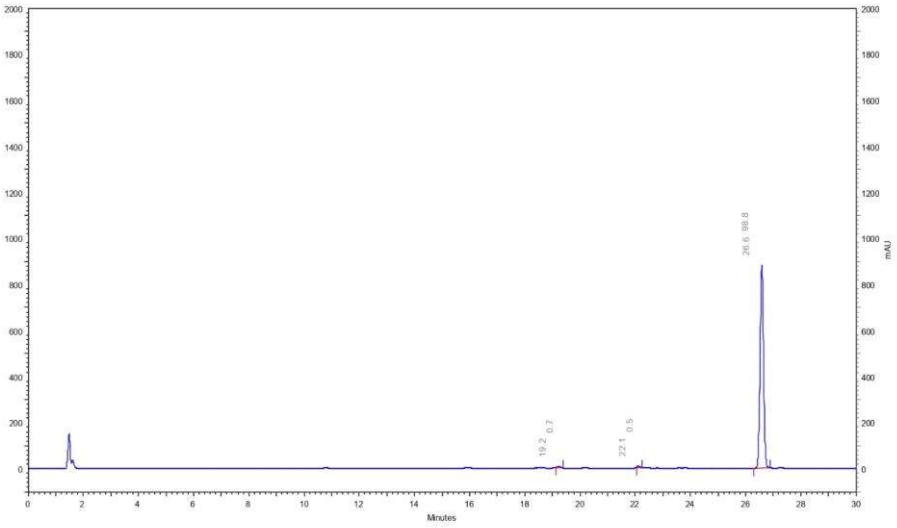


Figure S36. HPLC trace of **2f**.

Compound 2g

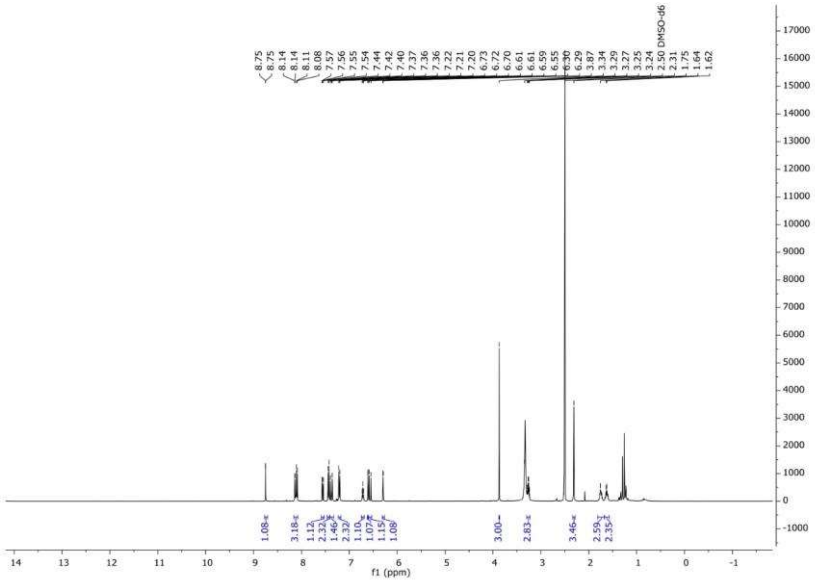


Figure S37. ^{1}H-RMN full spectrum (400 MHz, DMSO-d_6) of **2g**.

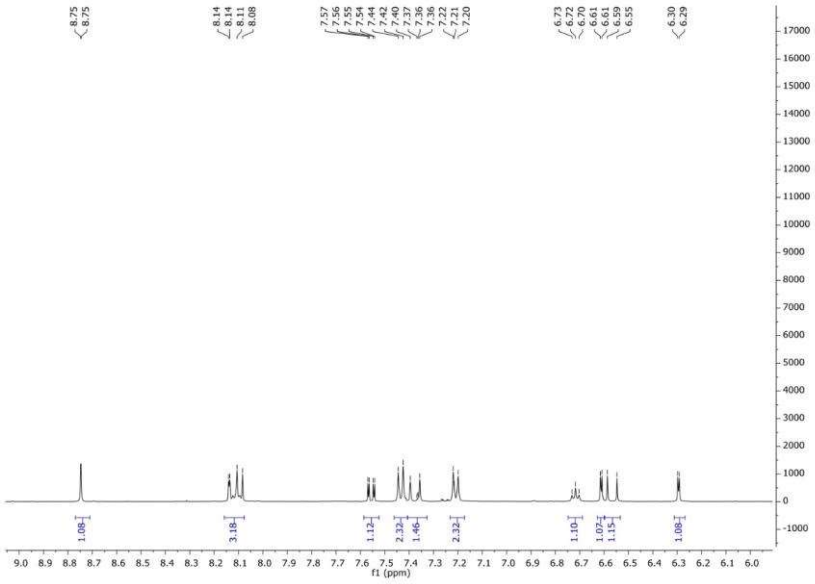


Figure S38. Aromatic region in the ^{1}H-RMN spectrum (400 MHz, DMSO-d_6) of **2g**.

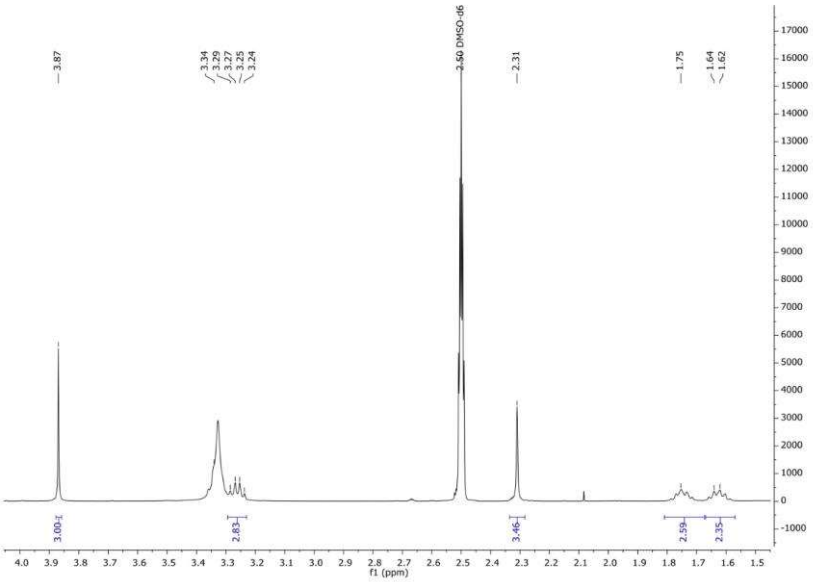


Figure S39. Aliphatic region in the ^{1}H-RMN spectrum (400 MHz, DMSO-d_6) of **2g**.

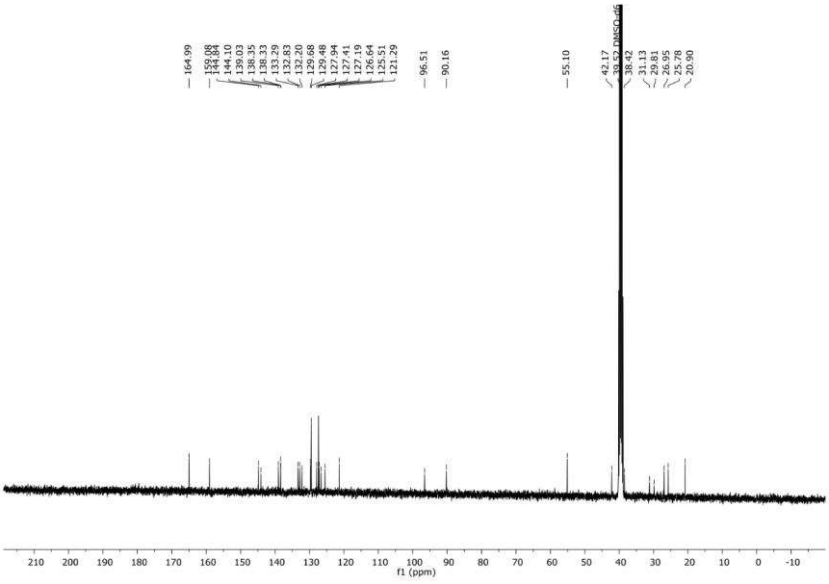


Figure S40. ^{13}C-RMN spectrum (100 MHz, DMSO-d_6) of **2g**.

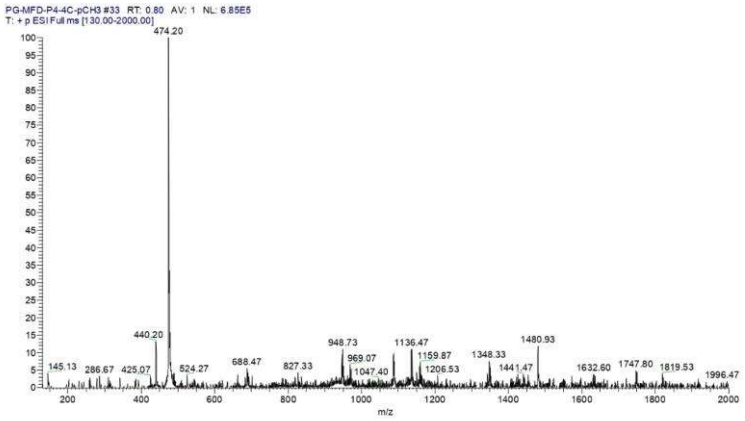


Figure S41. ESI-IT (+) spectrum of **2g**.

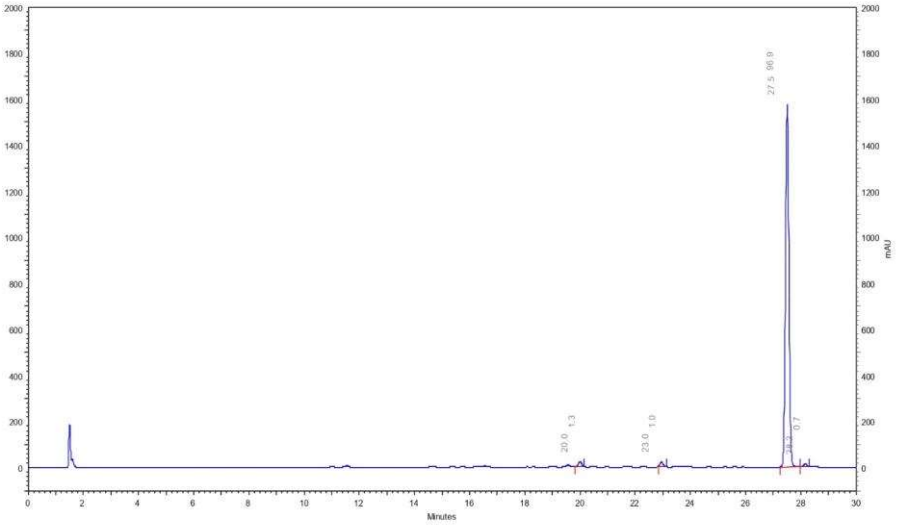


Figure S42. HPLC trace of **2g**.

Compound 2h

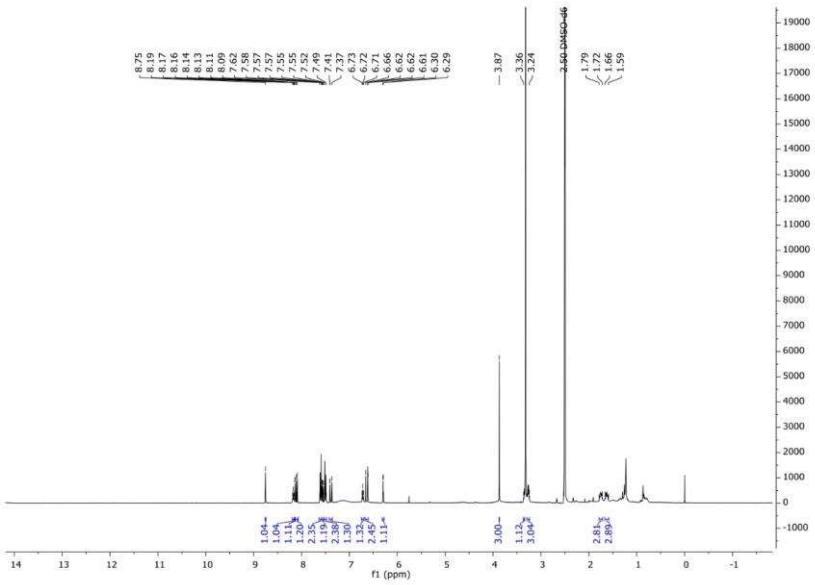


Figure S43. ^{1}H-RMN full spectrum (400 MHz, DMSO-d_6) of **2h**.

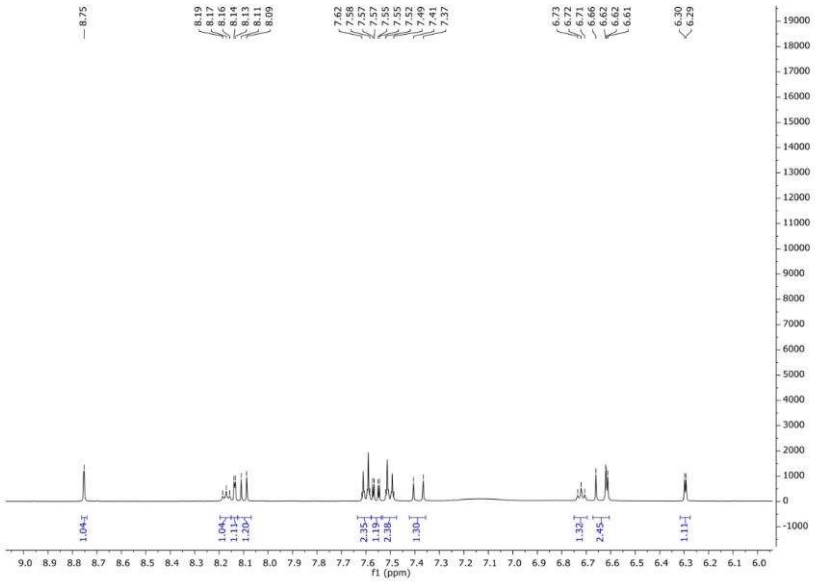


Figure S44. Aromatic region in the ^{1}H-RMN spectrum (400 MHz, DMSO-d_6) of **2h**.

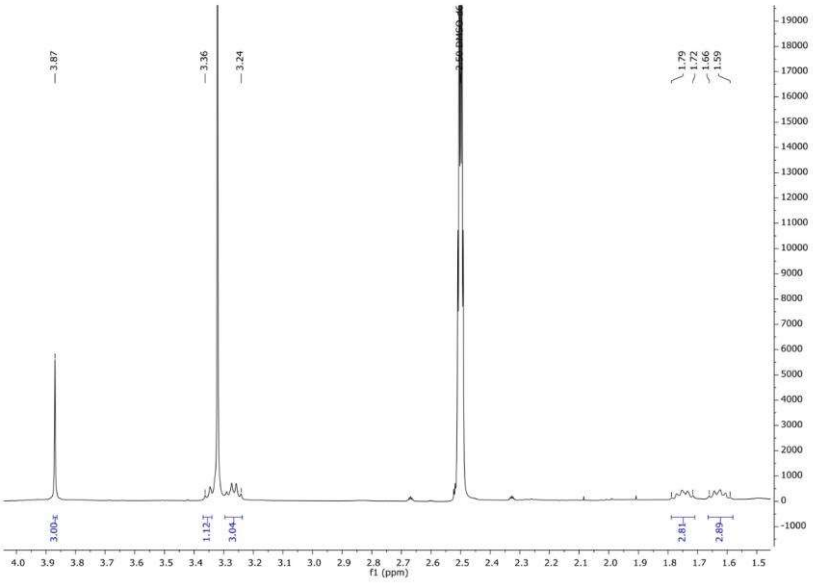


Figure S45. Aliphatic region in the ^{1}H-RMN spectrum (400 MHz, DMSO-d_6) of **2h**.

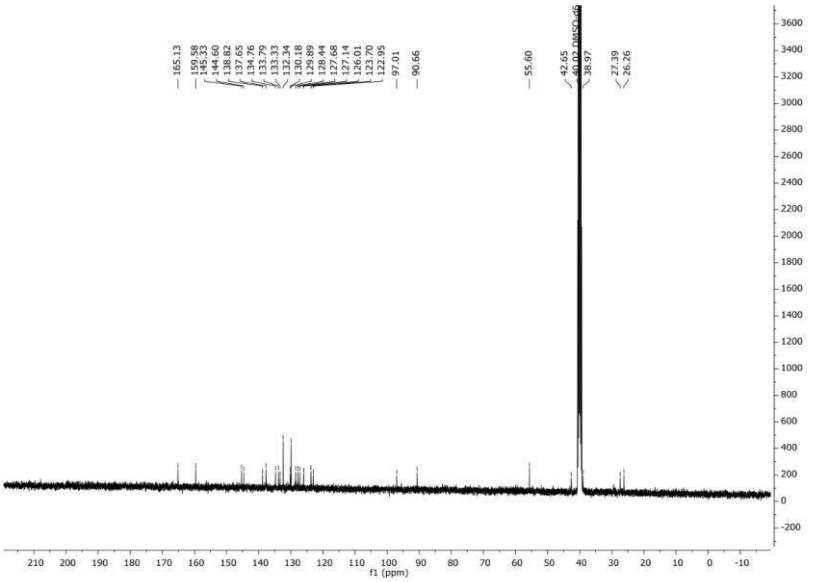


Figure S46. ^{13}C-RMN spectrum (100 MHz, DMSO-d_6) of **2h**.

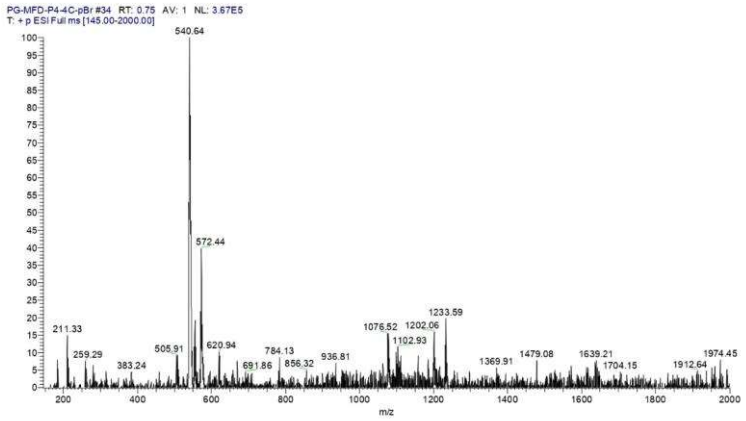


Figure S47. ESI-IT (+) spectrum of **2h**.

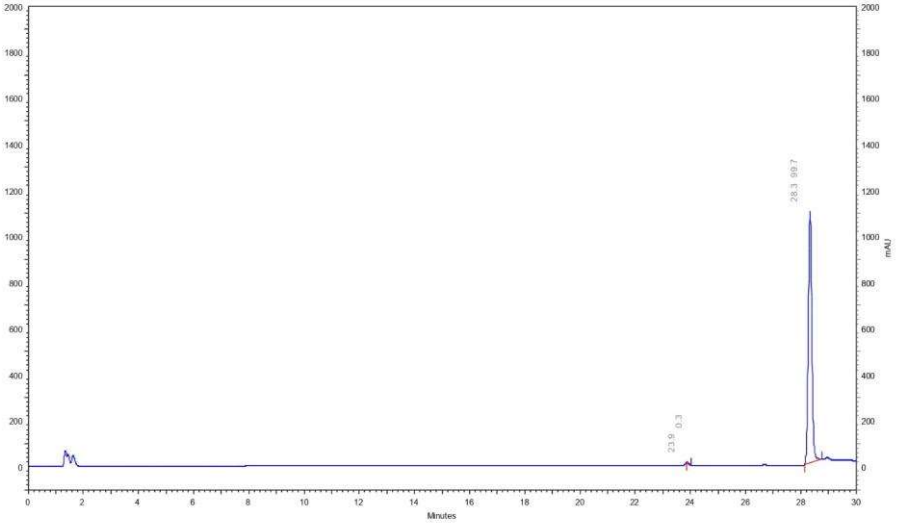


Figure S48. HPLC trace of **2h**.

Compound 2i

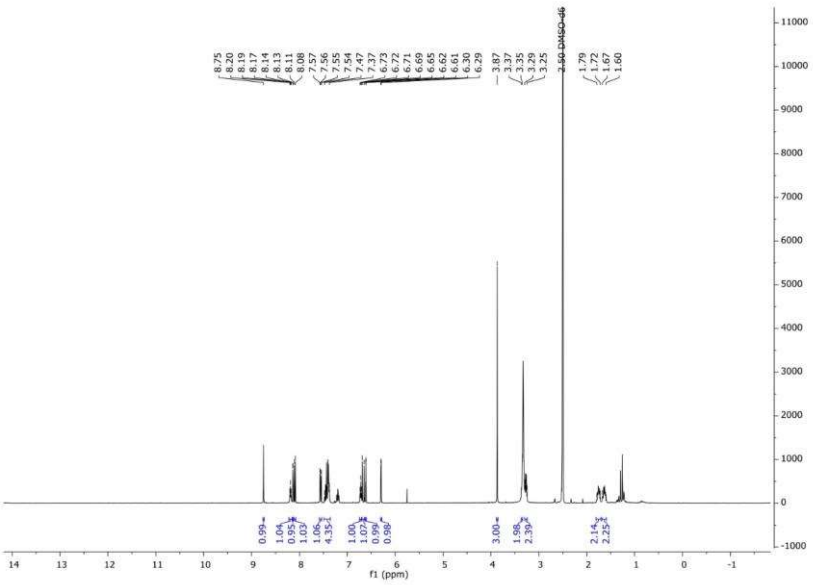


Figure S49. ^{1}H-RMN full spectrum (400 MHz, DMSO-d_6) of **2i**.

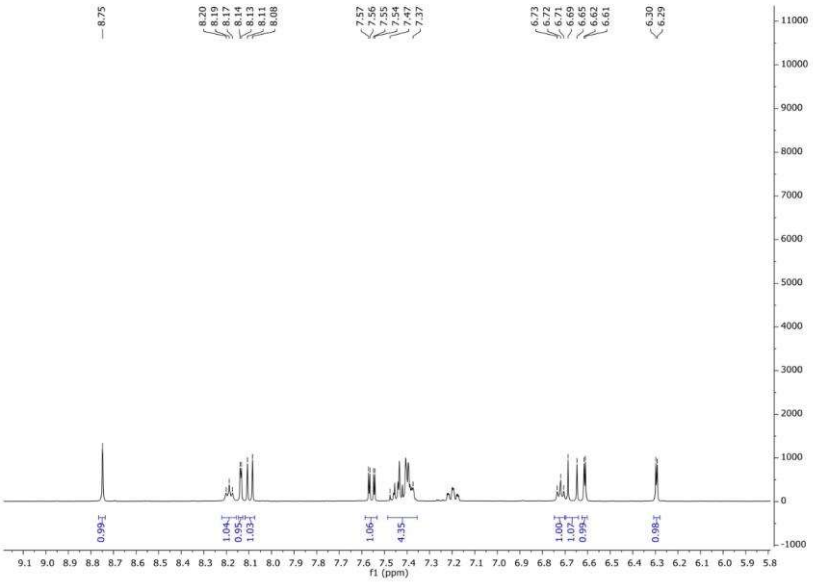


Figure S50. Aromatic region in the ^{1}H-RMN spectrum (400 MHz, DMSO-d_6) of **2i**.

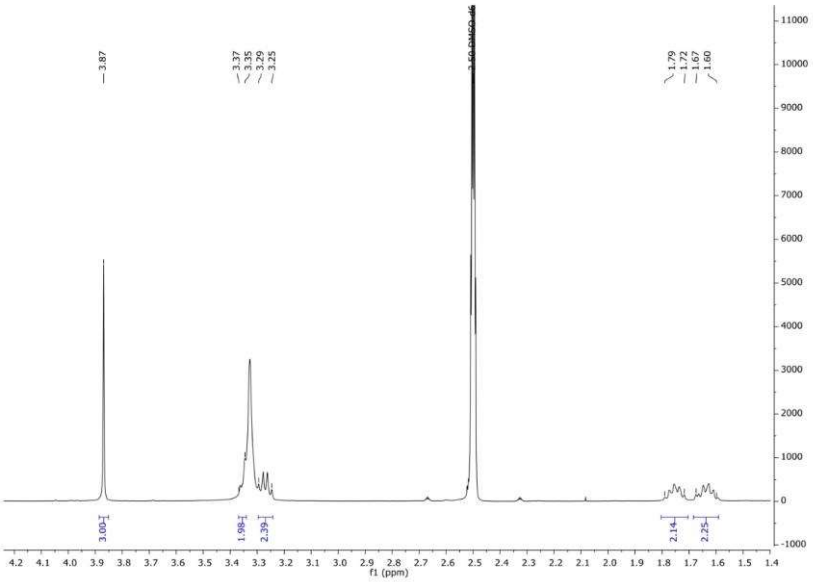


Figure S51. Aliphatic region in the ^{1}H-RMN spectrum (400 MHz, DMSO-d_6) of **2i**.

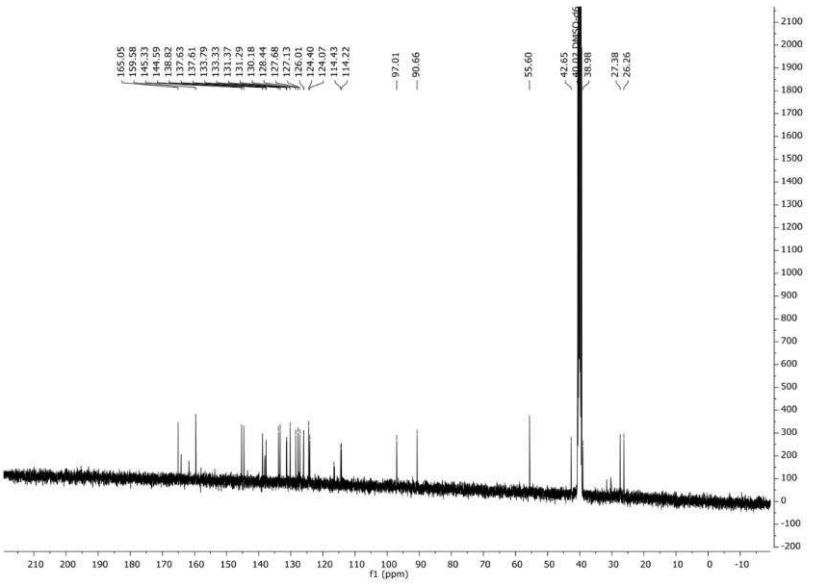


Figure S52. ^{13}C-RMN spectrum (100 MHz, DMSO-d_6) of **2i**.

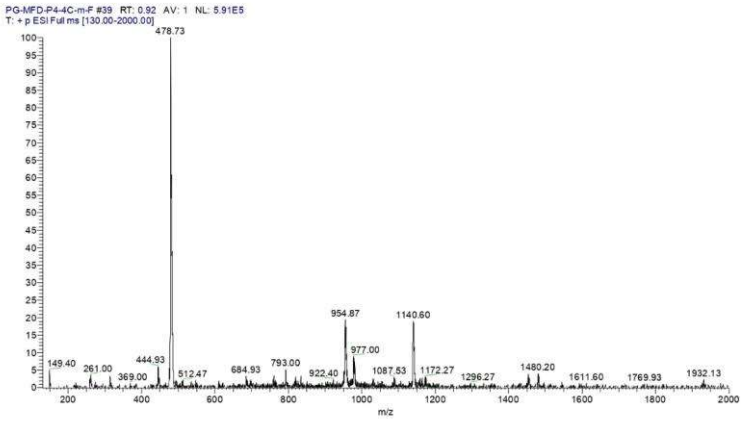


Figure S53. ESI-IT (+) spectrum of **2i**.

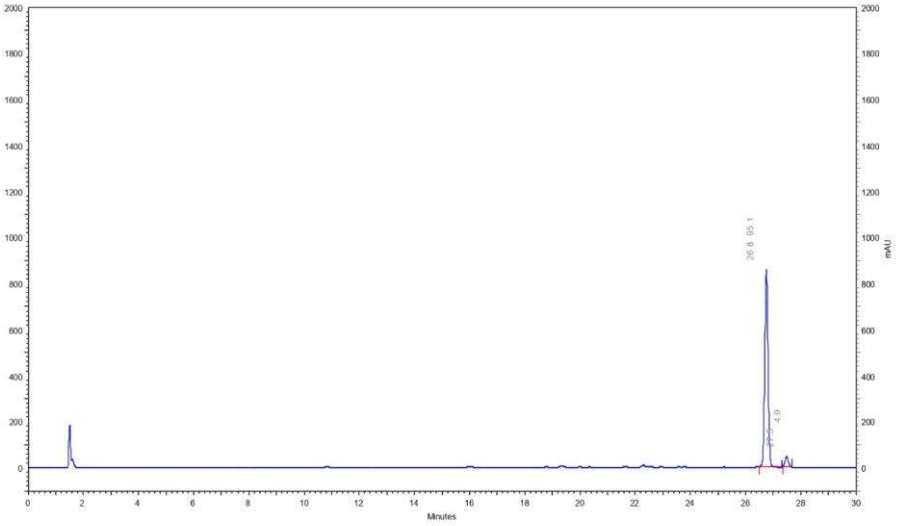


Figure S54. HPLC trace of **2i**.

Compound 2j

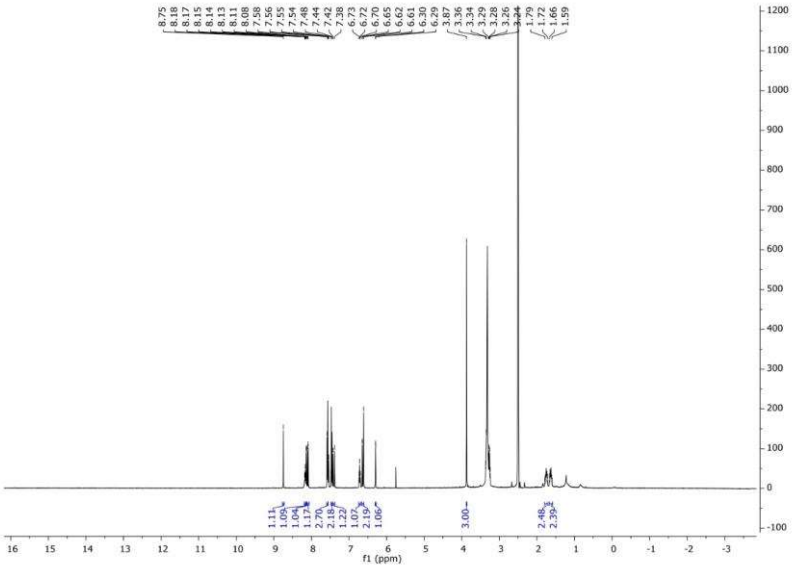


Figure S55. ^{1}H-RMN full spectrum (400 MHz, DMSO-d_6) of **2j**.

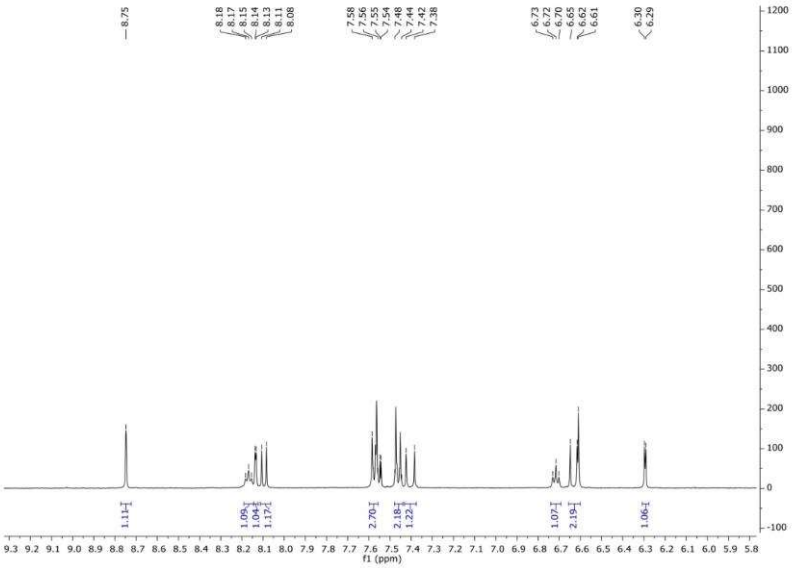


Figure S56. Aromatic region in the ^{1}H-RMN spectrum (400 MHz, DMSO-d_6) of **2j**.

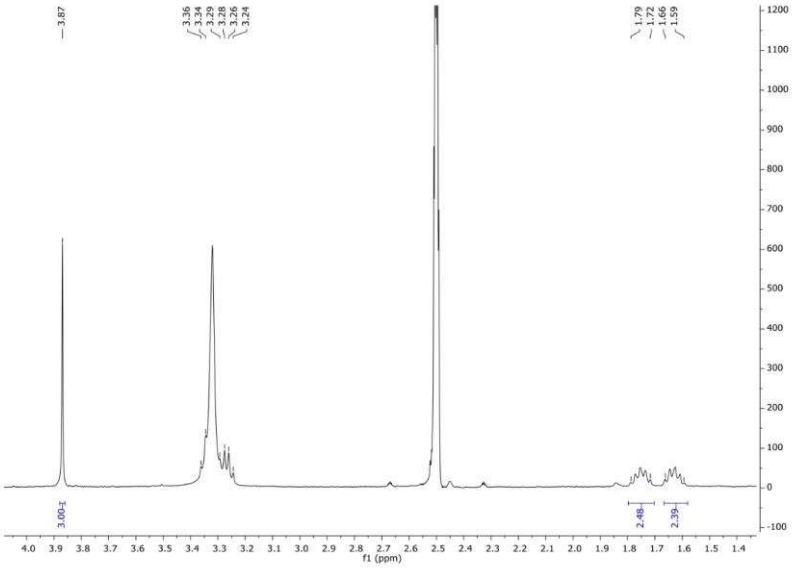


Figure S57. Aliphatic region in the ^{1}H-RMN spectrum (400 MHz, DMSO-d_6) of **2j**.

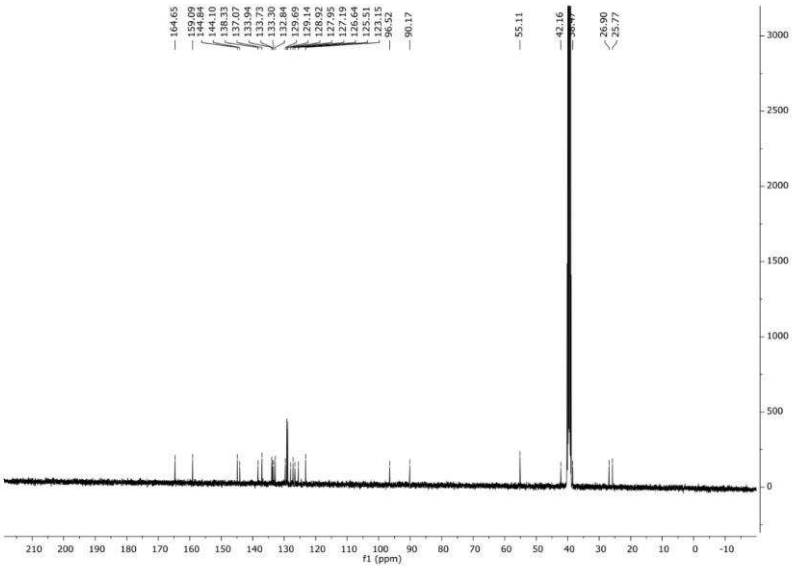


Figure S58. ^{13}C-RMN spectrum (100 MHz, DMSO-d_6) of **2j**.

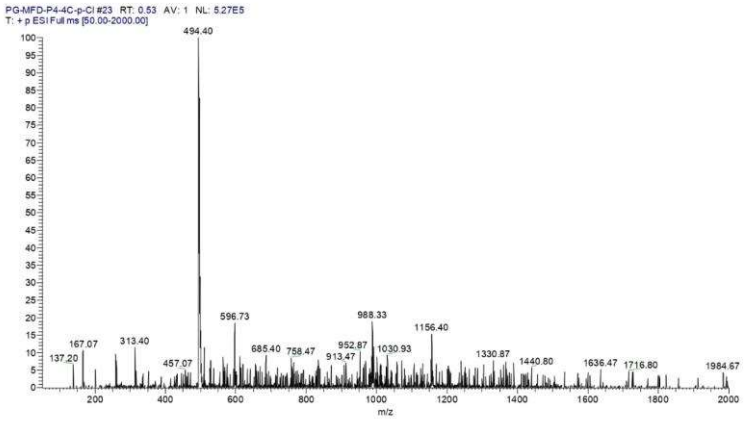


Figure S59. ESI-IT (+) spectrum of **2j**.

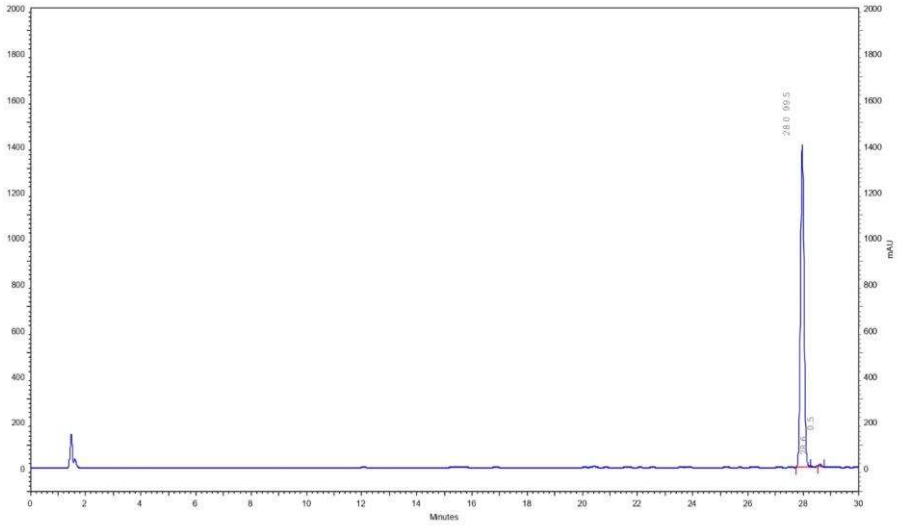


Figure S60. HPLC trace of **2j**.

Compound 2k

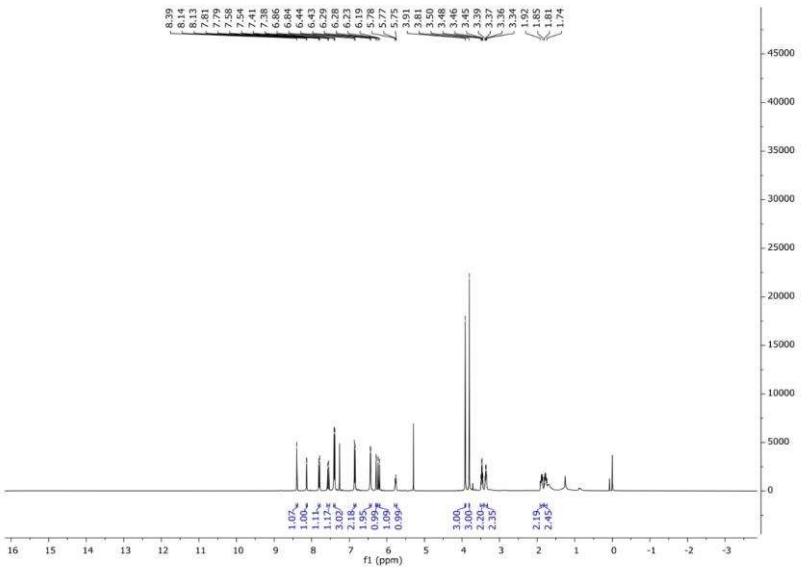


Figure S61. ^{1}H-RMN full spectrum (400 MHz, $CDCl_3$) of **2k**.

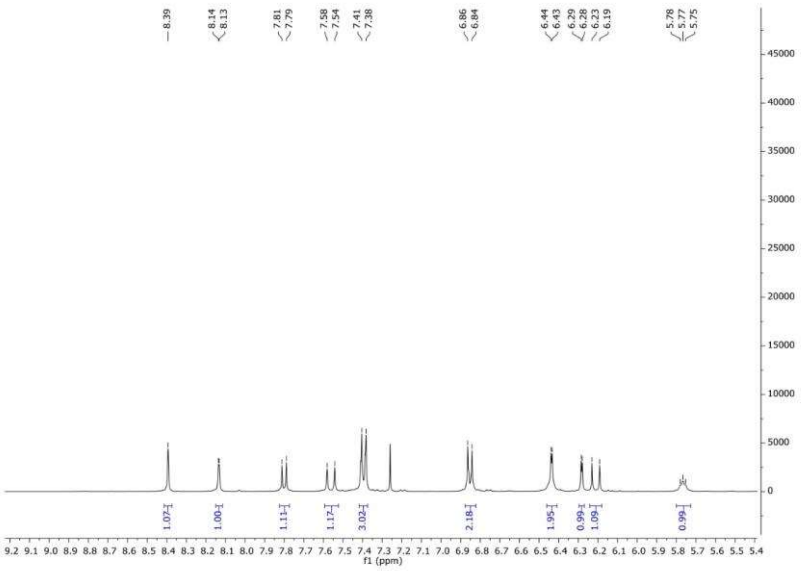


Figure S62. Aromatic region in the ^{1}H-RMN spectrum (400 MHz, $CDCl_3$) of **2k**.

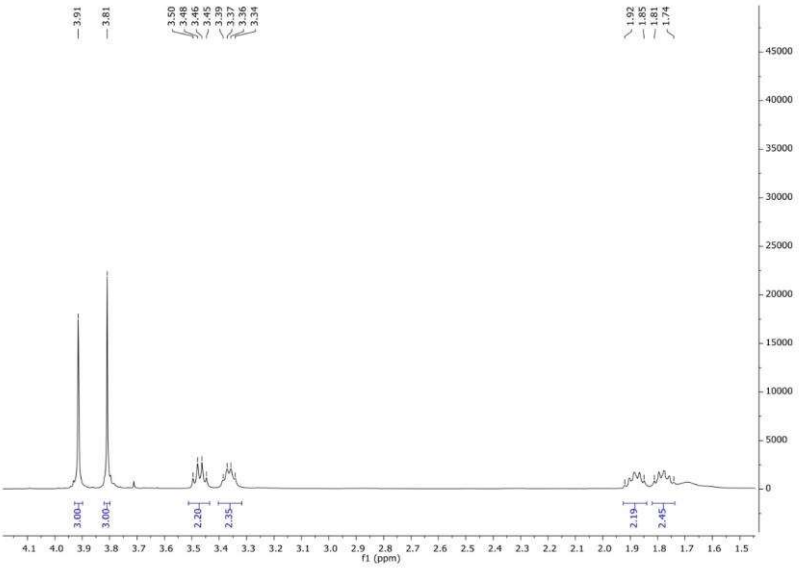


Figure S63. Aliphatic region in the ^{1}H-RMN spectrum (400 MHz, $CDCl_3$) of **2k**.

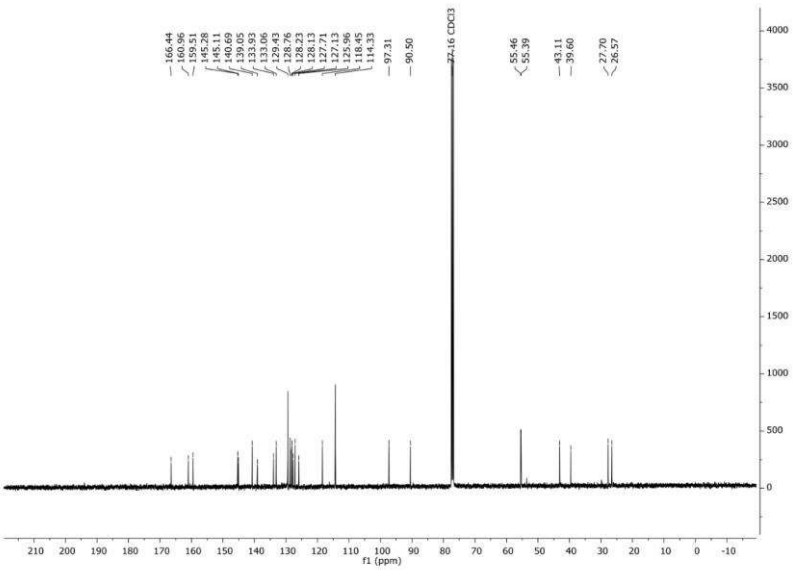


Figure S64. ^{13}C-RMN spectrum (100 MHz, $CDCl_3$) of **2k**.

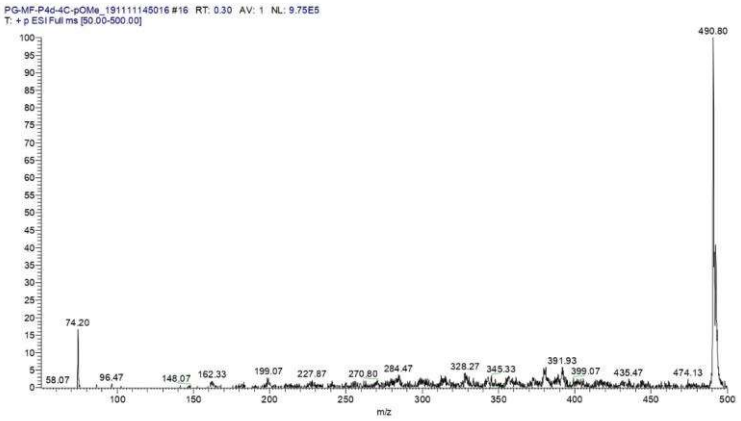


Figure S65. ESI-IT (+) spectrum of **2k**.

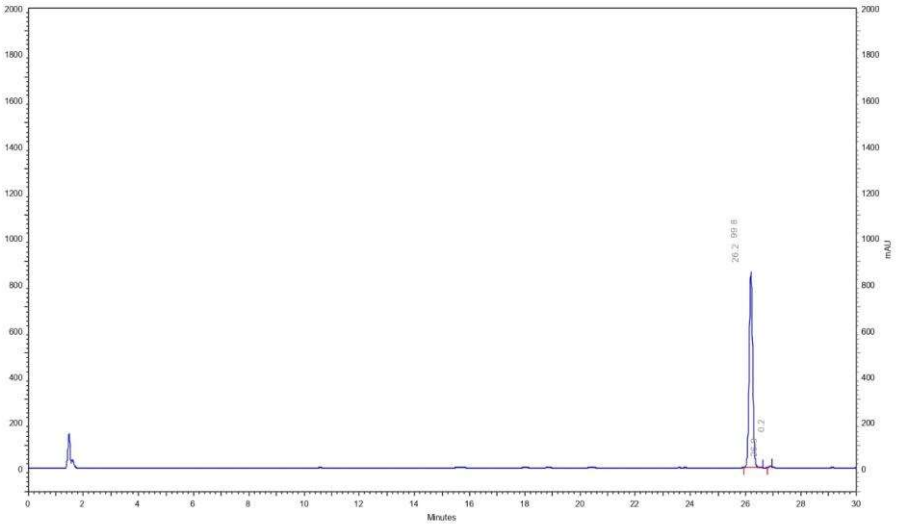


Figure S66. HPLC trace of **2k**.

Compound 2l

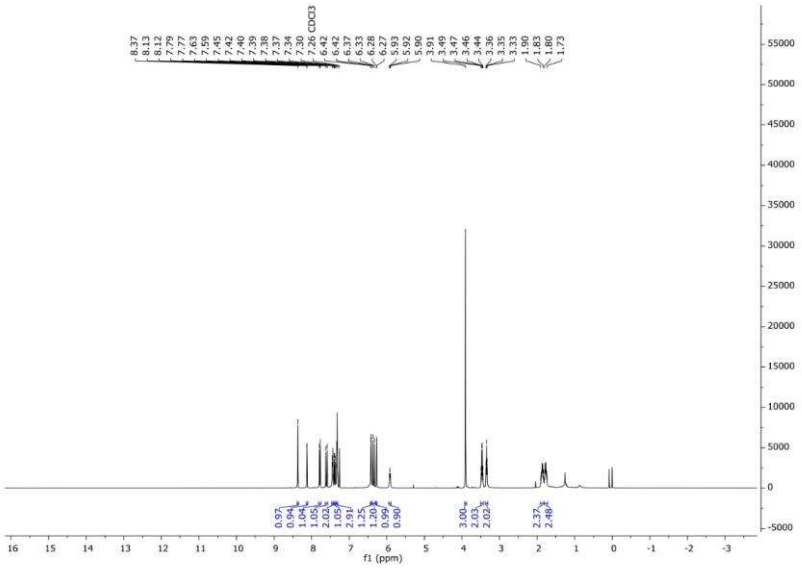


Figure S67. ^{1}H-RMN full spectrum (400 MHz, $CDCl_3$) of **2l**.

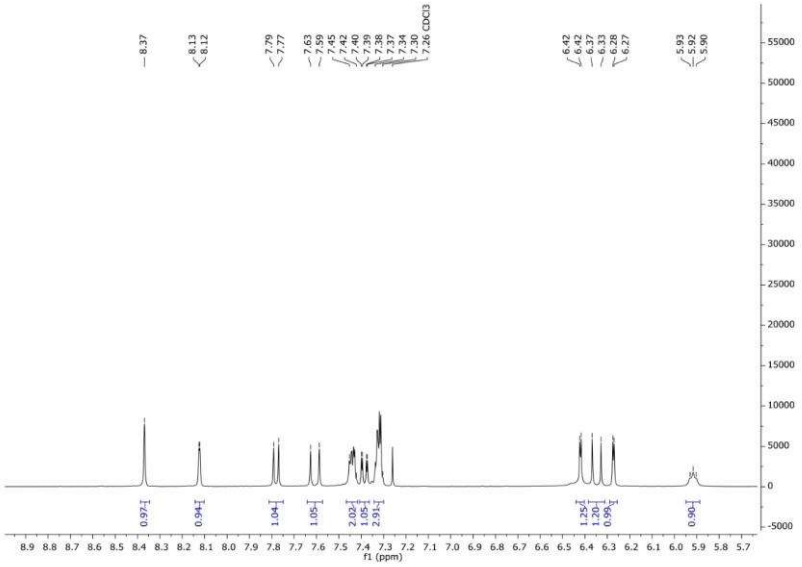


Figure S68. Aromatic region in the ^{1}H-RMN spectrum (400 MHz, $CDCl_3$) of **2l**.

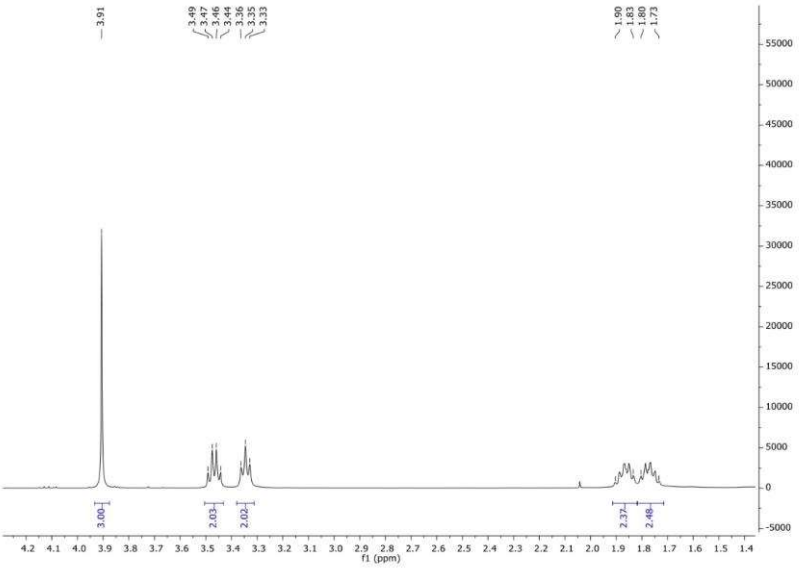


Figure S69. Aliphatic region in the ^{1}H-RMN spectrum (400 MHz, $CDCl_3$) of **2l**.

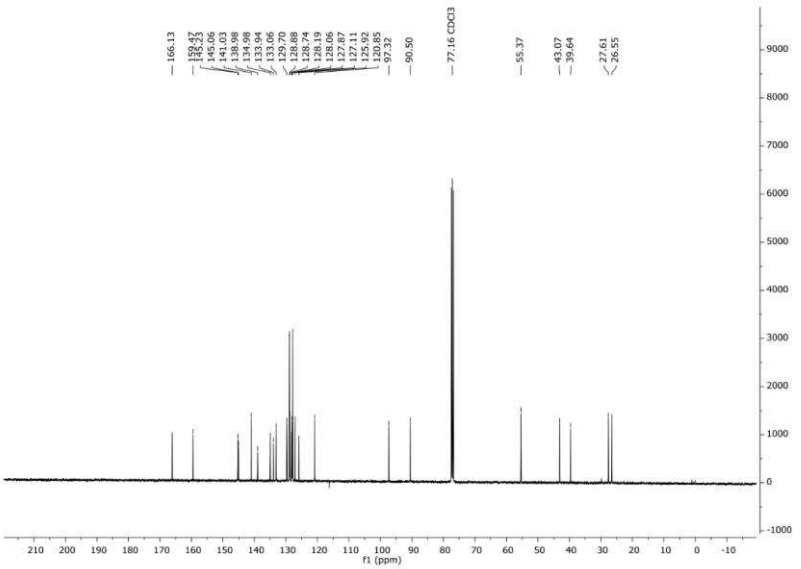


Figure S70. ^{13}C-RMN spectrum (100 MHz, $CDCl_3$) of **2l**.

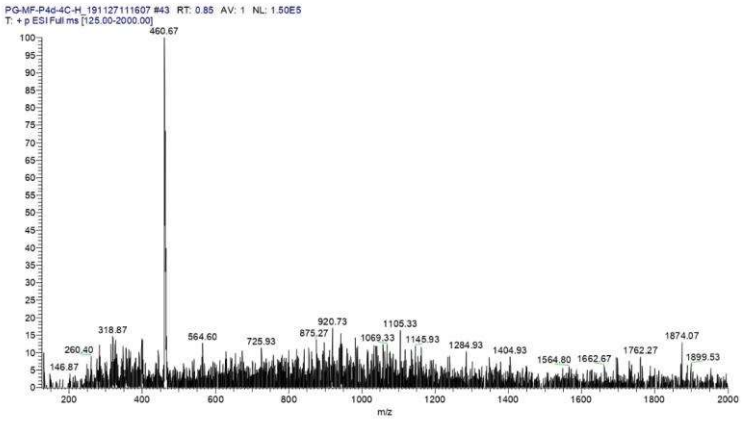


Figure S71. ESI-IT (+) spectrum of **2l**.

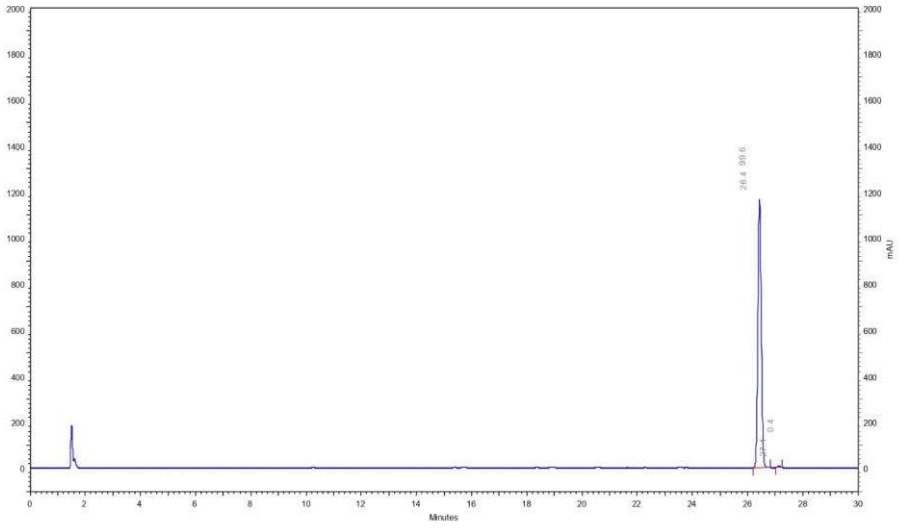
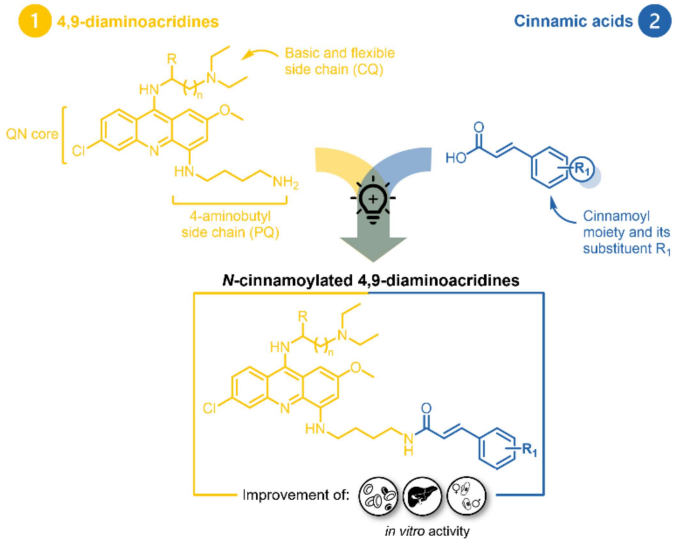


Figure S72. HPLC trace of **2l**.

Article IV

Disclosure of cinnamic acid/4,9-diaminoacridine conjugates as multi-stage antiplasmodial hits

Mélanie Fonte, Catarina Rôla, Sofia Santana, Yunuen Avalos-Padilla, Xavier Fernàndez-Busquets, Miguel Prudêncio, Paula Gomes, Cátia Teixeira



Bioorg. Med. Chem., **2024**, *104,* 117714 doi: 10.1016/j.bmc.2024.117714

Summary

The promising multi-stage activities observed for 4-(*N*-cinnamoylbutyl)aminoacridines, prompted us to apply the same covalent bitherapy approach to the other family of ACR-based hybrids, the 4,9-diaminoacridines, anticipating a similar outcome. Hence, this article is a sequel of the previous one, wherein 4,9-diamioacridines were coupled to different CAs. Eight new conjugates were produced that were also evaluated *in vitro* against three developmental stages of malaria parasites, and showed increased potency, particularly against blood stage forms, as compared to the reference drugs.

Declaration of authorship of published article IV: Disclosure of cinnamic acid/4,9-diaminoacridine conjugates as multi-stage antiplasmodial hits[4]

I, Mélanie Fonte, declare that the experimental design, laboratory work involving the synthesis, purification, and characterization of all compounds used in this study, and the data analysis and discussion were carried out by me, under the supervision of Prof. Paula Gomes, Dr. Cátia Teixeira and Dr. Miguel Prudêncio. Additionally, I participated in the *in vitro* evaluation of gametocytocidal activity of all the tested compounds under the guidance of Yunuen Avalos-Padilla and Xavier Fernàndez-Busquets. I was also responsible for the writing of the article's original draft that was next corrected and validated by all the co-authors.

We, Cátia Teixeira, Paula Gomes, and Miguel Prudêncio, as Mélanie Fonte's supervisors, hereby confirm that the information above is correct.

Mélanie Fonte

Mélanie Fonte

Paula Gomes | Cátia Teixeira | Miguel Prudêncio

[4] Copyright Elsevier 2024. Reproduced with permission.

Bioorg. Med. Chem. 104 (2024) 117714

Contents lists available at ScienceDirect

Bioorganic & Medicinal Chemistry

journal homepage: www.elsevier.com/locate/bmc

Disclosure of cinnamic acid/4,9-diaminoacridine conjugates as multi-stage antiplasmodial hits

Mélanie Fonte [a], Catarina Rôla [b], Sofia Santana [b], Yunuen Avalos-Padilla [c,d], Xavier Fernàndez-Busquets [c,d,e], Miguel Prudêncio [b], Paula Gomes [a,*], Cátia Teixeira [a,1]

[a] LAQV-REQUIMTE, Departamento de Química e Bioquímica, Faculdade de Ciências, Universidade do Porto, Portugal
[b] Instituto de Medicina Molecular, Faculdade de Medicina, Universidade de Lisboa, Portugal
[c] Nanomalaria Group, Institute for Bioengineering of Catalonia (IBEC), The Barcelona Institute of Science and Technology, Spain
[d] Barcelona Institute for Global Health (ISGlobal, Hospital Clínic-Universitat de Barcelona), Spain
[e] Nanoscience and Nanotechnology Institute (IN2UB), University of Barcelona, Spain

ARTICLE INFO

Keywords:
Antimalarial
Cinnamic acid
Covalent bitherapy
Diaminoacridine
Multi-target

ABSTRACT

4,9-diaminoacridines with reported antiplasmodial activity were coupled to different *trans*-cinnamic acids, delivering a new series of conjugates inspired by the covalent bitherapy concept. The new compounds were more potent than primaquine against hepatic stages of *Plasmodium berghei*, although this was accompanied by cytotoxic effects on Huh-7 hepatocytes. Relevantly, the conjugates displayed nanomolar activities against blood stage *P. falciparum* parasites, with no evidence of hemolytic effects below 100 μM. Moreover, the new compounds were at least 25-fold more potent than primaquine against *P. falciparum* gametocytes. Thus, the new antiplasmodial hits disclosed herein emerge as valuable templates for the development of multi-stage antiplasmodial drug candidates.

1. Introduction

Malaria is a life-threatening infectious disease caused by protozoan parasites of the genus *Plasmodium*. Six species of *Plasmodium* can infect humans, *Plasmodium falciparum* and *P. vivax* being the most prevalent in tropical and sub-tropical countries, where malaria represents a major health concern. While progress has been made in reducing malaria cases and deaths globally, complete eradication remains a complex and challenging goal.[1] The continued malaria burden is mainly due to (i) the complex parasite's life cycle, which undermines the prompt and successful development of effective drugs and vaccines, and (ii) the quick emergence and spread of drug-resistant strains of the parasite, compromising the efficacy of all the drugs developed so far.[1–3] Indeed, effective therapeutic options are becoming scarce since the current frontline artemisinin-based combination therapies (ACT) are facing a concerning decline in their effectiveness.[4–8] This highlights the urgent need to produce new potent antiplasmodial drugs that, ideally, overcome emerging drug resistance, whilst considering safety, especially in children and pregnant women, and improved dosing convenience.[9–11] Over the past decade, there has been significant attention directed towards multi-stage drugs, driven by their advantages in addressing complex diseases like malaria and issues related to drug resistance.[12–14] Since malaria mostly affects low-income populations, the challenge lies precisely in finding an affordable medicine that addresses all the desired characteristics. Most antimalarial drugs lack a clear and undisputed mechanism of action (MOA), which hampers the rational design of new drugs. Therefore, the development of antimalarials has been targeting the functionalization of existing pharmacophores, aiming at their re-

Abbreviations: ACT, Artemisinin-based combination therapies; ATP, adenosine triphosphate; CA, cinnamic acid; CQ, Chloroquine; DCM, dichloromethane; DIEA, *N,N*-diisopropylethylamine; DMSO, dimethyl sulfoxide; DNA, deoxyribonucleic acid; ESI-IT MS, electrospray ionization-ion trap mass spectrometry; HEPES, 4-(2-hydroxyethyl)-1-piperazine ethanesulfonic acid; HPLC-DAD, high-performance liquid chromatography with diode-array detection; IC_{50}, half-maximal inhibitory concentration; MOA, mechanism of action; n.d., not determined; NMR, nuclear magnetic resonance; *P.*, *Plasmodium*; PQ, Primaquine; QN, Quinacrine; RPMI, roswell Park Memorial Institute 1640 medium; RT, retention time; SAR, structure and activity relationship; SD, standard deviation; TBTU, O-(Benzotriazol-1-yl)-*N,N,N′,N′*-tetramethyluronium tetrafluoroborate; TLC, thin layer chromatography.

* Corresponding author.
E-mail address: pgomes@fc.up.pt (P. Gomes).
[1] Current affiliation: Gyros Protein Technologies Inc., Tucson, Arizona, USA.

https://doi.org/10.1016/j.bmc.2024.117714
Received 26 February 2024; Received in revised form 21 March 2024; Accepted 2 April 2024
Available online 3 April 2024
0968-0896/© 2024 The Authors. Published by Elsevier Ltd. This is an open access article under the CC BY-NC-ND license (http://creativecommons.org/licenses/by-nc-nd/4.0/).

introduction in the chemotherapy repository.[15–18] Thus, several research groups, including ours,[19–30] have been dedicated to the rescuing of traditional antimalarial drugs such as quinacrine (QN), primaquine (PQ), and chloroquine (CQ), whose use has been limited due to resistance and/or toxicity issues.[17,31,32] QN was the first effective synthetic antimalarial drug with blood-schizonticidal activity. However, due to its severe side effects, QN was soon overtaken by CQ, a low-cost medicine with higher efficiency, oral bioavailability, and safety. Yet, due to the rise and spread of CQ-resistant strains of *P. falciparum*, its use has been progressively abandoned.[33,34] While QN and CQ target blood-stage parasites, as do most of the available antimalarials, PQ is, alongside tafenoquine (TQ),[35] the only drug capable of eliminating (i) liver forms of *Plasmodium* species, including the dormant hypnozoites of *P. vivax* and *P. ovale* that may induce malaria relapses, and (ii) gametocytes, preventing transmission to the mosquito vector. Nevertheless, PQ exhibits high hemotoxicity and limited oral bioavailability, which restricts its clinical use.[36,37].

We recently developed a family of compounds where the pharmacophores of QN, CQ and PQ are merged into a single 4,9-diaminoacridine core (**1a-b**, Figure 1), as potential multi-stage antiplasmodials.[23,38] The best compounds of this family, **1a** and **1b**, retained the activities of the parent drugs, PQ and CQ, displaying substantial *in vitro* activity against both the blood and liver stages of malaria parasites.[23] Inspired by these encouraging results and by former findings in our group,[24–30,39,40] we have now conjugated **1a** and **1b** to *trans*-cinnamic acids (CAs), targeting new conjugates with improved multi-stage efficacy and safety, and less propensity to develop resistance. This conjugation strategy was inspired in the covalent bitherapy concept pioneered by Meunier, whose combination of two pharmacophores in one single chemical entity has been widely and successfully employed, including in the context of antimalarial drug development.[41,42] The choice of CAs as the ancillary bioactive moiety was based on their ability to cause, in *Plasmodium* parasites, (i) a decline in energy production (ATP) due to the inhibition of lactate transporters, and (ii) a change in mitochondrial respiration; in addition, CAs have been reported to reduce the translocation of amino acids and carbohydrates in *Plasmodium*-infected erythrocytes.[40,43–45] Moreover, due to their α,β-unsaturated carbonyl moiety, CAs may act as Michael acceptors inhibiting cysteine proteases, especially falcipain-2 and falcipain-3, which also have a crucial role in hemoglobin degradation, the blood stage parasite's primary food source.[44,46–48] Therefore, we have coupled **1a** and **1b** to four different CAs, selected on the basis of the electronic properties and positions of substituents in the CA's aromatic ring, and assessed the efficacy of the resulting conjugates (**2**, Figure 1) against the liver, blood, and gametocyte stages of *Plasmodium* parasites *in vitro*. Data obtained shows that the new conjugates have enhanced multi-stage activity, especially against blood stage parasite forms, compared to the parent 4,9-diaminoacridines.

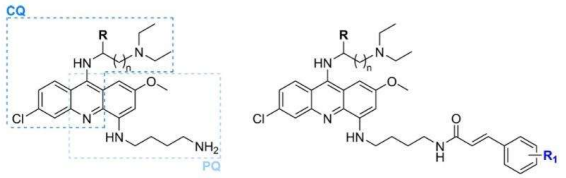


Figure 1. Dual-stage antiplasmodial 4,9-diaminoacridines (**1a,b**) previously developed by us,[23,38] and their cinnamic acid conjugates herein reported.

2. Results and discussion

2.1. Chemistry

The synthesis of target compounds **2a-h** was accomplished using the route outlined in Scheme 1**.** Detailed procedures and relevant spectroscopic data of the final compounds are provided in the Experimental Section, and the corresponding chromatographic and spectral traces are given in the Supporting Information (SI).

4,9-diaminoacridine derivatives **1a** and **1b** were first obtained by a seven-step synthetic route developed and optimized by us,[38,49] starting from methyl 2-amino-4-chlorobenzoate and 4-bromo-3-nitroanisole, as formerly described. Then, a classical *in situ* amide coupling method was used to couple **1a** and **1b** to a range of CAs, resulting in the synthesis of the target compounds **2a-h** (Scheme 1). For this purpose, the carboxylic acid group of each CA was initially activated in dichloromethane (DCM) for 1 h using *O*-(Benzotriazol-1-yl)-*N,N,N′,N′*-tetramethyluronium tetrafluoroborate (TBTU) and *N*-ethyl-*N,N*-diisopropylamine (DIEA) as a coupling agent and base, respectively. After the activation process, **1a** or **1b** was added to the mixture and the reaction proceeded at room temperature (r.t.) for approximately 4 h.

The target products were isolated by liquid chromatography on silica-gel columns in 94–98 % purity verified by high-performance liquid chromatography (HPLC). Structural analyses by electrospray ionization-ion trap mass spectrometry (ESI-IT MS), and by proton (^{1}H) and carbon-13 (^{13}C) nuclear magnetic resonance (NMR) validated the anticipated structures for all target compounds **2a-h**, which were achieved with moderate to good (24–82 %) overall yields.

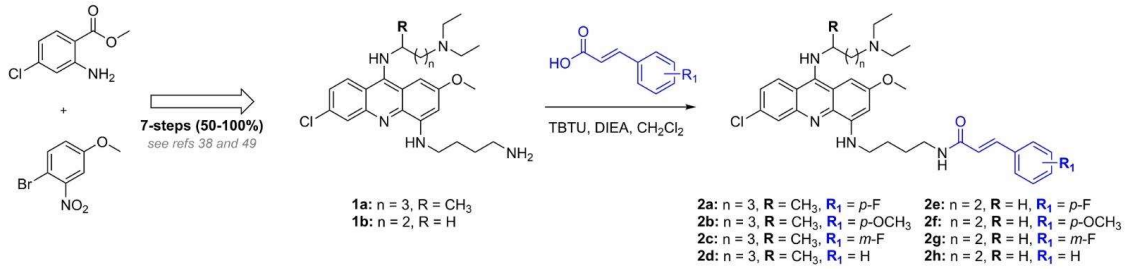
2.2. Biological assays

2.2.1. Blood stage activity

The efficacy of the compounds against blood-stage parasites of the *P. falciparum* 3D7 strain was assessed *in vitro* using flow cytometry, as described in the Experimental Section. The results obtained are summarized in Table 1 and show that all conjugates **2a-h** were active against the blood forms of *P. falciparum* (3D7 strain). Although none of the compounds presented a similar or better activity than that of CQ, all of them were much better than the parent drugs **1a** and **1b**, showing IC_{50} values in the nanomolar range. This result was not unexpected, as conjugates **2a-h** are analogues of QN, conserving a basic aminoalkyl chain linked to the C-9 of the acridine ring that is relevant to the accumulation of QN in the parasite's acidic digestive vacuole where it inhibits hemozoin formation. This process is vital for the parasite as a mechanism for the detoxification of the free heme group released upon hemoglobin digestion.[50–54] Additionally, these conjugates possess a CA moiety known to affect other vital processes in the asexual intra-erythrocytic stages of *Plasmodium*, as already highlighted in the Introduction. The relevance of the basic aminoalkyl substituent in the acridine's C-9 position on the blood stage activity is further supported by the fact that conjugates **2a-h** were also considerably more potent than similar CA conjugates of 4-aminoacridines previously reported by us (**3a–d**, Figure 2 and Table 1),[39] in which lack such substituent.

The IC_{50} values obtained for the new conjugates **2a–h** were dependent on (i) the substituent of the aryl ring in the cinnamoyl building block (R_1) and (ii) the length of the amino side chain on the C-9 of the acridine ring (R and n). In this regard, the following observations can be noted:

(a) a shorter side chain in the acridine's C-9 (n = 2, **2e–h**) improved activity independently of the substituent (R_1) in the aryl ring of the cinnamoyl moiety; this trend had already been observed for the parent 4,9-diaminoacridines, where **1b**, with the shorter side chain, displayed a lower IC_{50} value ($IC_{50} = 0.44 \pm 0.21$ μM) than **1a** ($IC_{50} = 0.68 \pm 0.24$ μM);



Scheme 1. Synthetic route to target compounds **2a-h**. 4,9-diaminoacridines **1a** and **1b** were first obtained in seven reaction steps starting from methyl 2-amino-4-chlorobenzoate and 4-bromo-3-nitroanisole, as previously described,[38,49] and next coupled to different CAs (highlighted in blue) under the following conditions: relevant CA (1.1 equiv), TBTU (1.1 equiv), DIEA (2 equiv) and DCM at r.t.

Table 1
In vitro activity of the new conjugates **2a-h**, their parent compounds (**1a,b**)[23] and reference drugs CQ and PQ against liver forms of *P. berghei*, as well as early gametocytes and ring stages of *P. falciparum* 3D7 strain. Data previously reported for similar CA conjugates of 4-aminoacridines (**3a-d**)[39] is also included, for comparison.

Compound	R	n	R_1	IC_{50} ± SD, μM		
				Blood stage[a]	Liver stage[b]	Gametocyte stage[c]
1a	CH_3	3	–	0.68 ± 0.24[d]	11.02 ± 0.44[d]	–
1b	H	2	–	0.44 ± 0.21[d]	n.d.[e]	–
2a	CH_3	3	*p*-F	0.178 ± 0.005	n.d.[e]	0.645 ± 0.045
2b	CH_3	3	*p*-OCH_3	0.3478 ± 0.0006	n.d.[e]	–
2c	CH_3	3	*m*-F	0.1528 ± 0.0003	n.d.[e]	–
2d	CH_3	3	H	0.164 ± 0.003	n.d.[e]	0.474 ± 0.032
2e	H	2	*p*-F	0.1637 ± 0.0002	n.d.[e]	–
2f	H	2	*p*-OCH_3	0.1605 ± 0.0001	n.d.[e]	~0.43
2 g	H	2	*m*-F	0.143 ± 0.057	n.d.[e]	0.461 ± 0.031
2 h	H	2	H	0.0802 ± 0.0001	n.d.[e]	–
3a	–	–	*p*-F	5.83 ± 1.02[f]	0.884 ± 0.046[f]	–
3b	–	–	*p*-OCH_3	10.30 ± 1.40[f]	1.182 ± 0.115[f]	0.52 ± 0.38[f]
3c	–	–	*m*-F	4.34 ± 0.96[f]	0.561 ± 0.179[f]	0.14 ± 0.43[f]
3d	–	–	H	>70[f]	0.496 ± 0.230[f]	6.66 ± 1.54[f]
CQ	–	–	–	0.006 ± 0.004	–	–
PQ	–	–	–	–	8.428 ± 3.384	17.66 ± 2.31

[a] blood-stage antiplasmodial activity was determined against the CQ-sensitive *P. falciparum* 3D7 strain, using CQ as reference drug.
[b] liver-stage antiplasmodial activity was determined against liver forms of *P. berghei*, using PQ as reference drug.
[c] gametocytocidal activity was determined in *P. falciparum* NF54-gexp02-Tom strain, using PQ as reference drug.
[d] values taken from ref [23].
[e] n.d., not determined (toxic to Huh-7 cells at 10 μM).
[f] Values taken from ref [39].

(b) in the conjugates with the longer side chain (n = 3, **2a-d**), the results suggest that an electron-withdrawing group R_1, such as *p*-F (**2a**, IC_{50} = 0.178 ± 0.005 μM) and *m*-F (**2c**, IC_{50} = 0.1528 ± 0.0003 μM) is preferable to the electro-donating one (**2b**, IC_{50} = 0.3478 ± 0.0006 μM);
(c) changing the position of the aryl substituent from *para* to *meta*, as in **2a** (R_1 = *p*-F; IC_{50} = 0.178 ± 0.005 μM) *versus* **2c** (R_1 = *m*-F; IC_{50} = 0.1528 ± 0.0003 μM) or in **2e** (R_1 = *p*-F; IC_{50} = 0.1637 ± 0.0002 μM) *versus* **2 g** (R_1 = *p*-F; IC_{50} = 0.143 ± 0.057 μM), slightly improves activity;
(d) interestingly, the presence of a substituent in the aryl ring of the cinnamoyl moiety was not advantageous for blood stage activity of conjugates with the shorter side chain (**2e-h**), since the most potent compound of this sub-series was **2 h** (R_1 = H, IC_{50} = 0.0802 ± 0.0001 μM).

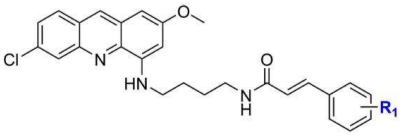


Figure 2. Cinnamic acid conjugates of 4-aminoacridines (**3a-d**) previously reported by us.[39]

Overall, conjugate **2 h** stood out for its higher activity against blood forms of *P. falciparum* (IC_{50} = 0.0802 ± 0.0001 μM), being approximately 5-fold more potent than its parent compound **1b** (IC_{50} = 0.44 ± 0.21 μM).

2.2.2. Hepatic stage activity

The effectiveness of conjugates **2a-h** against the hepatic stage of *P. berghei* parasites was assessed through a previously described bioluminescence-based method to quantify the *in vitro* parasite load of the human hepatoma (Huh-7) cell line.[55,56] Concomitantly, the cytotoxicity of the compounds towards this cell line was gauged by fluorescence-based assessment of cell confluency.

At the lowest concentration tested, 1 μM, the compounds did not effectively inhibit hepatic infection (Fig. 3). However, at 10 μM, all the compounds showed higher activity than PQ, the reference drug for this stage of infection. However, due to the high cytotoxicity displayed at this concentration, IC_{50} values were not determined and therefore no structure–activity relationships (SAR) could be inferred. Nevertheless, based on the impact that the introduction of the CA moiety had in conjugates **3a-d** and the lack of cytotoxicity of parent drugs **1a-b** at 10 μM (Fig. 3), we can hypothesize that the % of infection observed at this concentration for the new conjugates **2a-h** may be related to the incorporation of the CA moiety. However, further experiments are required to corroborate this hypothesis.

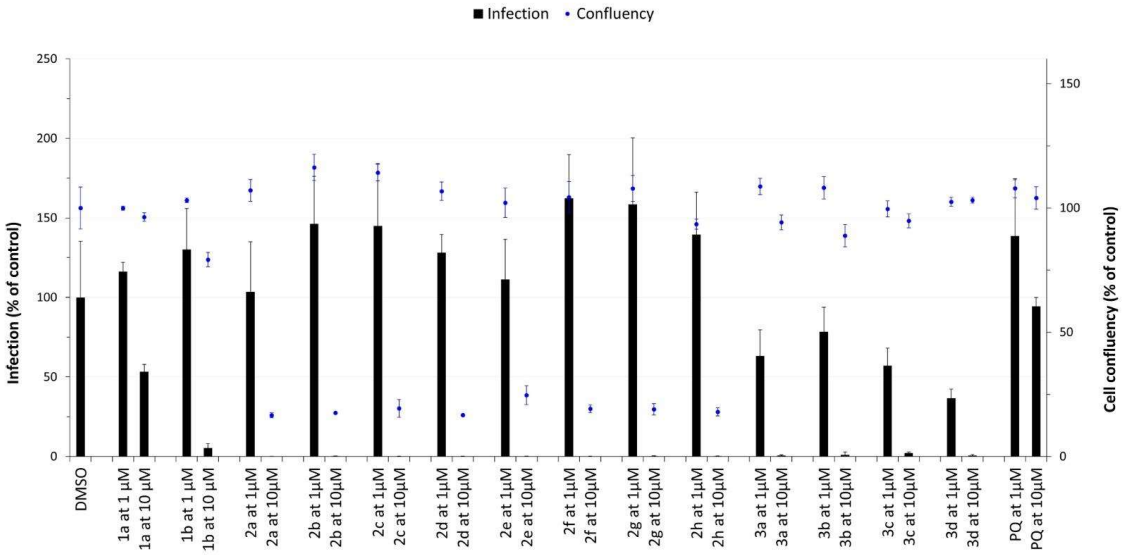


Figure 3. *In vitro* screening of the activity of conjugates **2a-h** and of their parent compounds **1a,b**[23] against liver forms of *P. berghei* (bars) and Huh-7 cells (dots) at 1 μM and 10 μM. Results previously obtained for CA conjugates of 4-aminoacridines **3a-d**[39] are included, for comparison. PQ was used as reference drug.

Relevantly, a comparison of the new CA conjugates of 4,9-diaminoacridines reported herein (**2a-h**) with their formerly disclosed analogues derived from 4-aminoacridines (**3a-d**),[39] shows that, while the presence of the aminoalkyl side chain in C-9 of the acridine ring has a clearly positive impact on blood stage activity (see previous section), the opposite happens in regard to toxicity to Huh-7 hepatocytes (Figure 3), as conjugates **3a-d** were not toxic to this cell line at 10 μM.[39].

Of note, owing to their ability to interact with DNA, among other MOA, many acridine-based compounds are known to have selective antiproliferative activity on tumor cell lines.[57–60] Thus, conjugates **2a-h** might be nontoxic or less toxic to primary (non-tumor) cell lines than to tumor ones as Huh-7 hepatocytes. A preliminary assessment of the cytotoxicity of these compounds to different tumor cell lines and one primary cell line, showed them to have a selective effect against cancer cells (undisclosed data). In other words, one cannot rule out the possibility that conjugates **2a-h** could have a selective action against hepatic forms of *Plasmodium* inside the liver cells.

2.2.3. Gametocytocidal activity

The gametocytocidal activity of compounds **2a-h** was assessed *in vitro* against early gametocytes of the *P. falciparum* NF54-*gexp02-Tom* strain, which contains a fluorescent protein that is under the control of a gametocyte-specific promoter leading to accurate and easy-to-perform quantification of gametocytes.[61] While a dose-dependent response was observed in all cases, reliable IC_{50} values could only be determined for compounds **2a**, **2d**, **2f,** and **2 g**. Remarkably, the IC_{50} values obtained for conjugates **2** (0.645 μM > IC_{50} > 0.461 μM) were at least 25-fold lower than that of the reference drug in this stage, PQ (IC_{50} = 17.66 ± 2.31 μM). Indeed, compounds that can efficiently eliminate gametocytes remain scarce, while they play a crucial role in preventing host-to-vector transmission.[62].

3. Concluding remarks

We disclose a new family of compounds (**2a-h**) as promising multi-stage antiplasmodial leads. These compounds were obtained by coupling different *trans*-cinnamic acids to 4,9-diaminoacridines previously identified as dual-stage antiplasmodial hits. Considering our earlier findings on the enhancement of the antiplasmodial activity of 4-aminoacridines through their coupling to cinnamic acids,[39] we hypothesized that using the same strategy on 4,9-aminoacridines **1a,b** could have a similar outcome. Overall, the data herein reported support the validity of this working hypothesis, since the conjugates **2a-h** exhibit enhanced multi-stage activity *in vitro*, especially against the erythrocytic and gametocyte stages, compared to the parent compounds **1a** and **1b**. While conjugate **2 h** (n = 2, R = H, R_1 = H) displayed the highest activity against blood stage parasites, conjugate **2 g** (n = 2, R = H, R_1 = *m*-F), which only differs from the former in the substituent R_1 of the aryl ring, showed the best combined activity against the blood and gametocyte stages of *P. falciparum*.

The activity against hepatic forms of *P. berghei* was also noteworthy, despite the high toxicity observed towards Huh-7 cells, which might not be observed in the case of primary (non-tumor) cell lines. This hypothesis is under investigation and preliminary undisclosed data support a selective action of conjugates **2a-h** against tumor cells.

The MOA(s) behind the multi-stage antiplasmodial activity of conjugates **2a-h** remain unknown. The significant differences in blood- and liver-stage activities between the conjugates herein reported (**2a-h**) and their earlier analogues derived from 4-aminoacridines (**3a-d**) highlight the influence of the aminoalkyl chain linked to the C-9 position of the acridine ring, but cannot be interpreted as indicative of similar or dissimilar MOA(s). The positive influence of this chain on blood stage activity could be related to an improved compound accumulation inside the acidic digestive vacuole of the parasite, followed by inhibition of hemozoin formation. However, other alternative or additional MOA(s) can be considered, such as the ability of cinnamic acids to (i) hinder the production of ATP, (ii) reduce the translocation of amino acids and carbohydrates to parasitized erythrocytes, (iii) upset the parasite's mitochondrial respiration, and (iv) inhibit cysteine proteases in intra-erythrocytic parasites.[40,43–48] Additionally, the planar acridine ring present in QN analogues like **2a-h**, is reported as capable of intercalating with DNA, which may account for the bioactivity of these conjugates.[57–60] Yet, these are new molecular entities that may owe their multi-stage antiplasmodial action to other mechanisms beyond those reported for structurally related compounds. Ongoing studies (undisclosed data) will hopefully shed some light into this matter.

In conclusion, the results herein reported highlight compounds **2a-h** as new multi-stage antiplasmodial hits. Given the importance of halting

the infection's progression within the human host from its very beginning in the liver and through its symptomatic stage in red blood cells to the gametocyte stage underlying disease propagation, these findings are a significant step forward towards the development of new valuable antiplasmodial candidates.

4. Experimental section

4.1. Chemistry

4.1.1. Synthesis of compounds 1a-b

4-(4-aminobutyl)amino-6-chloro-9-[*N*-(4-(diethylamino)pent-2-yl] amino-2-methoxy-acridine (**1a**) and 4-(4-aminobutyl)amino-6-chloro-9-[*N*-(3-(diethylamino)prop-1-yl]amino-2-methoxy-acridine (**1b**) were prepared by a seven-step route as previously described and optimized by us, and their structural analyses (see SI) agreed with formerly reported data.[38,49].

4.1.2. Synthesis of compounds 2a-h

The *trans*-cinnamic acid of interest (1 equiv) was dissolved in DCM and then TBTU (1.1 equiv) and DIEA (2 equiv) were added. Following an activation period of about 1 h, compound **1a** or **1b** (1 equiv) in DCM was added to the mixture and the reaction proceeded under stirring at r.t. until no additional advancement could be detected by thin-layer chromatography (TLC) (1–3 h). Next, the mixture underwent successive washes with saturated aq. $NaHCO_3$ (3 × 50 mL) and saturated aq. NaCl (3 × 50 mL), and the organic layers were pooled, dried over anhydrous Na_2SO_4, and filtered by gravity. The resulting filtrate was concentrated to dryness under reduced pressure. The crude product thus obtained was subjected to purification by column chromatography on silica gel using an elution mixture of DCM/CH_3OH 8:1 (v/v). This process yielded compounds **2a-h** with purity degrees ranging from 94 % to 99 % (HPLC) and correct structural data (NMR and ESI-IT-MS), as given in detail below. Chromatographic and spectral traces are provided in the SI.

4.1.2.1. Compound 2a. Orange oil, η = 42 % (0.0093 g); **^{1}H NMR** (400 MHz, $CDCl_3$) δ 8.11 (bs, 1H), 8.00 (d, *J* = 9.2 Hz, 1H), 7.55 (d, *J* = 15.6 Hz, 1H), 7.48 – 7.39 (m, 2H), 7.30 – 7.26 (m, 2H), 7.05 – 6.96 (m, 2H), 6.64 – 6.53 (m, 2H), 6.41 (d, *J* = 15.6 Hz, 1H), 6.25 (d, *J* = 2.2 Hz, 1H), 4.08 – 3.99 (m, 1H), 3.94 (s, 3H), 3.46 (q, *J* = 6.4 Hz, 2H), 3.34 – 3.23 (m, 2H), 2.92 (q, *J* = 7.9, *J* = 7.3 Hz, 4H), 2.87 – 2.80 (m, 2H), 1.94 – 1.73 (m, 9H), 1.32 (d, *J* = 6.3 Hz, 3H), 1.19 (t, *J* = 7.3 Hz, 6H); **^{13}C NMR** (101 MHz, $CDCl_3$) δ 166.22, 164.78, 162.30, 158.59, 139.46, 131.37, 129.65, 125.10, 124.77, 120.97, 116.04, 115.82, 55.74, 55.43, 52.04, 46.87, 43.43, 39.67, 35.44, 29.83, 27.57, 26.37, 22.82, 22.35, 21.25, 14.24, 8.67, 1.15; **$^m/_z$ (ESI-IT MS, +)** 634.87 (M + H^+); M^+ ($C_{36}H_{45}ClFN_5O_2$) requires 633.32; **HPLC-DAD:** RT, 15.550 min; purity degree (peak relative area), 97.9 %.

4.1.2.2. Compound 2b. Orange oil, η = 24 % (0.0066 g); **^{1}H NMR** (400 MHz, $CDCl_3$) δ 8.18 (bs, 1H), 8.02 (d, *J* = 9.2 Hz, 1H), 7.79 – 7.72 (m, 1H), 7.64 – 7.57 (m, 1H), 7.55 (d, *J* = 15.5 Hz, 1H), 7.45 – 7.37 (m, 2H), 7.25 – 7.22 (m, 1H), 6.87 – 6.81 (m, 2H), 6.70 (s, 1H), 6.56 (bs, 1H), 6.40 (d, *J* = 15.6 Hz, 1H), 6.27 (d, *J* = 2.2 Hz, 1H), 4.18 – 4.08 (m, 1H), 3.90 (s, 3H), 3.81 (s, 3H), 3.47 (q, *J* = 6.3 Hz, 2H), 3.28 (t, *J* = 6.4 Hz, 2H), 2.96 (q, *J* = 7.5, 6.6 Hz, 4H), 2.88 (t, *J* = 7.3 Hz, 2H), 2.05 – 1.60 (m, 8H), 1.37 (d, *J* = 6.3 Hz, 3H), 1.20 (t, *J* = 7.3 Hz, 6H); **^{13}C NMR** (101 MHz, $CDCl_3$) 166.87, 160.90, 158.54, 140.36, 129.49, 127.95, 127.84, 125.14, 125.05, 125.01, 118.86, 114.33, 55.78, 55.54, 55.48, 52.08, 46.83, 43.72, 39.64, 35.27, 27.68, 26.11, 22.27, 21.30, 8.54, 1.16; **$^m/_z$ (ESI-IT MS, +)** 646.67 (M + H^+); M^+ ($C_{37}H_{48}ClN_5O_3$) requires 645.34; **HPLC-DAD:** RT, 15.590 min; purity degree (peak relative area), 94.3 %.

4.1.2.3. Compound 2c. Orange oil, η = 44 % (0.0122 g); **^{1}H NMR** (400 MHz, $CDCl_3$) δ 8.09 (bs, 1H), 7.99 (d, *J* = 9.2 Hz, 1H), 7.54 (d, *J* = 15.7 Hz, 1H), 7.34 – 7.10 (m, 6H), 7.04 – 6.95 (m, 1H), 6.60 – 6.52 (m, 2H), 6.47 (d, *J* = 15.6 Hz, 1H), 6.24 (d, *J* = 2.2 Hz, 1H), 4.10 – 3.98 (m, 1H), 3.93 (s, 3H), 3.47 (q, *J* = 6.4 Hz, 2H), 3.35 – 3.25 (m, 2H), 2.93 (q, *J* = 7.5 Hz, 4H), 2.84 (t, *J* = 7.5 Hz, 2H), 1.95 – 1.57 (m, 8H), 1.32 (d, *J* = 6.4 Hz, 3H), 1.20 (t, *J* = 7.3 Hz, 6H); **^{13}C NMR** (101 MHz, $CDCl_3$) δ 165.93, 164.32, 161.88, 158.58, 139.40, 139.37, 137.51, 137.43, 130.46, 130.38, 125.13, 124.72, 124.07, 124.05, 122.61, 116.53, 116.32, 114.11, 113.89, 55.69, 55.39, 52.08, 46.89, 43.38, 39.72, 35.49, 29.83, 27.51, 26.39, 22.35, 21.26, 8.67, 1.15; **$^m/_z$ (ESI-IT MS, +)** 634.40 (M + H^+); M^+ ($C_{36}H_{45}ClN_5O_2$) requires 633.32; **HPLC-DAD:** RT, 15.610 min; purity degree (peak relative area), 97.0 %.

4.1.2.4. Compound 2d. Orange oil, η = 39 % (0.0079 g); **^{1}H NMR** (400 MHz, $CDCl_3$) δ 8.07 (bs, 1H), 7.99 (d, *J* = 9.2 Hz, 1H), 7.59 (d, *J* = 15.6 Hz, 1H), 7.50 – 7.43 (m, 2H), 7.35 – 7.27 (m, 5H), 6.59 – 6.50 (m, 2H), 6.47 (d, *J* = 15.6 Hz, 1H), 6.36 (bs, 1H), 6.24 (d, *J* = 2.3 Hz, 1H), 4.07 – 3.98 (m, 1H), 3.93 (s, 3H), 3.46 (q, *J* = 6.5 Hz, 2H), 3.34 – 3.24 (m, 2H), 2.91 (q, *J* = 7.3 Hz, 4H), 2.83 (t, *J* = 7.5 Hz, 2H), 1.91 – 1.57 (m, 8H), 1.30 (d, *J* = 6.4 Hz, 3H), 1.18 (t, *J* = 7.3 Hz, 6H); **^{13}C NMR** (101 MHz, $CDCl_3$) δ 166.35, 158.59, 144.95, 140.82, 135.07, 129.67, 128.90, 127.93, 125.11, 124.73, 121.13, 86.63, 55.69, 55.40, 52.06, 46.88, 43.39, 39.67, 35.44, 29.83, 27.66, 26.37, 22.82, 22.32, 21.26, 14.24, 8.70; **$^m/_z$ (ESI-IT MS, +)** 616.41 (M + H^+); M^+ ($C_{36}H_{46}ClN_5O_2$) requires 615.33; **HPLC-DAD:** RT, 15.467 min; purity degree (peak relative area), 98.7 %.

4.1.2.5. Compound 2e. Orange oil, η = 43 % (0.0087 g); **^{1}H NMR** (400 MHz, $CDCl_3$) δ 8.25 (bs, 1H), 8.00 (d, *J* = 9.3 Hz, 1H), 7.56 (d, *J* = 15.7 Hz, 1H), 7.51 – 7.44 (m, 2H), 7.15 (dd, *J* = 9.3, 2.1 Hz, 1H), 7.04 – 6.97 (m, 3H), 6.70 (Bs, 1H), 6.64 (d, *J* = 2.3 Hz, 1H), 6.58 (d, *J* = 15.7 Hz, 1H), 6.28 (d, *J* = 2.1 Hz, 1H), 4.06 – 3.98 (m, 2H), 3.91 (s, 3H), 3.49 (q, *J* = 6.0 Hz, 2H), 3.31 – 3.21 (m, 2H), 2.95 – 2.86 (m, 6H), 2.14 – 1.80 (m, 6H), 1.20 (t, *J* = 7.2 Hz, 6H); **^{13}C NMR** (101 MHz, $CDCl_3$) δ 166.53, 164.72, 162.24, 158.04, 139.06, 131.54, 129.70, 125.60, 124.15, 121.37, 115.97, 115.76, 109.39, 55.85, 51.05, 47.08, 43.98, 39.73, 29.84, 27.37, 26.07, 25.65, 14.25, 9.79, 1.15; **$^m/_z$ (ESI-IT MS, +)** 606.93 (M + H^+); M^+ ($C_{34}H_{41}ClFN_5O_2$) requires 605.29; **HPLC-DAD:** RT, 14.910 min; purity degree (peak relative area), 94.4 %.

4.1.2.6. Compound 2f. Orange oil, η = 66 % (0.0105 g); **^{1}H NMR** (400 MHz, $CDCl_3$) δ 8.20 (bs, 1H), 8.00 (d, *J* = 9.3 Hz, 1H), 7.55 (d, *J* = 15.6 Hz, 1H), 7.47 – 7.41 (m, 2H), 7.13 (dd, *J* = 9.3, 2.1 Hz, 1H), 6.87 – 6.81 (m, 2H), 6.75 – 6.66 (m, 2H), 6.48 (d, *J* = 15.6 Hz, 1H), 6.25 (d, *J* = 2.2 Hz, 1H), 4.01 (t, *J* = 5.8 Hz, 2H), 3.90 (s, 3H), 3.80 (s, 3H), 3.48 (q, *J* = 6.1 Hz, 2H), 3.30 – 3.18 (m, 2H), 2.99 – 2.90 (m, 6H), 2.20 – 1.76 (m, 6H), 1.21 (t, *J* = 7.2 Hz, 6H); **^{13}C NMR** (101 MHz, $CDCl_3$) δ 166.96, 160.82, 158.13, 140.07, 129.50, 127.98, 124.22, 119.13, 114.30, 55.89, 55.46, 46.90, 43.95, 39.67, 29.84, 27.53, 26.05, 25.59, 9.45; **$^m/_z$ (ESI-IT MS, +)** 618.60 (M + H^+); M^+ ($C_{35}H_{44}ClN_5O_3$) requires 617.31; **HPLC-DAD:** RT, 14.950 min; purity degree (peak relative area), 97.6 %.

4.1.2.7. Compound 2 g. Orange oil, η = 82 % (0.0132 g); **^{1}H NMR** (400 MHz, $CDCl_3$) δ 8.25 (bs, 1H), 7.99 (d, *J* = 9.3 Hz, 1H), 7.55 (d, *J* = 15.7 Hz, 1H), 7.34 – 7.07 (m, 4H), 7.07 – 6.93 (m, 1H), 6.79 – 6.58 (m, 3H), 6.28 (d, *J* = 2.2 Hz, 1H), 4.02 (t, *J* = 5.6 Hz, 2H), 3.90 (s, 3H), 3.49 (q, *J* = 6.0 Hz, 2H), 3.34 – 3.18 (m, 2H), 3.00 – 2.86 (m, 6H), 2.17 – 1.80 (m, 6H), 1.20 (t, *J* = 7.2 Hz, 6H); **^{13}C NMR** (101 MHz, $CDCl_3$) δ 166.21, 164.33, 161.89, 158.08, 139.00, 137.66, 130.38, 130.30, 125.58, 124.21, 123.99, 123.02, 116.35, 116.13, 114.28, 114.07, 55.84, 47.00, 43.96, 39.76, 29.85, 27.27, 26.08, 25.62, 9.64; **$^m/_z$ (ESI-IT MS, +)** 606.47 (M + H^+); M^+ ($C_{34}H_{41}ClFN_5O_2$) requires 605.29; **HPLC-DAD:** RT, 15.040 min; purity degree (peak relative area), 97.0 %.

4.1.2.8. Compound 2 h. Orange oil, η = 33 % (0.0063 g); **^{1}H NMR** (400

MHz, $CDCl_3$) δ 8.26 (bs, 1H), 8.00 (d, $J = 9.3$ Hz, 1H), 7.61 (d, $J = 15.7$ Hz, 1H), 7.54 – 7.45 (m, 2H), 7.37 – 7.27 (m, 3H), 7.15 (dd, $J = 9.3$, 2.1 Hz, 1H), 6.81 – 6.55 (m, 3H), 6.27 (d, $J = 2.2$ Hz, 1H), 4.05 – 3.99 (m, 2H), 3.92 (s, 3H), 3.50 (q, $J = 6.1$ Hz, 2H), 3.29 – 3.24 (m, 2H), 2.94 – 2.85 (m, 6H), 2.15 – 1.81 (m, 6H), 1.20 (t, $J = 7.2$ Hz, 6H); **^{13}C NMR** (101 MHz, $CDCl_3$) δ 166.62, 158.05, 140.41, 135.29, 129.50, 128.85, 127.99, 125.54, 124.14, 121.53, 55.89, 47.01, 43.93, 39.74, 29.84, 27.40, 26.09, 25.66, 9.73, 1.15; **$^{m}/_{z}$ (ESI-IT MS)** 588.45 ($M + H^+$); M^+ ($C_{34}H_{42}ClN_5O_2$) requires 587.30; **HPLC-DAD:** RT, 14.760 min; purity degree (peak relative area), 94.4 %.

4.2. In vitro assays

4.2.1. Blood stage activity

Asexual stages of the *P. falciparum* 3D7 strain were grown in group B human erythrocytes at 3 % hematocrit using Roswell Park Memorial Institute 1640 medium (RPMI) supplemented with 0.5 % (w/v) Albumax II (Life Technologies, New Zealand) and 2 mM L-glutamine. During the full experiment, parasites were maintained in standard culturing conditions (37 °C, 5 % O_2, 5 % CO_2, and 90 % N_2). The parasites were first synchronized in the ring stage with a 5 % sorbitol lysis as described in ref.[63] Then, the newly established parasite culture (0.75 % parasitemia) was transferred to 96-well plates and incubated with growing concentrations of the different compounds (0.0051–100 μM). As control, parasites were left untreated. After 48 h of incubation, cultures were diluted to ca. 1–10 × 10^6 cells/mL and incubated with Syto11 to stain the nuclei. Parasitemia was measured by flow cytometry using a LSRFortessa flow cytometer (BD Biosciences, USA) equipped with the 4 lasers, 20 parameters standard configuration. The single-cell population was selected on a forward-side scattergram. Syto 11 fluorescence signal was detected by exciting samples at 488 nm and collecting the emission with a 530/30-nm bandpass filter. Growth inhibition was calculated by referencing the growth rates of a chloroquine-treated culture (100 % inhibition) and of an untreated culture (0 % inhibition). The obtained data were subjected to sigmoidal fitting using the GraphPad Prism 8.4.2 software, allowing the determination of the compounds concentrations required to reduce *P. falciparum* viability by 50 % (IC_{50}).

4.2.2. Hepatic stage activity

The *in vitro* inhibition of hepatic infection was assessed by measuring the luminescence intensity in lysates of Huh-7 cells infected with a firefly luciferase-expressing *P. berghei* line, *PbGFP*-Luccon, as previously described.[55,56] Briefly, Huh-7 cells were cultured in RPMI supplemented with 10 % v/v fetal calf serum, 1 % v/v penicillin/streptomycin, 1 % v/v nonessential amino acids, 1 % v/v glutamine, and 10 mM 4-(2-hydroxyethyl)-1-piperazine ethanesulfonic acid (HEPES), pH 7, and maintained at 37 °C with 5 % CO_2. Huh-7 cells were seeded in 96-well plates on the day before drug treatment and infection. About 1 h prior to infection with sporozoites freshly obtained by disruption of salivary glands of infected female *Anopheles stephensi* mosquitoes, the culture medium in the wells was replaced by infection medium (culture medium supplemented with 50 μg/mL gentamicin and 0.8 μg/mL amphotericin B) containing the suitable concentration of each compound. In control wells, the cell culture medium was replaced by a medium containing the same percentage of dimethyl sulfoxide (DMSO) used in compound solutions (0.01 %), which is not cytotoxic. Following a 48-h infection period, the compounds' effect on the viability of Huh-7 cells was assessed by the AlamarBlue assay (Invitrogen, UK) using the manufacturer's protocol, and infection was measured by a bioluminescence assay (Biotium, USA), also according to the manufacturer's instructions. Nonlinear regression analysis was employed to fit the normalized results of the dose–response curves, and IC_{50} values were determined using GraphPad Prism 8.4.2. software. From the extrapolation of cell confluency data, the cytotoxicity of tested compounds was assessed.

4.2.3. Gametocytocidal activity

P. falciparum parasites of the high-gametocyte productive NF54-gexp02-Tom line (kindly supplied by Prof. Alfred Cortés) were utilized. This line features a genome-integrated tandem Tomato (tdTomato) fluorescent marker gene controlled by an early gametocyte promoter (gexp02).[61] The parasites were cultured in group B human erythrocytes at 3 % hematocrit using RPMI-based standard medium supplemented with 2 mM choline chloride, and incubated at 37 °C under hypoxic conditions (5 % O_2, 5 % CO_2, and 90 % N_2 at 37 ∘C). To induce sexual conversion, choline was removed from the medium, accompanied by synchronization through sorbitol lysis, and addition of 10 % Human serum. Subsequently, the induced cultures were then maintained without choline until the end of the experiment. The impact on gametocyte development was evaluated in three independent replicas by adding growing concentrations (0.0051–100 μM) of each compound to the culture. The appearance of stage V gametocytes was daily monitored by light microscopy, and approximately fifteen days after choline removal, nearly 80 % of gametocytes reached stages IV and V (mature forms). After this time, Giemsa-stained blood smears were prepared and at least 10,000 cells were manually counted for each condition. A positive control treated with the IC_{90} of PQ and a negative control culture without drugs were also included in the experiment. Growth inhibition was calculated as the total parasitemia relative to control cultures and expressed as a percentage. The data were then subjected to sigmoidal fitting to determine the IC_{50} values of compounds **2a-h**, using the GraphPad Prism 8.4.2. software.

Funding

This work received financial support from PT national funds (FCT/MCTES, Fundação para a Ciência e Tecnologia and Ministério da Ciência, Tecnologia e Ensino Superior) through project CIRCNA/BRB/0281/2019.

CRediT authorship contribution statement

Mélanie Fonte: Writing – original draft, Validation, Methodology, Investigation, Formal analysis, Data curation. **Catarina Rôla:** Methodology, Investigation, Data curation. **Sofia Santana:** Writing – original draft, Validation, Methodology, Investigation, Data curation. **Yunuen Avalos-Padilla:** Validation, Methodology, Investigation, Formal analysis, Data curation, Writing – original draft. **Xavier Fernàndez-Busquets:** Conceptualization, Formal analysis, Funding acquisition, Supervision, Validation, Writing – review & editing. **Miguel Prudêncio:** Writing – review & editing, Validation, Supervision, Funding acquisition, Formal analysis. **Paula Gomes:** . **Cátia Teixeira:** Writing – review & editing, Validation, Supervision, Investigation, Formal analysis, Conceptualization.

Declaration of competing interest

The authors declare that they have no known competing financial interests or personal relationships that could have appeared to influence the work reported in this paper.

Data availability

Data will be made available on request.

Acknowledgments

The authors thank FCT/MCTES for supporting Research Units LAQV-REQUIMTE (LA/P/0008/2020 DOI 10.54499/LA/P/0008/2020, UIDP/50006/2020 DOI 10.54499/UIDP/50006/2020 and UIDB/50006/2020 DOI 10.54499/UIDB/50006/2020) and for the Doctoral Grant to MF (SRFH/BD/147354/2019). MP further acknowledges the "la Caixa"

Foundation for Grant HR21-848. ISGlobal and IBEC are members of the CERCA Programme, Generalitat de Catalunya. We acknowledge support from the Ministerio de Ciencia e Innovación/Agencia Estatal de Investigación (MCIN/AEI/ 10.13039/501100011033) through the "Centro de Excelencia Severo Ochoa 2019-2023" Program (CEX2018-000806-S). This research is part of ISGlobal's Program on the Molecular Mechanisms of Malaria which is partially supported by the Fundación Ramón Areces.

Appendix A. Supplementary data

Supplementary data to this article can be found online at https://doi.org/10.1016/j.bmc.2024.117714.

References

1. World Health Organization, World malaria report, 2023.
2. Dhiman S. *Infect Dis Poverty*. 2019;8:14.
3. Antony HA, Parija SC. *Tropical Parasitology*. 2016;6:30–41.
4. World Health Organization, Artemisinin resistance and artemisinin-based combination therapy efficacy, 2018.
5. Balikagala B, Fukuda N, Ikeda M, et al. *N Engl J Med*. 2021;385:1163–1171.
6. Noreen N, Ullah A, Salman SM, Mabkhot Y, Alsayari A, Badshah SL. *Journal of Global Antimicrobial Resistance*. 2021;27:142–149.
7. Nsanzabana C. *Trop Med Infect Dis*. 2019;4:26.
8. Rosenthal PJ. *Lancet Infect Dis*. 2021;21:1056–1057.
9. Rosenthal PJ. *Am J Trop Med Hyg*. 2022;106:1565–1567.
10. King K. Holmes, S. Bertozzi, Barry R. Bloom, et al. Major Infectious Diseases: Key Messages from Disease Control Priorities. In: King K. Holmes, S. Bertozzi, Barry R. Bloom, Prabhat Jha, eds. 3 ed.; ch. 12 - *Malaria Elimination and Eradication*, 2017.
11. Burrows JN, Duparc S, Gutteridge WE, et al. *Malar J*. 2017;16:26.
12. Tibon NS, Ng CH, Cheong SL. *Eur J Med Chem*. 2020;188, 111983.
13. Makhoba XH, Viegas Jr C, Mosa RA, Viegas FPD, Pooe OJ. Drug design. *Development and Therapy*. 2020;14:3235–3249.
14. Talevi A. *Front Pharmacol*. 2015:6.
15. Siqueira-Neto JL, Wicht KJ, Chibale K, Burrows JN, Fidock DA, Winzeler EA. *Nat Rev Drug Discov*. 2023;22:807–826.
16. Teixeira C, Vale N, Pérez B, Gomes A, Gomes JRB, Gomes P. *Chem Rev*. 2014;114:11164–11220.
17. Pinheiro L, Feitosa L, Gandi M, Silveira F, Boechat N. *Molecules*. 2019:24.
18. Pandey SK, Anand U, Siddiqui WA, Tripathi R. *Advances in Medicine*. 2023;2023, 5060665.
19. Araújo MJ, Bom J, Capela R, et al. *J Med Chem*. 2005;48:888–892.
20. Matos J, Cruz FPD, Cabrita É, Gut J, Nogueira F, Rosário VED, Moreira R, Rosenthal PJ, Prudêncio M, Gomes P. *Antimicrob Agents Chemother*. 2012;56:1564–1570.
21. Vale N, Nogueira F, do Rosário VE, Gomes P, Moreira R. *Eur J Med Chem*. 2009;44:2506–2516.
22. Vale N, Prudêncio M, Marques CA, et al. *J Med Chem*. 2009;52:7800–7807.
23. Fonte M, Tassi N, Fontinha D, et al. *ChemMedChem*. 2021;16:788–792.
24. Gomes A, Machado M, Lobo L, et al. *ChemMedChem*. 2015;10:1344–1349.
25. Gomes A, Pérez B, Albuquerque I, et al. *ChemMedChem*. 2014;9:305–310.
26. Pérez B, Teixeira C, Albuquerque IS, et al. *MedChemComm*. 2012;3:1170–1172.
27. Pérez B, Teixeira C, Gomes AS, et al. *Bioorg Med Chem Lett*. 2013;23:610–613.
28. Pérez B, Teixeira C, Gut J, Rosenthal PJ, Gomes JRB, Gomes P. *ChemMedChem*. 2012;7:1537–1540.
29. Pérez B, Teixeira C, Albuquerque IS, et al. *J Med Chem*. 2013;56:556–567.
30. Pérez B, Teixeira C, Figueiras M, et al. *Eur J Med Chem*. 2012;54:887–899.
31. Fonte M, Tassi N, Gomes P, Teixeira C. *Molecules*. 2021;26:600.
32. Parvathaneni V, Kulkarni NS, Muth A, Gupta V. *Drug Discov Today*. 2019;24:2076–2085.
33. D. A. van Schalkwyk, in *Encyclopedia of Life Sciences*, pp. 1-5.
34. Schlitzer M. *ChemMedChem*. 2007;2:944–986.
35. Mayence A, Vanden eynde JJ. *Pharmaceuticals*. 2019;12:115.
36. Ashley EA, Recht J, White NJ. *Malar J*. 2014;13:418.
37. Vale N, Moreira R, Gomes P. *Eur J Med Chem*. 2009;44:937–953.
38. Fonte M, Fagundes N, Gomes A, et al. *Tetrahedron Lett*. 2019;60:1166–1169.
39. Fonte M, Fontinha D, Moita D, et al. *Eur J Med Chem*. 2023;258, 115575.
40. Ruwizhi N, Aderibigbe BA. *Int J Mol Sci*. 2020;21:5712.
41. Meunier B. *Polypharmacology in Drug Discovery*. 2012:423–439.
42. Meunier B. *Acc Chem Res*. 2008;41:69–77.
43. Kanaani J, Ginsburg H. *Antimicrob Agents Chemother*. 1992;36:1102–1108.
44. Silva AT, Bento CM, Pena AC, et al. *Molecules*. 2020;25:66.
45. De P, Bedos-Belval F, Vanucci-Bacque C, Baltas M. *Curr Org Chem*. 2012;16:747–768.
46. Santos MM, Moreira R. *Mini-Rev Med Chem*. 2007;7:1040–1050.
47. Rosenthal PJ, Olson JE, Lee GK, Palmer JT, Klaus JL, Rasnick D. *Antimicrob Agents Chemother*. 1996;40:1600–1603.
48. Previti S, Ettari R, Cosconati S, et al. *J Med Chem*. 2017;60:6911–6923.
49. Fonte M, Teixeira C, Gomes P. *RSC Adv*. 2024;14:6253–6261.
50. Coronado LM, Nadovich CT, Spadafora C. Biochimica et biophysica acta (BBA). - *General Subjects*. 1840, 2014,:2032–2041.
51. Deshpande S, Kay B. *Med Chem*. 2016:6.
52. Hu Y-Q, Gao C, Zhang S, et al. *Eur J Med Chem*. 2017;139:22–47.
53. Agnello S, Brand M, Chellat M, Gazzola S, Riedl R. *Angew Chem Int Ed*. 2018:58.
54. Rawe SL, McDonnell C. In: *G. L. Patrick*: Elsevier; 2020:65–98.
55. Ploemen IHJ, Prudêncio M, Douradinha BG, et al. *PLoS One*. 2009;4:e7881.
56. Prudêncio M, Mota MM, Mendes AM. *Trends Parasitol*. 2011;27:565–574.
57. Ehsanian R, Van Waes C, Feller SM. *Cell Communication and Signaling*. 2011;9:13.
58. Gomes A, Fernandes I, Teixeira C, Mateus N, Sottomayor MJ, Gomes P. *ChemMedChem*. 2016;11:2703–2712.
59. Kumar M, Sarkar A. *Sci Pharm*. 2022;90:12.
60. Kumar R, Kaur M, Kumari M. *Acta Pol Pharm*. 2012;69:3–9.
61. Portugaliza HP, Llorà-Batlle O, Rosanas-Urgell A, Cortés A. *Sci Rep*. 2019;9:14595.
62. Munro BA, McMorran BJ. *Parasitologia*. 2022;2:101–124.
63. Lambros C, Vanderberg JP. *J Parasitol*. 1979;65:418–420.

Supporting Information

Disclosure of cinnamic acid/4,9-diaminoacridine conjugates as multi-stage antiplasmodial hits

Mélanie Fonte,[1] Catarina Rôla,[2] Sofia Santana,[2] Yunuen Avalos-Padilla,[3,4] Xavier Fernàndez-Busquets,[3,4,5] Miguel Prudêncio,[2] Paula Gomes,[1*] Cátia Teixeira[1,6]

[1] LAQV-REQUIMTE, Departamento de Química e Bioquímica, Faculdade de Ciências, Universidade do Porto, Portugal;

[2] Instituto de Medicina Molecular, Faculdade de Medicina, Universidade de Lisboa, Portugal;

[3] Nanomalaria Group, Institute for Bioengineering of Catalonia (IBEC), The Barcelona Institute of Science and Technology, Spain;

[4] Barcelona Institute for Global Health (ISGlobal, Hospital Clínic-Universitat de Barcelona), Spain;

[5] Nanoscience and Nanotechnology Institute (IN2UB), University of Barcelona, Spain;

[6] Current affiliation: Gyros Protein Technologies Inc., Tucson, Arizona, USA

Contents:

General information 2

Spectral and chromatographic traces for compounds 2a-h (Figures S1-S32) 3

General information.

All solvents and commercial chemicals were used without further purification and purchased from Sigma-Aldrich (*trans*-3-fluorocinnamic acid), Bachem (TBTU), Alfa Aesar (DIEA, 4-fluorocinnamic acid), Acros Organics (*trans*-cinnamic acid and *trans*-4-methoxycinnamic acid), PanReac AppliChem (anhydrous Na_2SO_4), Biochem Chemopharma ($NaHCO_3$), VWR International (HPLC gradient grade, LC-MS grade, and p.a. grade solvents, i.e., acetonitrile and methanol), LabChem (synthesis grade solvents, i.e., DCM and methanol), and CortecNet ($CDCl_3$ for NMR analysis).

Aluminum foils coated with silica-gel 60 F254 from Merck were used for monitoring reaction progress, purification steps, and determination of compound retention factors (Rf) by thin-layer chromatography (TLC). TLC chromatograms obtained were revealed with ultra-violet light (254 nm), using a Viber Lourmat lamp, model CN-6, and/or using a phosphomolybdic acid stain (10 g of phosphomolybdic acid in 100 mL of absolute ethanol).

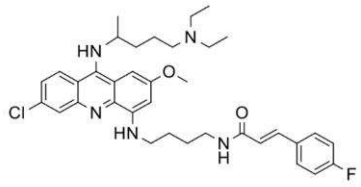
The purification of the compounds was performed by normal phase liquid chromatography in glass columns charged with silica gel 60, from Sigma Aldrich, as solid phase. A mixture of DCM and methanol 8:1 (v/v) was used as the mobile phase (eluent).

^{1}H-NMR and ^{13}C-NMR spectra were acquired on a Bruker Avance III spectrometer at frequencies of 400 and 100 MHz, respectively, from compound solutions in $CDCl_3$ with tetramethylsilane (TMS) as an internal reference. Chemical shifts for protons and carbons are reported in parts per million (ppm) downfield and are referenced to residual protium in the NMR solvent. Data are represented as follows: chemical shift, multiplicity (br = broad, s = singlet, d = doublet, t = triplet, q = quartet, m = multiplet, dd = doublet of doublets), coupling constants in Hertz (Hz) and integration.

Electrospray ionization-ion trap mass spectrometry (ESI-IT MS) analyses (direct injection with detection in positive mode) were achieved with solutions of the pure products in p.a. methanol, using a Finnigan Surveyor LCQ DECA XP MAX spectrometer, at the Department of Chemistry and Biochemistry of the Faculty of Sciences of the University of Porto.

The determination of the retention time (RT) and purity degree of the compounds was performed by analytical reverse-phase high-performance liquid chromatography (RP-HPLC), using a Hitachi-Merck Elite LaChrom system equipped with an L-2130 quaternary pump, an L-2200 thermostatted (Peltier effect) automated sampler, and an L-2455 diode-array detector (DAD). Compounds were dissolved in acetonitrile and injected in an end-capped octadecylsilane (C18) column Purospher star RP-C18 of 125 × 4.0 mm and 5 µm pore size. A gradient elution (1 to 100 % of acetonitrile in 0.05% aqueous trifluoroacetic acid) was run for 30 minutes at a flow rate of 1 mL/min, and detection was set at 290 nm.

(*E*)-*N*-(4-((6-chloro-9-((5-(diethylamino)pentan-2-yl)amino)-2-methoxyacridin-4-yl)amino)butyl)-3-(4-fluorophenyl)acrylamide (2a)



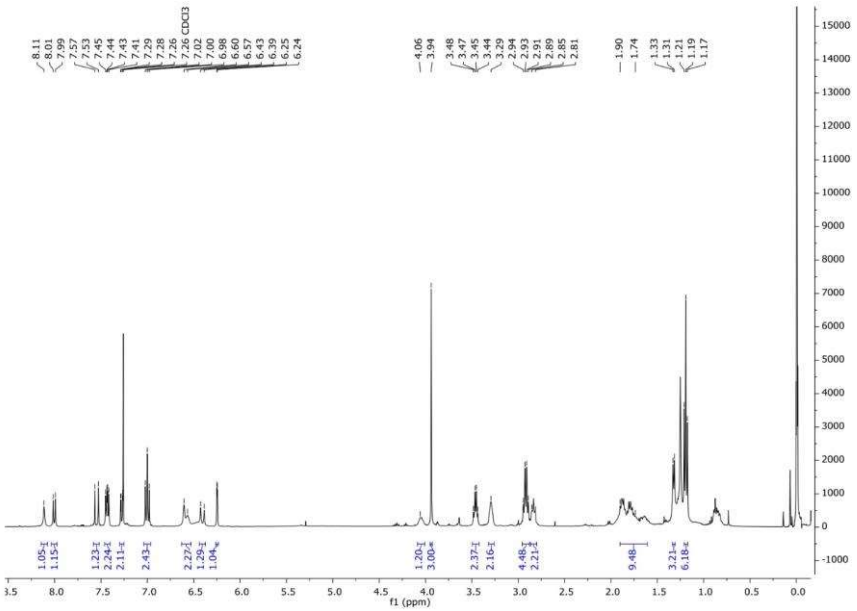


Figure S1. ^{1}H-NMR spectrum (400 MHz, $CDCl_3$) of **2a**.

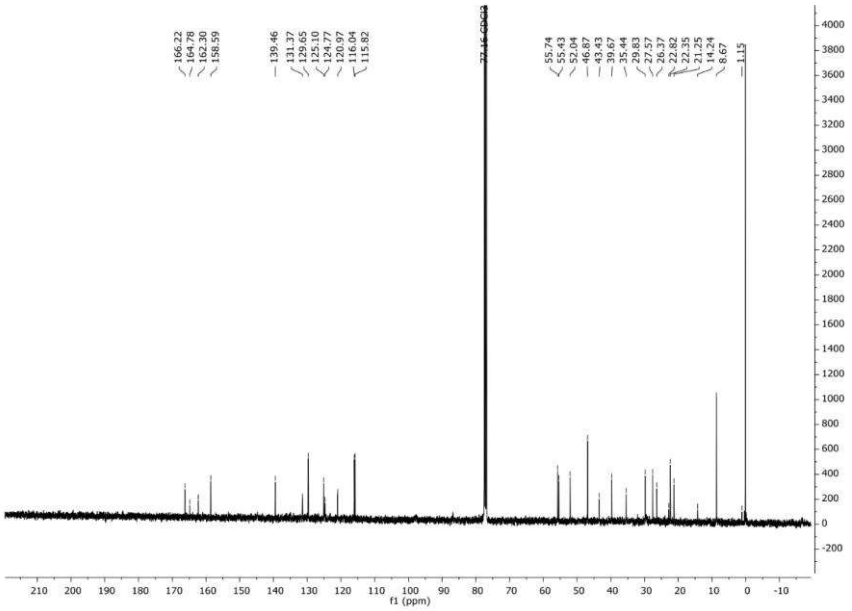


Figure S2. ^{13}C-NMR spectrum (100 MHz, $CDCl_3$) of **2a**.

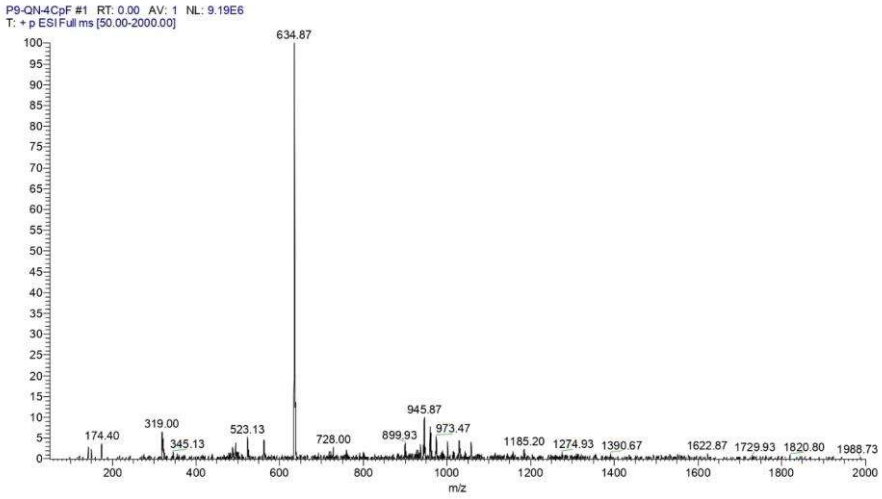


Figure S3. ESI-IT (+) spectrum of **2a**.

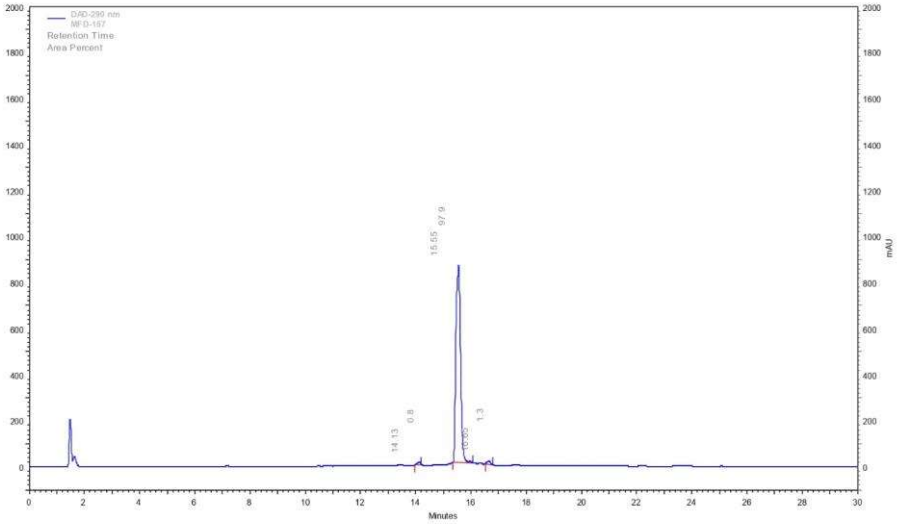
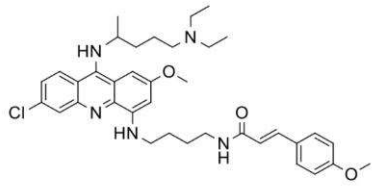


Figure S4. HPLC trace of **2a**.

(*E*)-*N*-(4-((6-chloro-9-((5-(diethylamino)pentan-2-yl)amino)-2-methoxyacridin-4-yl)amino)butyl)-3-(4-methoxyphenyl)acrylamide (2b)



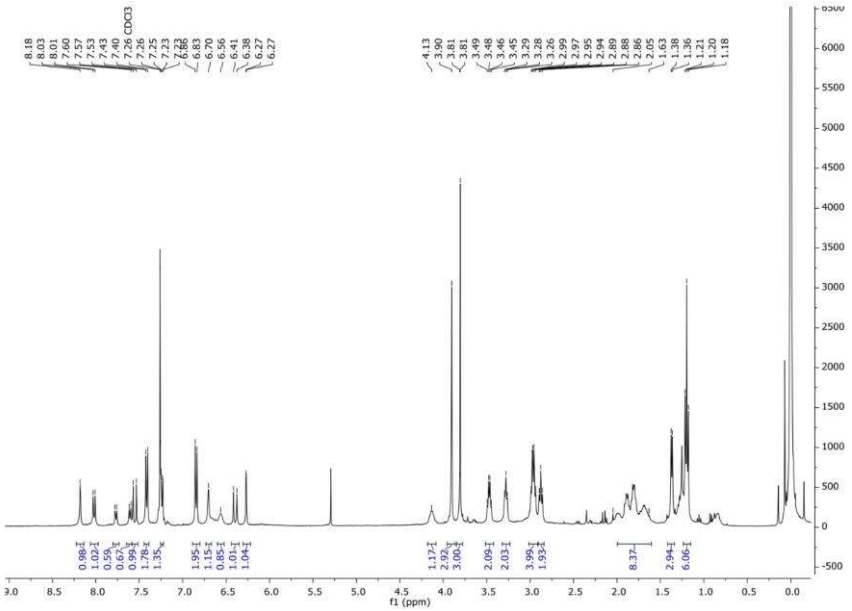


Figure S5. ^{1}H-NMR spectrum (400 MHz, $CDCl_3$) of **2b**.

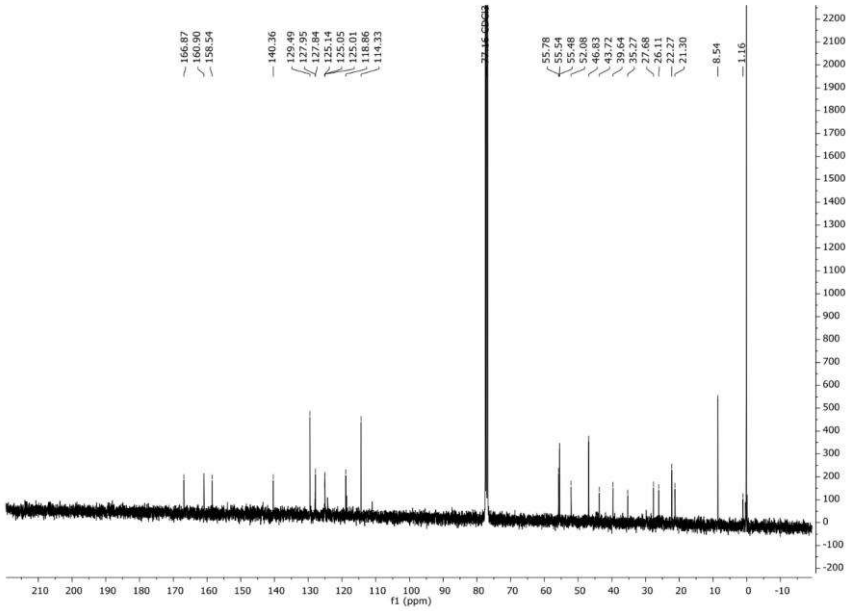


Figure S6. ^{13}C-NMR spectrum (100 MHz, $CDCl_3$) of **2b**.

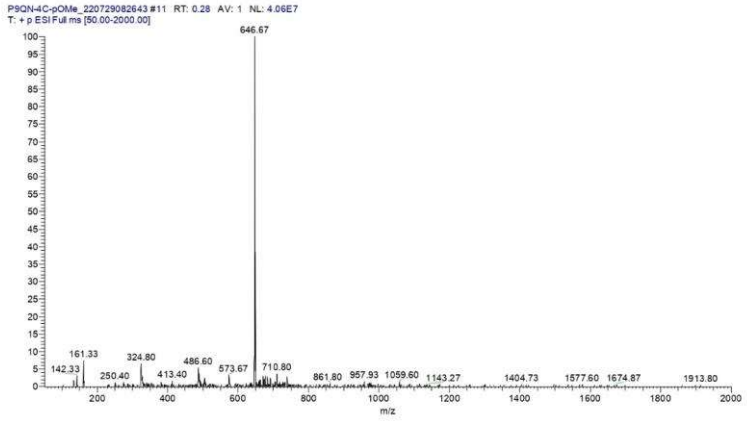


Figure S7. ESI-IT (+) spectrum of **2b**.

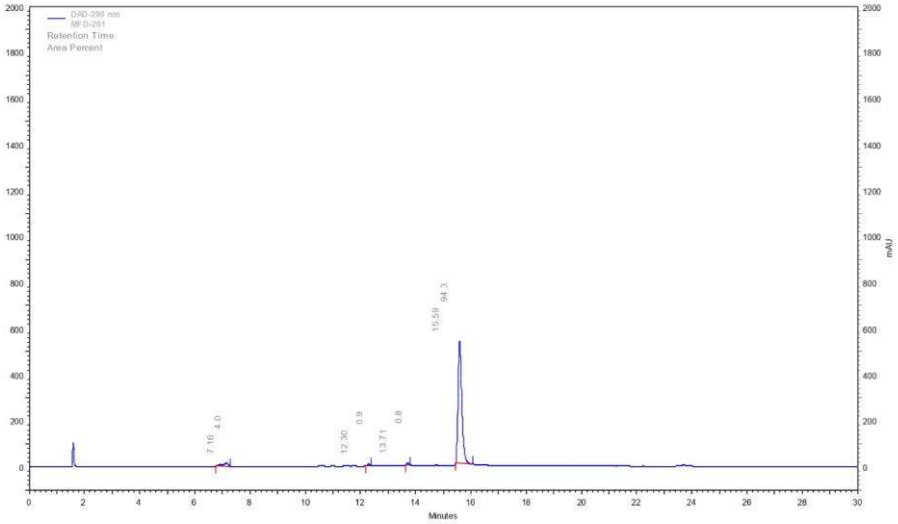
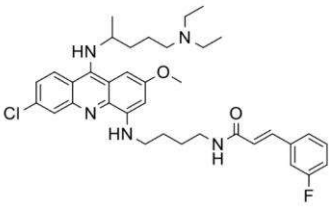


Figure S8. HPLC trace of **2b**.

(*E*)-*N*-(4-((6-chloro-9-((5-(diethylamino)pentan-2-yl)amino)-2-methoxyacridin-4-yl)amino)butyl)-3-(3-fluorophenyl)acrylamide (2c)



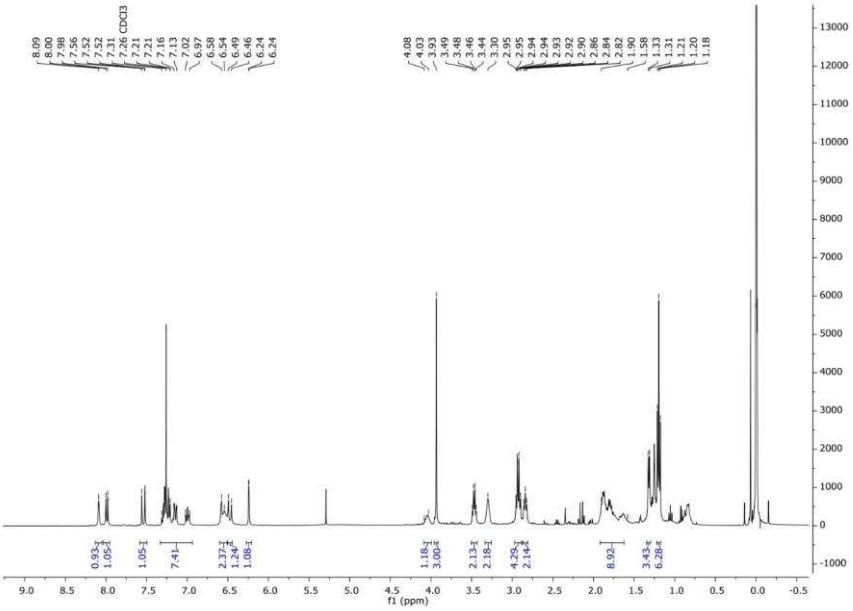


Figure S9. ^{1}H-NMR spectrum (400 MHz, $CDCl_3$) of **2c**.

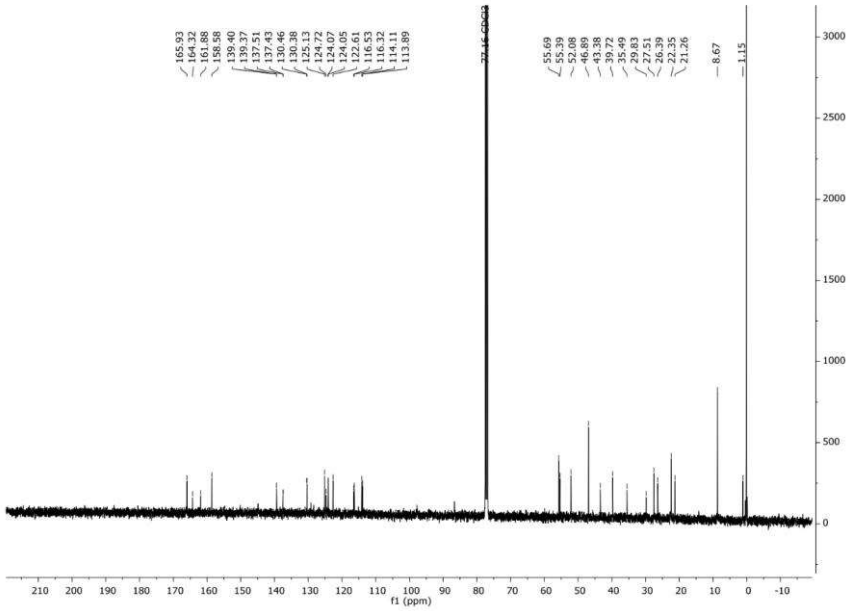


Figure S10. ^{13}C-NMR spectrum (100 MHz, $CDCl_3$) of **2c**.

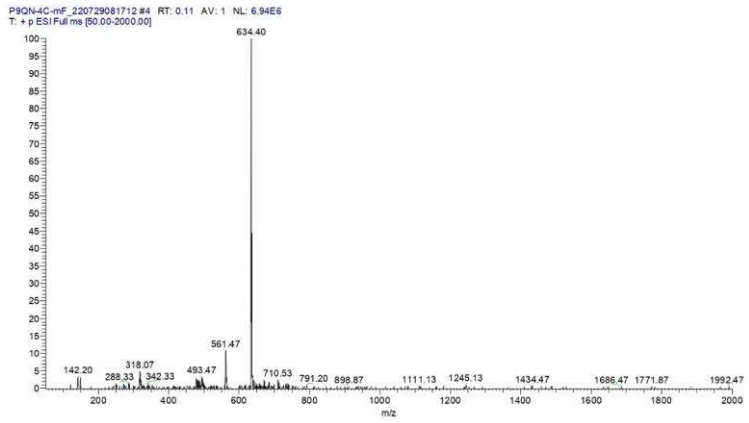


Figure S11. ESI-IT (+) spectrum of **2c**.

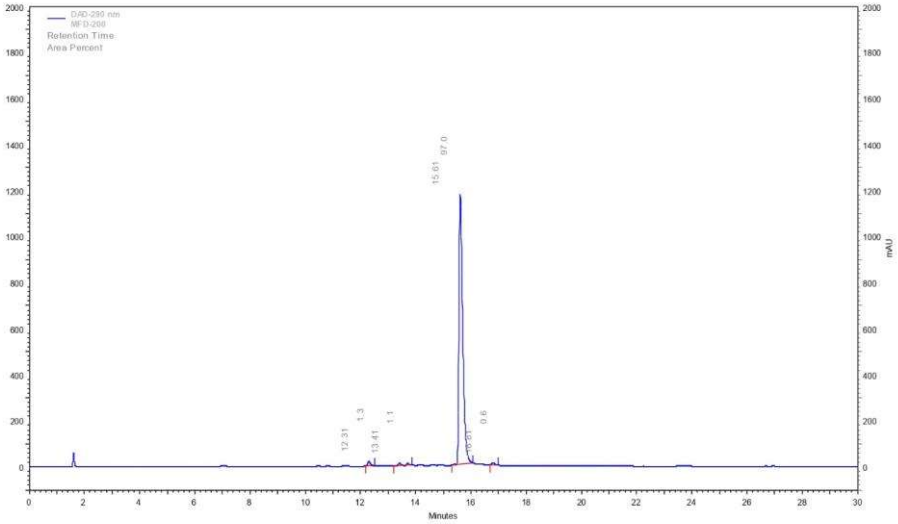


Figure S12. HPLC trace of **2c**.

***N*-(4-((6-chloro-9-((5-(diethylamino)pentan-2-yl)amino)-2-methoxyacridin-4-yl)amino)butyl)cinnamamide (2d)**

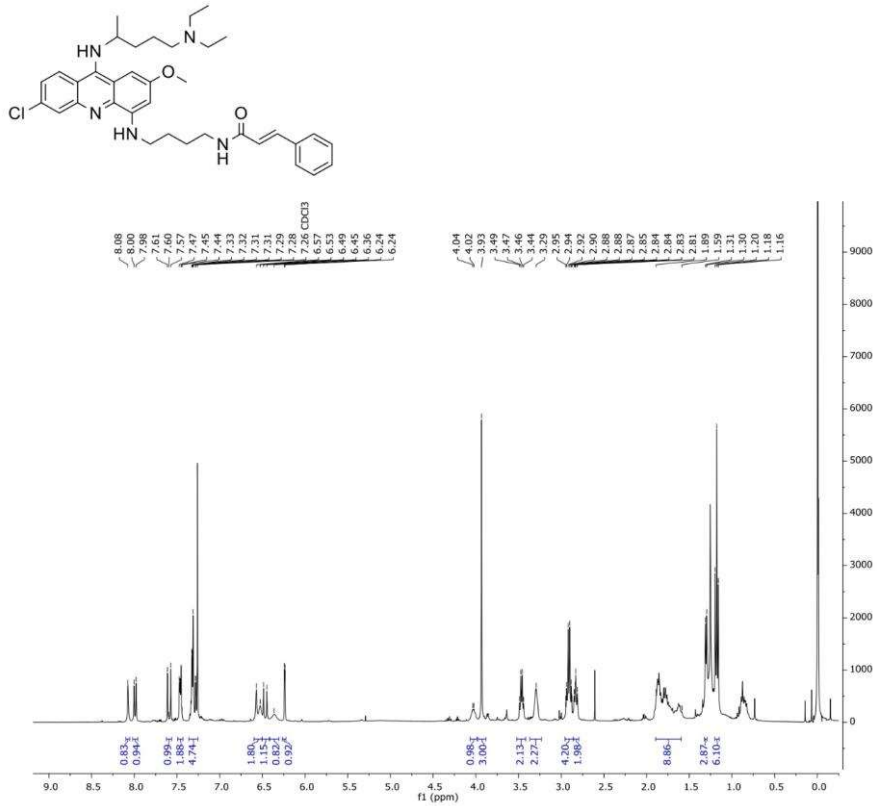


Figure S13. ^{1}H-NMR spectrum (400 MHz, $CDCl_3$) of **2d.**

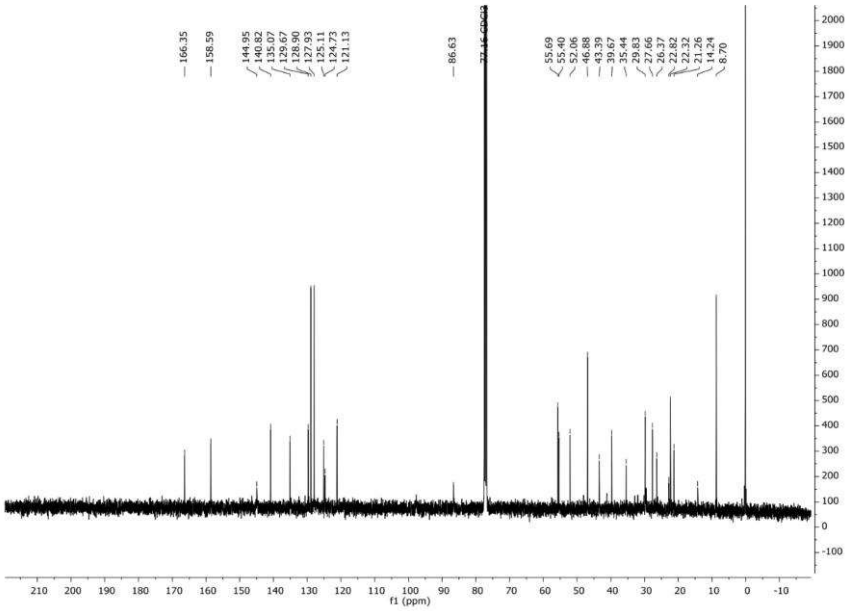


Figure S14. ^{13}C-NMR spectrum (100 MHz, $CDCl_3$) of **2d**.

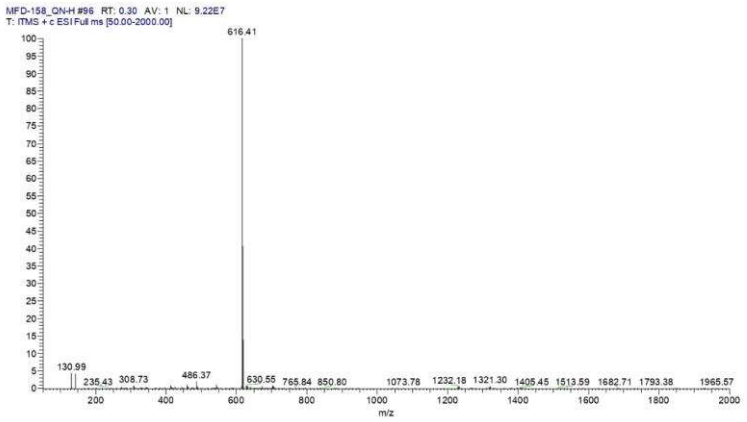


Figure S15. ESI-IT (+) spectrum of **2d**.

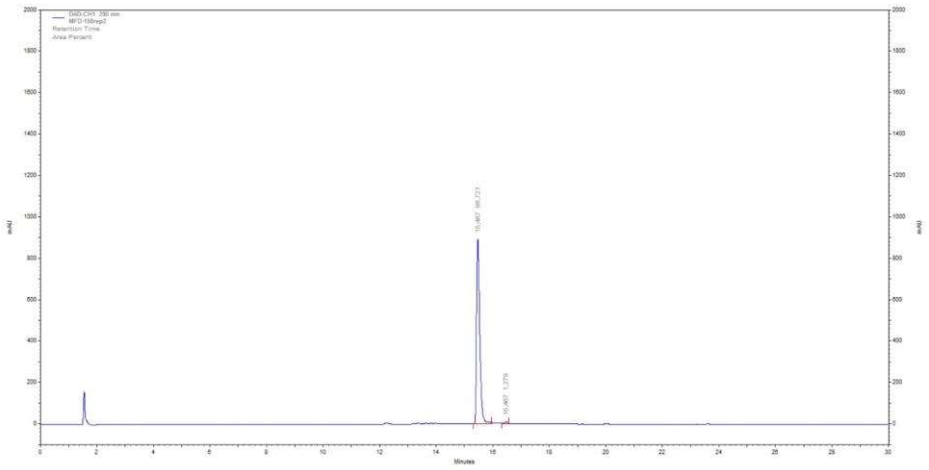


Figure S16. HPLC trace of **2d**.

(*E*)-*N*-(4-((6-chloro-9-((3-(diethylamino)propyl)amino)-2-methoxyacridin-4-yl)amino)butyl)-3-(4-fluorophenyl)acrylamide (2e)

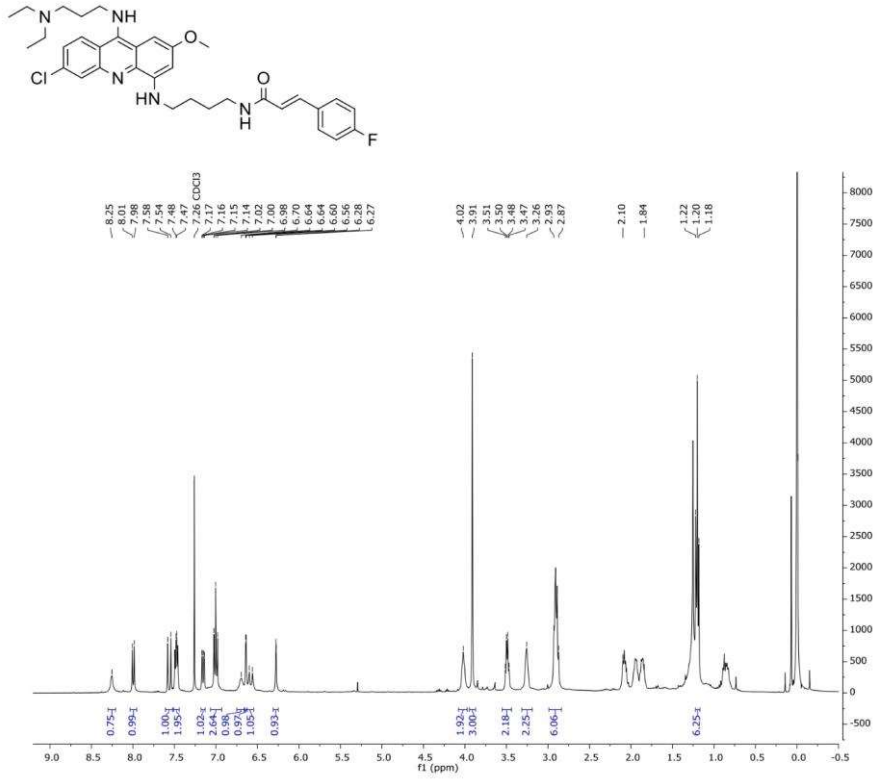


Figure S17. ^{1}H-NMR spectrum (400 MHz, $CDCl_3$) of **2e**.

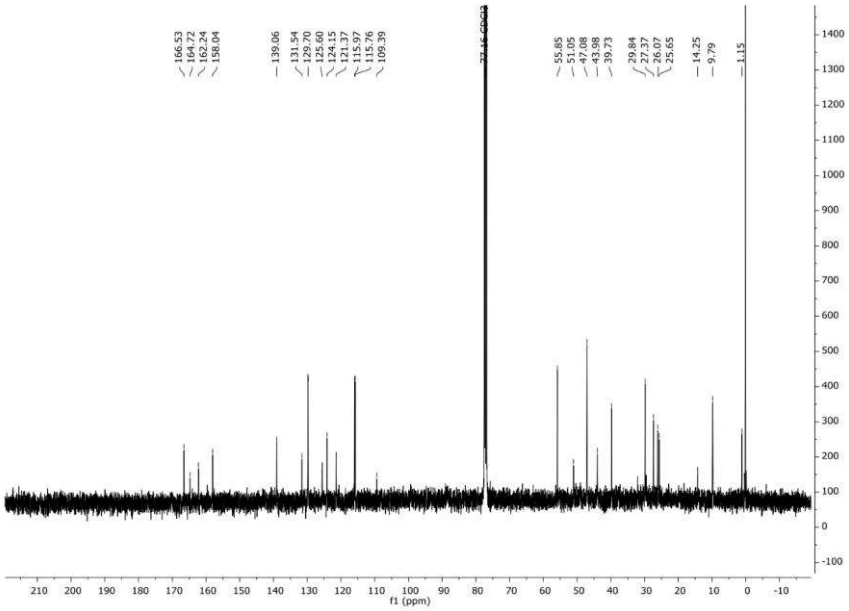


Figure S18. ^{13}C-NMR spectrum (100 MHz, $CDCl_3$) of **2e**.

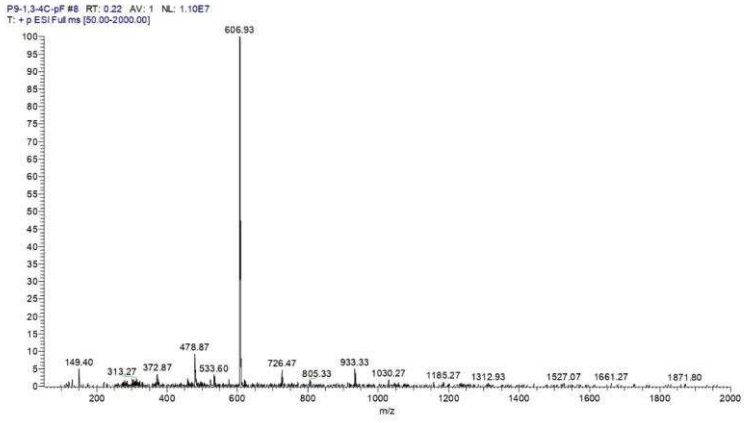


Figure S19. ESI-IT (+) spectrum of **2e**.

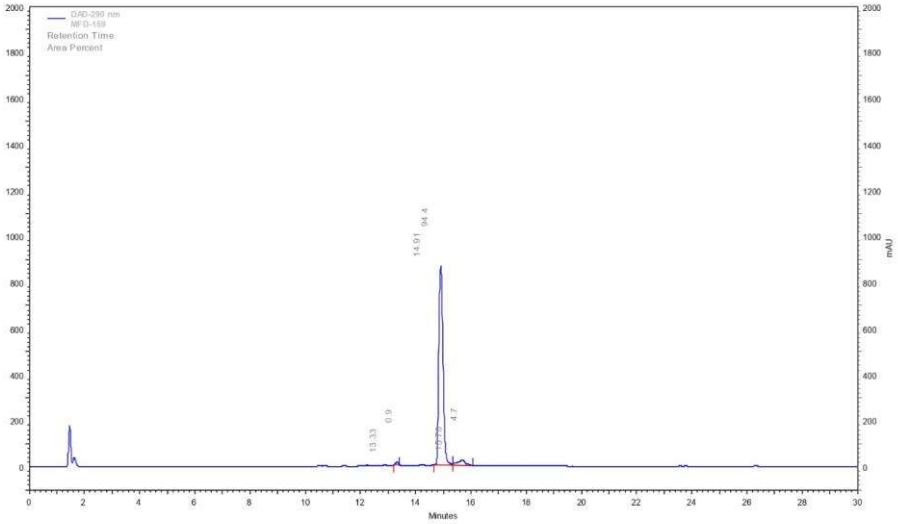


Figure S20. HPLC trace of **2e**.

(*E*)-*N*-(4-((6-chloro-9-((3-(diethylamino)propyl)amino)-2-methoxyacridin-4-yl)amino)butyl)-3-(4-methoxyphenyl)acrylamide (2f)

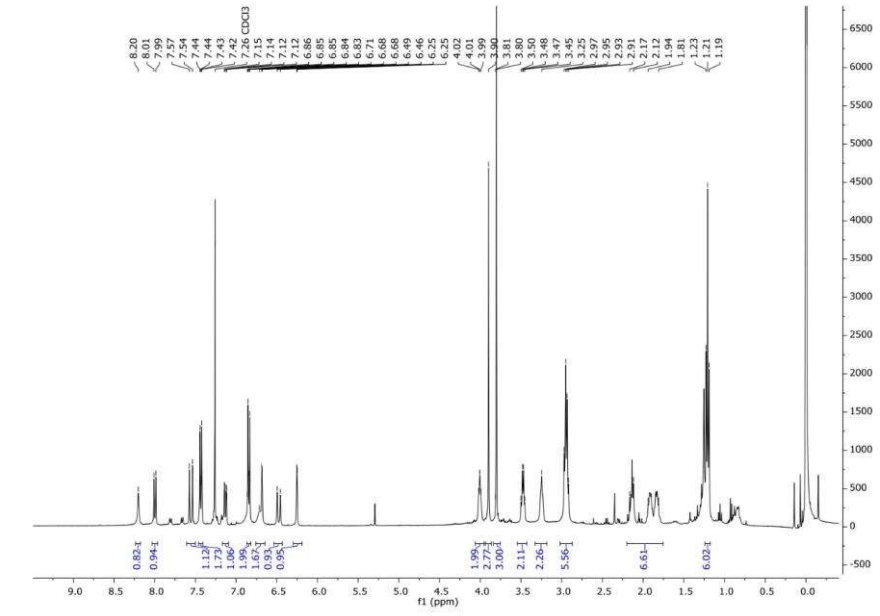


Figure S21. ^{1}H-NMR spectrum (400 MHz, $CDCl_3$) of **2f**.

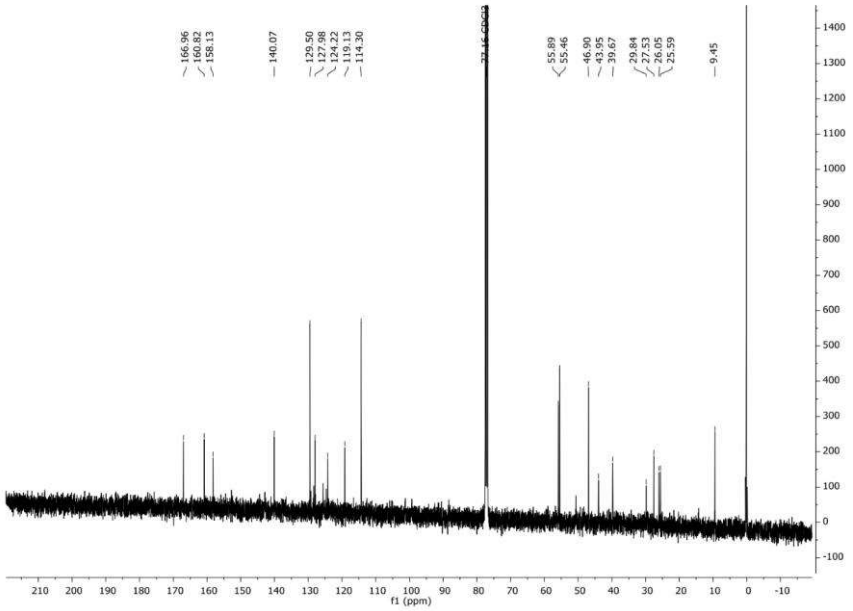


Figure S22. ^{13}C-NMR spectrum (100 MHz, $CDCl_3$) of **2f**.

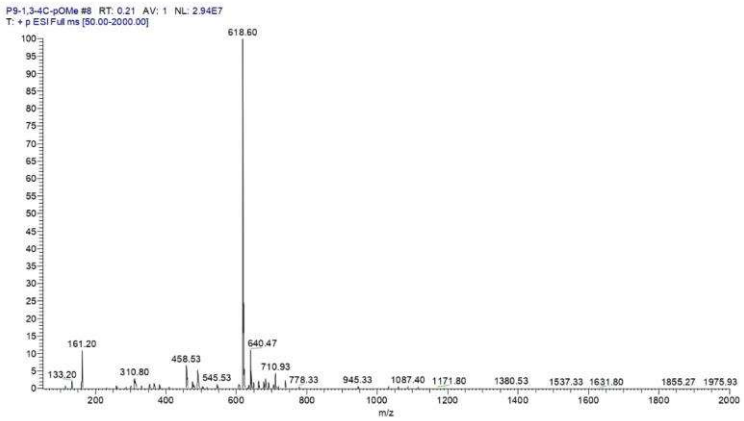


Figure S23. ESI-IT (+) spectrum of **2f**.

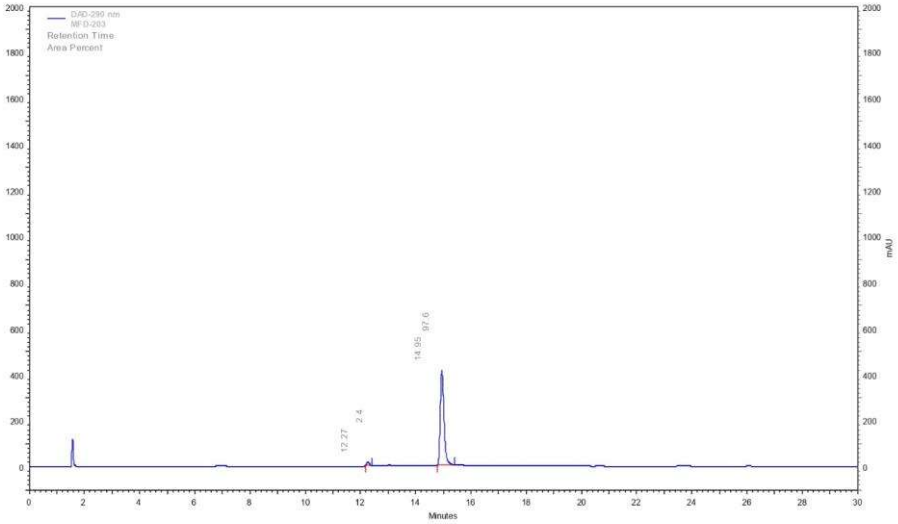


Figure S24. HPLC trace of **2f**.

(*E*)-*N*-(4-((6-chloro-9-((3-(diethylamino)propyl)amino)-2-methoxyacridin-4-yl)amino)butyl)-3-(3-fluorophenyl)acrylamide (2g)

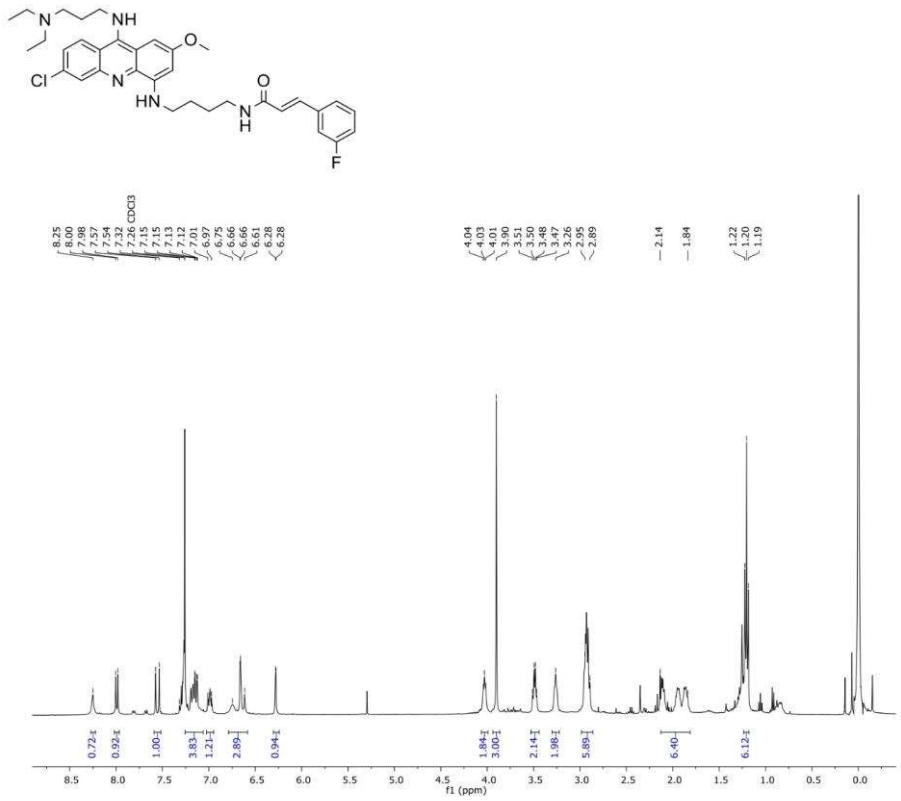


Figure S25. ^{1}H-NMR spectrum (400 MHz, $CDCl_3$) of **2g**.

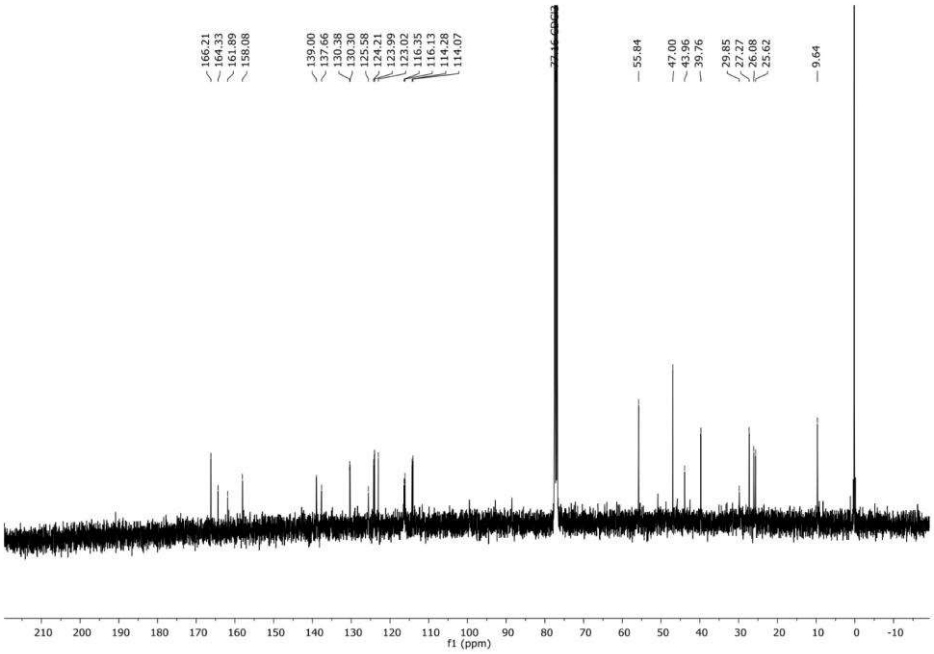


Figure S26. ^{13}C-NMR spectrum (100 MHz, $CDCl_3$) of **2g**.

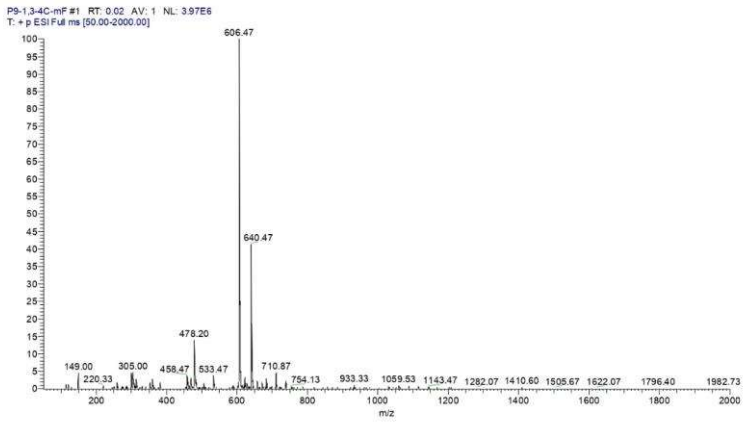


Figure S27. ESI-IT (+) spectrum of **2g**.

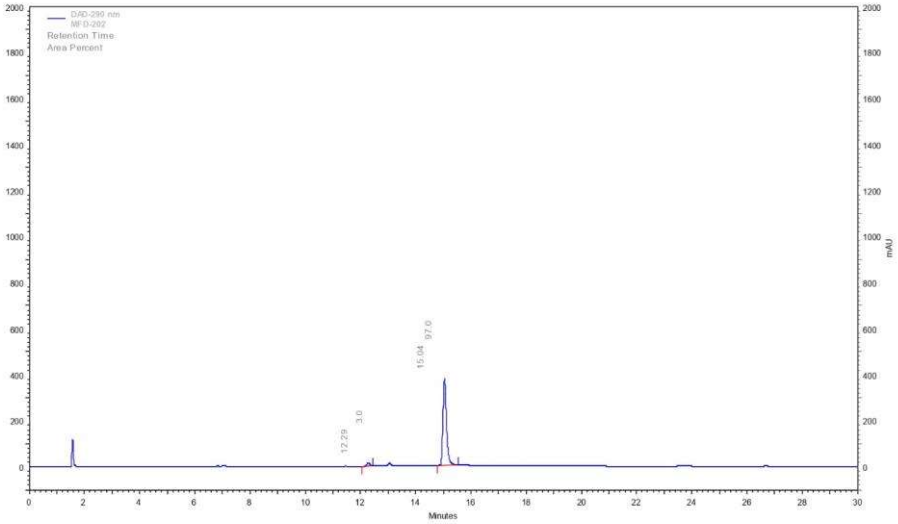


Figure S28. HPLC trace of **2g**.

***N*-(4-((6-chloro-9-((3-(diethylamino)propyl)amino)-2-methoxyacridin-4-yl)amino)butyl)cinnamamide (2h)**

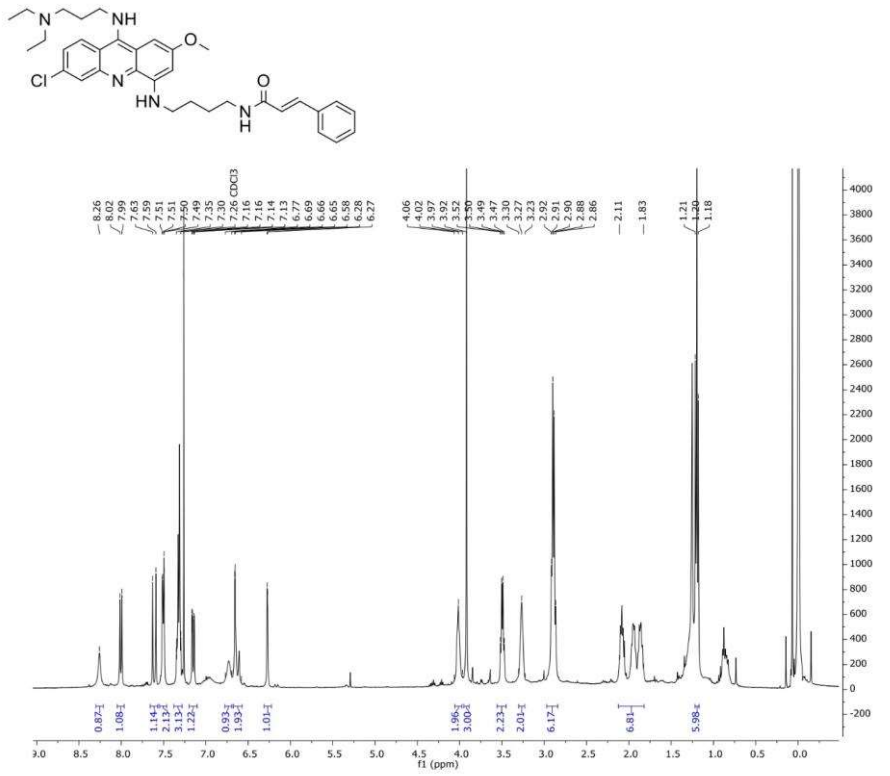


Figure S29. ^{1}H-NMR spectrum (400 MHz, $CDCl_3$) of **2h**.

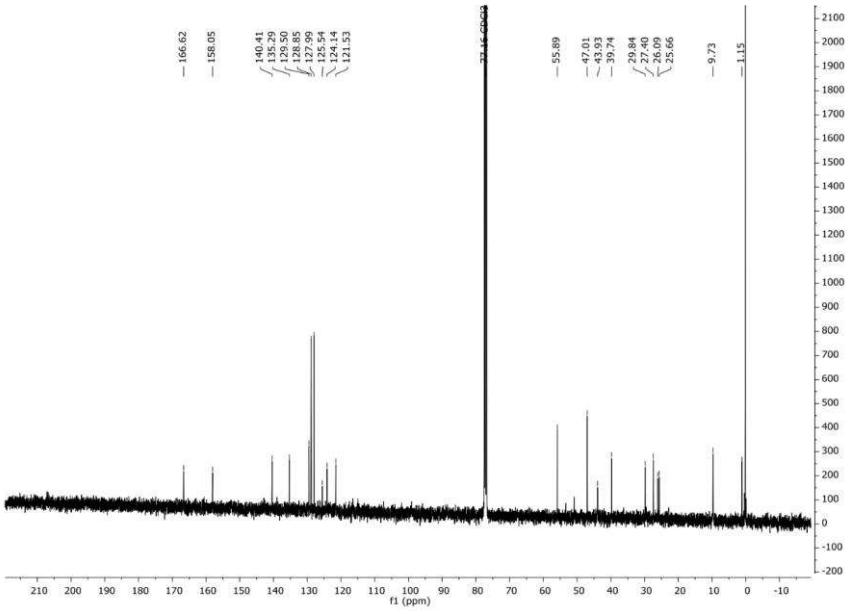


Figure S30. ^{13}C-NMR spectrum (100 MHz, $CDCl_3$) of **2h**.

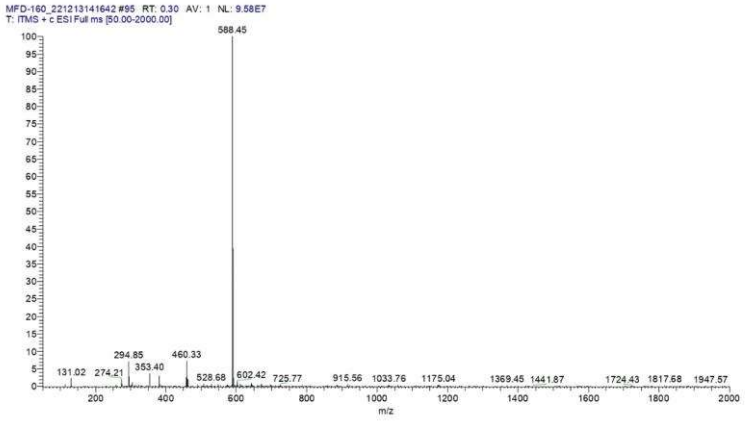


Figure S31. ESI-IT (+) spectrum of **2h**.

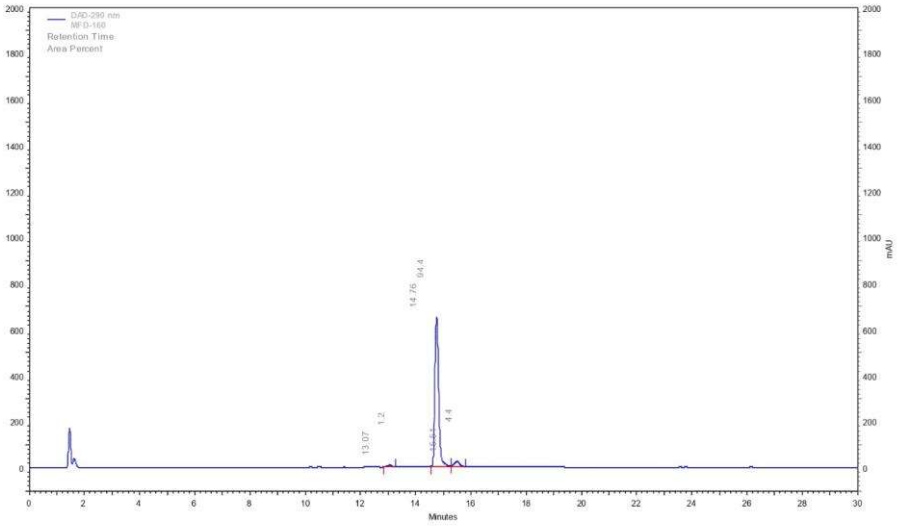
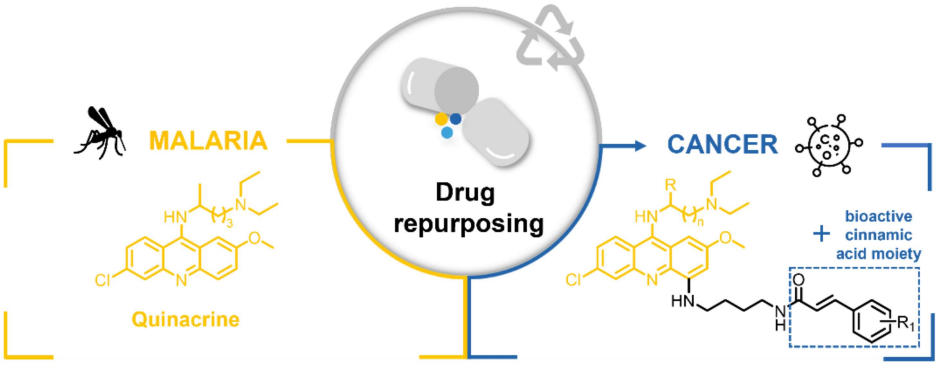


Figure S32. HPLC trace of **2h**.

Article V

Repurposing antiplasmodial leads for cancer: exploring the antiproliferative effects of *N*-cinnamoyl-aminoacridines

Mélanie Fonte, Catarina Rôla, Sofia Santana, Miguel Prudêncio, Joana Almeida, Ricardo Ferraz, Cristina Prudêncio, Cátia Teixeira, Paula Gomes



Bioorg. Med. Chem. Lett., **2024**, 111, 129894 doi.org/10.1016/j.bmcl.2024.129894

Summary

As malaria, cancer is one of the more serious health problems today. Drug repurposing and rescuing have emerged as cost-effective approaches to expand the collection of chemotherapeutic agents. The two families of conjugates formerly developed and discussed embeds both acridine and CA scaffolds, both of which are reported as having antitumor action. This triggered our curiosity to explore the antiproliferative properties of the *N*-cinnamoyl-acridine conjugates developed in this doctoral research project. The results revealed that the CA/4,9-diaminoacridine conjugates displays selective cytotoxicity against the tested tumor cell lines, without any toxic effects to non-carcinogenic cells.

Declaration of authorship of published article V: Repurposing antiplasmodial leads for cancer: exploring the antiproliferative effects of *N*-cinnamoyl-aminoacridines[5]

I, Mélanie Fonte, declare that the laboratory work involving the *in vitro* antiproliferative assays using MKN-28 and HDF cell lines of all compounds tested in this study, and the data analysis and discussion were carried out by me, under the supervision of Prof. Paula Gomes, Dr. Cátia Teixeira and Dr. Miguel Prudêncio. I was also responsible for the writing of the article's original draft that was follow corrected and validated by all the co-authors.

We, Cátia Teixeira, Paula Gomes, and Miguel Prudêncio, as Mélanie Fonte's supervisors, hereby confirm that the information above is correct.

Mélanie Fonte

Mélanie Fonte

Paula Gomes | Cátia Teixeira | Miguel Prudêncio

[5] Copyright Elsevier 2024. Reproduced with permission.

Bioorg. Med. Chem. Lett. 111 (2024) 129894

Contents lists available at ScienceDirect

Bioorganic & Medicinal Chemistry Letters

journal homepage: www.elsevier.com/locate/bmcl

Repurposing antiplasmodial leads for cancer: Exploring the antiproliferative effects of *N*-cinnamoyl-aminoacridines

Mélanie Fonte [a], Catarina Rôla [b], Sofia Santana [b], Miguel Prudêncio [b], Joana Almeida [c,d], Ricardo Ferraz [a,c,d], Cristina Prudêncio [c,d], Cátia Teixeira [a,e,1], Paula Gomes [a,*]

[a] LAQV-REQUIMTE, Departamento de Química e Bioquímica, Faculdade de Ciências, Universidade do Porto, Portugal
[b] Instituto de Medicina Molecular, Faculdade de Medicina, Universidade de Lisboa, Portugal
[c] Centro de Investigação em Saúde Translacional e Biotecnologia Médica (TBIO)/Rede de Investigação em Saúde (RISE-Health), Escola Superior de Saúde, Instituto Politécnico do Porto, Portugal
[d] Ciências Químicas e das Biomoléculas, Escola Superior de Saúde, Politécnico do Porto, Portugal
[e] Gyros Protein Technologies Inc., Tucson, AZ, USA

ARTICLE INFO

Keywords:
Antitumor
Cancer
Covalent bitherapy
Hybrid
Malaria
Mepacrine
Recycling
Selectivity

ABSTRACT

Drug repurposing and rescuing have been widely explored as cost-effective approaches to expand the portfolio of chemotherapeutic agents. Based on the reported antitumor properties of both *trans*-cinnamic acids and quinacrine, an antimalarial aminoacridine, we explored the antiproliferative properties of two series of *N*-cinnamoyl-aminoacridines recently identified as multi-stage antiplasmodial leads. The compounds were evaluated *in vitro* against three cancer cell lines (MKN-28, Huh-7, and HepG2), and human primary dermal fibroblasts. One of the series displayed highly selective antiproliferative activity in the micromolar range against the three cancer cell lines tested, without any toxicity to non-carcinogenic cells.

Cancer remains a pervasive and life-threatening disease worldwide.[4,5] Alongside surgery and radiotherapy, chemotherapy is one of the most common anticancer therapeutic approaches employed. However, it faces several limitations, such as high cost, low efficacy, resistance issues, and poor selectivity, translating into high toxicity.[6] Therefore, in spite of a constant quest for highly efficacious anticancer drugs and biopharmaceuticals, the traditional development pipeline is a costly, complex, and extensive process.[7] As such, drug repurposing and rescuing are being increasingly explored as strategies to find new uses for known drugs and pharmacophores, including for cancer. When rescuing or repurposing a well-known drug, prior knowledge regarding its safety, efficacy, and suitable administration route translates into a fast track towards more affordable medicines to treat conditions other than that for which the drug was originally licensed.[7–11] Indeed, there is growing evidence that several drugs may interact with multiple biological targets, which, in turn, may be implicated in more than one pathophysiological process.[12,13] Therefore, a single bioactive molecule holds the potential to play a therapeutic role in a wide range of diseases as diverse as, e.g., cancer and malaria.[14,15] For instance, the repurposing of antimalarials like chloroquine[16–19] or quinacrine (QN) [20–24] as anticancer agents has been widely explored.

QN (Fig. 1) and *trans*-cinnamic acids (CA, Fig. 1) are well-known bioactive scaffolds that have been extensively described for diverse medicinal purposes, including for cancer treatment.[20–22,25–33] Following its discovery in the 1920s as an antimalarial agent, QN has been widely documented for its anticancer potential.[21,34] Despite the exact mechanism(s) of action (MoA) underlying the anticancer activity of QN remaining unclear, it has been suggested that it may hinder cancer cell growth through (i) regulation of autophagy, (ii) intercalation into DNA, (iii) suppression of the nuclear factor-kappa B (NF-κB), (iv) alkalization of cellular compartments, (v) inhibition of topoisomerases, and (vi) activation of protein p53.[20–22, 35] In turn, the antineoplastic activity of CA derivatives has been linked to their ability to (i) induce apoptosis and cell cycle arrest through DNA damage in cancer cells, (iii) inhibit

Abbreviations: CA, cinnamic acid; DOX, doxorubicin; IC_{50}, half maximal inhibitory concentration; MoA, mechanism of action; MTT, 3-(4,5-dimethylthiazol-2-yl)-2,5-diphenyltetrazolium bromide; QN, quinacrine; SI, selective index.

* Corresponding author.
E-mail address: pgomes@fc.up.pt (P. Gomes).
[1] Current affiliation.

https://doi.org/10.1016/j.bmcl.2024.129894
Received 14 April 2024; Received in revised form 26 June 2024; Accepted 20 July 2024
Available online 21 July 2024
0960-894X/© 2024 The Author(s). Published by Elsevier Ltd. This is an open access article under the CC BY-NC-ND license (http://creativecommons.org/licenses/by-nc-nd/4.0/).

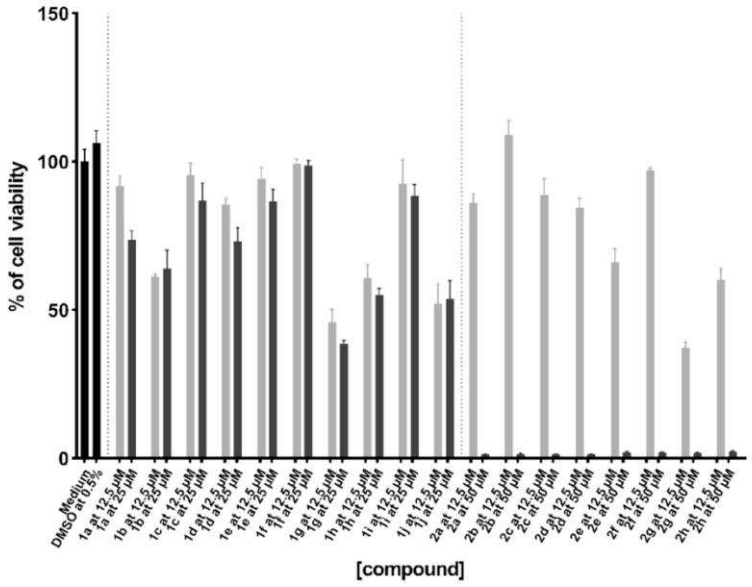


Fig. 2. Initial screening of conjugates **1a-j** (at 12.5 and 25 μM) and **2a-h** (at 12.5 and 50 μM) on MKN-28 cells.

Table 1
In vitro antiproliferative activity (IC_{50}) and selectivity (SI) of compounds **2a-h** against MKN-28, Huh-7, HepG2 and HDF cell lines. The antineoplastic drug doxorubicin (DOX) was included for reference.

Comp.	R	n	R_1	$IC_{50} \pm SD$, μM[a] MKN-28[b]	SI[c]	Huh-7[d]	SI[c]	HepG2[d]	SI[c]	HDF[b, e]
2a	CH_3	3	*p*-F	12.483 ± 1.366	> 4.0	12.425 ± 2.963	> 4.0	7.642 ± 2.420	> 6.5	> 50
2b	CH_3	3	*p*-OCH_3	13.667 ± 1.665	> 3.6	12.125 ± 0.983	> 4.1	3.328 ± 1.505	> 15.0	> 50
2c	CH_3	3	*m*-F	12.720 ± 0.276	> 3.9	12.905 ± 0.757	> 3.9	5.064 ± 0.107	> 9.9	> 50
2d	CH_3	3	H	9.998 ± 0.359	> 5.0	7.260 ± 0.410	> 6.9	4.166 ± 0.879	> 12.0	> 50
2e	H	2	*p*-F	12.250 ± 1.300	> 4.1	11.172 ± 1.964	> 4.5	6.319 ± 2.198	> 7.9	> 50
2f	H	2	*p*-OCH_3	15.540 ± 1.933	> 3.2	12.375 ± 2.199	> 4.0	5.383 ± 0.670	> 9.3	> 50
2 g	H	2	*m*-F	12.960 ± 1.964	> 3.8	11.535 ± 2.836	> 4.3	5.215 ± 0.612	> 9.6	> 50
2 h	H	2	H	15.430 ± 1.814	> 3.2	12.130 ± 0.693	> 4.1	4.110 ± 0.730	> 12.2	> 50
QN	–	–	–	2.46 ± 0.11[e]	–	8.696 ± 0.284	–	4.480 ± 0.680	–	nd
DOX	–	–	–	0.34 ± 0.01[e]	–	6.053 ± 0.401	–	0.425 ± 0.045	–	nd

[a] IC_{50}: compound concentration causing inhibition of cell growth by 50 %; [b] antiproliferative activity evaluated at the Escola Superior de Saúde (ESS), using the MTT assay; [c] Selectivity index (SI): IC_{50}(HDF cells)/IC_{50} (cancer cells); [d] antiproliferative activity evaluated at the Institute of Molecular Medicine (iMM), using the Alamar Blue assay in; [e] 50 μM was the highest concentration tested; [d] taken from reference [37]; nd, not determined.

been highlighted as both a hallmark and a therapeutic target for anti-cancer agents.[41] Yet, one cannot rule out other relevant factors or MoA (s) for these or similar compounds. Indeed, the MoA(s) through which *N*-cinnamoyl-4,9-diaminoacridines **2a-h** exert their antiproliferative activity remains to be elucidated. One possibility is that, due to the planarity of their heteroaromatic core, and resemblance to QN, these compounds might be able to intercalate into DNA, disrupting its structure and interfering with its replication and transcription.[20–22,35] On the other hand, the presence of a CA moiety that may act as Michael acceptor through its α,β-unsaturated carbonyl moiety might induce formation of covalent complexes with nucleophilic groups (e.g., cysteine side-chain thiols) in key proteins directly or indirectly involved in cell signaling, apoptosis, and other cellular processes relevant for the growth of carcinogenic cells.[30–33] Still, other possibilities cannot be ruled out, as the acridine (QN) and Michael acceptor (CA) moieties might further (or alternatively) engage in other biochemical processes contributing to the hindrance of tumor cell growth; an additional and relevant observation is that both these moieties are equally present in conjugates **1a-j** that do not display the same bioactivity profile. This further reinforces the hypothesis that the aminoalkyl side chain present in **2a-h** and absent in **1a-j** could be making a difference in regard to the ability of the former to accumulate inside their target cells. Anyway, this highlights the need to carry out further studies envisaging the establishment of the mechanisms of internalization and action of these compounds.

In summary, two families of *N*-cinnamoyl-aminoacridines (**1a-j** and **2a-h**), previously reported as potent multi-stage antiplasmodial leads, were evaluated for their antiproliferative activity. While conjugates **1a-j** were not cytotoxic against either cancer (MKN-28) or healthy (HDF) cells, conjugates **2a-h** exhibited selective low micromolar activity against MKN-28, Huh-7, and HepG2 cancer cells. As such, compounds **2a-h**, particularly **2d**, represent a promising starting point for the pursuit of novel affordable leads against malignant tumor cells. Further structural optimization, and elucidation of their MoA(s) may pave the way towards more selective and potent antineoplastic candidates. Altogether, our findings reinforce the therapeutic value of repurposing scaffolds based on QN for cancer therapy.

the Doctoral Grant to MF (SRFH/BD/147354/2019). MP further acknowledges the "la Caixa" Foundation for Grant HR21-848.

Abbreviations

CA	cinnamic acid
DOX	doxorubicin
IC_{50}	half maximal inhibitory concentration
MoA	mechanism of action
MTT	3-(4,5-dimethylthiazol-2-yl)-2,5-diphenyltetrazolium bromide
QN	quinacrine
SI	selective index

References and notes

1. Fonte M, Fontinha D, Moita D, et al. New 4-(*N*-cinnamoylbutyl)aminoacridines as potential multi-stage antiplasmodial leads. *European Journal of Medicinal Chemistry.* 2023;258: 115575.
2. Fonte M, Rôla C, Santana S, et al. Disclosure of cinnamic acid/4,9-diaminoacridine conjugates as multi-stage antiplasmodial hits. *Bioorganic & Medicinal Chemistry.* 2024;104: 117714.
3. Fonte M, Teixeira C, Gomes P. Improved synthesis of antiplasmodial 4-aminoacridines and 4,9-diaminoacridines. *RSC Advances.* 2024;14(9): 6253–6261.
4. WHO. Global Cancer Observatory; https://gco.iarc.fr/en. Accessed 13th February 2024.
5. Siegel RL, Giaquinto AN, Jemal A. Cancer statistics, 2024. *CA: A Cancer Journal for Clinicians.* 2024;74(1): 12-49.
6. Shnaider PV, Ivanova OM, Malyants IK, et al. New Insights into Therapy-Induced Progression of Cancer. *International journal of molecular sciences.* 2020;21(21): E7872.
7. Parvathaneni V, Kulkarni NS, Muth A, Gupta V. Drug repurposing: a promising tool to accelerate the drug discovery process. *Drug Discovery Today.* 2019;24(10): 2076-2085.
8. Kulkarni VS, Alagarsamy V, Solomon VR, Jose PA, Murugesan S. Drug Repurposing: An Effective Tool in Modern Drug Discovery. *Russian Journal of Bioorganic Chemistry.* 2023;49(2): 157-166.
9. Schein CH. Repurposing approved drugs for cancer therapy. *British Medical Bulletin.* 2021;137(1): 13-27.
10. Mohi-ud-din R, Chawla A, Sharma P, et al. Repurposing approved non-oncology drugs for cancer therapy: a comprehensive review of mechanisms, efficacy, and clinical prospects. *European Journal of Medical Research.* 2023;28(1): 345.
11. Langedijk J, Mantel-Teeuwisse AK, Slijkerman DS, Schutjens MH. Drug repositioning and repurposing: terminology and definitions in literature. *Drug Discovery Today.* 2015;20(8): 1027-1034.
12. Haupt VJ, Daminelli S, Schroeder M. Drug Promiscuity in PDB: Protein Binding Site Similarity Is Key. *PLOS ONE.* 2013;8(6): e65894.
13. Campillos M, Kuhn M, Gavin AC, Jensen LJ, Bork P. Drug target identification using side-effect similarity. *Science.* 2008;321(5886): 263-266.
14. Qu XA, Gudivada RC, Jegga AG, Neumann EK, Aronow BJ. Inferring novel disease indications for known drugs by semantically linking drug action and disease mechanism relationships. *BMC Bioinformatics.* 2009;10(5): S4.
15. Keiser MJ, Setola V, Irwin JJ, et al. Predicting new molecular targets for known drugs. *Nature.* 2009;462(7270): 175-181.
16. Abdel-Aziz AK, Saadeldin MK, Salem AH, et al. A Critical Review of Chloroquine and Hydroxychloroquine as Potential Adjuvant Agents for Treating People with Cancer. *Future Pharmacology.* 2022;2(4): 431-443.
17. Eloranta K, Cairo S, Liljeström E, et al. Chloroquine Triggers Cell Death and Inhibits PARPs in Cell Models of Aggressive Hepatoblastoma. *Frontiers in Oncology.* 2020;10.
18. Anand K, Niravath P, Patel T, et al. A Phase II Study of the Efficacy and Safety of Chloroquine in Combination With Taxanes in the Treatment of Patients With Advanced or Metastatic Anthracycline-refractory Breast Cancer. *Clinical Breast Cancer.* 2021;21(3): 199-204.
19. Zhou W, Wang H, Yang Y, Chen Z-S, Zou C, Zhang J. Chloroquine against malaria, cancers and viral diseases. *Drug Discovery Today.* 2020;25(11): 2012-2022.
20. Varakumar P, Rajagopal K, Aparna B, et al. Acridine as an Anti-Tumour Agent: A Critical Review. *Molecules.* 2023;28(1): 193.
21. Kumar M, Sarkar A. Repurposing of Anti-Malarial Drug Quinacrine for Cancer Treatment: A Review. *Scientia Pharmaceutica.* 2022;90(1): 12.
22. Oien DB, Pathoulas CL, Ray U, Thirusangu P, Kalogera E, Shridhar V. Repurposing quinacrine for treatment-refractory cancer. *Seminars in Cancer Biology.* 2021;68: 21-30.
23. Thirusangu P, Pathoulas CL, Ray U, et al. Quinacrine-Induced Autophagy in Ovarian Cancer Triggers Cathepsin-L Mediated Lysosomal/Mitochondrial Membrane Permeabilization and Cell Death. *Cancers.* 2021;13(9): 2004.
24. Oien DB, Ray U, Pathoulas CL, et al. Quinacrine Induces Nucleolar Stress in Treatment-Refractory Ovarian Cancer Cell Lines. *Cancers.* 2021;13(18): 4645.
25. Gensicka-Kowalewska M, Cholewiński G, Dzierzbicka K. Recent developments in the synthesis and biological activity of acridine/acridone analogues. *RSC Advances.* 2017;7(26): 15776-15804.
26. Kozurkova M, Sabolova D, Kristian P. A new look at 9-substituted acridines with various biological activities. *Journal of Applied Toxicology.* 2021;41(1): 175-189.
27. Prasher P, Sharma M. Medicinal chemistry of acridine and its analogues. *MedChemComm.* 2018;9(10): 1589-1618.
28. Silva AT, Bento CM, Pena AC, et al. Cinnamic Acid Conjugates in the Rescuing and Repurposing of Classical Antimalarial Drugs. *Molecules.* 2020;25(1): 66.
29. Prithwiraj De FB-BCV-BMB. Cinnamic Acid Derivatives in Tuberculosis, Malaria and Cardiovascular Diseases - A Review. *Current Organic Chemistry.* 2012;16(6): 747-768.
30. Feng L-S, Cheng J-B, Su W-Q, et al. Cinnamic acid hybrids as anticancer agents: A mini-review. *Archiv der Pharmazie.* 2022;355(7): 2200052.
31. De P, Baltas M, Bedos-Belval F. Cinnamic acid derivatives as anticancer agents-a review. *Current Medicinal Chemistry.* 2011;18(11): 1672-1703.
32. De P, Bedos-Belval F, Vanucci-Bacque C, Baltas M. Cinnamic Acid Derivatives in Tuberculosis, Malaria and Cardiovascular Diseases - A Review. *Current Organic Chemistry.* 2012;16(6): 747-768.

Funding

This work received financial support from PT national funds (FCT/MCTES, Fundação para a Ciência e Tecnologia and Ministério da Ciência, Tecnologia e Ensino Superior) through project CIRCNA/BRB/0281/2019.

CRediT authorship contribution statement

Mélanie Fonte: Writing – original draft, Methodology, Investigation, Data curation. **Catarina Rôla:** Investigation, Formal analysis, Data curation. **Sofia Santana:** Validation, Investigation, Formal analysis, Data curation. **Miguel Prudêncio:** Writing – review & editing, Supervision, Resources, Formal analysis. **Joana Almeida:** Writing – review & editing, Validation, Supervision, Methodology, Formal analysis. **Ricardo Ferraz:** Writing – review & editing, Resources, Methodology, Formal analysis. **Cristina Prudêncio:** Validation, Supervision, Resources. **Cátia Teixeira:** Supervision, Methodology, Investigation, Formal analysis, Conceptualization. **Paula Gomes:** .

Declaration of competing interest

The authors declare that they have no known competing financial interests or personal relationships that could have appeared to influence the work reported in this paper.

Data availability

Data will be made available on request.

Acknowledgments

The authors thank Professors Iva Fernandes (Food Quality and Technology group, Faculdade de Ciências da Universidade do Porto, Portugal) and Pedro Coelho (T.Bio Laboratory, Escola Superior de Saúde do Politécnico do Porto, Portugal), for the kind gift of MKN-28 and HDF cells, respectively. The authors further thank FCT/MCTES for supporting Research Units LAQV-REQUIMTE (LA/P/0008/2020 DOI 10.54499/LA/P/0008/2020, UIDP/50006/2020 DOI 10.54499/UIDP/50006/2020 and UIDB/50006/2020 DOI 10.54499/UIDB/50006/2020) and for the Doctoral Grant to MF (SRFH/BD/147354/2019). MP further acknowledges the "la Caixa" Foundation for Grant HR21-848.

Appendix A. Supplementary data

Supplementary data to this article can be found online at https://doi.org/10.1016/j.bmcl.2024.129894.

References

1. Fonte M, Fontinha D, Moita D, et al. New 4-(*N*-cinnamoylbutyl)aminoacridines as potential multi-stage antiplasmodial leads. *Eur J Med Chem*. 2023;258, 115575.
2. Fonte M, Rôla C, Santana S, et al. Disclosure of cinnamic acid/4,9-diaminoacridine conjugates as multi-stage antiplasmodial hits. *Bioorg Med Chem*. 2024;104, 117714.
3. Fonte M, Teixeira C, Gomes P. Improved synthesis of antiplasmodial 4-aminoacridines and 4,9-diaminoacridines. *RSC Adv*. 2024;14:6253–6261.
4. WHO. Global Cancer Observatory; https://gco.iarc.fr/en. Accessed 13th February 2024.
5. Siegel RL, Giaquinto AN, Jemal A. Cancer statistics, 2024. CA: A Cancer J Clinic 2024; 74(1): 12-49.
6. Shnaider PV, Ivanova OM, Malyants IK, et al. New Insights into Therapy-Induced Progression of Cancer. *Int J Mol Sci*. 2020;21:E7872.
7. Parvathaneni V, Kulkarni NS, Muth A, Gupta V. Drug repurposing: a promising tool to accelerate the drug discovery process. *Drug Discov Today*. 2019;24:2076–2085.
8. Kulkarni VS, Alagarsamy V, Solomon VR, Jose PA, Murugesan S. Drug Repurposing: An Effective Tool in Modern Drug Discovery. *Russ J Bioorg Chem*. 2023;49:157–166.
9. Schein CH. Repurposing approved drugs for cancer therapy. *Br Med Bull*. 2021;137:13–27.
10. Mohi-ud-din R, Chawla A, Sharma P, et al. Repurposing approved non-oncology drugs for cancer therapy: a comprehensive review of mechanisms, efficacy, and clinical prospects. *Eur J Med Res*. 2023;28:345.
11. Langedijk J, Mantel-Teeuwisse AK, Slijkerman DS, Schutjens MH. Drug repositioning and repurposing: terminology and definitions in literature. *Drug Discov Today*. 2015;20:1027–1034.
12. Haupt VJ, Daminelli S, Schroeder M. Drug Promiscuity in PDB: Protein Binding Site Similarity Is Key. *PLoS One*. 2013;8:e65894.
13. Campillos M, Kuhn M, Gavin AC, Jensen LJ, Bork P. Drug target identification using side-effect similarity. *Science*. 2008;321:263–266.
14. Qu XA, Gudivada RC, Jegga AG, Neumann EK, Aronow BJ. Inferring novel disease indications for known drugs by semantically linking drug action and disease mechanism relationships. *BMC Bioinf*. 2009;10:S4.
15. Keiser MJ, Setola V, Irwin JJ, et al. Predicting new molecular targets for known drugs. *Nature*. 2009;462:175–181.
16. Abdel-Aziz AK, Saadeldin MK, Salem AH, et al. A Critical Review of Chloroquine and Hydroxychloroquine as Potential Adjuvant Agents for Treating People with Cancer. *Future Pharmacol*. 2022;2:431–443.
17. Eloranta K, Cairo S, Liljeström E, et al. Chloroquine Triggers Cell Death and Inhibits PARPs in Cell Models of Aggressive Hepatoblastoma. *Front Oncol*. 2020;10.
18. Anand K, Niravath P, Patel T, et al. A Phase II Study of the Efficacy and Safety of Chloroquine in Combination With Taxanes in the Treatment of Patients With Advanced or Metastatic Anthracycline-refractory Breast Cancer. *Clin Breast Cancer*. 2021;21:199–204.
19. Zhou W, Wang H, Yang Y, Chen Z-S, Zou C, Zhang J. Chloroquine against malaria, cancers and viral diseases. *Drug Discov Today*. 2020;25:2012–2022.
20. Varakumar P, Rajagopal K, Aparna B, et al. Acridine as an Anti-Tumour Agent: A Critical Review. *Molecules*. 2023;28:193.
21. Kumar M, Sarkar A. Repurposing of Anti-Malarial Drug Quinacrine for Cancer Treatment: A Review. *Sci Pharm*. 2022;90:12.
22. Oien DB, Pathoulas CL, Ray U, Thirusangu P, Kalogera E, Shridhar V. Repurposing quinacrine for treatment-refractory cancer. *Semin Cancer Biol*. 2021;68:21–30.
23. Thirusangu P, Pathoulas CL, Ray U, et al. Quinacrine-Induced Autophagy in Ovarian Cancer Triggers Cathepsin-L Mediated Lysosomal/Mitochondrial Membrane Permeabilization and Cell Death. *Cancers*. 2021;13:2004.
24. Oien DB, Ray U, Pathoulas CL, et al. Quinacrine Induces Nucleolar Stress in Treatment-Refractory Ovarian Cancer Cell Lines. *Cancers*. 2021;13:4645.
25. Gensicka-Kowalewska M, Cholewiński G, Dzierzbicka K. Recent developments in the synthesis and biological activity of acridine/acridone analogues. *RSC Adv*. 2017;7:15776–15804.
26. Kozurkova M, Sabolova D, Kristian P. A new look at 9-substituted acridines with various biological activities. *J Appl Toxicol*. 2021;41:175–189.
27. Prasher P, Sharma M. Medicinal chemistry of acridine and its analogues. *MedChemComm*. 2018;9:1589–1618.
28. Silva AT, Bento CM, Pena AC, et al. Cinnamic Acid Conjugates in the Rescuing and Repurposing of Classical Antimalarial Drugs. *Molecules*. 2020;25:66.
29. Prithwiraj De FB-BCV-BMB. Cinnamic Acid Derivatives in Tuberculosis, Malaria and Cardiovascular Diseases - A Review. *Curr Org Chem*. 2012;16:747–768.
30. Feng L-S, Cheng J-B, Su W-Q, et al. Cinnamic acid hybrids as anticancer agents: A mini-review. *Arch Pharm*. 2022;355:2200052.
31. De P, Baltas M, Bedos-Belval F. Cinnamic acid derivatives as anticancer agents-a review. *Curr Med Chem*. 2011;18:1672–1703.
32. De P, Bedos-Belval F, Vanucci-Bacque C, Baltas M. Cinnamic Acid Derivatives in Tuberculosis, Malaria and Cardiovascular Diseases - A Review. *Curr Org Chem*. 2012;16:747–768.
33. Ruwizhi N, Aderibigbe BA. Cinnamic Acid Derivatives and Their Biological Efficacy. *Int J Mol Sci*. 2020;21:5712.
34. Samanta A, Sarkar A. Fighting New Wars with old Weapons: Repurposing of Anti-Malarial Drug for Anticancer Therapy: Quinacrine role in BC treatment. *Arch Breast Cancer*. 2022;9:439–449.
35. Ehsanian R, Van Waes C, Feller SM. Beyond DNA binding - a review of the potential mechanisms mediating quinacrine's therapeutic activities in parasitic infections, inflammation, and cancers. *Cell Commun Signal*. 2011;9:13.
36. Pérez BC, Fernandes I, Mateus N, Teixeira C, Gomes P. Recycling antimalarial leads for cancer: Antiproliferative properties of *N*-cinnamoyl chloroquine analogues. *Bioorg Med Chem Lett*. 2013;23:6769–6772.
37. Gomes A, Fernandes I, Teixeira C, Mateus N, Sottomayor MJ, Gomes P. A Quinacrine Analogue Selective Against Gastric Cancer Cells: Insight from Biochemical and Biophysical Studies. *ChemMedChem*. 2016;11:2703–2712.
38. Fonte M, Fagundes N, Gomes A, et al. Development of a synthetic route towards N^4,^{N}9-disubstituted 4,9-diaminoacridines: On the way to multi-stage antimalarials. *Tetrahedron Lett*. 2019;60:1166–1169.
39. Wiser MF. The Digestive Vacuole of the Malaria Parasite: A Specialized Lysosome. *Pathogens*. 2024;13.
40. Coban C. The host targeting effect of chloroquine in malaria. *Curr Opin Immunol*. 2020;66:98–107.
41. Bogdanov A, Bogdanov A, Chubenko V, Volkov N, Moiseenko F, Moiseyenko V. Tumor acidity: From hallmark of cancer to target of treatment. *Front Oncol*. 2022;12, 979154.

Supporting Information

Repurposing antiplasmodial leads for cancer: exploring the antiproliferative effects of *N*-cinnamoyl-aminoacridines

Mélanie Fonte,[1] Catarina Rôla,[2] Sofia Santana,[2] Miguel Prudêncio,[2] Joana Almeida,[3, 4] Ricardo Ferraz,[1,3,4] Cristina Prudêncio,[3,4] Cátia Teixeira,[1,5] Paula Gomes[1]

[1] LAQV-REQUIMTE, Departamento de Química e Bioquímica, Faculdade de Ciências, Universidade do Porto, Portugal;

[2] Instituto de Medicina Molecular, Faculdade de Medicina, Universidade de Lisboa, Portugal;

[3] Centro de Investigação em Saúde Translacional e Biotecnologia Médica (TBIO)/Rede de Investigação em Saúde (RISE-Health), Escola Superior de Saúde, Instituto Politécnico do Porto, Portugal;

[4] Ciências Químicas e das Biomoléculas, Escola Superior de Saúde, Politécnico do Porto, Portugal;

[5] Current affiliation: Gyros Protein Technologies Inc., Tucson, Arizona, USA.

Contents:

1. Experimental section 2

1.1. MTT assay 2

1.2. AlamarBlue assay 2

1. Experimental Section - *In vitro* cytotoxicityassay

The MKN-28 cells originating from human gastric adenocarcinoma and the human dermal fibroblasts (HDF) were kindly provided by Iva Fernandes from Food Quality and Technology group (FCUP, Porto, Portugal) and Pedro Coelho from T.Bio Laboratory (Escola Superior de Saúde, Porto, Portugal), respectively. The human hepatoma cell lines (HepG2 and Huh7) were purchased from ATCC and kindly provided by Cenix Bioscience GmbH, respectively.

Cells were cultured in 25 cm^2 plates as a monolayer and were routinely maintained in (i) HDF cells: Dulbecco's modified Eagle's medium (DMEM, Sigma-Aldrich), supplemented with 20% v/v fetal bovine serum (FBS, Corning®) and 1% penicillin/streptomycin (Corning®); (ii) MKN-28 cells: Roswell Park Memorial Institute 1640 medium (RPMI-1640, Sigma-Aldrich) supplemented with 10% v/v FBS and 1% penicillin/streptomycin; (iii) Huh-7 cells: RPMI-1640 supplemented with 10% (v/v) FBS, 1% (v/v) glutamine, 1% (v/v) penicillin/streptomycin, 1% non-essential amino acids, and 10mM HEPES; and (iv) HepG2 cells: DMEM supplemented with 10% FBS, 1% (v/v) glutamine and 1% (v/v) penicillin/streptomycin, under a humidified atmosphere with 5% CO_2 at 37 °C. Fresh complete medium was added every 2 days. Except for HDF, cells were harvested by trypsinization twice a week. At confluence, the subculture was split, and the cells were seeded on 96-well plates.

1.1. MTT assay

MKN-28 or HDF cells were seeded into 96-well plates and allowed to grow for 24 h under a humidified atmosphere with 5% CO_2 at 37 °C. Then, the culture medium in the wells was substituted by a medium containing serially diluted concentrations of each compound (50.0, 25.0, 12.5, 6.25, 3.12, 1.56, and 0.50 µM), with a maximal dimethyl sulfoxide (DMSO, LabChem) concentration of 0.1 %, which is not cytotoxic. Following a 24 h period of incubation, the medium was removed, and a solution of 3-(4,5-dimethylthiazol-2-yl)-2,5-diphenyltetrazolium bromide (MTT, Alfa Aesar) at 0.5 mg/mL in the medium was added. After 1.5 h of incubation, the MTT solution was removed, and the resulting crystals were dissolved in DMSO and quantified photometrically at a dual wavelength of 570/690 nm using the Multiskan SkyHigh microplate reader (Thermo ScientificTM, USA). The percentage of viable cells was determined, a nonlinear regression analysis was employed to fit the normalized results of the dose-response curves, and IC_{50} values were determined using GraphPad Prism 8.4.2. software.

1.2. AlamarBlue assay

Huh7 or HepG2 cells were seeded into 96-well plates and, 24 h later, the culture medium in the wells was replaced by medium containing the suitable concentration of each compound (15, 12, 8.0, 4.0, 2.0, 0.50, 0.10 µM or 30, 25, 20, 15, 10, 5.0, 1.0 µM, depending on the compound). In control wells, the cell culture medium was replaced by medium containing the same percentage of DMSO used in compound solutions (0.01%), which is not cytotoxic. Following a 24 h incubation period, growth inhibition was assessed by the AlamarBlue assay (Invitrogen, UK) using the manufacturer's protocol. Nonlinear regression analysis was employed to fit the normalized results of the dose-response curves, and IC_{50} values were determined using GraphPad Prism 8.4.2. software.

CHAPTER IV

Conclusions and Future Perspectives

This final chapter summarizes the main achievements and conclusions of the present doctoral thesis, as well as future perspectives.

Summary of main conclusions

Malaria remains a leading cause of death in tropical countries, particularly affecting children and pregnant women. Despite extensive efforts, the fast adaptative evolution of *Plasmodium* parasites and mosquito vectors to the current antimalarial chemotherapeutics and insecticidal drugs has aggravated this huge threat to health and wellbeing. Drug resistance has rendered previously effective treatments less reliable, and signs of resistance to ACTs, the current first-line treatment, highlight the urgent need to develop new antimalarials before complete failure of available therapies. Future treatments must efficiently clear asexual blood-stage parasitemia and all hepatic forms of the parasite, including dormant hypnozoites, while also blocking transmission. Ideally, they should also be simple and feasible for use in developing countries. Traditional drug development strategies are not a long-term option, making it crucial to explore alternative approaches to identify novel antimalarials that address these challenges. Thus, the main aim of the present work was to develop a multi-stage antimalarial candidate capable of targeting multiple processes in the malaria parasite's life cycle, thereby enhancing efficacy, and reducing the likelihood of emerging resistance. This was achieved by applying the covalent bitherapy concept to merge CQ and PQ chemical structures into a single molecular construct comprising an aminoacridine core, anticipating that the new molecules would retain the parent drugs' activity across different stages of the *Plasmodium* life cycle. To accomplish our overarching aim, this doctoral project was divided into four experimental goals, whose pursuit and achievement were reported and discussed in preceding chapters and resulted in five original research articles. Overall, the work combined traditional organic synthesis and analytical techniques with biological *in vitro* evaluation of antiplasmodial and antiproliferative properties. In summary, this work allowed us to draw the following conclusions:

Chapter II

1. **The unprecedented synthesis of 4-aminoacridines and 4,9-diaminoacridines was successful achieved.**

The new synthetic routes developed during this journey led to the correct production of the target aminoacridines. The route established comprised two main parts: Part A - synthesis of the 6,9-dichloro-2-methoxy-4-nitroacridine precursor, and Part B - functionalization of this core with the desired amino alkyl chains. Specifically, the

precursor was obtained via five reaction steps in a global yield of 24%, whereas final 4-aminoacridines and 4,9-diaminacridines were produced through five and four reaction steps in 21% and 13% global yields, respectively. The chemical structures of the target compounds were successfully confirmed by proton and carbon NMR and ESI-IT MS, while their high purity (> 96%) was verified by HPLC.

2. The target 4-aminoacridines and 4,9-diaminoacridines have dual-action against *Plasmodium*.

The *in vitro* assessment of the two first-generation families of acridine-based molecules developed herein revealed that these novel compounds, which merge the structures of CQ and PQ, preserved the antiplasmodial properties of the parent drugs, emerging as dual-action antiplasmodial hits with activity against the erythrocytic stages of CQ-sensitive and CQ-resistant *P. falciparum* strains, and against the hepatic stages of *P. berghei*. Noteworthy, 4,9-diaminoacridines exhibited superior activity against blood forms of the parasite compared to 4-aminoacridines. Conversely, 4-aminoacridines showed more promising activities against hepatic forms of the parasite, even surpassing that of the reference drug PQ, whereas 4,9-diaminoacridiines were notably toxic to the hepatic Huh-7 cell line. Among the whole set, hybrids with the *N*-butylamino chain in C-4 of the acridine ring were considered the best candidates within each family to take forward into additional studies.

3. Efforts aimed at optimizing the synthetic routes of 4-aminoacridines and 4,9-diaminoacridines led to significant progress in the overall synthesis scheme.

The modest global yields obtained in the initial synthesis scheme used to produce 4-aminoacridines and 4,9-diaminoacridines, as well as the harsh and/or time-consuming procedures involved, were the driving force to work on the optimization of the synthesis route. Optimization efforts allowed to reduce the reaction steps needed to produce the 6,9-dichloro-2-methoxy-4-nitroacridine common precursor from five to three (Part A of the overall synthetic route), with a two-fold increase in the overall yield (63%), compared to that previously achieved (24%).

Improvements were also possible for Part B of the global synthesis route. Thus, in the pathway from 6,9-dichloro-2-methoxy-4-nitroacridine to 4,9-diaminoacridines, the introduction of the amino side chains in the C-9 and C-4 positions of the acridine ring were also significantly ameliorated by the use of MW heating and reductive amination, respectively. In the pathway from the same precursor to 4-aminoacridines, the efforts targeted the experimental conditions of the reduction steps. Taken together,

modifications to the overall synthesis scheme allowed to produce 4,9-diaminoacridines in four steps with a 21% overall yield, and 4-aminoacridines in five steps with a 34% yield, which in both cases is superior to previous methods (13% and 21%, respectively). Moreover, the new synthesis scheme is simpler and faster than previous approaches, while making use of milder conditions. Altogether, these findings enable a more accessible and sustainable production of functionalized acridines, laying the groundwork for future synthetic approaches focused on acridine-based compounds.

Achievements - Chapter II

In short, the results reported in Chapter II allowed us to validate our initial working hypothesis in that the conjugation of PQ and CQ in one single molecule would result in merged hybrids with multi-stage action towards *Plasmodium* parasites. Alongside, the reported efforts in synthetic optimization facilitate the easier acquisition of these promising 4-amino and 4,9-diaminoacridines hits.

Chapter III

4. The coupling of CAs to 4-aminoacridines and to 4,9-diaminoacridines had a positive impact on the global antiplasmodial activity.

Two new second-generation families of hybrids were obtained through the coupling of a series of CAs to the aliphatic amine of either the 4-aminoacridines or the 4,9-diaminoacridines that were previously found to display the best dual-stage antiplasmodial activity *in vitro* (Chapter II). The new conjugates were produced in moderate to good yields (24-98%) and high purities (94-99%), using the previously described synthetic route (Chapter II) to which a final coupling step was added. *In vitro* assessment of the antiplasmodial activity of the conjugates allowed us to confirm that coupling of the aminoacridines with CAs did have a positive impact, as an overall enhancement of activity against the three phases of the *Plasmodium* life cycle in human host, liver, blood, and gametocyte stages, could be observed.

The 4-aminoacridine-based conjugates displayed superior activity than the parent aminoacridine against liver and gametocyte forms of parasite. On the other hand, their blood-stage activities were not so remarkable, although a few conjugates also showed improvement over the parent compound. Importantly, none of these new conjugates showed significant toxicity to either hepatic Huh-7 cells or erythrocytes.

Similarly, 4,9-diaminoacridine-based conjugates displayed enhanced activity against gametocyte and liver forms of parasite compared to the parent diaminoacridine, although the hepatic activity was accompanied by cytotoxic effects on Huh-7 cells. Remarkably, this family of second-generation hybrids displayed nanomolar activities against blood forms of *P. falciparum*, which makes them more potent than the parent diaminoacridine.

5. **Conjugation with *m*-fluorocinnamic acid leads to the most promising second-generation hybrids.**

Interestingly, in both families of second-generation hybrids, conjugation with *m*-fluorocinnamic acid led to the best-performing conjugates. This finding aligns with literature reports advocating that incorporation of fluorine to bioactive compounds typically enhances pharmacological properties, such as lipophilicity, metabolic stability, and binding affinity when compared to their counterparts. Notably, several well-known antimalarials, including mefloquine, halofantrine, and tafenoquine, are fluorinated.

6. **The presence of an amino alkyl substituent on C-9 of the acridine ring notably affects activity and toxicity.**

The substantial differences in antiplasmodial activities and in cytotoxicity, between first- and second-generation 4-aminoacridines as compared to first- and second-generation 4,9-diaminoacridines, emphasize the significant influence of the amino alkyl substituent in C-9 of the acridine ring of the latter. Thus, 4,9-diaminoacridine-based hybrids showed more potent activity against blood forms and higher toxicity to Huh-7 cells compared to their 4-aminoacridine counterparts. While this is an important observation regarding future development of ACR-based antimalarials, it is equally relevant if considering a possible repurposing of these compounds as templates for novel anti-tumoral agents.

7. **The 4,9-diaminoacridine/cinnamic acid conjugates are selectively toxic to tumor cell lines**

Following our previous findings, in particular the observation that 4,9-diaminoacridine-based conjugates were toxic to human hepatoma cells of the Huh-7 cell line, additional antiproliferative assays were conducted *in vitro* on Huh-7, HepG2, MKN-28 tumoral cell lines, as well as on human primary dermal fibroblasts (non-carcinogenic cells). This confirmed that 4,9-diaminoacridine-based have selective toxicity towards tumor cell lines, which indicates the potential of these scaffolds for repurposing as antineoplastic agents. Conversely, 4-aminoacridine-based constructs showed no toxicity towards either tumor or non-tumor cells, which once more emphasizes the significant influence of the

amino side chain in C-9 of the acridine ring on the biological properties of the ACR-based compounds developed and explored herein.

Achievements - Chapter III

Briefly, the results presented in Chapter III allowed us to confirm that conjugation of CAs with first-generation ACR-based merge hybrids is a good approach to enhance their global antiplasmodial activity. Additionally, further antiproliferative assays *in vitro* disclosed 4,9-diaminoacrdine-based structures as relevant templates for future development of selective antitumoral agents.

In conclusion…

The results of this project constitute a significant step forward towards the development of multi-stage antimalarial drug candidates, with the potential to fill the two most critical gaps in malaria control and elimination: new therapeutic alternatives to the current ACTs whose efficacy is declining, and medicines able to elude the resistance issues recurrent in malaria chemotherapy. The data presented firmly establish the potential of aminoacridines as a promising scaffold with multi-stage antiplasmodial activity, one of the key desired features for next generation antimalarials. Given the importance of halting the progression of infection within the human host from its initial stages in the liver, throughout its symptomatic stage in red blood cells, up until the gametocyte stage underlying disease propagation, these findings offer a significant contribution towards the development of new valuable antiplasmodial candidates. Additionally, the development and optimization of synthetic routes for 4-aminoacridines and 4,9-diaminoacridines, alongside the synthesis pathway to a precursor that may serve to produce other ACR-based compounds, pave the way for future synthetic approaches targeting compounds of this chemotype.

Drug discovery and development is a lengthy process that extends well beyond the scope of a doctoral thesis. Nevertheless, in an era where we still largely rely on antimalarial drugs, this work may serve as a starting point for the development of potential multi-stage ACR-based candidates, offering a new pathway towards tackling and ideally eradicating malaria.

Future Perspectives

As commonly occurs during a doctoral research project, irrespective of how much has been done and achieved, a lot more remains to be explored going forward. In the present work, substantial research remains to be conducted towards transition of the compounds developed from hit-to-lead to from lead-to-candidate. In this regard, relevant future experiments to complement this work include:

1. Structural optimization.

Although second-generation conjugates revealed enhanced features over first-generation ones, we cannot exclude that other structural modifications of the latter can bring higher benefits to antiplasmodial activity, toxicity, as well as to pharmacokinetic-pharmacodynamic properties (which were not addressed within the scope of this work). Also, to obtain promising leads for lead-to-candidate development, extensive SAR studies should be undertaken.

2. Liver-stage activity of 4,9-diaminoacridine conjugates in primary hepatocytes.

The liver-stage activity of all the conjugates in this study was assessed using the Huh-7 cell line, a well-differentiated hepatocyte-derived carcinoma cell line commonly used as a substitute for primary hepatocytes due to the drawbacks associated with primary cells. The 4,9-diaminoacridine-based compounds herein reported exhibited toxicity to this cell line, but not for a non-carcinogenic line of human fibroblasts. Therefore, we cannot rule out that these compounds might have relevant liver-stage activity that was hindered by the fact that *in vitro* assays were conducted on Huh-7 cells. Therefore, it would be important to implement and use an *in vitro* assay enabling the use of primary hepatocytes. While testing the compounds *in vivo* on a rodent malaria model could be an alternative approach to check the liver-stage efficacy of 4,9-diaminoacridine-based compounds, unnecessary animal sacrifice should be avoided, i.e., *in vivo* studies should be considered only if test compounds have been confirmed as highly effective *in vitro*.

3. Activity against drug-resistant *P. falciparum* strains and resistance selection.

A major concern with new compounds regards investigating whether they can (i) effectively kill drug-resistant parasites, and (ii) induce the development of resistant parasite strains. Thus, it will be crucial to test the compounds herein reported against various drug-resistant *P. falciparum* strains, as well as to use them in resistance induction assays. Since drug resistance is correlated with specific genetic mutations,

monitoring these molecular markers may help uncover mechanisms not only of parasite resistance, but also of the compounds' antiplasmodial action.

4. Disclosure of the antiplasmodial MoA(s) of the new compounds.

The MoA(s) underlying the antiplasmodial activity of the compounds herein investigated are unknown. However, understanding these mechanisms could lead to potential chemical optimizations and, therefore, the development of more potent compounds. Both acridine and cinnamic acid, the components of these hybrids, have some possibles MoA(s), that might contribute to the conjugates' bioactivity. Yet, these new molecular entities might exhibit multi-stage antiplasmodial action through mechanisms other than those reported for structurally related compounds. Hence, it is important to complement the work with mechanistic studies, such as examining (i) β-hematin inhibition, (ii) accumulation in the parasite's digestive vacuole, or (iii) DNA interaction, to gain further insights.

5. Further investigations on the antiproliferative action of 4,9-diaminoacridines.

Given the selective activity of the 4,9-diaminoacridine-based conjugates against three different tumor cell lines, further exploration of those conjugates and of other structures based on the 4,9-diaminoacridine scaffold towards new antineoplastic agents is warranted. Starting by testing the compounds *in vitro* against colorectal, breast (including triple-negative), and pancreatic tumor cell lines, which are amongst the deadliest cancers, will surely be insightful. The use of primary cell lines from each corresponding tissue as controls (e.g.: human rectal fibroblasts, human mammary fibroblasts, and human pancreatic stellate cells), instead of HDF used herein, should also be considered.

Once all studies outlined above have been completed, and compounds with proven value as promising antimalarial and/or antineoplastic leads are identified, the next phase should involve in-depth *in vivo* studies on efficacy, pharmacokinetics, and pharmacodynamics.

Annexes

JOHN WILEY AND SONS LICENSE
TERMS AND CONDITIONS

May 23, 2024

This Agreement between FCUP -- Mélanie Fonte ("You") and John Wiley and Sons ("John Wiley and Sons") consists of your license details and the terms and conditions provided by John Wiley and Sons and Copyright Clearance Center.

License Number	5794690852373
License date	May 23, 2024
Licensed Content Publisher	John Wiley and Sons
Licensed Content Publication	ChemMedChem
Licensed Content Title	4,9-Diaminoacridines and 4-Aminoacridines as Dual-Stage Antiplasmodial Hits
Licensed Content Author	Cátia Teixeira, Paula Gomes, Miguel Prudêncio, et al
Licensed Content Date	Dec 7, 2020
Licensed Content Volume	16
Licensed Content Issue	5
Licensed Content Pages	5
Type of use	Dissertation/Thesis
Requestor type	Author of this Wiley article
Format	Print and electronic

Portion	Full article
Will you be translating?	No
Title of new work	Novel 4-amino- and 4,9-diamino-acridines as multi-stage antimalarials
Institution name	FCUP
Expected presentation date	Jul 2024
Order reference number	1
Requestor Location	FCUP Rua do Campo Alegre, 1021 Porto, 4169-007 Portugal Attn: FCUP
Publisher Tax ID	EU826007151
Total	0.00 EUR

Terms and Conditions

TERMS AND CONDITIONS

This copyrighted material is owned by or exclusively licensed to John Wiley & Sons, Inc. or one of its group companies (each a"Wiley Company") or handled on behalf of a society with which a Wiley Company has exclusive publishing rights in relation to a particular work (collectively "WILEY"). By clicking "accept" in connection with completing this licensing transaction, you agree that the following terms and conditions apply to this transaction (along with the billing and payment terms and conditions established by the Copyright Clearance Center Inc., ("CCC's Billing and Payment terms and conditions"), at the time that you opened your RightsLink account (these are available at any time at http://myaccount.copyright.com).

Terms and Conditions

- The materials you have requested permission to reproduce or reuse (the "Wiley Materials") are protected by copyright.
- You are hereby granted a personal, non-exclusive, non-sub licensable (on a stand-alone basis), non-transferable, worldwide, limited license to reproduce the Wiley

Materials for the purpose specified in the licensing process. This license, **and any CONTENT (PDF or image file) purchased as part of your order,** is for a one-time use only and limited to any maximum distribution number specified in the license. The first instance of republication or reuse granted by this license must be completed within two years of the date of the grant of this license (although copies prepared before the end date may be distributed thereafter). The Wiley Materials shall not be used in any other manner or for any other purpose, beyond what is granted in the license. Permission is granted subject to an appropriate acknowledgement given to the author, title of the material/book/journal and the publisher. You shall also duplicate the copyright notice that appears in the Wiley publication in your use of the Wiley Material. Permission is also granted on the understanding that nowhere in the text is a previously published source acknowledged for all or part of this Wiley Material. Any third party content is expressly excluded from this permission.

- With respect to the Wiley Materials, all rights are reserved. Except as expressly granted by the terms of the license, no part of the Wiley Materials may be copied, modified, adapted (except for minor reformatting required by the new Publication), translated, reproduced, transferred or distributed, in any form or by any means, and no derivative works may be made based on the Wiley Materials without the prior permission of the respective copyright owner.**For STM Signatory Publishers clearing permission under the terms of the STM Permissions Guidelines only, the terms of the license are extended to include subsequent editions and for editions in other languages, provided such editions are for the work as a whole in situ and does not involve the separate exploitation of the permitted figures or extracts,** You may not alter, remove or suppress in any manner any copyright, trademark or other notices displayed by the Wiley Materials. You may not license, rent, sell, loan, lease, pledge, offer as security, transfer or assign the Wiley Materials on a stand-alone basis, or any of the rights granted to you hereunder to any other person.

- The Wiley Materials and all of the intellectual property rights therein shall at all times remain the exclusive property of John Wiley & Sons Inc, the Wiley Companies, or their respective licensors, and your interest therein is only that of having possession of and the right to reproduce the Wiley Materials pursuant to Section 2 herein during the continuance of this Agreement. You agree that you own no right, title or interest in or to the Wiley Materials or any of the intellectual property rights therein. You shall have no rights hereunder other than the license as provided for above in Section 2. No right, license or interest to any trademark, trade name, service mark or other branding ("Marks") of WILEY or its licensors is granted hereunder, and you agree that you shall not assert any such right, license or interest with respect thereto

- NEITHER WILEY NOR ITS LICENSORS MAKES ANY WARRANTY OR REPRESENTATION OF ANY KIND TO YOU OR ANY THIRD PARTY, EXPRESS, IMPLIED OR STATUTORY, WITH RESPECT TO THE MATERIALS OR THE ACCURACY OF ANY INFORMATION CONTAINED IN THE MATERIALS, INCLUDING, WITHOUT LIMITATION, ANY IMPLIED WARRANTY OF MERCHANTABILITY, ACCURACY, SATISFACTORY QUALITY, FITNESS FOR A PARTICULAR PURPOSE, USABILITY, INTEGRATION OR NON-INFRINGEMENT AND ALL SUCH WARRANTIES ARE HEREBY EXCLUDED BY WILEY AND ITS LICENSORS AND WAIVED BY YOU.

- WILEY shall have the right to terminate this Agreement immediately upon breach of this Agreement by you.

- You shall indemnify, defend and hold harmless WILEY, its Licensors and their respective directors, officers, agents and employees, from and against any actual or threatened claims, demands, causes of action or proceedings arising from any breach of this Agreement by you.

- IN NO EVENT SHALL WILEY OR ITS LICENSORS BE LIABLE TO YOU OR ANY OTHER PARTY OR ANY OTHER PERSON OR ENTITY FOR ANY SPECIAL, CONSEQUENTIAL, INCIDENTAL, INDIRECT, EXEMPLARY OR PUNITIVE DAMAGES, HOWEVER CAUSED, ARISING OUT OF OR IN CONNECTION WITH THE DOWNLOADING, PROVISIONING, VIEWING OR USE OF THE MATERIALS REGARDLESS OF THE FORM OF ACTION, WHETHER FOR BREACH OF CONTRACT, BREACH OF WARRANTY, TORT, NEGLIGENCE, INFRINGEMENT OR OTHERWISE (INCLUDING, WITHOUT LIMITATION, DAMAGES BASED ON LOSS OF PROFITS, DATA, FILES, USE, BUSINESS OPPORTUNITY OR CLAIMS OF THIRD PARTIES), AND WHETHER OR NOT THE PARTY HAS BEEN ADVISED OF THE POSSIBILITY OF SUCH DAMAGES. THIS LIMITATION SHALL APPLY NOTWITHSTANDING ANY FAILURE OF ESSENTIAL PURPOSE OF ANY LIMITED REMEDY PROVIDED HEREIN.

- Should any provision of this Agreement be held by a court of competent jurisdiction to be illegal, invalid, or unenforceable, that provision shall be deemed amended to achieve as nearly as possible the same economic effect as the original provision, and the legality, validity and enforceability of the remaining provisions of this Agreement shall not be affected or impaired thereby.

- The failure of either party to enforce any term or condition of this Agreement shall not constitute a waiver of either party's right to enforce each and every term and condition of this Agreement. No breach under this agreement shall be deemed waived or excused by either party unless such waiver or consent is in writing signed by the party granting such waiver or consent. The waiver by or consent of a party to a breach of any provision of this Agreement shall not operate or be construed as a waiver of or consent to any other or subsequent breach by such other party.

- This Agreement may not be assigned (including by operation of law or otherwise) by you without WILEY's prior written consent.

- Any fee required for this permission shall be non-refundable after thirty (30) days from receipt by the CCC.

- These terms and conditions together with CCC's Billing and Payment terms and conditions (which are incorporated herein) form the entire agreement between you and WILEY concerning this licensing transaction and (in the absence of fraud) supersedes all prior agreements and representations of the parties, oral or written. This Agreement may not be amended except in writing signed by both parties. This Agreement shall be binding upon and inure to the benefit of the parties' successors, legal representatives, and authorized assigns.

- In the event of any conflict between your obligations established by these terms and conditions and those established by CCC's Billing and Payment terms and conditions, these terms and conditions shall prevail.

- WILEY expressly reserves all rights not specifically granted in the combination of (i) the license details provided by you and accepted in the course of this licensing transaction, (ii) these terms and conditions and (iii) CCC's Billing and Payment terms and conditions.

- This Agreement will be void if the Type of Use, Format, Circulation, or Requestor Type was misrepresented during the licensing process.

- This Agreement shall be governed by and construed in accordance with the laws of the State of New York, USA, without regards to such state's conflict of law rules. Any legal action, suit or proceeding arising out of or relating to these Terms and Conditions or the breach thereof shall be instituted in a court of competent jurisdiction in New York County in the State of New York in the United States of America and each party hereby consents and submits to the personal jurisdiction of such court, waives any objection to venue in such court and consents to service of process by registered or certified mail, return receipt requested, at the last known address of such party.

WILEY OPEN ACCESS TERMS AND CONDITIONS

Wiley Publishes Open Access Articles in fully Open Access Journals and in Subscription journals offering Online Open. Although most of the fully Open Access journals publish open access articles under the terms of the Creative Commons Attribution (CC BY) License only, the subscription journals and a few of the Open Access Journals offer a choice of Creative Commons Licenses. The license type is clearly identified on the article.

The Creative Commons Attribution License

The Creative Commons Attribution License (CC-BY) allows users to copy, distribute and transmit an article, adapt the article and make commercial use of the article. The CC-BY license permits commercial and non-

Creative Commons Attribution Non-Commercial License

The Creative Commons Attribution Non-Commercial (CC-BY-NC)License permits use, distribution and reproduction in any medium, provided the original work is properly cited and is not used for commercial purposes.(see below)

Creative Commons Attribution-Non-Commercial-NoDerivs License

The Creative Commons Attribution Non-Commercial-NoDerivs License (CC-BY-NC-ND) permits use, distribution and reproduction in any medium, provided the original work is properly cited, is not used for commercial purposes and no modifications or adaptations are made. (see below)

Use by commercial "for-profit" organizations

Use of Wiley Open Access articles for commercial, promotional, or marketing purposes requires further explicit permission from Wiley and will be subject to a fee.

Further details can be found on Wiley Online Library
http://olabout.wiley.com/WileyCDA/Section/id-410895.html

Other Terms and Conditions:

v1.10 Last updated September 2015